INVESTIGATIONS INTO THE RESPONSES OF AXES OF RECALCITRANT SEEDS TO DEHYDRATION AND CRYOPRESERVATION

by

JAMES WESLEY-SMITH

Submitted in partial fulfilment of the academic requirements for the degree of Doctor in Philosophy of the Faculty of Science, Unversity of Natal, Durban

School of Life and Environmental Sciences
University of Natal
Durban, South Africa

PREFACE

The experimental work described in this thesis was carried out was carried out in the School of Life and Environmental Sciences of the University of Natal, Durban, under the supervision of Profs Patricia Berjak and NW Pammenter, and at the National Seed Storage Laboratory, USDA-ARS, Ft Collins CO. 80521, US., under the supervision of Dr Christina Walters.

These studies represent original work by the author, and have not otherwise been submitted in any form for any degree or diploma to any tertiary institution. Where use has been made of the work of others it is duly acknowledged in the text.

I dedicate this thesis to my parents, a small gesture that pales in comparison with all they have done for me in the past. Thank you!

ACKNOWLEDGEMENTS

To my supervisors Pat Berjak, Norman Pammenter and Chris Walters, my gratitude for believing in me, for your guidance and assistance, as well as for sharing openly your knowledge in aspects relating to this thesis, and beyond. I am truly indebted.

I would also like to acknowledge colleagues who helped me at various stages during the course of this work. To Paula Watt, for sharing many biotechnological secrets of that 'witchcraft' called tissue culture. To Rob Slotow for his highly significant (P <0.0001) assistance with statistical analysis. To Derek Dixon and the team from the Workshop of the School of Pure and Applied Physics for their skill in making the spring-loaded plunger and many other contraptions used during this thesis. To Bob Lee (Colorado State University) and Tom Giddings (University of Colorado, Boulder) for their able assistance with freeze-fracturing. To Pirrie Maartens for her friendship, efficiency and support while this thesis was nearing completion. To Quinton.com, our resident "IT-lighty", thank you for keeping gremlins away from my PC. Finally, to all those of you from both, University of Natal and from the National Seed Storage Laboratory in Ft Collins, CO. US - too many to single out - thanks for your friendship and support.

I would like to thank in particular Anthea, Bianca and Lauren for their love, encouragement, and patient understanding during my long periods of absence from home. This one is also for you!

Last, but not least, I thank God for being with me all along, for helping me see this work through to completion, and for giving me strength when I needed it most.

TABLE OF CONTENTS

CHAPTER 8. A cryopreservation study of embryonic axes of *Acer saccharinum*. Ultrastructural assessment of freezing damage and subsequent recovery *in vitro*

CHAPTER 9. Rapid drying and cooling as a reliable approach to cryopreserve embryonic axes of recalcitrant seeds: A critical appraisal

ABSTRACT

Achieving long-term storage of germplasm is critical for the conservation of plant biodiversity. Seed storage practices require that degradative reactions causing ageing be limited. By reducing the water content, cytoplasmic viscosity is increased to levels that minimise deteriorative reactions. Reducing the storage temperature additionally increases the storage lifespan by further reducing the rate at which such deleterious processes occur. Two broad categories of seeds can be distinguished based on their storage behaviour. Orthodox seeds are desiccation-tolerant; generally shed in the dry state and are metabolically quiescent. Such seeds are usually stored at low water contents (e.g. 5%), and their high cytoplasmic viscosity prevents freezing damage during cooling to subzero temperatures. On the other hand, desiccation-sensitive (recalcitrant) seeds do not undergo a maturation-drying phase, they are metabolically active at shedding, and sensitive to extreme or prolonged drying. Accordingly, recalcitrant seeds cannot be stored under conventional conditions because they do not survive drying to low water contents and are damaged by sub-zero temperatures, even when dried to the lowest water content tolerated. Therefore, procedures that facilitate harmless drying and cooling to low temperatures are required to achieve long-term storage of recalcitrant germplasm.

Recalcitrant seeds that are dried rapidly can attain relatively lower water contents without injury. However, these seeds are usually large and this limits the drying rates that can be achieved even under favourable conditions. Isolating embryonic axes from the rest of the seed facilitates faster drying, and a consequent reduction in the water content at which damage occurs. In axes of many species, the level of drying attained before lethal desiccation damage occurs is sufficient to limit freezing damage during cryogenic exposure and facilitate survival *in vitro*. However, many others are damaged when dried to water contents that preclude freezing, and also are killed if cooled to sub-zero temperatures at higher water contents. In such instances, the

window of permissible water contents leading to survival may be small or non-existent.

A basic premise explored in this thesis is that by restricting the growth of intracellular ice crystals using increasingly rapid cooling rates, the range of permissible water contents can be widened, facilitating survival of axes at higher water contents. An overview of the problems associated with the long-term storage of recalcitrant germplasm, and the rationale behind such rapid cooling approach are presented in Chapter 1 of the present thesis. Subsequent chapters report investigations on the effects of variables required to dry and cryopreserve embryonic axes with minimum damage, in keeping with this approach. Collectively, those studies aimed at establishing a robust cryopreservation procedure for the conservation of recalcitrant germplasm with broad applicability across species.

The approach presently adopted entailed manipulating the water content of excised axes using rapid drying to discrete water content ranges, and also using different methods to cool axes to cryogenic temperatures at various rates. The calorimetric properties of water in axes were investigated for *Camellia sinensis* (L.) O. Kuntze using differential scanning calorimetry (DSC). For all species, the effect of any drying or cooling treatment tested was determined by assessing the survival of axes *in vitro*, which provided the most reliable indicator of cellular damage. Additionally, the effects of different treatments upon the structural and functional integrity of axes were assessed using light and electron microscopy as well as measurement of electrolyte leakage. The studies undertaken are presented in a similar sequence to that in which they took place during the course of the experimental phase of this work. These are summarised below.

Partial drying plays a pivotal role in the approach developed, and microscopy has contributed towards increasing present understanding of desiccation damage. Microscopy was used to determine the effects of drying rate upon the ultrastructure of recalcitrant axes. It was necessary to find reliable protocols to prepare specimens for

light and electron microscopy that did not alter the architecture of the cells in the dry state. Freeze-substitution and conventional aqueous fixation were compared in Chapter 2 using variously dried material from three species. The results obtained revealed that an unacceptably high extent of artefactual rehydration occurs during aqueous fixation, and highlight the need for anhydrous processing of dehydrated samples. Significantly, that study also revealed that many cellular events commonly associated with desiccation damage (e.g. withdrawal, tearing and/or vesiculation of the plasmalemma) are not seen in freeze-substituted preparations, and are likely artefacts of aqueous fixation.

Freeze-substitution was used subsequently (Chapter 3) to assess the effects of slow drying (2 - 3 days) or rapid drying (min) upon the survival of embryonic axes of jackfruit (*Artocarpus heterophyllus* Lamk.) Results confirmed the beneficial effects of rapid drying, and also provided insights into ultrastructural changes and probable causes underlying cellular damage that occur during a drying/rehydration cycle.

Efforts subsequently focused on determining the effect of cooling rate upon survival of recalcitrant axes at various water contents. The study on embryonic axes of recalcitrant *Camellia sinensis* (tea; Chapter 4) tested the hypothesis that rapid cooling facilitates survival of axes at higher water content by restricting the growth of ice crystals to within harmless dimensions. The presence of sharp peaks in DSC melting thermograms was indicative of decreased survival *in vitro.* These peaks were attributed to the melting of ice crystals sufficiently large to be detected by DSC as well as to cause lethal damage to axes. Increasing the cooling rate from 10°C min^{-1} to that attained by forcibly plunging naked axes into sub-cooled nitrogen increased the upper limit of water content facilitating survival *in vitro* from *c.* 0.4 to 1.1 – 1.6 g H_2O g^{-1} (dry mass [dmb]). Subsequent studies tested whether a similar trend occurred in other recalcitrant species cooled under similar conditions.

In order to investigate further the relationship between water content, cooling rate and survival it was necessary to achieve cooling rates reproducibly, and to quantify these reliably. The plunging device required to achieve rapid cooling, and instruments

required to measure the cooling rates attained, are described in Chapter 5. That study investigated the effects of cryogen type, depth of plunge and plunging velocity on the cooling rates measured by thermocouples either bare or within tissues of similar size and water content as encountered in cryopreservation experiments. This plunger was used in subsequent studies to achieve the fastest cooling conditions tested. Favourable cooling conditions were selected, and the efficacy of this procedure to cryopreserve relatively large axes was tested (Chapter 6) using embryonic axes of horse chestnut (*Aesculus hippocastanum* L.) Axes at water contents above *c.* 0.75 g g^{-1} could not be cooled faster than *c.* 60 °C s^{-1}, but cooling rates of axes below this water content increased markedly with isopentane, and to a lesser extent with sub-cooled nitrogen. Axes were killed when cooled at water contents above 1.0 g g^{-1} but survived fully (albeit abnormally) when cooled in isopentane between 1.0 and 0.75 g g^{-1}. Complete survival and increasingly normal development was attained at water contents below 0.75 g g^{-1}, especially if isopentane was used.

The study on horse chestnut axes emphasised that water content and cooling rate are co-dependent during non-equilibrium cooling. Accordingly, that study could not determine whether survival at lower water contents increased because of the corresponding increase in cooling rates measured, or because of the higher cytoplasmic viscosity that resulted from drying. That uncertainty was addressed by the study discussed in Chapter 7, using axes of the trifoliate orange (*Poncirus trifoliata* [L.] RAF.) That study investigated the effect of cytoplasmic viscosity upon survival of axes cooled and warmed at different rates. Survival and normal development was high at lower water contents, and seemingly independent of cooling rate at about 0.26 g g^{-1}. At higher water contents the range of cooling rates facilitating survival became narrower and displaced towards higher cooling rates. This study revealed two conspicuous inconsistencies that questioned the beneficial effect of rapid cooling. Firstly, the fastest cooling rates did not necessarily facilitate the highest survival. Secondly, survival of fully hydrated axes was higher when cooled under conditions that encouraged - rather than restricted - the growth of intracellular ice crystals.

These inconsistencies were explored further using embryonic axes of silver maple (*Acer saccharinum* L.). Freeze-fracture replicas and freeze-substitution techniques provided valuable insights into the way in which ice crystals were distributed in cells cooled using different methods at rates ranging between 3.3 and 97°C s^{-1}. Extensive intracellular freezing was common to all treatments. Unexpectedly, fully hydrated axes not only survived cryogenic exposure, but many axes developed normally when cooled using the relatively slower methods (77 and 3.3°C s^{-1}) if warming was rapid. The most conspicuous ultrastructural difference between plunge cooling and the relatively slower methods was the exclusion of ice from many intracellular compartments in the latter. It is possible that even the fastest warming cannot prevent serious cellular damage if ice crystals form within such 'critical' compartments. It is proposed that the intracellular location of ice is a stronger determinant of survival that the size attained by ice crystals.

The study of *A. saccharinum* also investigated the recovery of axes cooled fully hydrated either rapidly (97°C s^{-1}) or slowly (3.3°C s^{-1}). This facet of the study showed that cell lysis became apparent immediately after warming only where damage was most extensive. In other cells damage became apparent only after 2.5 to 6 h had elapsed, thus cautioning against inferring survival from the ultrastructural appearance of cells immediately after warming. Microscopy enabled cell repair as well as the pattern of growth of cryopreserved tissues to be appraised at the cellular, tissue and organ levels. Similar studies are required to understand further the nature of freezing damage, and how those events affect cell function.

The salient trends observed in previous chapters are brought together in Chapter 9.

CHAPTER 1

Introduction

Conserving plant biodiversity by means of long-term storage of seeds is of paramount importance in the face of a growing list of species threatened with extinction, and genetic erosion arising from highly selective breeding programs designed increase yield in agricultural crops (Chin, 1992). Genebanks preserve genetic diversity by capturing suitably large samples of individuals within populations, and storing these accessions for periods in excess of 30 years under conditions where deteriorative conditions are reduced or, preferably eliminated (Walters, 1998). Selecting favourable storage conditions is critical to prevent genetic shifts and ensure long-term stability. The conditions providing favourable storage are determined primarily by the water content of the seed and on the storage temperature. The water content and the procedure followed to reach the storage temperature vary among species, and provide the basis for categorisation of seeds according to their storage behaviour.

Seed Storage Behaviour - An overview

Two broad categories of seeds are distinguished by significant differences in their physiology and post-harvest behaviour, *viz.* orthodox and recalcitrant (Roberts, 1973), although it is probable that these represent the extremes of a continuum of responses by which seeds may be categorised (Berjak and Pammenter, 1994; Pammenter and Berjak, 1999). Orthodox seeds are those which undergo a developmentally-programmed period of maturation drying on the parent plant to water contents of 20% or less of the fresh mass, and which can be dried further to 5% without loss of viability (Roberts and King, 1980). This maturation drying phase is preceded and/or accompanied by physiological changes that culminate in a reduction of metabolic activity to a state of relative quiescence (Bewley, 1979; Kermode *et al.*, 1985). Most agricultural and horticultural crops with annual or biennial seed production belong to this category, and can survive years of storage under cold, dry conditions. On the other hand, recalcitrant seeds do not undergo a similar maturation-drying phase, are

shed in a hydrated condition and are killed by extreme desiccation and sub-zero temperatures (Roberts and King, 1980). Species producing recalcitrant seeds are common in, but not exclusive to, aquatic or moist environments in tropical and temperate climates (Roberts and King, 1980). A further behavioural category – constituted by seeds that are neither orthodox nor recalcitrant has been defined (intermediate types, e.g. Hong and Ellis [1996]). It is probable that the principles described in this thesis can be extended to this third category of seeds, although this will not be considered in the present work.

Recalcitrant seeds are metabolically active at shedding (Berjak *et al.*, 1992, 1993; Farrant *et al.*, 1992, 1993) and although this activity is seemingly lowest at that stage, germination-related events continue during storage (Berjak *et al.,* 1984; Pammenter *et al.*, 1984; Farrant *et al.*, 1985, 1992; Finch-Savage, 1992, 1993). The apparent absence of a clear developmental marker during recalcitrant seed ontogeny makes it extremely difficult to distinguish where seed maturation ends and germination begins (Berjak *et al.*, 1989; Farrant *et al.*, 1992, 1998). The occurrence of precocious germination of seeds in fruits while still attached to the parent plant in some seeds are those which usually undergo a developmentally-programmed period of maturation drying on the parent plant to water contents of 20% or less of the fresh mass, and which can be dried further to 5% without loss of viability (Roberts and King, 1980).

Initially, germination-associated events of recalcitrant seeds may occur in the absence of additional water (Berjak *et* al., 1984, 1989; Pammenter *et al.*, 1994; Farrant *et al.*, 1986, 1988) and seeds are capable of tolerating moderate water loss immediately after shedding (Berjak *et al.*, 1989). However, the seeds become increasingly dependent upon additional water becoming available with further development along the germination pathway (Pammenter *et al.*, 1984; Farrant *et al.*, 1985, 1986, 1988), and this coincides with the occurrence of cell division and increased vacuolation in meristematic cells (Farrant *et al.*, 1985, 1986). At this stage seeds become far more sensitive to water loss, although the degree of drying tolerated appears to be inversely related to the extent to which germination has proceeded (Farrant *et al.*, 1986). Berjak *et al.* (1984) suggested that the ultrastructural

changes that occurred during drying of recalcitrant seeds resemble those occurring during dehydration of imbibed, germinating orthodox seedlings rather than events observed during maturation drying, as described by e.g. Klein and Pollock (1968). Increased sensitivity to desiccation in germinating embryos of orthodox seeds coincides with an increase in the rate and spectrum of metabolic processes following imibibtion (Farrant *et al.*, 1988). This also coincides with the initiation of cell division and extensive vacuolation (Bewley, 1979) in a manner analogous to that observed post-harvest in recalcitrant seeds. The basis for recalcitrance has been suggested to be the apparent absence or inadequacies of mechanisms akin to those conferring stability to orthodox seeds during the maturation stage (Farrant *et al.*, 1988; Berjak *et* al., 1990; Vertucci and Farrant, 1995; Pammenter and Berjak, 1999), and this may arise due to the premature termination of development of recalcitrant seeds (Finch-Savage, 1992).

Recalcitrant seed tissues are sensitive to changes in water status. Water is required to sustain normal metabolic functions, which are likely to be compromised by increasing drying. Discrete changes in metabolic activity have been associated with the loss of water with particular calorimetric properties (e.g. 1990). Vertucci and Farrant (1995) have described the cellular processes that are affected by different levels of drying. Removing cellular water above 0.7 g H_2O g dry mass (g g^{-1}; corresponding to a water potential [Ψ] of *c.* –1.5 MPa; hydration level 5) concentrates the relatively dilute cytoplasm of fully hydrated cells, and results in growth and cell division being inhibited. Drying between 0.7 and 0.4 g g^{-1} (Ψ= > -3 MPa; hydration level 4) affects the pattern of protein synthesis, and many recalcitrant seed tissues tolerate this extent of drying, but for a limited period only (Walters *et al.*, 2001). Water in this hydration level is described as concentrated, or water that is associated with pores or capillaries. The altered nature of this type of water is denoted by its lower freezing point relative to dilute solution water (Franks, 1980). Metabolic activities are severely impaired with further drying to 0.45-0.25 g g^{-1} (Ψ= > -11MPa; hydration level 3), resulting in unregulated catabolism and the accumulation of harmful levels of free radicals (reviewed by Vertucci and Farrant,

1995; Pammenter and Berjak, 1999, Walters *et al.,* 2002). The lower level of this hydration range marks the limit of desiccation tolerance of recalcitrant seed tissues even in the short-term and, significantly, the beginning of the hydration range (0.25 - 0.08 g g^{-1}; Ψ= > -150 MPa; hydration level 2) where translational molecular motion is restricted by the viscous ('glassy') state of the cytoplasm (Vertucci 1989b, 1990; Williams and Leopold, 1989; Meryman and Williams, 1980; Leprince and Walters-Vertucci, 1995; Buitink *et al.,* 1996; Williams *et al.,* 1993). Orthodox seeds are damaged by drying below 0.08 g g^{-1} (Ψ= < -150 MPa; hydration level 1 water), albeit slowly.

Numerous factors make it difficult to identify with accuracy the lower limit of desiccation tolerance of recalcitrant seeds. The degree of water loss tolerated by recalcitrant seeds varies among species (Farrant *et* al., 1989; Hong and Ellis, 1990; Tompsett, 1987) and developmental status (Farrant *et* al., 1986, 1988, 1989; Hong and Ellis, 1990; Berjak *et* al., 1992, 1993; Finch-Savage, 1992; Tompsett and Pritchard, 1993). Germination behaviour can also vary in seeds at equivalent stages of maturity within the same growing season, and also between seasons (Pammenter and Berjak, 1999). Further complexity is added by the fact that the response to desiccation of different species is inextricably linked to a time component (Pammenter *et al.*, 1991, 1998; Pritchard, 1991; Finch-Savage *et al.*, 1993; Vertucci and Farrant, 1995; Walters *et al.,* 2001) that obscures the accurate description of water contents critical for survival (Pammenter *et al.*, 1998; Pammenter and Berjak, 1999).

It is equally hard to determine accurately those water contents that maximise the limited storage lifespan of recalcitrant seeds. Evidence indicates that increasing the drying rate allows lower water contents to be reached without injury, either because the time of exposure to conditions promoting uncontrolled metabolism are minimised (Pammenter *et* al., 1991, 1998; Pritchard, 1991; Berjak *et* al., 1993; Vertucci and Farrant, 1995; Walters *et al.,* 2001) or because seeds are prevented from progressing along the germination pathway (Farrant *et al.*, 1985, 1986, 1988, 1989). Conversely, seeds stored at high relative humidity survive longer in storage, but eventually lose

viability. In highly recalcitrant seeds the period in which this process occurs can be extremely short (e.g. 2 weeks for *Avicennia marina*, Farrant *et* al., 1985) and is often curtailed by the activity of the associated mycoflora (Calistru *et al.*, 2000), which highlights the need for the development of long-term conservation strategies.

Challenges of long-term storage

Long-term storage of seeds requires limiting metabolic reactions that cause ageing. This is done in the short term by reducing the water content and therefore increasing cytoplasmic viscosity to levels where glasses are formed (hydration level 2; [Vertucci and Farrant, 1995]), and in the long-term by additionally reducing the storage temperature. In genebanks, orthodox seeds are conventionally stored at water contents of *c.* 5 ±1% and at -18°C (e.g. Stanwood, 1985). The high cytoplasmic viscosity of cells in these seeds not only reduces the rate metabolic reactions, but precludes ice crystal damage during cooling to -18°C as well. In contrast, recalcitrant seeds cannot be stored under conventional conditions because they do not survive drying to such low water contents even in the short-term. While rapid drying of whole seeds allows lower water contents to be attained while still retaining viability (Farrant *et al.*, 1986; Berjak *et al.*, 1989, 1990; Pritchard, 1991; Kioko *et al.*, 1998; Pammenter *et al.,* 1998), even partially dehydrated seeds are susceptible to freezing damage during exposure to ≤ -18°C. This means that with few notable exceptions such as seeds of *Piper nigrum* (Chaudhury and Chandel, 1994), tea (Hu et al., 1993), neem (Berjak and Dumet, 1996) and some citrus varieties (Normah and Sitti Dewi Serimala, 1997) cooled to -196°C, low temperature storage of whole seeds of most recalcitrant species is presently unattainable. Protocols to preserve recalcitrant germplasm in the long-term must thus facilitate harmless drying to levels that preclude freezing damage during cooling to temperatures sufficiently low to halt all metabolic processes.

Embryonic axes as propagules

The physical constraints that limit the drying rate of whole seeds can be circumvented by using isolated embryonic axes. Embryonic axes are small structures, accounting in many cases for only 0.25% (Chin et al., 1989) - or less - of the dry mass of whole

seeds. Exposing excised embryonic axes to an air stream either by rapid (flash) drying (Berjak et al., 1989, 1990; see Chapter 3) or by the commonly-used laminar flow hood method (see Table 3 in Berjak et al., [1996]; Table1 in Chandel et al., [1996]) has facilitated drying of axes to water contents previously unattained with whole seeds yet with minimal loss of viability (Normah et al., 1986; Pritchard and Prendergast, 1986; Berjak et al., 1989; Pammenter et al., 1991 Pritchard, 1991; Pritchard and Manger, 1998). Significantly, the ability to dry embryonic axes of recalcitrant seeds to lower water contents without injury increases the likelihood of survival following cryogenic exposure, thus strengthening the potential of cryopreservation as a tool to achieve long-term storage.

Microculture

Advances in the field of biotechnology have led to significant progress in the ex situ conservation of recalcitrant germplasm. The development of growth media with substrates that replace nutrients provided by the storage tissues in intact seeds, as well as techniques suitable for aseptic culture, have facilitated in vitro germination of embryonic axes isolated from recalcitrant seeds (Chin et al., 1988). Furthermore, development of axes in vitro can be stimulated or retarded by manipulating growing conditions or the relative concentration of growth factors in the medium. For example, pre-growth media with high concentrations of sucrose or other osmotica have been shown to increase survival of somatic embryos following exposure to liquid nitrogen (Dumet et al., 1993, 1994). The presence of growth regulators such as gibberellic acid (GA_3) in the culture medium has been reported to enhance the recovery of cryopreserved axes (Abdelnour-Esquivel et al., 1992). The advantages afforded by biotechnology to plant conservation (reviewed by Engelmann, 1997) are beyond the scope of the present introduction. It suffices to say that by circumventing the need to work with whole seeds, in vitro technology has increased the likelihood of achieving long-term cryogenic storage of recalcitrant embryonic axes. This is already evident by the increasing number of successful studies since the inception of this approach (Grout et al., 1983; Normah et al., 1986; Pritchard and Prendergast, 1986; Chaudhury

et al., 1991; Vertucci et al., 1991; Wesley-Smith et al., 1992, 1995, 2001b; Chandel et al., 1995; Berjak *et al.*, 1999; Thammasiri, 1999; Chapters 4, 6, 8 and 9, this volume).

The benefits conferred by rapid drying

The mechanisms by which rapid drying allows lower water contents to be tolerated in recalcitrant material have not yet been fully elucidated, but evidence indicates that the duration of the benefit conferred is short (Pammenter *et al.*, 1998; Walters *et al.,* 2001; reviewed by Vertucci and Farrant, 1995; Walters *et al.,* 2002). This is presumed to be due to normal cell functions being disrupted at water contents intermediate between full hydration and the lower limit of survival, resulting in deleterious reactions due to unregulated metabolism (Berjak *et al.,* 1990; Pammenter *et al.,* 1991, 1998; Pritchard, 1991; Leprince and Hoekstra, 1998; Leprince *et al.,* 1999, 2000; Walters *et al.,* 2001; reviewed by Vertucci and Farrant, 1995; Berjak and Pammenter, 1997; Pammenter and Berjak, 1999; Walters *et al.,* 2002). Accordingly, reducing the time of exposure of axes to intermediate hydration levels is likely to minimise dehydration damage that accumulates during the short drying period. However, the beneficial effect of rapid drying is obscured by the fact that previous studies have compared slow drying of whole seeds with rapid drying of excised embryonic axes (Pritchard and Prendergast, 1986; Pammenter *et al.,* 1991; Berjak *et al.,* 1990, 1993; Pritchard *et al.*, 1995; Kioko *et al.*, 1998; Pritchard and Manger, 1998). Such comparisons introduce uncertainty regarding the contribution of the storage tissues towards the water status of the axis during drying. Therefore, the effects of drying rate upon survival of embryonic axes deserve attention (Wesley-Smith *et al.,* 2001a; Walters *et al.,* 2001; Chapter 3).

A window of optimal water content for cryopreservation

It is necessary to optimise the water content of axes prior to storage. Although smaller than seeds, isolated embryonic axes of recalcitrant seeds are nevertheless fully hydrated at shedding and must be pre-conditioned in order to withstand exposure to cryogenic temperatures (reviewed by Reed, 1996; Engelmann, 1997). Since fully hydrated cells freeze at *c.* -2°C, and ice crystal growth arrested at -80°C (Moor,

1973), these cells must traverse this critical temperature region extremely rapidly to prevent growth of ice to lethal sizes. In cells producing high levels of endogenous sugars (e.g. cortical cells of cold-acclimated mulberry; [Sakai and Otsuka, 1967]), or in those which undergo programmed maturation drying to low water contents, the span of this critical region is reduced, or even eliminated altogether (Moor, 1973; Robards and Sleytr, 1985; Vertucci, 1989a,b). This is because during drying the resulting increase in cytoplasmic viscosity reduces the intracellular mobility of water (Buitink *et al.,* 1998b, 2000), and thus the readiness with which ice crystals are formed during cryogenic cooling (Luyet *et al.,* 1962; Rall and Fahy, 1985; Rall, 1987).

Drying to low water contents reduces the availability of water and therefore the risk of lethal ice crystal damage within cells during exposure to freezing temperatures (Meryman and Williams, 1985). Many recalcitrant axes tolerate loss of water corresponding to hydration levels 5 and 4 (≥ 0.45 g g^{-1}; Vertucci and Farrant, 1995), but are damaged by attempts to dry axes below this lower level. Measurements using differential scanning calorimetry (DSC; see Chapter 4) and differential thermal analysis (DTA; e.g. Becwar *et al.,* 1983) show that at water contents above this level a large amount of intracellular water freezes, and that this is usually accompanied by a precipitous decrease in survival. Therefore, evidence suggests that a window of optimal hydration exists, which is limited by desiccation damage at the lower end and by lethal freezing damage at the other (Grout *et al.*, 1983; Normah *et* al., 1986; Pritchard and Prendergast, 1986; Vertucci *et al.,* 1991; Wesley-Smith *et al.*, 1992, 1995, 2001b; Vertucci *et al.,* 1994, 1995; Chapter 4). Protocols commonly used to cryopreserve recalcitrant embryonic axes rely on dehydrating axes to levels within this typically narrow window in order to minimise damage due to freezing or extreme drying (see Table 1.1, below).

Alternative procedures to minimise freezing damage

Alternative methods are also used to optimise the water content and thus hinder crystallisation. Two-step cooling is an alternative method of physically dehydrating cells prior to cooling to cryogenic temperatures (Sakai and Otsuka, 1967; Sakai *et al.*,

1968; Kasai *et al.*, 1980; Wood and Farrant, 1980; reviewed by Mazur, 1990). That procedure relies upon drying induced by extracellular freezing during a period of exposure to sub-zero temperatures. The duration of this period, and thus the extent of drying, is determined empirically, and must ensure the cytoplasm is sufficiently concentrated to withstand subsequent immersion in liquid nitrogen. In cold-acclimated plants, the intracellular concentration of solutes is increased naturally by endogenously-produced sugars or compounds that help prevent intracellular freezing either by supercooling (George *et al.*, 1982) or by forming aqueous glasses within cells (Hirsh *et al.*, 1985; reviewed by Bryant *et al.*, 2001). Permeating cryoprotectants (see Finkle *et al.*, 1985) or vitrification mixtures (Fahy *et al.*, 1984; Rall, 1987) also raise cytoplasmic concentrations and hinder ice crystal growth during cryogenic cooling, thus relaxing the need for very rapid cooling and very small samples (Moor, 1973).

Table 1.1. Maximum survival reported of cryopreserved embryonic axes dehydrated to various water contents

SPECIES	WATER CONTENT ($g\ g^{-1}$)	MAXIMUM SURVIVAL (%)	REFERENCE
Camellia sinensis	0.15 - 0.33	95	Chaudhury *et al.*, 1991
Poncirus trifoliata	0.12 - 0.19	68	Radhamani and Chandel, 1992
Citrus spp.	0.12 - 0.19	60-100	Normah and Serimala, 1997
Artocarpus heterophyllus	0.14 - 0.17	30	Chandel *et al.*, 1995
Hevea brasiliensis	0.16 - 0.25	69	Normah *et al.*, 1986
Aesculus hippocastanum	0.23 - 0.28	100% (shoots only)	Pence, 1992

Conventional cryopreservation procedures (reviewed by Engelmann, 1997) exploit these processes to reduce freezing damage in cryopreserved tissues. But while cryoprotectants either alone (de Boucaud *et al.*, 1991; Thammasiri, 1999) or combined with partial air-drying (Pence, 1991; Assy-Bah and Engelmann, 1992;

Dumet *et* al., 1993, 1994; Mycock *et al.*, 1995; Kioko *et al.*, 1998; Stewart *et al.*, 2000) have been used with varied success to minimise freezing damage in explants of recalcitrant species, their use has not proved widely successful in zygotic embryonic axes. The large diversity of cell types within axes, which presumably have very different intracellular properties (e.g. different membrane permeability), has been suggested as a probable explanation for this failure (Dumet *et* al., 1993; Berjak *et al.*, 1996; Withers and Engelmann, 1997). Additionally, cryoprotective solutions are most effective at concentrations sufficiently high to become cytotoxic (e.g. Plattner *et* al., 1972; Morris, 1976; Finkle *et al.*, 1985; Chmielarz, 1997; Berjak *et al.*, 1998). Attempts to reduce cryoprotectant cytotoxicity by permeating axes at sub-ambient temperatures prior to cooling can injure recalcitrant axes that are chilling-sensitive (Chin and Roberts, 1980; Morris *et al.*, 1983). Furthermore, optimal cryoprotectant treatments are usually determined empirically, and this time-consuming exercise for one species often has limited applicability to other species. Therefore, where success allows it, most of these methods are abandoned in favour of the simpler approach of reducing the water content of axes by drying in an air stream (e.g. Normah *et al.*, 1986; Pritchard and Prendergast, 1986; Pence, 1990, 1992, 1995; Wesley-Smith *et al.*, 1992, 1995, 2001a,b; Chapters 3, 4, 6, 8 and 10)

Optimising the water content of axes prior to cooling is one of many steps involved in most cryopreservation protocols, but evidence presented in this thesis strongly suggests that it is a strong determinant of the cooling conditions subsequently required to maintain viability.

Conventional cooling methods

Single cells

Conventionally, hydrated cells are usually cooled slowly (<1-10°C min^{-1}) in the presence of cryoprotectants using protocols that encourage extracellular freezing. Extracellular freezing induces a chemical potential dis-equilibrium relative to the supercooled cell interior. This becomes the driving force causing water to leave the cell to restore thermodynamic equilibrium as the temperature is gradually decreased.

As the conditions on either side of the cell membrane usually approach equilibrium, this cooling method is commonly referred as 'equilibrium freezing' (reviewed by Mazur, 1990). The cytoplasm of these cells becomes increasingly concentrated and, at empirically determined optima, cells may be exposed to cryogenic temperature without injury. However, cells that fail to achieve the necessary intracellular concentration and supercool more than *c.* 2°C are likely to endure lethal intracellular freezing if the temperature is suddenly decreased further (reviewed by Mazur, 1990).

Embryonic axes

A protocol commonly used to cryopreserve isolated embryonic axes of desiccation-sensitive (recalcitrant) seeds involves partial drying, enclosure in polypropylene cryovials and immersion in liquid nitrogen (e.g. Pritchard and Prendergast, 1986; Pence, 1990, 1992, 1995; Chaudhury *et al.,* 1991; de Boucaud *et al.,* 1991; Abdelnour-Esquivel *et al.,* 1992; Chandel *et al.,* 1995; Pritchard *et al.,* 1995). Cooling rates attained by this procedure approximate to 3°C s^{-1} (Vertucci, 1989b), and it is critical that embryonic axes from recalcitrant seeds be dried below 0.4 - 0.3 g g^{-1} in order to prevent freezing damage during cooling ([Table 1.1]; Becwar *et al.,* 1983; Pritchard and Prendergast, 1986; Vertucci 1989a, b; Pence, 1990, 1992, 1995; Chaudhury *et al.,* 1991; de Boucaud *et al.,* 1991; Vertucci *et al.,* 1991; Abdelnour-Esquivel *et al.,* 1992; Chandel *et al.,* 1995; Pritchard *et al.,* 1995). The low water contents required to avoid freezing damage could be likened to those attained during slow freezing as described above (e.g. Sakai *et al.*, 1968; reviewed by Mazur, 1990). The unavailability of water for freezing below 0.4 - 0.3 g g^{-1} is supported by the absence of freezing or melting transitions in DSC thermograms of mature axes from several species at those water contents (Vertucci, 1989a,b, 1990; Pammenter *et al.,* 1991; Vertucci *et al.,* 1991; Berjak *et al.,* 1992; Wesley-Smith *et al.,* 1992; Farrant and Walters, 1995; Pritchard *et al.,* 1995; Pritchard and Manger, 1998).

Drawbacks of conventional approaches – Embryonic axes

Survival of cryopreserved axes in many of those studies occurred not only at very low water contents, but within a very narrow range as well (Table 1.1). Furthermore, it is

often unclear whether 'survival' reported describes axes that enlarge and display normal development of roots and shoots, or partial development of either root, shoot or disorganised callus growth. It is contended that the need for such severe drying inherent to conventional cooling methods poses several problems. Firstly, survival of only a small percentage of the initial sample of axes begs the question regarding possible genetic shifts if embryos with a particular genotype were to be selectively eliminated or retained during this procedure. This event would seriously challenge the goal of cryopreserving axes as a means of conserving genetic diversity. Secondly, abnormalities such as disorganised callus growth and loss of shoot or root function at low water content have been reported *even in the absence of cooling* (e.g. Pence, 1992). The ability of such abnormal embryos to regenerate into normal, healthy plants is uncertain. Lastly, even when axes survive drying to low water contents at ambient temperature, severe damage can nevertheless occur when they are exposed to the combined stress of low water content and cryogenic temperatures (Vertucci, 1989a; Vertucci and Roos, 1993; Vertucci *et al.,* 1994, 1995; Berjak *et al.,* 1999). While cooling axes at higher water contents ameliorates this type of damage, it also increases the likelihood of lethal intracellular freezing. Collectively, evidence suggests that the extent of drying required by conventional protocols prior to cooling is detrimental, and that cooling methods that allow axes to be cryopreserved at higher water contents without injury would be highly desirable.

An alternative approach - Rapid (non-equilibrium) cooling

Luyet and co-workers (e.g. Luyet and Gonzales, 1951; Luyet 1960, 1965,1970; Luyet *et al.,* 1962) pioneered the use of rapid cooling rates as an alternative method to retain structure and function of cryopreserved cells. Cooling cells at velocities that exceed equilibrium rates almost invariably leads to supercooling and intracellular freezing, which is usually regarded as being lethal (Mazur, 1966). According to the rapid cooling approach, less than maximum amount of ice is formed within dilute solutions if the solution is prevented from reaching thermodynamic equilibrium within the temperature range where ice crystal growth is possible during cooling and warming (Luyet, 1960, 1965; MacKenzie, 1977; Roos and Karel, 1991). This

approach has facilitated the preservation of erythrocytes (Fujikawa, 1981) yeast cells (Moor and Mühlethaler, 1963; Anderson *et al.,* 1966; Mazur and Schmidt, 1968; MacKenzie, 1970; Bank, 1973; Nei, 1977), 20-30 μm sections of cortical parenchyma of cold-acclimated mulberry (Sakai, 1966, 1970; Sakai and Otsuka, 1967; Sakai *et al.,* 1968), ascites tumour cells (Asahina *et al.,* 1967, 1970), and after permeation with vitrification solutions, protoplasts of plant cells (Langis and Steponkus, 1990), mouse embryos (Rall and Fahy, 1985; Rall, 1987) and *Drosophila* embryos (Steponkus *et al.,* 1990; Mazur *et al.,* 1993). However, avoiding equilibrium and restricting the growth of lethal ice crystals demands stringent cooling and warming conditions. The necessarily high cooling rates required to prevent lethal freezing (particularly where no cryoprotectants were used) were facilitated in those studies by favourable surface to volume ratio of single cells, and by the efficient dissipation of heat while during cooling. Favourable surface area to volume ratios increase heat transfer during convective cooling, especially when specimens do not exceed 0.1 mm linear dimensions (Bailey and Zasadzinski, 1991).

Attempts to cool hydrated specimens larger than this usually results in slower cooling and increasing amounts of ice formed, as observed microscopically in model specimens (e.g. Meryman, 1960; Van Venrooij *et al.,* 1975) or survival studies (e.g. Mohr and Stein, 1969). Rapid cooling in large biological specimens is hampered by the relatively inefficient conduction of heat through many cell layers (Meryman, 1957, 1960), by the increasing heat capacity of supercooled water prior to freezing (MacKenzie, 1977; Franks, 1980) and by the release of latent heat of fusion when this occurs (Meryman, 1956, 1966; Bald, 1987). Therefore, in order to avoid freezing damage within biological tissues during non-equilibrium cooling the heat capacity of the sample needs to be reduced by reducing the amount of material, increasing the surface area to volume ratio, and maximising the rate of heat exchange (Elder *et al.*, 1982; Gilkey and Staehelin, 1986; Ryan, 1992; Bachmann and Mayer, 1987; Bald, 1987; Bailey and Zasadzinsky, 1991).

Overcoming physical constraints imposed by axes

It is not possible to manipulate the surface area to volume ratio of embryonic axes, because complex cell and tissue structure dictate particular geometries that cannot be altered. Similarly, the heat capacity cannot be lowered by reducing the size of the sample if intact axes are to be cryopreserved. However, since water holds the largest reserve of heat within cells (Bachmann and Mayer, 1987) it was presently hypothesised that partial drying could reduce the heat capacity of axes sufficiently to compensate for the necessary disadvantage of their size. If this were possible, the next step would be to determine the minimum cooling rate required to prevent freezing damage and facilitate survival in axes at various water contents. This question was addressed (Chapter 4) and provided the basis for the rapid cooling approach adopted in the remaining studies reported in this thesis. This approach examined the complex interaction between heat transfer, cooling and warming rates and viscosity required to reduce freezing damage sufficiently to facilitate normal development of axes *in vitro*.

Developing a cryopreservation model

Water content influences cytoplasmic viscosity and, therefore, the mobility of water within cells (Vertucci and Roos, 1990; Williams *et al.*, 1993; Buitink *et al.*, 1998b, 2000; Leprince and Hoekstra, 1998; Leprince *et al.*, 1999). When axes are exposed to rapid (non-equilibrium) cooling, the mobility of water and the cooling rate required to prevent the formation of lethal ice crystals are closely related (Luyet *et al.*, 1962; Rall and Fahy, 1985; Rall, 1987). Evidence suggests that the intracellular viscosity attained by drying to *c.* 0.25 g g^{-1} (Ψ= -12 MPa) is sufficient to limit ice formation during relatively slow cooling, making survival of axes independent of cooling rate (Vertucci, 1989a,b). It was hypothesised that since water molecules acquire greater mobility with increasing hydration, axes would require increasingly faster cooling if the growth of ice crystals to lethal sizes is to be avoided. A threshold is likely to exist, determined by the difficulty of dissipating the greater heat load of hydrated specimens sufficiently rapidly before freezing damage occurs. The water content characterising this limit is presumably determined by the properties of axes, such as specific heat,

dry mass and geometry, and by the conditions at the interface between the axes and the coolant (Meryman, 1956, 1966; Stephenson, 1956; Luyet, 1960; Mazur, 1966; Bachmann and Mayer, 1987; Bald, 1987; Ryan, 1992). It is also highly possible that differences in the degree of vacuolation, or type and abundance of storage reserves, could also influence the cooling rate required to avoid freezing damage. This thesis explores the responses of axes from seeds of various species cooled under conditions that yielded various cooling rates. A basic premise was that successful cryopreservation protocols would strike a balance between intracellular viscosity, achieved by manipulating water content, and the minimum cooling rate required to avoid damage during non-equilibrium cooling.

Aim of this thesis

Evidence suggests that conventional approaches are inadequate to cryopreserve zygotic embryonic axes of desiccation-sensitive species, especially those that lose viability when dried to water contents that can also promote lethal freezing. The purpose of this thesis is to develop a robust procedure to cryopreserve embryonic axes of recalcitrant seeds. The investigations presently reported did not endeavour to establish cryopreservation protocols 'fine-tuned' for particular recalcitrant species. Instead the present thesis explores fundamental biophysical, physiological and ultrastructural phenomena underlying success or failure of axes to survive cryogenic exposure.

The present thesis investigates the hypothesis that rapid cooling enhances cryopreservation and extends the range of permissible water content. This hypothesis is based on the finding that nucleation of ice and subsequent crystal growth occur at a rate that is dependent on the extent of supercooling, the sample temperature, and on the mobility of water at that temperature (Luyet *et al.,* 1962; MacKenzie, 1977; Franks, 1980). To prevent large ice crystals from forming, specimens must be cooled to temperatures that do not support crystallization faster than ice can grow (Meryman, 1956, 1966; Stephenson, 1956; Luyet, 1965; Mazur, 1966). Thus, survival of axes depends on whether the rate of traversal of the critical temperature zone for freezing

transitions exceeds the rate at which ice is formed. It is expected that studying the physiological response of axes to rapid cooling will ultimately lead to the development of a reliable alternative to conventional approaches to cryopreservation.

The work presented encompasses results obtained using embryonic axes from different recalcitrant species. While focussing on the same species may have facilitated a more in-depth study of the response of axes to rapid cooling, this was not possible because of the limited seasonal availability and restricted life in storage of recalcitrant seeds. Conversely, it could be argued that the diverse requirements that characteristically arise from working with axes from different species tests the broad applicability of this approach. Furthermore, observations made on one species were frequently confirmed during subsequent studies using others. This increases confidence in generalising from the present finding on the conditions required for favourable cryopreservation, to axes of other temperate - and probably many tropical - recalcitrant species.

Thesis outline

The studies undertaken are presented in a sequence which follows developments that took place during the course of the experimental phase of this thesis. The rationale behind each study, and an outline of each chapter, are described briefly below.

Lowering the water content is an important step in most cryopreservation protocols, as it increases the likelihood of survival following cryogenic exposure (e.g. Sakai *et al.*, 1968; Meryman and Williams, 1983). Transmission electron microscopy has provided valuable insights into the structure of cells in the dehydrated state. However, many of those studies relied on aqueous fixation protocols to prepare dehydrated specimens for ultrastructural analysis, introducing uncertainty regarding the extent of rehydration that occurred during processing. **Chapter 2** compared the ultrastructure of tissues from desiccation-sensitive and desiccation-tolerant tissues processed for microscopy using either an aqueous-based protocol, or anhydrously by freeze-

substitution. Freeze-substitution precluded rehydration artefacts, facilitating reliable ultrastructural assessment of cells in the dehydrated state. Freeze-substitution was used subsequently to assess reliably the ultrastructure of partially hydrated axes in a study that investigated the effects of drying rate upon the survival of embryonic axes of jackfruit (*Artocarpus heterophyllus* Lamk. [Moraceae]; **Chapter 3**). Drying is required to optimise the water content of axes for cryogenic exposure, and that study examined survival, electrolyte leakage and ultrastructural characteristics of axes dried either slowly (2 - 3 days) or rapidly (≤ 90 min) to various water contents. Results confirmed the beneficial effects of rapid drying, as observed previously using whole seeds (Farrant *et al.*, 1986; Berjak *et al.*, 1989, 1990; Pritchard, 1991; Kioko *et al.*, 1998; Pammenter *et al.,* 1998). Furthermore, it also provided insights into ultrastructural changes and probable causes underlying cellular damage that occur during a drying/rehydration cycle. Based on results obtained, rapid (flash) drying became the method of choice for cryopreservation studies.

Having established how to optimise the water content without injury, a subsequent study investigated the effects of cooling rate upon survival of embryonic axes of recalcitrant *Camellia sinensis* (L.) O. Kuntze (Theaceae; tea) seeds dried to various water contents (**Chapter 4**). Results from that study indicated that by increasing the cooling rate from 10°C min^{-1} to that attained by plunging naked axes forcibly into sub-cooled nitrogen the upper limit of water content facilitating survival *in vitro* was correspondingly increased from *c.* 0.4 to 1.1 – 1.6 g g^{-1}. Among other significant findings, results from that study supported the contention that rapid cooling can restrict the growth of intracellular ice within levels, thus allowing axes at higher water content to survive cryogenic exposure.

It became desirable to investigate further the relationship between cooling rate and survival of axes at various water contents. Achieving this goal required quantifying reproducibly the cooling rates achieved by various methods tested in order to allow reliable comparisons among treatments as well as among species. The plunging device required to achieve rapid cooling, and instruments required to measure the cooling rates attained, are described in **Chapter 5**. Additionally, that chapter also

outlines the procedure followed for cryopreserving axes, as well as highlighting how rapid cooling is limited by size and water content in tissues with similar properties to those encountered in survival studies.

The effectiveness of the plunging device to cryopreserve relatively large axes was assessed in **Chapter 6** using embryonic axes of horse chestnut (*Aesculus hippocastanum* L.; [Hippocastanaceae]. Survival and leakage data showed that in spite of its large size (*c.* 6 mg dry mass), complete survival and normal development were attained at higher water contents than attained previously using slower methods (Pence, 1992). That study emphasised that water content and cooling rate are closely related during non-equilibrium cooling. Thus, it was unclear whether survival of horse chestnut axes increased at lower water contents because of the increase in cooling rates measured, or because of the higher cytoplasmic viscosity that resulted from drying. That uncertainty was addressed in **Chapter 7** using axes of the trifoliate orange (*Poncirus trifoliata* [L.] RAF.; [Rutaceae]). These axes are far smaller (*c.* 0.4 mg dry mass) than those of *A. hippocastanum*, and could therefore be cooled at rates ranging between 0.1 and >1 300°C s^{-1} by various methods. Additionally, that study investigated the effects of warming rate upon survival of axes cooled at different rates and water contents. While results from this study largely supported the findings from previous chapters, two apparent contradictions emerged. Firstly, normal development of partially hydrated axes cooled above *c.* 1 000°C s^{-1} decreased beyond an apparent optimum attained at lower rates. Secondly, survival of fully hydrated axes was higher when cooled at conditions that encouraged - rather than restricted - the growth of intracellular ice crystals, thus contradicting the accepted view that similar conditions are usually lethal (Mazur and Schmidt, 1968; Sakai, 1968, 1970; Mazur *et al.,* 1969; Asahina *et al.,* 1970; Bank and Mazur, 1973; Bank, 1974; Fujikawa, 1988; Vertucci, 1989a,b; Wesley-Smith *et al.,* 1992; Vertucci *et al.,* 1995).

The last cryopreservation study presently reported explored survival characteristics of embryonic axes of silver maple (*Acer saccharinum* L. [Aceraceae]) at three water contents, following cooling and warming at three different rates each (**Chapter 8**). In

particular, that study explored whether or not the seemingly incongruous survival of slowly cooled, fully hydrated axes of *P. trifoliata* also occurred in axes of silver maple cooled under similar conditions. Freezing patterns formed within fully hydrated axes cooled by the methods tested were assessed using freeze-fracture and freeze-substitution, and related to the survival *in vitro* of axes treated similarly. It was also desirable to characterise the physiological response of axes to freezing stress at the cellular, tissue and organ levels. Recovery of axes warmed rapidly after cooling at either 97°C s^{-1} or 3.3°C s^{-1} was monitored at intervals ranging from minutes to 3 days using light and transmission electron microscopy, and related to the ultrastructural appearance of similar axes in the solidified state.

Results from the studies reported are discussed critically in **Chapter 9**.

The term 'rapid cooling' is used in preference to 'ultra-rapid cooling' throughout this thesis to distinguish the cooling rates presently attained from faster ones required to cryofix hydrated specimens for electron microcopy (see Gilkey and Staehelin, 1986). Likewise, the term rapid cooling is used in preference to freezing, highlighting the fact that the former approach seeks to *avoid* crystallisation, unlike conventional methods that *rely* on extracellular freezing to prevent damage.

CHAPTER 2*

Anhydrous processing of dehydrated plant tissues using freeze-substitution

* Also published as Wesley-Smith J (2001) Freeze-substitution of dehydrated plant tissues: artefacts of aqueous fixation revisited. *Protoplasma* **218**: 154-167

Introduction

Mature seeds, pollen and, in a few cases, vegetative tissues of a variety of plants can withstand exposure to extreme desiccation for different periods. In contrast, many others exhibit varying degrees of sensitivity to water loss and die following exposure to severe dehydration. Ultrastructural studies have contributed significantly towards increasing current understanding of the processes underlying the acquisition, or lack, of desiccation tolerance. However, many of those investigations have relied on the use of aqueous-based preparative protocols, which introduces uncertainty about the extent of rehydration that occurs during tissue processing. Rehydration of plant cells in the dry state can occur in a matter of seconds or minutes following immersion in aqueous media (Swift and Buttrose, 1972; Buttrose, 1973; Tiwari *et al.,* 1990). Straightening of otherwise convoluted cell walls, discontinuity of the plasmalemma, and rounding of organelles showing diffuse membranes have been reported to occur during aqueous fixation (Swift and Buttrose, 1972; Buttrose, 1973; Webb and Arnott, 1982; Vigil *et al.,* 1984; Öpik, 1985). Thus, use of aqueous-based fixatives is unlikely to give an accurate impression of cells and tissues as they occur in the dehydrated state.

Attempts to circumvent rehydration artefacts during processing of plant tissues have been made by truly anhydrous chemical processing methods using osmium vapour fixation (Perner, 1965; Hallam, 1976; Öpik, 1980, 1985; Smith, 1991) or aldehyde-based fixatives in anhydrous di-methyl sulfoxide or glycerol (Hallam, 1976; Hallam and Gaff 1978; Smith, 1991). In other studies rehydration was

avoided initially by using anhydrous primary fixation, but introduced later by exposure to aqueous media during subsequent processing (Thomson, 1979; Altus and Hallam, 1980; Fincher Chabot and Leopold, 1982; Yatsu, 1983; Vigil *et al.,* 1984, 1985). Since the advent of cryotechniques (reviewed by Robards, 1974; Robards and Sleytr, 1985; Gilkey and Staehelin, 1986; Echlin 1992), ultra-rapid cooling of partially hydrated specimens in combination with freeze-fracture (Swift and Buttrose, 1972; Buttrose, 1973; Fincher Chabot and Leopold, 1982; Vigil *et al.,* 1984, 1985; Platt *et al.,* 1994) and freeze-drying (Lott, 1974) have also been successfully used to prevent rehydration artefacts. Although these protocols yield a relatively more accurate representation of cells in the dry state than does conventional (aqueous) fixation, each technique has inherent limitations. Anhydrous chemical fixation using osmium vapour, which is undesirably prolonged (from 4 weeks [Hallam, 1976] to 11 months [Öpik, 1980]), can result in cytoplasmic shrinkage (Perner, 1965), coalescence of oil bodies, reduced staining of organelles (Öpik, 1980), limited perfusion and poor sectioning quality (Yatsu, 1983; Smith, 1991). Similarly, use of aldehydes in glycerol or DMSO can result in poor definition of organelles and plasmalemma abnormalities (Thomson, 1979; Smith, 1991) as well as straightening of cell walls (Hallam, 1976; Hallam and Luff, 1980). While freeze-fracture is regarded as giving the most reliable ultrastructural preservation (e.g. Buttrose, 1973; Swift and Buttrose, 1972; Vigil *et al.,* 1984), highly dehydrated tissues can cleave in unpredictable and irregular planes (Fincher Chabot and Leopold, 1982; Vigil *et al.,* 1985) and establishing the original location of cells in the sample can be hindered by extensive fragmentation of replicas during cleaning (Fincher Chabot and Leopold 1982; Platt *et al.,* 1994).

Freeze-substitution and resin embedding for TEM is an alternative low-temperature preparative technique that combines the advantages afforded by cryofixation with the convenience of room temperature sectioning (Steinbrecht and Müller, 1987; Parthasarathy, 1995). It involves the replacement of solidified water in the sample by an anhydrous solvent at temperatures precluding ice crystal growth. Following optimal cryofixation, freeze-substitution can overcome

most shortcomings of other anhydrous protocols, facilitating superior morphological preservation of hydrated plant tissues (Browning and Gunning, 1977; Mersey and McCully, 1978; McCully and Canny, 1985; Lancelle *et al.,* 1986; Kiss *et al.,* 1990; Lancelle and Hepler, 1992; Kellenberger, 1991; Davidson and Newcomb, 2000).

The relevance of freeze-substitution to the study of desiccation was highlighted by studies on pollen (Tiwari *et al.,* 1990) and the resurrection plant, *Selaginella lepidophylla* (Hook and Grev; [Platt *et al.,* 1997; Thomson and Platt, 1997]). Advances in the field of cryofixation (reviewed by Sitte, 1996), and refinements to freeze-substitution protocols (e.g. Steinbrecht and Müller, 1987; Ding *et al.,* 1991; Parthasarathy, 1995) make it possible to re-assess critically rehydration artefacts that occur during preparation of dehydrated tissues for microscopy. The present phase of the investigation evaluated the ultrastructural preservation of dehydrated plant specimens using cryofixation and freeze-substitution, and compared it with that attained following aqueous two-step glutaraldehyde–osmium tetroxide fixation. Embryonic or mature vegetative tissues from three species were chosen for their developmentally diverse characteristics at the cellular level and relevance to the study of desiccation. Seeds of desiccation-tolerant (orthodox) species undergo a genetically programmed phase of drying to equilibrium with ambient relative humidity, during which metabolic activity is reduced to quiescence (Bewley, 1979; Kermode and Bewley, 1985). Radicles from embryonic axes of air-dried pea (*Pisum sativum* L.; [Fabaceae]) seeds were selected to illustrate the situation of cells of orthodox seeds following maturation drying. In contrast, desiccation-sensitive (recalcitrant) seeds do not undergo a similar drying phase, and are shed at high water content as metabolically active propagules. Radicles excised from embryonic axes of *Artocarpus heterophyllus* Lamk. (jackfruit), dehydrated to a non-lethal 20% of their water content at shedding, represent the condition of desiccation-sensitive cells during dehydration stress. Finally, inner leaves of the resurrection plant, *Eragrostis nindensis* (Ficalho & Hiern; [Poaceae]) tolerate extreme desiccation (Vander Willigen *et al.,* 2001) and illustrate the third category. Unlike meristematic tissues

in embryonic axes, the vegetative cells of the mature leaves are fully differentiated and adjust their metabolism to withstand water stress.

The present investigation assessed the extent of rehydration that occurs in dehydrated plant tissues during aqueous fixation for microscopy and compared it to the preservation attained following freeze-substitution. In addition to the morphological appearance at the light and electron microscopical levels, the area of cells resulting from each processing protocol was measured using image analysis software and contrasted.

Materials and Methods

Collection and preparation of plant material for fixation

Pea seeds (*Pisum sativum* L. cv. Greenfeast) were obtained commercially and maintained at the initial water content of 0.08 g H_2O g^{-1} dry mass (g g^{-1}). The embryonic radicles from these seeds were excised, and either immersed in aqueous fixative or further sliced into 1-2 mm transverse sections and immediately cryofixed as described below. In order to assess the structural changes that take place during imbibition, pea radicles were immersed in distilled water for 2 h prior to conventional fixation.

Hydrated specimens were partially dried using different methods. Axes of desiccation sensitive *Artocarpus heterophyllus* Lamk. (jackfruit) seeds were dehydrated from an initial water content of 3.5 to 0.7 g g^{-1}. Drying was achieved over two days by placing the excised axes on a nylon mesh suspended inside a closed chamber containing a saturated salt solution of KH_2PO_4 that yielded a relative humidity of 96% at 25°C (Winston and Bates, 1960). Following drying, radicles were excised and either immersed in aqueous fixative or sliced into 1-2 mm transverse sections and cryofixed immediately. Dried axes were also placed in distilled water and allowed to rehydrate at 20°C for 30 min before fixing and processing conventionally for microscopical analysis. The resurrection plant, *E. nindensis*, was grown under greenhouse conditions in Cape Town, South Africa.

Drying was effected *in planta* by withholding watering and allowing the plants to air-dry over 14 d. Transverse sections (1-2 mm thickness) were cut from an area 50 mm above the base of innermost leaves. The water content at the time of sampling ranged between 0.02 and 0.05 g g^{-1}. These sections were fixed either conventionally or by cryofixation. Sections were also immersed in distilled water for 30 min prior to conventional fixation, which allowed the structure of rehydrated cells to be assessed microscopically. For material from all three species, segments from three replicates per treatment were randomly selected for microscopy and analysis of cell area.

Water contents were determined gravimetrically following drying to constant mass in an oven at 80°C for 16 h. Values are expressed on a g H_2O g^{-1} dry matter (g g^{-1}).

Conventional processing protocol

Excised hypocotyls of axes of pea and jackfruit, and inner leaf segments of *E. nindensis* were immersed with agitation in a solution of 2.5% (v/v) glutaraldehyde in 0.1M Sørensen phosphate buffer (pH 7.2) for 2 h at room temperature. Although longer primary fixation at 4°C has been suggested to increase preservation of plant cell structure (Dong *et al.,* 1994), the aqueous fixation protocol used in this study is typical of that commonly used in desiccation studies (e.g. Webster and Leopold, 1977; Sack *et al.,* 1988; Quartacci *et al.,* 1997). Following primary fixation and buffer rinsing, specimens were post-fixed in 0.5% (w/v) osmium tetroxide for 1 h, rinsed with buffer, dehydrated in a graded acetone series, gradually infiltrated with low viscosity epoxy resin (Spurr, 1969) for 16 h and finally polymerised at 70°C for 10 h.

Cryofixation and substitution

Transverse sections of hypocotyls from embryonic axes and leaves were mounted edgeways on ultramicrotomy specimen supports (Leica, Austria) using a very small amount of low temperature adhesive (Tissue-Tek, Miles Scientific, USA). A Leica CPC cryofixation instrument (Leica, Austria) was used to plunge

specimens rapidly into liquid propane at 83 K (-190°C) immediately after mounting. Cooled specimens were placed in handling devices made using Beem™ embedding capsules (Catalogue No. G360, Agar Scientific, UK) where 5 mm holes made in the base and lid were sealed by heat-fusing fine stainless-steel mesh across these openings. Short segments of wire attached to the handling devices facilitated transfer of cooled specimens to the freeze-substitution medium pre-cooled to 193 K (-80°C) without warming. A protocol modified from Ding *et al.* (1991) was used, and consisted of specimen immersion in 0.1% (w/v) tannic acid in acetone at 193 K (-80°C) for 1 d followed by 3 d in a medium containing 2% (v/v) anhydrous glutaraldehyde in methanol (Electron Microscopy Sciences, Fort Washington, PA, USA), 2% (w/v) osmium tetroxide and 2% (w/v) uranyl acetate in acetone[1] at the same temperature. Subsequently, specimens were warmed in a stepwise manner (-60°C for 18 h, -40°C for 12 h, -20°C for 12 h and 0°C for 6 h) using a temperature-controlled substitution chamber (Reid and Associates, South Africa) placed inside a 193 K (-80°C) deep freezer. Specimens were subsequently rinsed twice in acetone, infiltrated with increasing concentrations of low viscosity epoxy resin (Spurr 1966) in acetone (1:3, 1:1, 3:1, 1:0) for 8-12 h at each stage and heat polymerised. The longer pot-life, lower viscosity formulation of the low viscosity resin first described by Spurr (1969) was used to enhance the permeation of freeze-substituted specimens during the prolonged infiltration times used. Polymerised specimens were sectioned using an Ultracut E (Leica, Austria) ultramicrotome. Semi-thin (1 μm) sections were stained with toluidine blue prior to viewing. Ultra-thin sections for transmission electron microscopy showing copper/gold interference colours were collected on 600 mesh copper grids that provided increased support during subsequent handling. Sections were contrasted for electron microscopy using a standard double-staining procedure.

[1] This medium contained a final concentration of 20% methanol introduced by the anhydrous glutaraldehyde solution.

Microscopy, image recording and analysis

Semi-thin sections were viewed using a Nikon Biophot (Nikon, Japan) transmitted light microscope. Ultra-thin sections were viewed using a JEOL JEM 1010 transmission electron microscope (JEOL, Japan) at 100 kV. Images from both instruments were recorded photographically and digitally. Measurements were performed on digitised images using Zeiss KS100 image analysis software (Carl Zeiss Vision, GmbH, Germany) following calibration to the appropriate magnification. In radicles of pea and jackfruit, cell areas were determined along four transects through the outermost 15-20 layers in transverse sections from each of three replicates. Leaves of *E. nindensis* prepared by either freeze-substitution or aqueous fixation were sectioned transversely, and the areas within the cell wall of mesophyll cells were also measured and contrasted.

Measurement of cell area is described by a single mean value in specimens where the plasmalemma remained adpressed against the cell wall. Alternatively, separate values are reported for either the area enclosed by the cell wall or that enclosed by the plasmalemma where separation between these structures had taken place. For greater clarity, results from light and electron microscopical observations are presented separately below.

Results

Light microscopy

Desiccation-tolerant tissues: pea

The protoplasm of cells from freeze-substituted pea hypocotyls appeared dense and tightly enclosed by moderately folded cell walls (Fig. 2.1 a). Measurements taken between the epidermis and the pericycle in transverse sections (comprising *c.* 20 cell layers) showed that the average area enclosed within the cell wall was 203 μm^2 (Table 2.1).

Table 2.1. Measurement of cell area (± standard deviation) in transverse sections of pea radicles following fixation.

	BOUNDARY[a]	AREA ±SD (μm^2)	% INCREASE IN CELL AREA [b]	DIFFERENCE IN ABSOLUTE CELL AREA [c]
Freeze-substitution	PL = CW	203 ±47	-	a
Aqueous fixation – dry	PL	350 ±92	41	b
	CW	463 ±106	55	c
Aqueous fixation - imbibed	PL = CW	492 ±131	55	c

[a] Only one value of cell area is given where contact between the plasmalemma and cell wall was maintained (PL=CW), or separately for area within the plasmalemma (PL) or within the cell wall (CW) where loss of contact was noted.

[b] Values represent percentage of the mean area occupied by corresponding freeze-substituted cells.

[c] Treatments with the same letter are not significantly different as established by one-way analysis of variance (LSD, P <0.05) and multiple range test (LSD).

Following conventional fixation, cells had a rounder appearance and instances where the cell wall and the plasmalemma had separated could be seen in several layers below the epidermis (Fig. 2.1 b). The area enclosed by the plasmalemma was 41% greater than that in freeze-substituted specimens (Table 2.1). One-way analysis of variance and multiple range tests showed that this difference was significant (P <0.05). In cells where separation from the plasmalemma had occurred, the area enclosed by the cell wall increased by a further 14% (Table 2.1), which was identical to that from axes imbibed for 2 h prior to aqueous fixation (Fig. 2.1 c; Table 2.1; P >0.05). Thus, equivalent rehydration of cell walls had occurred during the course of aqueous fixation and during imbibition. In contrast, plasmalemma and cell walls maintained close contact if radicles were imbibed prior to conventional fixation (Fig. 2.1 c). This indicated that both boundaries had expanded simultaneously and to the same extent during imbibition, and that their close apposition was unaffected by aqueous fixation.

Desiccation-sensitive axes: jackfruit

Cells of cortical tissues dehydrated to 0.7 g g^{-1} and processed by freeze-substitution appeared tightly packed and bound by moderately folded cell walls. The cytoplasm of these cells had a dense, compacted appearance, and vacuoles were prominent and irregularly shaped (Fig. 2.2 a). Conventional fixation of axes at similar water content resulted in relatively rounded contours of cells and vacuoles, as well as the appearance of spaces between the plasmalemma and cell walls of corresponding cortical cells (Fig. 2.2 b). The average area within the cell wall of the outermost 15 layers in transverse sections of aqueously fixed axes was 389 ±127 μm, which represented an increase of *c.* 25 % over the average 294 ±88 μm from corresponding freeze-substituted specimens. Student's T-test showed this increase to be significant (P <0.05). Cortical cells from axes rehydrated for 30 min prior to aqueous fixation showed plasmalemma closely appressed to the cell wall (Fig. 2.2 c)

Resurrection plants: *E. nindensis*

The highly folded appearance of the walls of mesophyll cells from air-dried *E. nindensis* leaves was evident after freeze-substitution even at the light microscope level (Fig. 2.3 a). Mesophyll cells stained intensely relative to their aqueously fixed counterparts (Fig. 2.3 b and c). Aqueous fixation of dehydrated leaves resulted in notable expansion of cell walls in these cells (Fig. 2.3 b), and reduced the curled appearance characteristic of *E. nindensis* leaves in the dry state (Vander Willigen *et al.*, 2001). Immersing leaves in distilled water for 30 min prior to conventional fixation had a similar effect, and very frequently resulted in mesophyll cells showing disrupted cell walls (Fig. 2.3 c; Vander Willigen *et al.*, 2001). This type of damage was not observed in FS specimens, suggesting that it had not been caused mechanically during cutting. Accurate measurement of cell areas within mesophyll cells was difficult due to the highly convoluted character of cell walls, especially after freeze-substitution. The average area within the cell wall of freeze-substituted mesophyll cells was 53 ±20 μm^2, and increased significantly (P <0.001; [Student's t-test]) by approximately 30% to 76 ±20 μm^2 after conventional fixation.

For all micrographs, FS= freeze-substitution; CF= conventional fixation

Figs 2.1 a, b, c. LM of transverse sections of dry embryonic axes of pea. **a** FS. Radicle tissues had a dense, tightly packed appearance. **b** CF. An increase in cell area and separation of the plasmalemma from the wall (asterisks) was observed in cells after aqueous fixation. **c** CF. Tissue rehydrated for 2 h prior to conventional fixation. No separation of the plasmalemma and cell wall was observed. Scale bar for **a** - **c**: 40 μm.

Figs 2.2 a, b, c. LM of transverse sections of dehydrated embryonic axes of recalcitrant jackfruit. **a** FS. Cells were tightly packed within these tissues, and walls moderately folded. Vacuoles (*vac*) and starch deposits (*s*) were prominent. **b** CF. The outline of cells and vacuoles showed a rounded appearance not seen in freeze-substituted axes. Asterisks indicate areas where the plasmalemma and cell wall became separated. **c** CF. Tissue rehydrated for 30 min prior to conventional fixation. No separation of the plasmalemma and cell wall was observed. Scale bar for **a** - **c**: 20 μm.

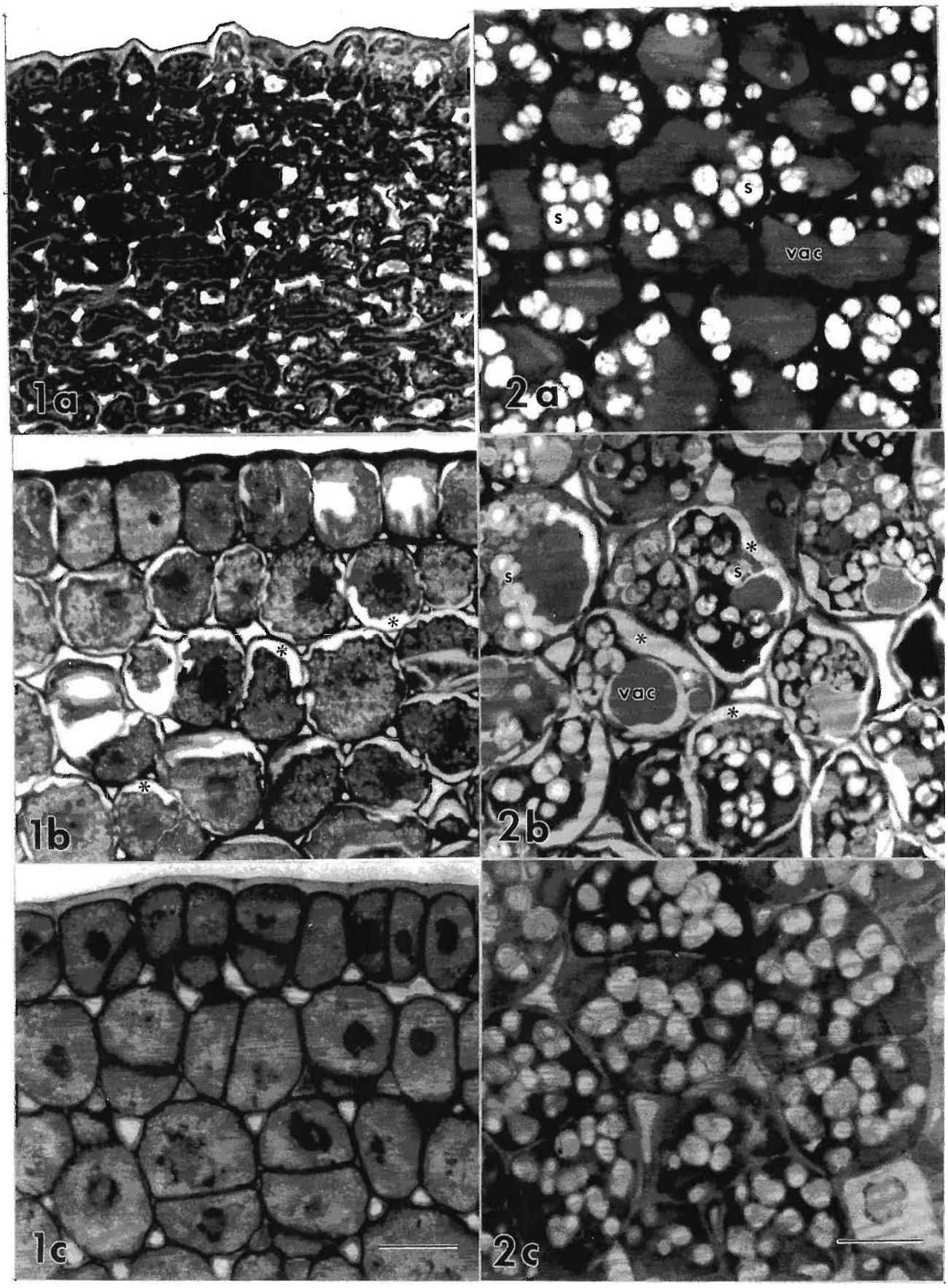
1a
2a
s
s
vac
1b
2b
s
s
vac
1c
2c

Electron microscopy

Desiccation-tolerant tissues: pea

The cytoplasm of freeze-substituted cortical cells of pea was densely packed with dissociated ribosomal subunits (Fig. 2.4 a). The plasmalemma of these cells was closely adpressed to the walls, and showed a continuous, tri-laminar appearance in favourable cross sections (Figs 2.4 a, b). Numerous discrete oil bodies lined the plasmalemma intracellularly, and these were closely associated with tubular structures presumed to be cisternae of endoplasmic reticulum ([ER]; Fig. 2.4 a). Similar cisternae were observed in close proximity to protein vacuoles, oil bodies and other structures within these cells (not shown). Irregularly shaped mitochondria and plastids were observed (Fig. 2.4 c). Mitochondrial matrices were extremely electron dense, which obscured internal detail. On the other hand, membranes within plastids could be resolved clearly in negative contrast against the dense background (Fig. 2.4 c).

Aqueous fixation introduced marked ultrastructural distortion of dehydrated cells. Separation of plasmalemma and cell walls was commonly observed (Fig. 2.4 d), and this was often accompanied by other ultrastructural abnormalities at the cell boundary. Oil bodies previously observed lining the inside of the plasmalemma (Fig. 2.4 a) often fused into large pools that lacked visible boundaries (Fig. 2.4 d, and compare with Fig. 4 a). Loss of plasmalemma integrity and extensive vesiculation of this bounding membrane was also observed, with many resultant vesicles situated in spaces between the plasmalemma and the cell wall (Fig. 2.4 e). Oil-body associated cisternae of ER could not be discerned in aqueously fixed cells (Fig. 2.4 e). Aqueous fixation also seemed to result in sectioned plastids having rounded profiles (Fig. 2.4 d) and in uneven distribution of ribosomal subunits, which gave the cytoplasm of these cells a patchy appearance (Fig. 2.4 e).

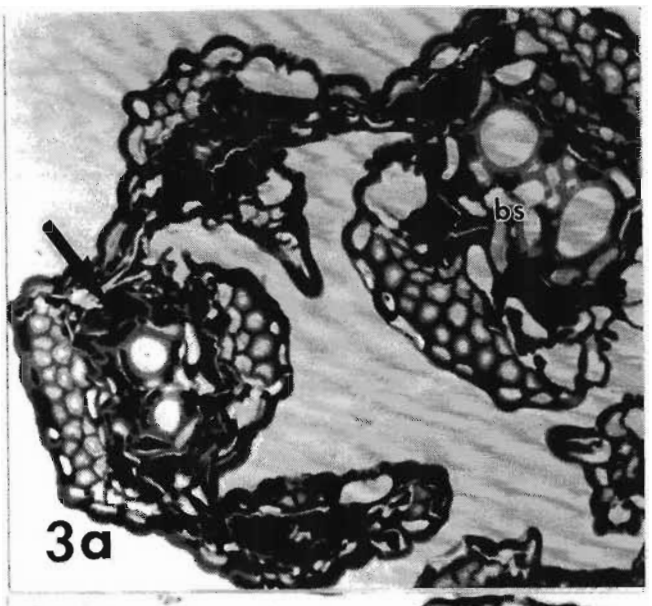

3a

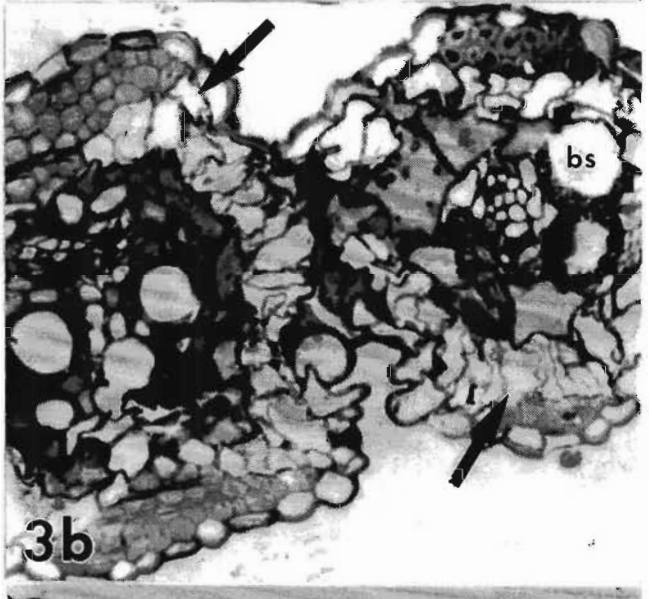

3b

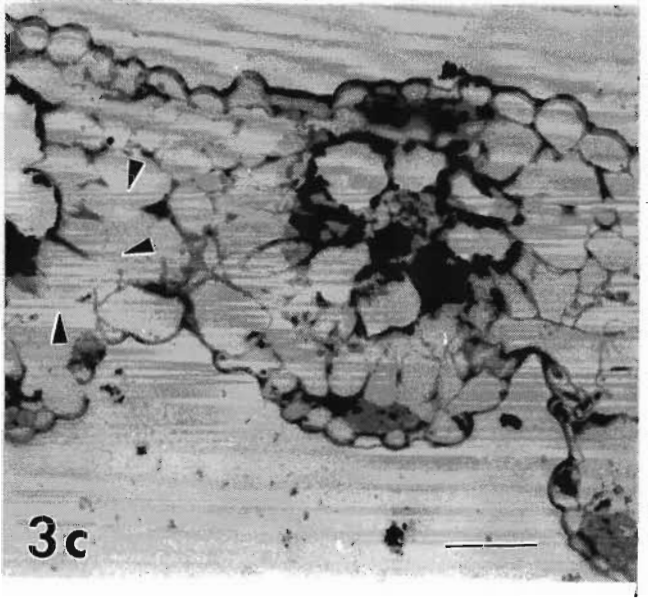

3c

Figs 2.4 a - e. TEM of dry pea hypocotyls. **a** FS. Oil bodies (*OB*) lined the clearly tri-laminate plasmalemma (*arrow*) and were closely associated with cisternae of endoplasmic reticulum (*er*). Scale bar: 0.2 μm. **b** FS. Cell membranes appeared intact and closely adpressed to walls (*CW*). Scale bar: 0.1 μm. **c** FS. Densely staining mitochondria (*m*) and plastids (*P*) showing internal differentiation were observed. Note the even distribution of ribosomal subunits in the cytoplasm of FS cells. Scale bar: 0.1 μm. **d** CF. Separation of the plasmalemma and cell wall (*double-headed arrow*) and coalescence of oil bodies (*arrowheads*) were frequently observed following aqueous fixation. Note the swollen appearance of mitochondria (*m*) and plastids (*P*) lacking internal structure. Scale bar: 0.5 μm. **e** CF. Numerous vesicles (*v*) presumably originating from the plasmalemma were observed to accumulate between this bounding membrane and the cell wall (*CW*). Ribosomal subunits were irregularly distributed, which gave the cytoplasm a patchy appearance. Scale bar: 0.25 μm.

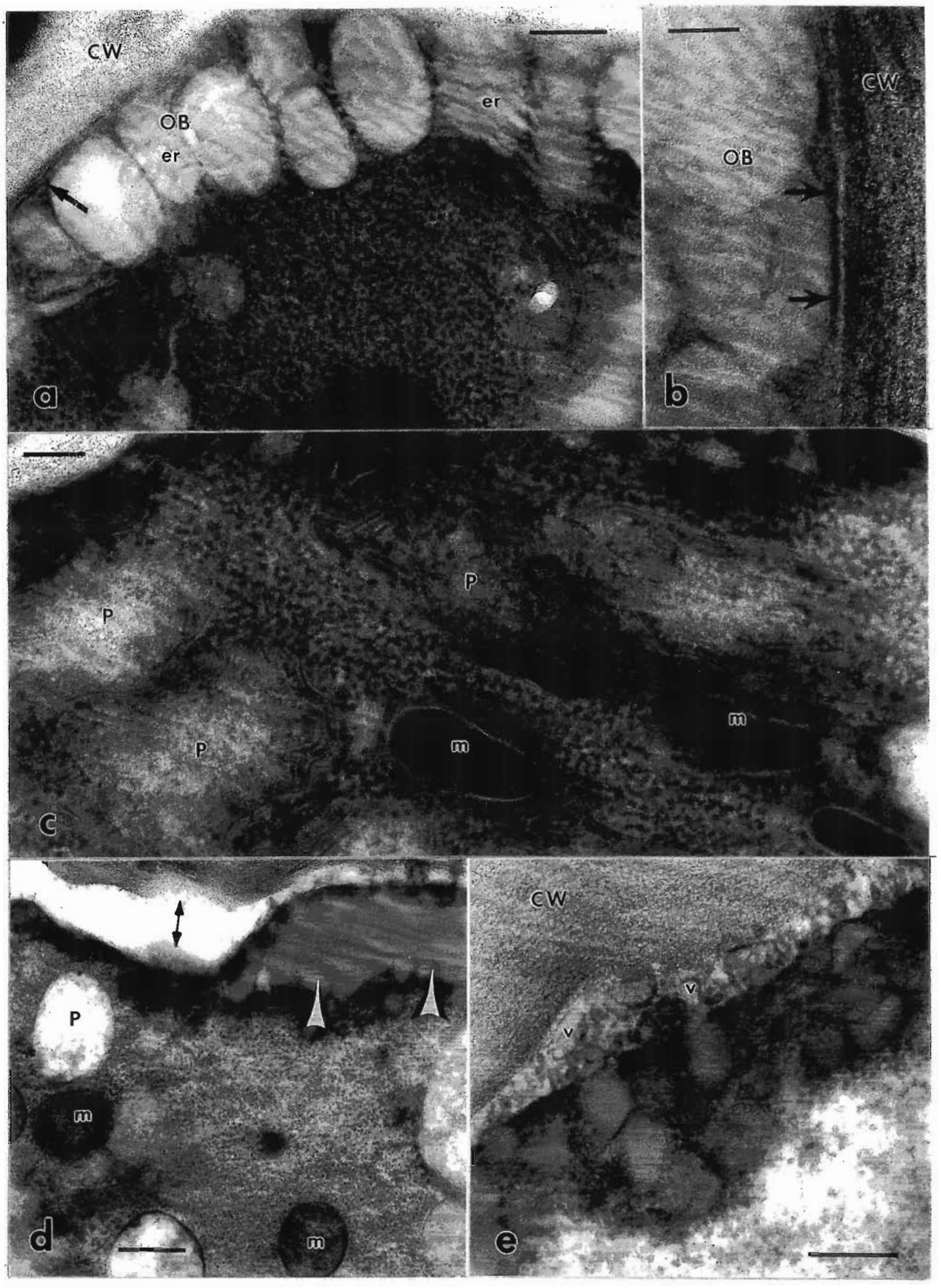
CW
OB
er
er
a
CW
OB
b
P
P
P
m
m
c
P
m
m
d
CW
v
v
e

Desiccation-sensitive axes: jackfruit

Freeze-substitution of dehydrated cells revealed reduced cell volumes, condensed nuclear chromatin as well compaction of organelles and other cellular compartments (Fig. 2.5 a), compared with the hydrated condition (not shown). Cell-wall folding was common in these cells but, significantly, separation of the plasmalemma and the wall was not observed (Figs 2.5 a, b). Furthermore, plasmalemma and tonoplast integrity was invariably maintained in partially dehydrated cells prepared by freeze-substitution (Figs 2.5 b, c, respectively). Ribosomal subunits were evenly distributed, Golgi bodies appeared well-developed (Fig. 2.5 a) and close associations of ER profiles with nuclear envelope, plasmalemma and mitochondria (Figs 2.5 a – c, respectively) were observed.

Aqueous fixation led to the separation of plasmalemma and cell wall in cells of partially hydrated jackfruit axes (Fig. 2.5 d). This separation was almost invariably accompanied by severing of plasmodesmatal connections between cells, tearing of the plasmalemma and structural abnormalities that occasionally included irregularity between the membranes of the nuclear envelope (Fig. 2.5 d). Membrane-bound organelles appeared distended after aqueous fixation, and mitochondria also showed electron translucent areas that were not observed in freeze-substituted preparations (Fig. 2.5 d).

Resurrection plants: *E. nindensis*

Mesophyll cells from freeze-substituted leaves of *E. nindensis* showed extensive wall folding, but no separation of plasmalemma and cell wall was observed (Fig. 2.6 a). In many cells a large central vacuole reduced the cytoplasm of mesophyll cells to a narrow band along the periphery (Fig. 2.6 a). Vacuoles were irregularly shaped, and in bundle sheath cells these often interdigitated with adjacent plastids containing very large starch grains (Fig. 2.6 b). Dehydration induced severe compaction of the cytoplasm and organelles in cells of *E. nindensis*, which also gave membranes a negatively stained appearance (Fig. 2.6 c, d). In spite of this compaction, structural integrity was apparently maintained, as illustrated by the favourable preservation of

Figs 2.5 a - d. TEM of cortical cells of jackfruit. **a** FS. Nuclear chromatin (*Nu*) appeared condensed, and cellular compartments were brought into close proximity by the drying treatment. In spite of this, the integrity of Golgi stacks (*G*), protein vacuoles (*Pv*) and plasmalemma was maintained. Scale bar: 0.2 μm. **b** FS. Plasmalemma (*arrows*) were intact and closely adpressed to cell walls (*CW*) in partially hydrated cells. Cisternae of ER (*er*) were frequently observed in close proximity to the plasmalemma. Scale bar: 0.1 μm. **c** FS. Protein vacuoles (*Pv*) were delineated by well-defined bounding membranes (*arrowheads*). ER cisternae (*er*) were also found in close association with protein vacuoles (*Pv*) and oval mitochondrial profiles (*m*). Scale bar: 0.1 μm. **d** CF. Separation of the plasmalemma from walls was observed following aqueous fixation (*double-headed arrow*). Tearing and vesiculation of the plasmalemma, and severing of plasmodesmatal connections were observed. Underlying structures were also affected by conventional fixation, as evidenced by the localised distension of the nuclear envelope (*arrowheads*), protein bodies (*Pb*) and mitochondria (*m*), which also showed abnormal clearings within their matrices. Scale bar: 0.5 μm.

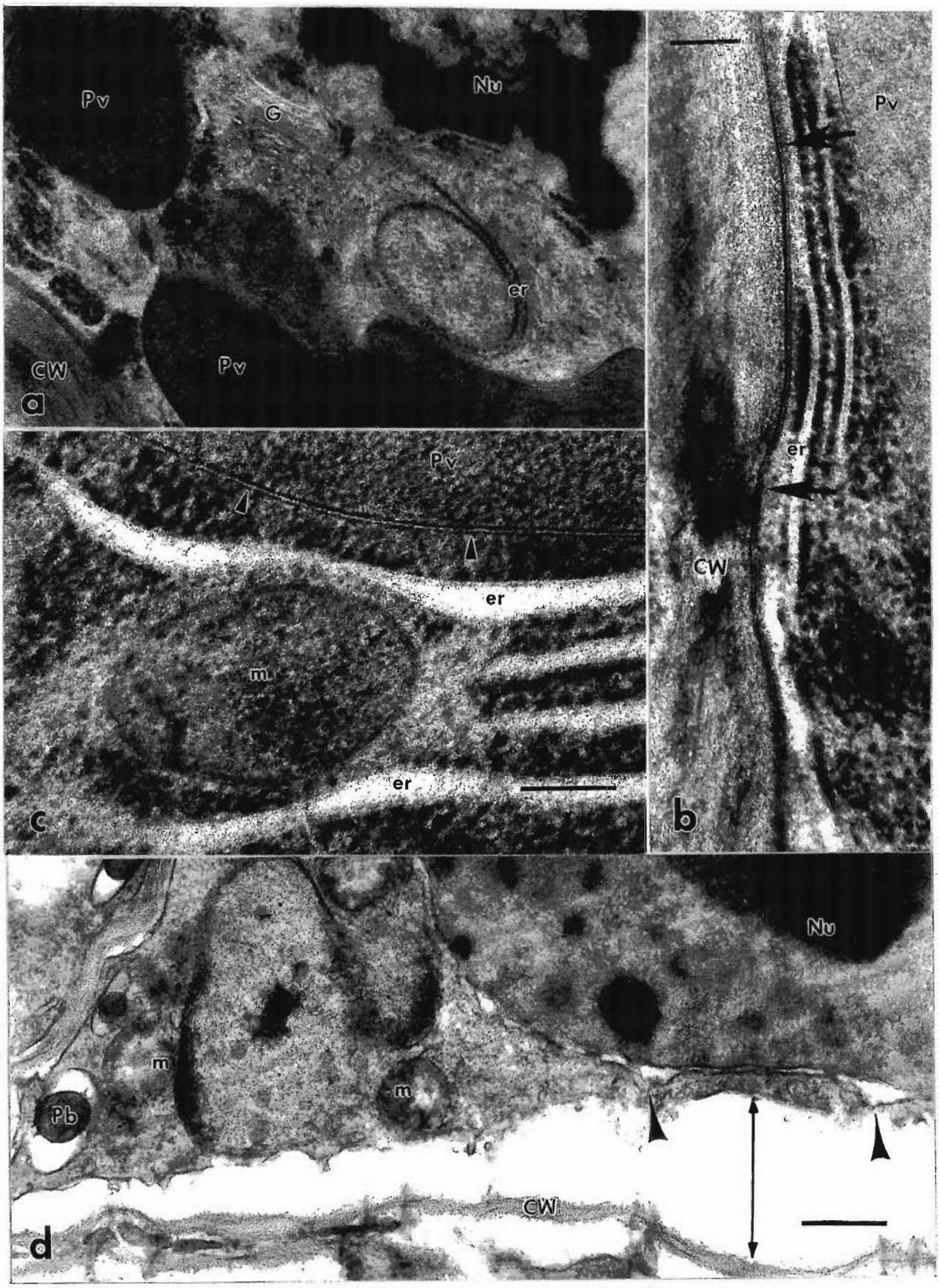
Pv
G
Nu
er
CW
Pv
a
Pv
er
CW
b
Pv
er
m
er
c
Nu
m
m
Pb
CW
d

Figs 2.6 a - f. TEM of transverse sections of dehydrated leaves of *E. nindensis*. **a** FS. Mesophyll cells showed extensive infolding of cell walls and large central vacuoles (*vac*) that limited the cytoplasm to a narrow peripheral band. Scale bar: 1 μm. **b** FS. Vacuoles (*vac*) had irregular outlines, and in bundle sheath cells vacuoles often interdigitated with neighbouring plastids (*arrowheads*) containing prominent starch grains (s). Scale bar: 0.5 μm. **c** FS. The cytoplasm of mesophyll cells appeared compacted and electron dense. The extent of this compaction is illustrated by the close proximity of a well-preserved mitochondrion (*m*), and plastids (*P*) between cell walls (*CW*). Scale bar: 0.1 μm. **d** FS. Freeze-substitution facilitated the orderly preservation of structure, such as thylakoids of chloroplasts. Scale bar: 0.1 μm. **e** CF. Tonoplast dissolution (*arrowheads*) and plasmalemma discontinuities (*asterisks*) became apparent after aqueous fixation. Scale bar: 0.5 μm. **f** CF. Distortion of chloroplast structure and clearings in the cytoplasm (*asterisks*) were also frequently observed. Scale bar: 0.25 μm.

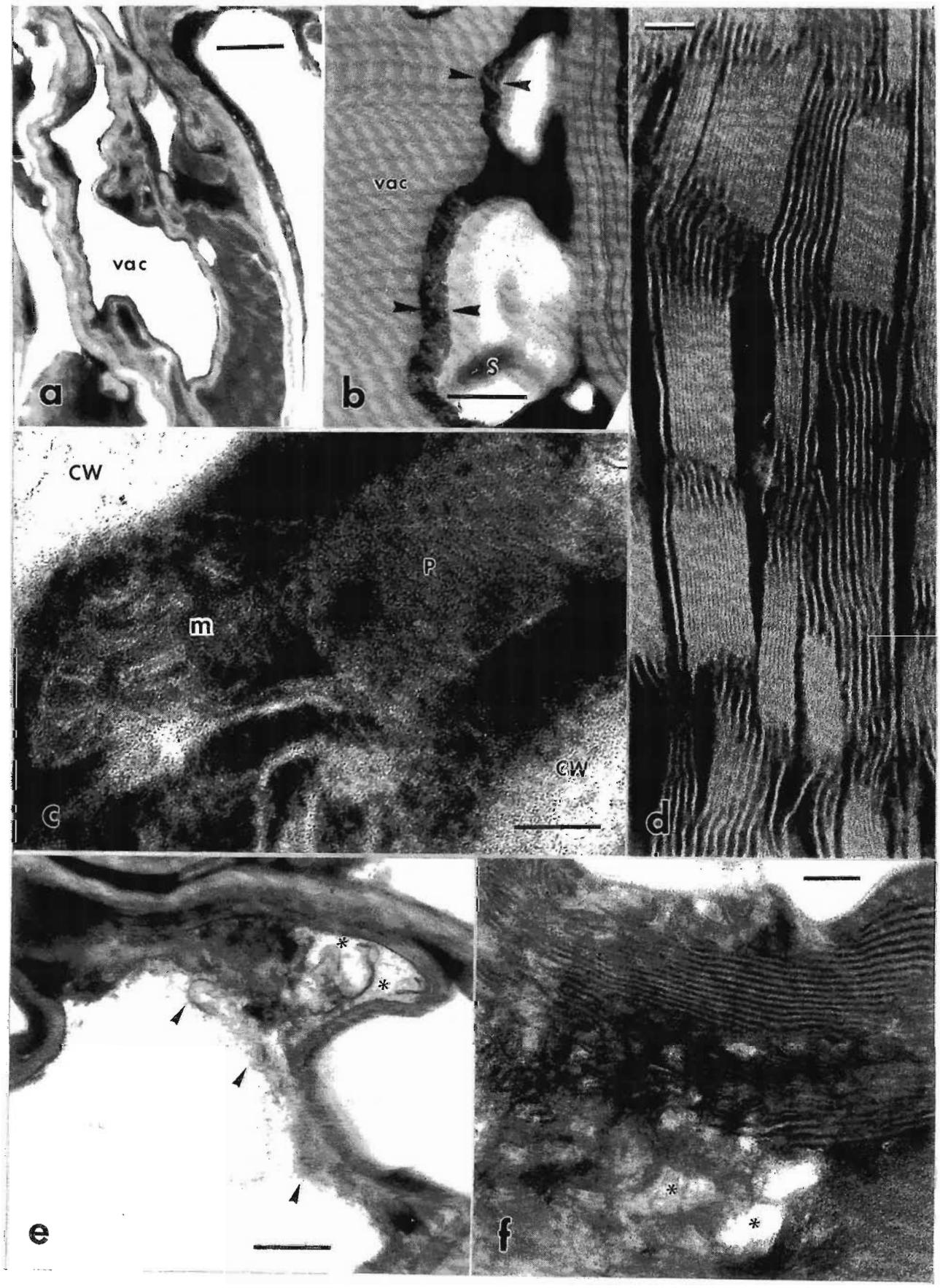
vac
a
vac
S
b
CW
P
m
CW
c
d
e
f

mitochondria (Fig. 2.6 c) and the orderly distribution of thylakoid membranes in sections of chloroplasts (Fig. 2.6 d).

The orderly ultrastructural preservation observed after freeze-substitution was absent from leaves that were fixed conventionally. Tonoplasts frequently appeared ruptured, leading to mixing of vacuolar and cytoplasmic contents (Fig. 2.6 e). Irregularities of the plasmalemma (Fig. 2.6 e), disruption of chloroplast structure and localised cytoplasmic clearing were also commonly observed (Fig. 2.6 f).

Discussion

The occurrence of rehydration artefacts during fixation of dehydrated cells in aqueous media has been recognised since the initial study of Perner (1965). In spite of this, aqueous fixation has continued to be used in desiccation studies, possibly due to expediency in contrast to the relatively more demanding anhydrous protocols. The uncertainty regarding the magnitude of rehydration that occurs during aqueous fixation prompted the present study. The assessment of rehydration artefacts using freeze-substitution was facilitated by the increasing number of works outlining this procedure (e.g. Robards and Sleytr, 1985; Gilkey and Staehelin, 1986; Lancelle *et al.*, 1986; Kellenberger, 1991; Echlin, 1992; Parthasarathy, 1995). Results from the present investigation showed that similar kinds of artefacts were found in dehydrated tissues of widely different origins following aqueous fixation, *viz.* separation of the cell wall and the plasmalemma, membrane irregularities and distortions of cellular sub-structure. These are considered below.

Separation of plasmalemma and cell walls was not observed in cells that had been freeze-substituted (Figs 2.1 a, 2.2 a, 2.5 b) or imbibed prior to conventional fixation (Figs 2.1 c, 2.2 c), but was evident in dehydrated specimens after aqueous fixation (Figs 2.1 b, 2.2 b, 2.4 d, 2.5 d). This indicates that the close apposition between plasmalemma and cell walls observed in freeze-substituted tissues had been maintained during imbibition and was not altered during subsequent conventional fixation. Swift and Buttrose (1972) proposed that during aqueous fixation of

dehydrated tissues, a hydration front precedes that of the crosslinking chemical, resulting in ultrastructural changes that resemble early stages of imbibition. Hallam (1976) reported cell walls to "spring away" from the cytoplasm during fixation, and later Öpik (1980) added to this view by suggesting that crosslinking chemicals restrict the expansion of protoplasts during this process. While there is no direct evidence to support the existence of such hydration fronts, differences between the composition of cell walls and the protoplasm are likely to result in different responses to aqueous fixation. Glutaraldehyde and osmium tetroxide are efficient crosslinking agents of proteins and lipids, respectively (Weakley, 1981; Bullock, 1984), and therefore affect predominantly the plasmalemma and cellular contents without stabilising cell wall components. The folded conformation of walls in dehydrated cells (as observed in freeze-substituted preparations) appears to relax during aqueous fixation (compare Figs 2.1 - 3 a with 2.1-3 b, respectively). This observation is supported by the study of Lott (1974), which showed that cell wall conformational changes were determined by the water status of the tissue and not influenced by glutaraldehyde fixation itself. It is possible that when the plasmalemma and cellular contents are immobilised early during fixation, expansion of the cell wall in the presence of water leads to loss of contact (Figs 2.1 b, 2.2 b, 2.4 d and 2.5 d) and possibly to the plasmalemma abnormalities observed (Figs 2.4 e and 2.5 d). Therefore, description of the phenomenon commonly referred to as "withdrawal of the plasmalemma from the cell wall" as a sign of desiccation stress (or injury) could be inaccurate and should be revised. Instead, this separation is likely to reflect the artefactual expansion of the cell wall away from the plasmalemma during aqueous fixation.

Distortion of structures during aqueous fixation of dehydrated material was not limited to the cell wall, but occurred intracellularly as well. A significant (P <0.05) increase in the area enclosed by the plasmalemma was observed in cells from pea radicles (Table 2.1), and the rehydrated appearance of cells from jackfruit axes and leaves of *E. nindensis* was also evident even at the light microscope level (Figs 2.2 b and 2.3 b). Ultrastructural evidence from this and other investigations shows that plastids and mitochondria acquire a relatively rounded appearance after aqueous fixation ([Figs

2.4 d and 2.5 d]; Buttrose, 1973; Swift and Buttrose, 1972; Vigil *et al.,* 1984; Platt *et al.,* 1997). The close association between cisternae of ER and discrete oil bodies visible in freeze-substituted cortical cells of pea (Fig. 2.4 a) was not observed following aqueous fixation (Figs 2.4 d, e), as also reported by others comparing anhydrous and conventional fixation protocols (Öpik, 1985; Smith, 1991). Extensive fusion of oil bodies occurred (Fig. 2.4 d), and this was also reported following prolonged osmium vapour fixation (Öpik, 1980). Coalescence of oil bodies is thus not particular to aqueous fixation, but may indicate sensitivity of oleosins to changes in pH (Huang, 1992) during fixation. Electron translucent areas in the ground cytoplasm of pea (Fig. 2.4 e) and in mitochondria of jackfruit (Fig. 2.5 d) were not observed in freeze-substituted cells, and may also be ascribed to artefacts of aqueous fixation. Loss of vacuolar integrity in mesophyll cells of *E. nindensis* (Fig. 2.6 e) is in agreement with the observations of Platt *et al.* (1997) on dehydrated cells of the resurrection plant *Selaginella lepidophylla* following aqueous fixation. Collectively, these findings highlight the relatively slow nature of conventional fixation (Mersey and McCully, 1978) and changes that can occur during this process (McCully and Canny 1985; reviewed by Gilkey and Staehelin, 1986)

In contrast, cryofixation can immobilise cellular process within milliseconds (Staehelin and Chapman, 1987; Craig and Staehelin, 1988; reviewed by Gilkey and Staehelin, 1986), and subsequent processing of cells under anhydrous conditions precludes rehydration artefacts. The plasmalemma of freeze-substituted cells was invariably adpressed to cell walls, and appeared intact in all specimens examined (Figs 2.4 b, 2.5 b). The cytoplasm of dehydrated cells appeared compacted and very electron dense, especially in mesophyll cells of *E. nindensis* (Fig. 2.6 c). The cytoplasm was studded with evenly distributed ribosomal subunits in cells of pea (Figs 2.4 a, c) and jackfruit (Fig. 2.5 c). Mitochondria and plastids were mostly elliptical and well defined (Figs 2.4 c, 2.5 c, 2.6 d) although internal detail was sometimes obscured by highly electron-dense matrices. Cisternae of endoplasmic reticulum were prominent and clearly resolved in cells of pea and jackfruit (Figs 2.4 a and 2.5 b, c, respectively). Nuclei in jackfruit cells had regular outlines and the chromatin appeared condensed.

Tonoplast integrity was also preserved in freeze-substituted cells of jackfruit and *E. nindensis* (Figs 5 c, 6 b, respectively). In bundle sheath cells of *E. nindensis*, clearly demarcated interdigitation was maintained between the vacuoles and surrounding starch-containing plastids. The tightly packed distribution of organelles in mesophyll cells of *E. nindensis* (Fig. 2.6 c) agrees with the findings of Platt *et al. (*1997) and Thomson and Platt (1997) on *S. lepidophylla*. The highly ordered structure of the chloroplasts attests to the excellent preservation attainable by freeze-substitution (Fig. 2.6 d). The superior ultrastructural preservation of plant structures attained by cryotechniques is well documented (Staehelin and Chapman, 1987; Craig and Staehelin, 1988; Kiss *et al.,* 1990; Davidson and Newcomb, 2000; reviewed by Gilkey and Staehelin, 1986), which enhances the reliability of observations made on tissues prepared by such methods.

Evidence suggests that cellular volume was reduced during drying by cell wall folding, irrespectively of whether cells were desiccation-tolerant or desiccation–sensitive. However, this does not exclude the possibility of plasmolysis *sensu stricto* occurring in species where the rigidity of the cell wall does not allow folding in response to drying (Webb and Arnott, 1982) or to extra-protoplasmic freezing (Murai and Yoshida, 1998). Electron microscopy revealed that the plasmalemma maintains its tri-laminar structure, continuity and apposition against cell walls even at the very low water content of 0.08 g g^{-1} (Figs 2.4 a and b). This is in agreement with previous freeze-fracture studies (e.g. Platt *et al.,* 1994) and TEM studies using truly anhydrous tissue processing (Browning and Gunning, 1977; Öpik 1980 1985; Kiss *et al.,* 1990; Tiwari *et al.,* 1990; Smith, 1991; Platt *et al.,* 1997; Thomson and Platt, 1997; Davidson and Newcomb, 2000) but different from observations following exposure to aqueous media during processing (Webster and Leopold, 1977; Thomson, 1979; Fincher Chabot and Leopold, 1982; Yatsu, 1983). Nuclear magnetic resonance and X-ray studies of orthodox seeds have also shown that membrane integrity is maintained even in the dry state and that membranes retain a lamellar configuration (Seewaldt *et al.,* 1981). Plasmalemma discontinuities and vesiculation were presently observed only following aqueous fixation from the dehydrated state, and particularly in areas

where separation of this membrane and the cell wall had occurred (Fig. 2.3 b). These findings provide a *caveat* that interpreting plasmalemma irregularities at the electron microscope level as a sign of desiccation damage, or as a mechanism to conserve membranes during cycles of dehydration/rehydration (e.g. Fincher Chabot and Leopold, 1982), demands careful consideration of the processing conditions (see Platt *et al.,* 1997, and compare e.g. Webster and Leopold [1977], Sargent *et al.,* [1981], with Staehelin and Chapman [1987], Tiwari *et al.,* [1990], Thomson and Platt [1997]).

Results from this investigation are particularly relevant to desiccation studies relating ultrastructure and survival. It is generally agreed that maintenance of plasmalemma and tonoplast integrity is critical for cell survival. Therefore, it seems counter-intuitive to attempt reconciling recovery of plants from sub-lethal desiccation with ultrastructural evidence obtained using aqueous fixation, which almost invariably shows artefacts similar to those described above. It must be stressed that those artefacts have often been cited as indicating the nature of dehydration damage in a diversity of plant material by many authors using TEM (e.g. Webster and Leopold, 1977; Fincher Chabot and Leopold, 1982; Sargent *et al.,* 1981; Sack *et al.,* 1988; Berjak *et al.,* 1989; Schneider *et al.,* 1993; Quartacci *et al.,* 1997; reviewed by Walters *et al.,* 2002). Therefore, conventional preparative methods for microscopy do not allow unequivocal distinction between damage caused by rehydration *per se* and ultrastructural changes induced during aqueous fixation.

The confounding effects of aqueous fixation on dried and rehydrating vegetative tissues of the lower order resurrection plant *S. lepidophylla* were previously addressed by Platt *et al.* (1997). Those authors endorsed the superiority of freeze-substitution and concluded that ultrastructural damage to dehydrated vegetative cells occurred upon rapid rehydration, either during imbibition of detached tissues in water or during aqueous fixation. Results from the present investigation not only support their findings, but also extend those observations to vegetative cells of an angiosperm resurrection plant (*E. nindensis*), and to developmentally diverse tissues such as

embryonic axes of both desiccation-tolerant pea and desiccation-sensitive jackfruit seeds. Additionally, measurement of cell areas provides convincing evidence of the distortion of cell structure introduced during aqueous fixation, and of the unreliability of ultrastructural information obtained from tissues processed in this way.

In conclusion, freeze-substitution is ideally suited for ultrastructural investigations of dehydrated plant tissues. The low water content in desiccated specimens reduces - or even precludes - the biggest obstacle to any cryotechnique: *viz.* the distortion of ultrastructure due to intracellular crystallisation during cooling. Similarly, re-crystallisation during freeze-substitution at $\geq$ -80°C is also unlikely due to the high solute concentration within dehydrated cells. Hence, ultrastructural abnormalities seen after freeze-substitution can far more convincingly be ascribed to dehydration *per se* than to any other factor. A drawback associated with freeze-substitution is the likely extraction of lipids in organic solvents (Lancelle *et al.,* 1985; Lancelle and Hepler, 1992; Thomson and Platt, 1997). Additionally, obtaining adequate thin sections can be challenging due to inadequate resin infiltration into cells. However, this problem is common to most anhydrous protocols for plant tissues using resin embedding (e.g. Öpik, 1980; Smith, 1991; Thomson and Platt, 1997). Ironically, this obstacle may arise from the superior preservation of the plasmalemma attained by such methods. Nevertheless, while freeze-substitution is technically more demanding than conventional aqueous fixation, the resultant improvement in the preservation of structure in the dry state (e.g. Tiwari *et al.,* 1990; Platt *et al.,* 1997; Thomson and Platt, 1997) more than rewards the effort invested.

CHAPTER 3*

Optimising the water content of embryonic axes for cryopreservation: the effects of drying rate on the desiccation tolerance of jackfruit

* Also published in Wesley-Smith J, Pammenter NW, Walters C, Berjak P (2001) The effects of two drying rates on the desiccation tolerance of embryonic axes of recalcitrant jackfruit (*Artocarpus heterophyllus* Lamk.) seeds. *Ann. Bot.* **88**: 653-664

Introduction

The lower limit of desiccation tolerance varies among species, and even within species depending upon the developmental status (Farrant *et al.,* 1986, 1989; Hong and Ellis, 1990; Berjak *et al.*, 1992, 1993; Finch-Savage, 1992; Tompsett and Pritchard, 1993). Rapid drying of excised embryonic axes in an air stream (flash drying; Berjak *et al.,* 1989, 1990) has facilitated drying of axes to water contents previously unattained with whole seeds yet with minimal loss of viability (Normah *et al.,* 1986; Pritchard and Prendergast, 1986; Berjak *et al.*, 1989; Pammenter *et al.,* 1991 Pritchard, 1991; Pritchard and Manger, 1998). In spite of this a lower limit to desiccation tolerance still exists, and exposure to such low water contents can result in desiccation damage (reviewed by Vertucci and Farrant, 1995; Pammenter and Berjak, 1999 Walters *et al.,* 2002).

Partial drying is a method commonly used to reduce the water content of recalcitrant axes prior to cryogenic exposure, as this step reduces the likelihood of lethal freezing damage (e.g. Normah *et al.*, 1986; Pritchard and Prendergast, 1986; Pence, 1990, 1992, 1995; Wesley-Smith *et al.*, 1992, 1995, 2001b; Reed, 1996; Engelmann, 1997). Evidence from previous studied suggests that drying should be rapid, as recalcitrant axes are reportedly injured by prolonged exposure to water contents intermediate between full hydration and *c.* 0.4 g H_2O per g dry matter (approximately Ψ= -3 MPa; Berjak *et al.,* 1990; Pammenter *et al.,* 1991, 1998; Pritchard, 1991; Leprince *et al.,* 1999, 2000; Walters *et al.,* 2001; reviewed by Vertucci and Farrant, 1995; Berjak and Pammenter, 1997; Pammenter and Berjak, 1999; Walters *et al.,* 2001). However,

determining how rapidly axes be should be dried is confounded by several issues. Firstly, most of the studies conducted have compared slow drying of whole seeds with rapid drying of excised embryonic axes (Pritchard and Prendergast, 1986; Pammenter *et al.,* 1991; Berjak *et al.,* 1990, 1993; Pritchard *et al.*, 1995; Pritchard and Manger, 1998), which introduces uncertainty about the contribution of the storage tissues towards the physiological status of the axis. In second place, studies comparing drying rates of embryonic axes of recalcitrant seeds have reported rapid drying to be either beneficial (Walters *et al.,* 2002), damaging (Fu *et al.,* 1993) or unrelated to the extent of water loss tolerated (Leprince *et al.,* 1999). Lastly, ultrastructural appraisal of damage presumed to occur during desiccation is obscured by rehydration artefacts that invariably occur during the preparation of partially hydrated tissues for microscopy (Wesley-Smith, 2001; Chapter 2). Therefore, the effects of drying rates on the ultrastructure and survival characteristics of excised embryonic axes of recalcitrant seeds must be the subject of further attention.

This facet of the investigation examines the effects of two very different drying regimes on the survival, ultrastructure and membrane leakage characteristics of excised embryonic axes of desiccation-sensitive seeds of jackfruit (*Artocarpus heterophyllus*). Survival of axes was assessed *in vitro*, and the integrity of membranes following drying was estimated by measurement of electrolyte leakage during rehydration. Rehydration artefacts were avoided by processing partially hydrated axes anhydrously for light and electron microscopy using freeze-substitution as described in the previous chapter (Ding *et al.,* 1991; Wesley-Smith, 2001).

The aims of these studies were:

1. To confirm the effects of differential drying rate when both rapid and slow drying are applied to isolated axes of jackfruit, as opposed to axes *vs.* seeds, as done for other species (Berjak *et al.,* 1990, 1993; Pritchard, 1991; Pritchard and Manger, 1998; Pritchard *et al.*, 1995) or seeds *vs.* seeds (Farrant *et al.*, 1986; Pammenter *et al.*, 1998).

2. To use freeze-substitution in order to observe the status of the tissue in the partially hydrated state, and so;
3. To compare ultrastructural characteristics of tissues dehydrated either slowly or rapidly to levels at which desiccation damage is incipient.
4. To assess ultrastructural changes that occur on rehydration of tissues partially dehydrated at different rates.

Materials and methods

Seeds

Mature multiple fruits of *Artocarpus heterophyllus* Lamk. were hand-harvested from the same tree in Durban, South Africa. The multiple fruits of jackfruit were considered mature when tears developed in the rind and the fleshy interior was relatively soft. All seeds within each fruit were collected for use in the present investigation. Seeds were surface sterilised in 1:3 dilution of commercial bleach (NaOCl) for 10 min and rinsed in three changes of sterile distilled water. They were temporarily stored at 8°C in plastic bags and used within 3 d. Only axes ≥2 mm were used, and these were surface sterilised again and rinsed (using the same parameters), blotted dry with sterile filter paper prior to dehydration.

Drying procedures

a) *Rapid drying* (Fig. 3.1). Nylon gauze was inserted across a PVC pipe of 35 mm diameter and 90 mm length, which acted as a support for the axes. A computer C.P.U. cooling fan (12V, 1W) was mounted in the middle of this pipe, with airflow directed towards the gauze end. This assembly was placed in a jar 115 mm high and 350 ml capacity containing 100 g of activated silica gel. The design ensured that the air inlet into the pipe was buried in the silica gel, and allowed sufficient clearance above the axes for unrestricted airflow. The electrical connections to the fan were sealed in a small perforation made in the screw cap of the jar. A digital thermometer was used to monitor the temperature during drying.

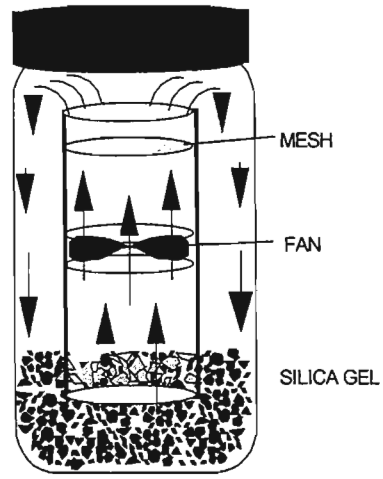

Fig. 3.1. Rapid drying apparatus. (See text for description.)

b) *Slow drying*. Axes were placed in plastic weighing boats and floated over saturated salt solutions yielding the required relative humidity (Winston and Bates, 1960). Drying was performed inside glass Petri dishes with a 60 ml head-space. Axes were dried over a solution of KH_2PO_4 (96% relative humidity [RH] at 25°C) for up to 3 d and for an additional 30 and 60 min over KCl (85% RH) where further drying was required. Both salt solutions and plastic weighing boats were sterilized to prevent microbial contamination of the axes during the experiment.

The temperature during drying for both drying methods was maintained between 22 and 25°C. Water contents were determined gravimetrically after drying at 80°C for 36 h. Values represent the mean of five axes ± standard deviation, and are expressed on a g H_2O per g dry matter (g g^{-1}) and on a fresh weight basis (fmb) indicated in parentheses.

Leakage measurements

In recalcitrant seeds, increased electrolyte leakage from cells has been directly linked to plasmalemma abnormalities, and is a good indicator of viability (Pammenter *et al.*, 1991, 1993). Five axes per drying stage of each treatment were placed individually in 1 ml of distilled water in separate wells and conductivity measured using a CM 100 conductivity meter (Reid and Associates cc., Durban, South Africa). Leakage was

measured after 130 min, where conductivity of the bathing solutions of the various treatments reached a plateau. Thereafter, embryonic axes were individually subjected to two freeze-thaw cycles to induce total membrane breakdown. The conductivity of the leachate from each axis in its original well was again measured after 2 h of soaking. Leakage data are expressed as a percentage of the total recorded for each axis, and represented graphically as the mean ± standard deviation of these five values at each water content.

Survival studies

The ability of embryonic axes for organised growth was assessed *in vitro*. Axes that had either not been dried, or immediately after drying to various water contents, were immersed in distilled water at 20°C for 30 min. They were subsequently surface sterilised (as above) and cultured aseptically on a reduced strength (¼) MS medium (Murashige and Skoog, 1962) containing 3% (w/v) sucrose and solidified with 0.7% (w/v) agar. Axes were grown under a light intensity of 66 μmol $m^{-2}s^{-1}$ and a 16h:8h light:dark photoperiod. Survival was assessed using ten axes per treatment, and axes were scored as surviving when the radicle doubled in length within two weeks *in vitro.*

Microscopy

The apical 3 mm of radicles from axes were processed for light (LM) and transmission electron microscopy (TEM) using anhydrous or aqueous protocols, depending on their water status. This ensured that the resulting preservation reflected the ultrastructure of dehydrated cells, or changes occurring early during recovery, respectively (Chapter 2). Fully hydrated axes (either undried or dehydrated axes imbibed for 30 min) were fixed in 2.5% (v/v) glutaraldehyde in 0.1 M sodium phosphate buffer with 0.5% (w/v) caffeine (pH 7.2) for 2 h. Caffeine was added to contain phenolics within vacuoles and thereby prevent artefactual polymerisation that can occurr during primary fixation (Drennan and Berjak, 1982). Subsequent specimen processing followed that described for aqueously fixed specimens in Chapter 2. For partially hydrated axes, 1 mm thick transverse sections were cut within the distal 2 mm, plunged into liquid propane at –180°C, freeze-substituted, embedded, sectioned

and stained using the procedures described in Chapter 2. Semi-thin sections were viewed with a Nikon Biophot (Nikon, Japan) transmitted light microscope. Ultra-thin sections were viewed with a JEOL JEM 1010 transmission electron microscope (JEOL, Japan) at 100 kV. The ultrastructure of meristem and –derivative cells from each of five axes of either control or treated material was assessed. Images that represented the general appearance of cells from each treatment were captured both photographically and digitally for subsequent analysis.

Image analysis

Measurement of cell and vacuolar areas was performed using Zeiss KS100 image analysis software (Carl Zeiss Vision GmbH, Germany) following calibration to the appropriate image magnification. The effects of drying rate on whole embryonic axes were assessed by examining transverse sections through the distal 2 mm of embryonic radicles. The area enclosed within the cell wall of cells along 3 - 4 randomly selected transects inwards from the epidermis (one section from each of five axes) was measured using LM. The extent of vacuolation was quantified at TEM level by measuring vacuolar areas in sections through *c.* 50 meristem and immediate meristem- derivative cells from five axes per treatment. The area within the wall of each cell was also measured, and the corresponding percentage area occupied by vacuoles was calculated and reported.

Results

Drying time courses

The water contents of axes dried by the two methods are shown in Table 3.1. Rapid drying reduced the water content to 0.37 g g^{-1} within 60 min. It took 3 d for a similar water content to be reached on slow drying.

Survival and leakage measurements

The relation among axis water content, electrolyte leakage and survival is shown in Figure 3.2. Survival of axes that were dried rapidly decreased from 100% at 0.4 g g^{-1} (29% fmb) to 60% at 0.19 g g^{-1} (16% fmb). The average conductivity of corresponding

axes mirrored this trend, showing a steep increase between 0.4 g g^{-1} and 0.2 g g^{-1} (the lowest water content tested). In axes dried slowly, a decline in viability was first observed at 0.8 g g^{-1} (44% fmb), i.e. twice the 'critical' water content of axes dried rapidly. Survival had declined to around 85% at 0.7 g g^{-1} (41% fmb) and this was followed by a precipitous drop to 0% at 0.36 g g^{-1} (26% fwb). Leakage from axes dried slowly to 0.8 g g^{-1} was similar to that of axes dried rapidly to 0.4 g g^{-1}, but increased significantly (P <0.05) following drying to 0.36 g g^{-1} ([26% fmb]; the lowest water content attained with the slow drying protocol). Although there was no significant difference in the leakage from axes dried rapidly to 0.2 g g^{-1} and those dried slowly to 0.36 g g^{-1}, survival of axes *in vitro* (60 and 0%, respectively) clearly set these treatments apart. In all instances, surviving axes germinated within a week. With the exception of the control (not dried) axes, no shoot development was noted in any of the treatments.

Table 3.1. Drying courses and water content of embryonic axes following slow or rapid drying. Values represent the mean of five axes, with standard deviations in parenthesis.

TREATMENT	DRYING TIME	WATER CONTENT (g g^{-1})
Fresh	0	3.54 (±0.48)
Rapid drying	30 min	0.70 (±0.06)
	60 min	0.37 (±0.04)
	90 min	0.19 (±0.05)
Slow drying 96% RH	1 d	1.49 (±0.24)
	2 d	0.81 (±0.01)
	3 d	0.67 (±0.01)
	3d + 30 min*	0.36 (±0.05)
	3d + 60 min*	0.29 (± 0.01)

Microscopy

Survival and leakage data suggest that for axes dried slowly, a water content of approximately 0.7 g g^{-1} (41% fmb) marked the onset of desiccation damage.

Therefore, the ultrastructure of axes dried slowly to this water content was assessed because of the potential to reveal the nature of the incipient desiccation damage suggested by other methods (Fig. 3.2). This ultrastructural information permitted a comparison with axes dried rapidly to the same water content, but which appeared relatively unaffected by the drying treatment.

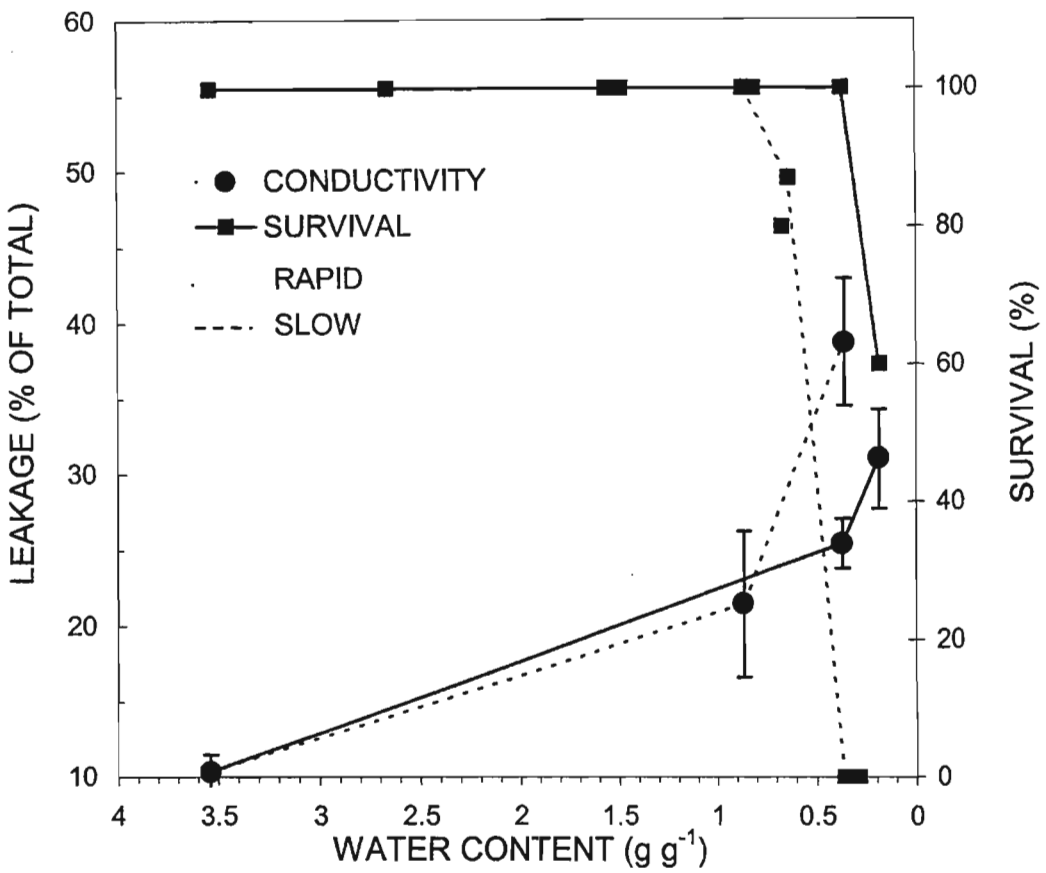

Fig. 3.2. Relationship between survival and electrolyte leakage of variously hydrated axes following rapid or slow drying. Survival data were gathered from *in vitro* culture of ten axes at each water content, and expressed as a percentage. Leakage data represent the average of individual measurements from five axes at each water content, and expressed as a function of total leakage from each axis ± standard deviation.

At the light microscope level, transverse sections from control axes (water content 3.5 g g^{-1} [78% fwb]) showed apparently fully turgid cells in the epidermis and cortical parenchyma (Fig. 3.3 a). Following rapid drying for 30 min to 0.7 g g^{-1} (41% fwb) cell

compaction of the outermost layers of became evident, while cells in the core of the axes appeared relatively more hydrated (Fig. 3.3 b). Cells from axes dried slowly for 2 d to a similar water content revealed irregular cell wall profiles throughout the section, suggesting a relatively even loss of water (Fig. 3.3 c). The apparent uneven distribution of water in axis tissues following rapid or slow drying is supported by measurements of areas within the cell wall shown in Figure 3.4. Statistical analysis showed significant differences (P <0.05) between drying treatments. Cells from axes dried rapidly were smaller seven rows away from the epidermis and largest within the stele. Cells from slowly dried axes showed the opposite trend, i.e. they were relatively larger within the first seven cell layers and smaller within the stele. No difference between treatments was found in cells 12 rows away from the epidermis.

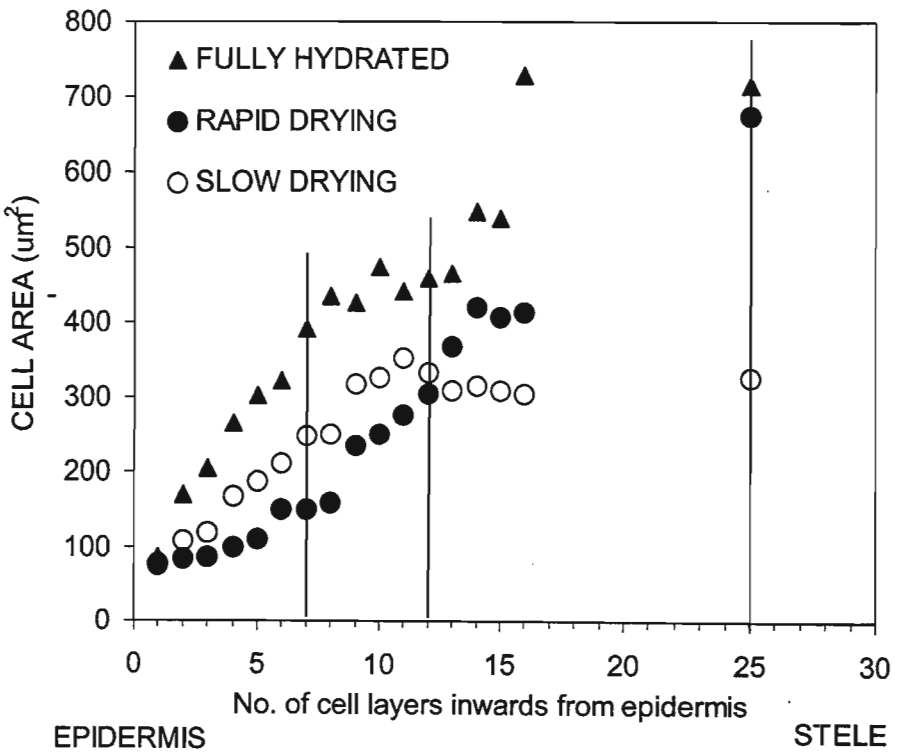

Fig. 3.4. Area enclosed by the cell wall in transverse sections of undried (control) and dehydrated axes. Measurements of cell area were made on 4-5 radial transects inwards from the epidermis of five axes per treatment. Fully hydrated (solid triangles), rapidly dried (solid circles) and dried slowly (open circles). Vertical lines indicate the measurements of cell area from axes dried rapidly or slowly that were tested for differences using a Student's T-test. The sectional area of dried cells was similar 12 layers in from the epidermis, but differed significantly (P <0.05) in rows 7 and 25.

For all micrographs, FS= freeze-substitution; CF= conventional fixation

Fig. 3.3. Transverse sections from radicles of embryonic axis of jackfruit. **a**, Fully hydrated (CF), **b** and **c** (FS) dehydrated to 0.7 g g^{-1} either rapidly for 30 min (b) or slowly over 2 d (c). *ep*, epidermis; Bar 75 μm

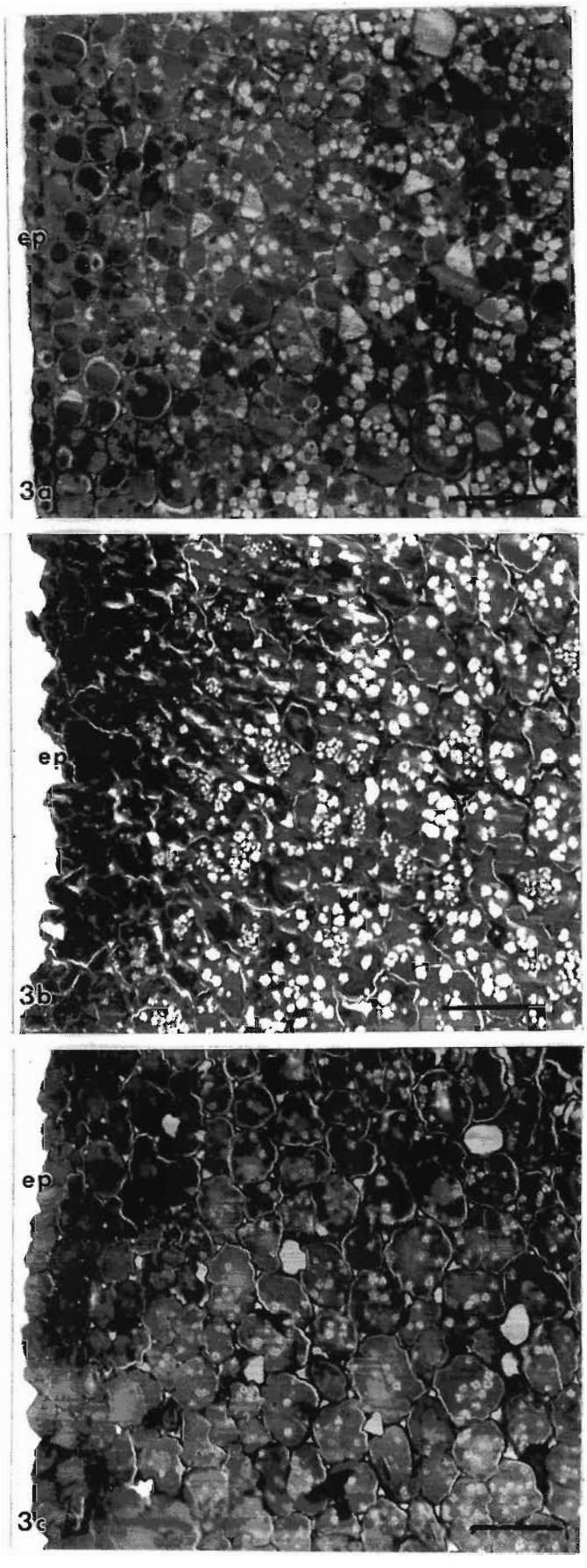
ep
3a
ep
3b
ep
3c

Ultrastructurally, meristematic cells in undried control axes showed prominent nuclei, many small vacuoles, plastids and moderately differentiated mitochondria (Fig. 3.5). Short profiles of endoplasmic reticulum (ER) were observed, usually in close proximity of the plasmalemma. Following rapid drying and freeze-substitution, meristem-derivative cells appeared normal and the cytoplasm densely packed with polysomes, which were occasionally observed bound to the nuclear envelope (insert; Fig. 3.6). Vacuoles were rounded and had intact boundaries (Fig. 3.6). The plasmalemma appeared intact, tri-laminate and adhered closely to the cell wall (Fig. 7). Tubular profiles of smooth ER (*c.* 30 nm diameter) were observed close to the plasmalemma (Fig. 3.7), and to bundles of microfilaments (Fig. 3.8) and Golgi stacks (Fig. 3.9). Dilated cisternae of smooth ER were also observed in the cell periphery, often sequestering areas of cytoplasm as shown in Figure 3.7. Spherical structures 60-100 nm in diameter were observed between ER cisternae and the plasmalemma, but it is not clear whether these were vesicles or transverse sections through ER profiles. Golgi stacks showing densely staining cisternae and vesicles were also observed in the vicinity of the plasmalemma (Fig. 3.9) often in close proximity, but without physical continuity with smooth ER cisternae.

In some respects, the ultrastructure of meristem and meristem-derivative cells of axes dried slowly was similar to that described for rapidly dehydrated material, although some irregularities were apparent and are highlighted. Nuclear chromatin appeared condensed in most cells (Fig. 3.10), and occasional swelling of the nuclear envelope was observed. Polysomes as observed in control and rapidly dried axes, had dissociated into ribosomal subunits on slow drying, which gave the cytomatrix an even, densely packed appearance (Figs 3.10 and 11). Plasmalemmae and tonoplasts appeared intact, although cell wall distortions occasionally brought these membranes into close contact (Fig. 3.11). Whorls of ER cisternae as well as long ER profiles with ribosomes still attached were also observed in these cells (Fig. 3.11). Electron-translucent Golgi stacks and numerous vesicles, presumably fragmented ER cisternae, were observed close to the cell walls (Fig. 3.12). Autophagy of cytoplasm

and organelles (particularly mitochondria) into newly-forming lytic compartments was commonly observed (Fig. 3.13).

Rehydrated cells from both drying treatments appeared to regain full turgidity, indicating that plasmalemma integrity had been maintained. After 30 min of rehydration, the ultrastructure of axes dried rapidly resembled that of the control (Figs 3.14 and 5, respectively). ER profiles appeared fragmented and dispersed throughout the cell. Fusion and dilation of other ER profiles and apparent lysis of cytoplasmic inclusions suggested *de novo* formation of vacuoles in these rapidly dried cells (Fig. 3.15). Rehydration of axes dried slowly frequently resulted in damaged tonoplasts, uneven distribution of ribosomal subunits in the cytoplasm and localised distention of the nuclear envelope (Fig. 3.16).

Results from measurement of vacuolar areas in cells of control and dried axes are shown in Table 3.2. There were no differences (P >0.05) in the absolute area occupied by vacuoles in cells from axes that were not dried, and those dried to *c.* 0.7 g g^{-1} either rapidly or slowly.

However, the proportion of the area occupied by vacuoles increased, possibly reflecting the reduced total cell area of dehydrated cells (Table 3.2). Rehydrated cells showed a significant increase in absolute vacuolar area, and this was similar in cells dried either rapidly or slowly. Cell areas of rehydrated axes also increased significantly (P <0.05) even above those from undried (control) material, and this effect was greatest in axes that had been dried slowly (Table 3.2). The proportion of the area occupied by vacuoles remained stable at *c.* 50% after drying and subsequent rehydration in cells from both drying treatments (Table 3.2).

Fig. 3.5. **CF**. Meristematic cell from the radicle of an undried (control) axis showing prominent nuclei (*N*), thin cell walls, discrete vacuoles (*Vac*), mitochondria (*m*) and plastids (*p*). Bar 2 μm

Fig. 3.6. FS. Rapid drying. Nuclear and vacuolar (*Vac*) integrity was preserved. Polysomes abounded in the cytoplasm, and were occasionally observed bound to the nuclear envelope (*insert*). Bar 0.5 μm; insert x 66 000 magnification

Fig. 3.7. **FS**. Rapid drying. Profiles of endomembrane origin were observed in close association with mitochondria (*m*) and the plasmalemma. Areas of the cytoplasm sequestered within dilated ER cisternae possibly indicate *de novo* vacuolation in these cells (*arrowheads*). Bar 0.2 μm

Fig. 3.8. **FS**. Rapid drying. Tubules presumed to be smooth ER, microfilament bundles and cisternae of rough ER (rer) were frequently observed in close proximity at the periphery of cells dried rapidly. Note the abundance of polysomes in the cytoplasm. Bar 0.2 μm

Fig. 3.9. **FS**. Rapid drying. Golgi stack showing vesiculation near the cell wall (*CW*). Note the densely stained areas within *trans* Golgi cisternae. Bar 0.1 μm

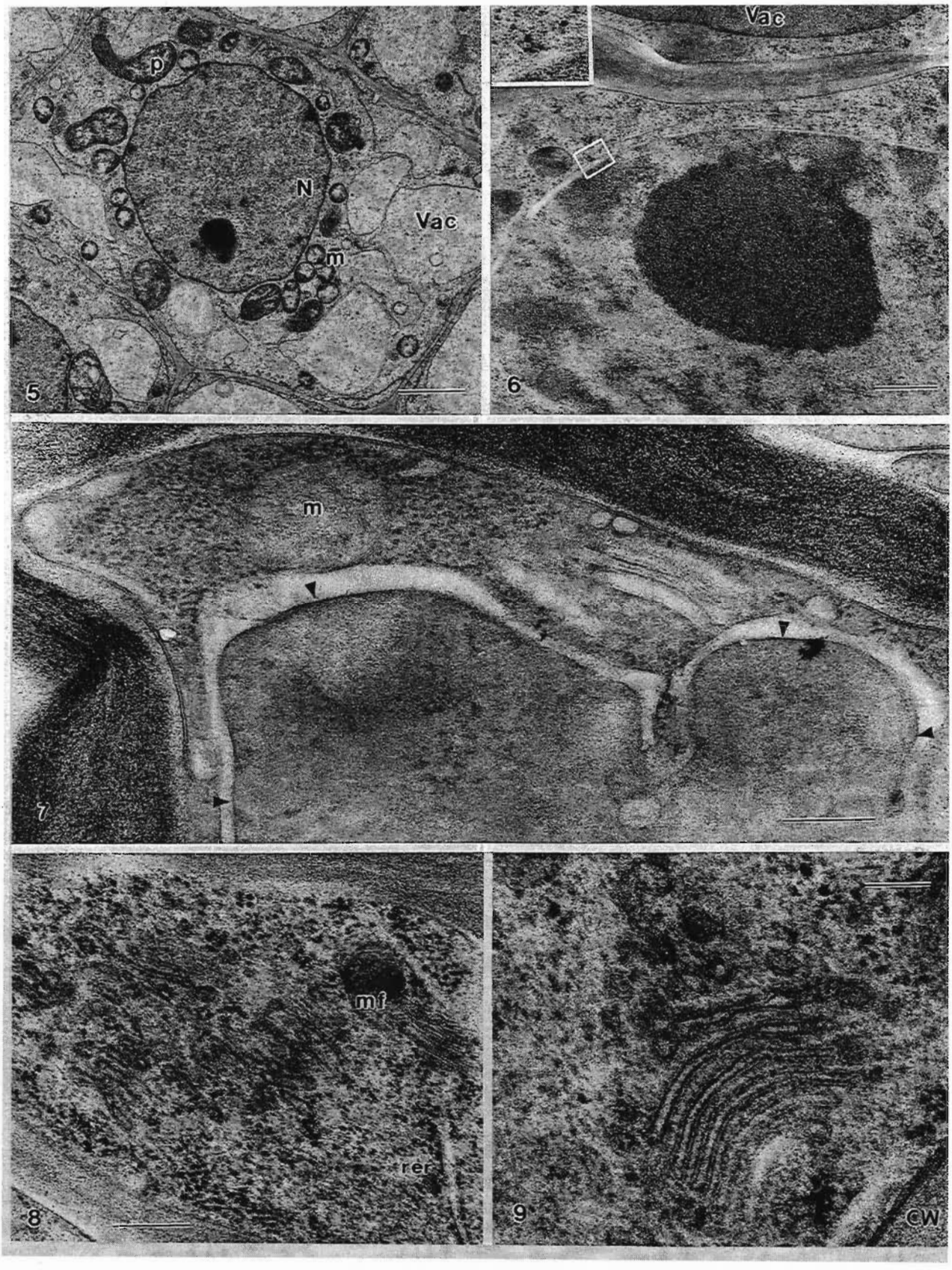
p
N
Vac
m
5
Vac
6
m
7
mi
rer
8
9
CW

Fig. 3.10. **FS**. Slow drying. Nuclei showed condensed chromatin not observed in rapidly dried axes. Golgi bodies (*G*), vesicles of presumed ER origin (*er*) and seemingly intact vacuoles (*Vac*) were observed. Evenly distributed ribosomal subunits gave the cytoplasm a dense appearance. Bar 0.25 μm

Fig. 3.11. **FS**. Slow drying. Cell dehydration led to a dense appearance of the cytoplasm and frequent folding of cell walls, bringing areas of the plasmalemma into close contact. In spite of this, the integrity and tri-laminar nature of tonoplasts and plasmalemma were maintained. ER profiles (*er*) were observed either as long cisternae or as concentric whorls (*arrowheads*). Bar 0.25 μm

Fig. 3.12. **FS**. Slow drying. A Golgi body (*G*) and surrounding matrix observed between a vacuole (*Vac*) and the cell wall (*CW*). Note the intact appearance of plasmalemma and tonoplast, as well as the electron translucent lumen of Golgi cisternae. Bar 0.1 μm

Fig. 3.13. **FS**. Slow drying. Evidence of autophagic inclusion of organelles into a vacuole or, alternatively, a highly convoluted vacuole in a slowly-dried cell. Bar 0.25 μm

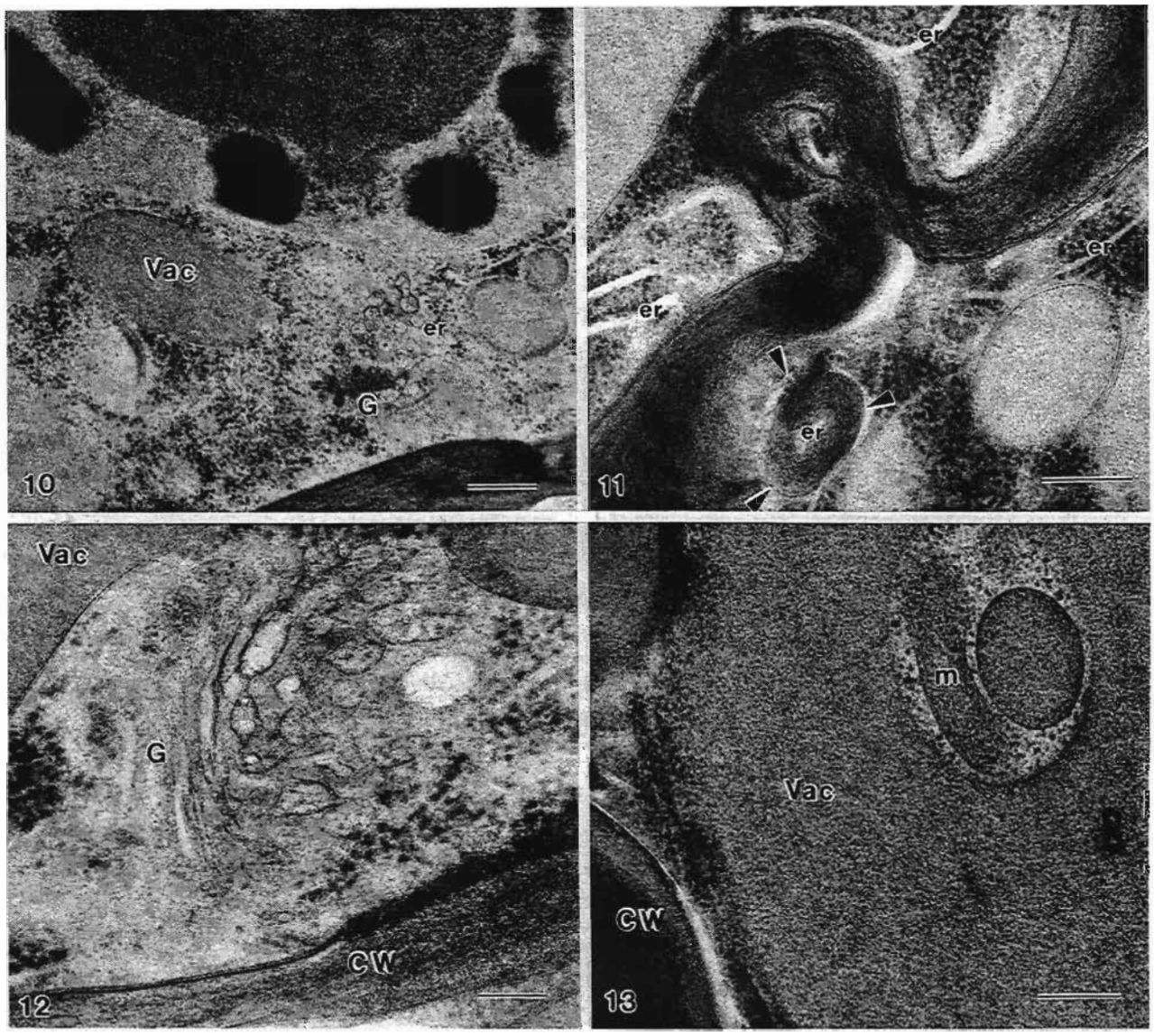
Vac
er
G
10
er
er
er
11
Vac
G
CW
12
m
Vac
CW
13

Table 3.2. One-way analysis of variance and LSD multiple range tests of vacuolar areas and cell sizes of variously manipulated axes. Each value represents the mean of measurements performed on >40 meristem and –derivative cells from five embryonic axes per treatment. Treatments within each measurement showing the same letters are not significantly different (P >0.05). The areas occupied by vacuoles were compared statistically (as described above) after transforming data by the formula log {p / (1 - p)}, where p= percentage / 100 (Dyke, 1997)

TREATMENT	AVERAGE ABSOLUTE VACUOLAR AREA ($\mu m^2 \pm SD$)	AVERAGE CELL SIZE ($\mu m^2 \pm SD$)	AVERAGE AREA OCCUPIED BY VACUOLES (% TOTAL)
Control	31 ±15 a	98 ±27 a	32 ±15 a
Rapid Drying (RD)	24 ±12 a	50 ±19 b	47 ±15 b
Slow Drying (SD)	20 ±13 a	36 ±17 b	49 ±16 b
RD and rehydrated	77 ±39 b	144 ±66 c	49 ± 14 b
SD and rehydrated	93 ±60 b	167 ±69 d	52 ± 15 b

Discussion

This investigation compared the physiological and ultrastructural properties of embryonic axes of jackfruit dried over a period of min or days. Rapid drying to 0.37 g g^{-1} (27% fmb) over 60 min resulted in 100% survival of axes, whereas none survived slow drying to this water content. These results contrast with the findings of Fu *et al.* (1993), who reported no survival of isolated jackfruit axes below 0.8 g g^{-1} (44% fmb) following drying under vacuum with activated silica gel at a rate equivalent to that presently attained using flash drying. It is likely that factors other than the drying rate *per se* (e.g. reduced pressure or anoxic conditions [Fu *et al.*, 1993]) were responsible for these contrasting results. Previous observations from this laboratory and other workers (Chandel *et al.*, 1995; Fu *et al.*, 1993; Thammasiri, 1999) have shown that drying rates slower than flash drying result in 40 – 80% mortality of jackfruit axes below 0.5 g g^{-1}. It is possible that the presumably faster flash drying method described here, and the limited time (≤90 min) spent at reduced water contents, may have facilitated 100% survival at 0.4 g g^{-1}, and 60% survival at 0.2 g g^{-1} (Fig. 3.2). This finding is supported indirectly by Chandel *et al.* (1995), who reported 60%

Fig. 3.14. CF. Rehydration following rapid drying. Meristematic cells resembled those from undried controls. Tonoplast and plasmalemma integrity was maintained. Bar 2 μm

Fig. 3.15. CF. Rehydration following rapid drying. ER profiles appeared fragmented and dispersed (*arrowheads*). Existing vacuoles, presumably damaged organelles and cytoplasmic ground substance were sequestered by enveloping ER cisternae, indicating autophagy and *de novo* vacuolation (*double arrowheads*) occurred in these cells. A second autophagic vacuole (*AV*) at a more advanced stage can also be seen. Bar 1 μm

Fig. 3.16. CF. Rehydration following slow drying. Dissolution of tonoplast, and mixing of vacuolar contents and the cytoplasm (*arrowheads*) was often observed. Other irregularities included clearing of the cytoplasm (*asterisks*) and localised distention of the nuclear envelope (*arrows*). Bar 1μm

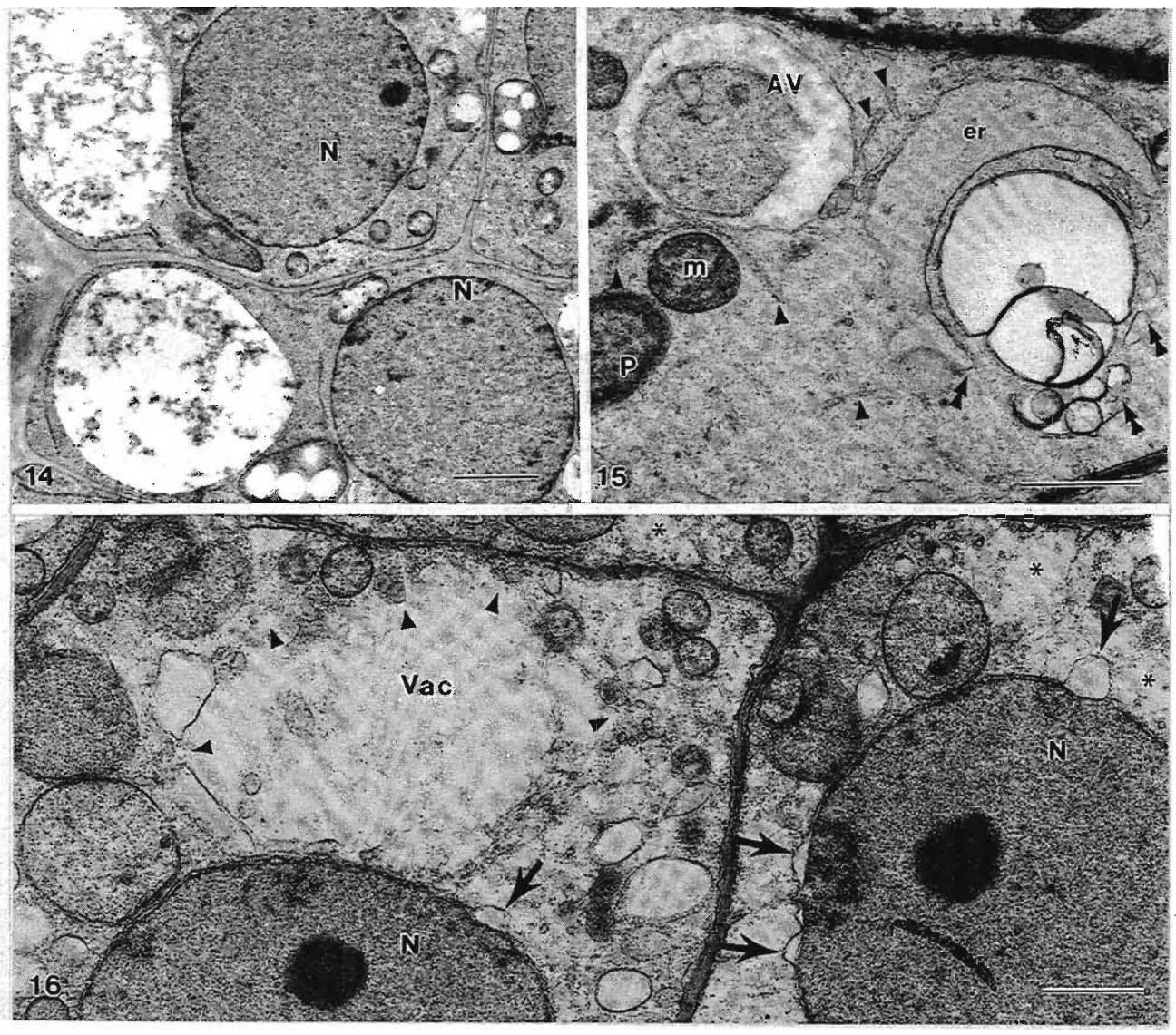
N
N
14
AV
er
m
P
15
Vac
N
N
16

survival of axes dehydrated to 0.15 g g^{-1} (13.7% fmb) within 120 min. In addition to drying rate, the variable lower limit of desiccation tolerance of jackfruit axes reported could also be due to differences in cultivars (Thammasiri, 1999) or developmental status (Chandel *et al.,* 1995).

Measurements of cell area indicated that the rate of drying determined the distribution of water among tissues of embryonic axes. This behaviour is analogous to that reported by Pammenter *et al. (*1998) for whole seeds of *Ekebergia capensis*, and could be explained as follows. A short (e.g. 30 min) exposure of axes to rapid drying resulted in the preferential withdrawal of water from the outermost tissue layers and a corresponding contraction of these cells, while those in the core of the axis (stele) remain relatively unaffected (Fig. 3.4). In contrast, slow drying over 2 - 3 d resulted in a more even distribution of water throughout the entire embryonic axis (Fig. 3.4). This finding has implications for axes dried slowly: core cells vital for survival and germination endure a greater degree of dehydration - and for longer periods - than similar cell in axes dried rapidly. On the other hand, cells from the epicotyl are relatively more exposed during drying than those of the hypocotyl. Failure (or a marked delay) to produce shoots in all axes dried by the methods described could have occurred because of greater dehydration of these cells, increased sensitivity to desiccation, rehydration, or a combination of these factors. The variable sensitivity of recalcitrant tissues to dehydration stress has been highlighted previously (Farrant *et al.,* 1986; Pritchard and Prendergast, 1986; Pence, 1992, 1995; Pritchard, 1991; Pritchard *et al.*, 1995; Pritchard and Manger, 1998; Berjak *et al.* 1999).

Increasing drying resulted in changes in electrolyte leakage and survival. In axes dried slowly, incipient metabolism-related damage (Pammenter and Berjak, 1999; Walters *et al.,* 2001) became apparent, indirectly by an increase in leakage and directly by a corresponding 15 - 20% decline in survival at *c.* 0.8-0.7 g g^{-1}, leading to complete mortality with further drying to 0.4 g g^{-1} (Fig. 3.2). In contrast, axes dried rapidly showed increased leakage only at 0.4 g g^{-1}, in agreement with previous observations for other species (Pammenter *et al.,* 1993). Full survival of axes at 0.4 g g^{-1} and even 60% survival at *c.* 0.2 g g^{-1} were attained, thus affirming the beneficial

rôle of rapid drying in reducing desiccation injury. Remarkably, Chandel *et al.* (1995) found no increase in leakage from jackfruit axes dehydrated to 0.15 g g^{-1}, and only a small increase following exposure of axes to -196°C in spite of decreased survival and visible ultrastructural damage. It is possible that the disruptions of membrane integrity observed in that study may have occurred during aqueous fixation of cells in the dehydrated state (e.g. Wesley-Smith, 2001; Chapter 2) and not during drying, cooling or rehydration.

Cells from partially hydrated axes prepared for TEM observation using conventional (aqueous) protocols usually show distorted cellular ultrastructure caused by rehydration that occurs during this process (Wesley-Smith, 2001; Chapter 2). Rehydration artefacts were avoided in the present study by the use of freeze-substitution, which facilitated ultrastructural preservation superior to that attained with other anhydrous preparative protocols for conventional TEM (Smith, 1991, and references therein). The superior preservation of plant structure attained by freeze-substitution is well documented (e.g. Staehelin and Chapman, 1987; Craig and Staehelin, 1988), which enhances the reliability of observations presently made on dehydrated tissues prepared by this method.

If the increase in leakage from axes dried slowly to 0.7 g g^{-1} were due to loss of membrane integrity, then it could be expected that transmission electron microscopy would reveal evidence of early stages of membrane breakdown. However, lesions were not immediately evident in cells after drying, as the plasmalemma and membranes of organelles and vacuoles appeared intact. Two explanations for this apparent contradiction are proposed. Membrane perturbations caused by slow drying may have been severe enough to increase membrane permeability, but insufficient to cause abnormalities visible at the ultrastructural level. Alternatively, disruptions of membrane structure may have occurred, but were not resolved in ultra-thin sections of resin embedded specimens at TEM level. Analogously, the plasmalemma in cells from of dry pea radicles appears intact in freeze-substitution preparations (Wesley-Smith, 2001; Chapter 2) and yet high electrolyte leakage occurs early during

imbibition (e.g. Simon and Raja Harun, 1972). However, membrane abnormalities were evident after rehydration in jackfruit axes previously dried slowly to 0.7 g g^{-1} (Fig. 3.16), suggesting that lesions may have occurred during drying, but required the presence of additional water to be manifested. A chemical (e.g. oxidative stress; Walters *et al.,* 2001) rather than physical (i.e. structural) damage is inferred from the observation that membrane abnormalities were most frequent in slowly dried axes in spite of both treatments having similar water contents.

Membranes are commonly proposed to be the primary site of desiccation injury (e.g. Senaratna and McKersie, 1986; Hoekstra *et al.*, 1989; Bryant *et al.*, 2001). The lowered water contents used here are greater than those reported to induce structural damage to membranes (equivalent to Ψ= -12 MPa; [Vertucci and Farrant, 1995]), and are therefore more likely to support lesions caused by dysfunctional metabolism (Leprince *et al.,* 1999, 2000; Vertucci, 1993; Salmen Espindola *et al.,* 1994; reviewed by Vertucci and Farrant, 1995; Pammenter and Berjak, 1999). Walters *et al.* (2001) have proposed that early damage caused by drying stress may be subtle and reversible although, given sufficient time at water potentials between -2 and -5 MPa (Leprince *et al.,* 2000; Walters *et al.,* 2002), can initiate events analogous to ageing and lead to cell death. Results from this study are in agreement with this view: although dehydrating cells to 0.7 g g^{-1} induced some ultrastructural disruption, this did not affect survival or cause membrane abnormalities if achieved within 30 min. The detrimental effect of longer drying time and lower water content on membrane integrity is emphasised by the contrasting survival and leakage of axes dried slowly (3 d) or rapidly (60 min) to 0.4 g g^{-1} (Fig. 3.2).

Cells from axes dried to 0.7 g g^{-1} over 30 min or ≥2 d shared many ultrastructural features, such as the presence of Golgi stacks, profiles of smooth and rough ER and relatively undifferentiated mitochondria in cortical areas. Other features were seen predominantly in material from one particular drying treatment and these are contrasted. In cells of axes dried rapidly, tubular and sheet-like cisternae of ER were seen closely associated with what are presumably vesicles and with plasmalemma,

as previously reported (Craig and Staehelin, 1988). Whether this association mediates an adjustment of the phospholipid composition of the plasmalemma (Staehelin and Chapman, 1987) or the removal of excess membranes in response to dehydration stress (Steponkus, 1984) cannot be established with certainty here. Similarly, cortical ER cisternae were observed closely associated with Golgi bodies (Craig and Staehelin, 1988) but the nature of this association in rapidly dried cells is speculative at present. Areas of cytoplasm (and occasionally organelles) sequestered within dilated ER cisternae (Fig 3.7; Matile, 1975; Hilling and Amelunxen, 1985) suggest the onset of *de novo* vacuolation in rapidly dried axes (discussed below). In contrast, most cells from axes dried slowly show condensed nuclear chromatin (Fig. 3.10), an event that was described as a sign of desiccation injury in germinating kernels of *Zea mays* (Crévecoeur *et al.*, 1976). Cytoplasmic polysomes dissociated into ribosomal subunits, in sharp contrast to the abundance of polysomes noted in cells dried rapidly. Additionally, ER cisternae in axes dried slowly often became re-arranged into concentric rings (Fig. 3.11), a phenomenon previously associated with cessation of growth in drought-stressed mustard seeds (Bergfeld and Schopfer, 1984), and with inhibition of protein synthesis in heat-shocked pollen tubes (Kandasamy and Kristen, 1989). These results strongly suggest the probable onset of metabolic stress in axes dried slowly, and that the ER may play a pivotal rôle during dehydration (e.g. Bergfeld and Schopfer, 1984). The dynamic and varied response of ER to stress has also been highlighted by conformational changes that occur during equilibrium freezing in parenchyma cells of cold-acclimated mulberry (Fujikawa and Takabe, 1996). Involvement of ER-derived structures in autophagy of cellular substrates is often observed in stressed cells, and this event has been suggested to be an important survival mechanism (Marty, 1999).

Autophagy was evident in cells of axes either dried rapidly or slowly, and could represent a mechanism to re-establish cellular homoiostasis. Autophagy of cellular reserves was reported to occur in plant cells during sucrose starvation as a mechanism to generate substrates for mitochondrial respiration (Aubert *et al.*, 1996; Moriyasu and Oshumi, 1996). It is possible that in the present investigation the

absence of an exogenous carbon source influenced the ultrastructural appearance of isolated embryonic axes, particularly those dried over 2-3 d. The autophagic digestion of mitochondria observed in slowly dried axes (Fig. 3.13) is in agreement with previous observations on plant cells stressed by sucrose deprivation (Journet *et al.*, 1986). However, autophagy and *de novo* vacuolation were also reported to occur in newly excised recalcitrant axes within 10 min of flash drying (Berjak *et al.*, 1989, 1990), suggesting that this process can be triggered almost immediately by signals other than reduced respiratory substrates. In partially hydrated, desiccation-sensitive cells autophagy probably provides a mechanism for the removal of structures that are either not immediately essential for survival or potentially susceptible to drying damage, or those damaged during drying (Berjak *et al.*, 1989). Hydrolysis of a variety of substrates during autophagy is likely to result in an increase of osmotically active solutes within cells, which possibly reduces water loss (reviewed by Walters *et al.*, 2002).

The absolute area occupied by vacuoles in meristematic and meristem-derived cells did not decrease on drying, and a significant increase over dried and undried cells occurred on axis rehydration (Table 3.2). It is conceivable that drying could lead to relatively higher solute concentrations within vacuoles, and that these compartments consequently become increasingly susceptible to osmotic swelling upon rehydration particularly after prolonged axis drying. The relatively greater propensity of slowly dried axes to osmotic swelling is indicated by the larger increase in cell size observed (Table 3.2). Although absolute vacuolar areas were similar after rapid or slow drying, evidence of tonoplast lysis was apparent in axes dried slowly (Fig. 3.16). Murai and Yoshida (1998) also reported increased sensitivity of vacuoles to rehydration in non-acclimated tubers of Jerusalem artichoke following freeze-dehydration. Vacuoles are critical to the maintenance of homoiostasis within cells (Marty, 1999) and loss of tonoplast integrity is usually considered lethal (e.g. Matile, 1975; Murai and Yoshida, 1998). The merits of slower rehydration protocols in ameliorating what could be imbibition-related must be weighed against the risks of prolonging the exposure of axes to intermediate water contents. Although axes of *Zizania palustris* appear to be

insensitive to the rate of rehydration (Vertucci *et al.*, 1995), partially dried axes of recalcitrant *Artocarpus heterophyllus, Podocarpus henkelii* and *Trichilia dregeana* seeds were harmed more by rehydration in a saturated atmosphere than over moistened filter paper or direct immersion in water (unpublished observations).

In conclusion, the evidence presented supports the contention that rapid drying increases the extent of water loss tolerated by recalcitrant material (Normah *et al.*, 1986; Farrant *et al.*, 1986; Berjak *et al.*, 1989, 1990; Pammenter *et al.*, 1991, 1998; Pritchard, 1991) by reducing the time of exposure to potentially-harmful intermediate water contents (reviewed by Vertucci and Farrant, 1995; Pammenter and Berjak, 1999; Walters *et al.*, 2001). Dehydration of recalcitrant axes to water contents facilitating cryopreservation should ensure the survival of at least a critical number of cells (Berjak *et al.*, 1999; Leprince *et al.*, 1999). Preferably, those cells should also enable the axes to initiate germination (Pritchard and Prendergast, 1986). This study shows that flash drying to sub-lethal water contents achieves this goal not only by reducing the time, but also the intensity of the dehydration stress to which most germinative cells are exposed. The advantages afforded by rapid drying, especially when combined with rapid cooling at $\geq 100°C\ s^{-1}$, has resulted in the cryopreservation of zygotic embryonic axes of recalcitrant (Wesley-Smith *et al.*, 1992, 2001; Berjak *et al.*, 1998, 1999; Chapters 4, 6, 8 and 9) and hydrated orthodox (Wesley-Smith *et al.*, 1995) seeds, as well as somatic embryos of both seed types (Mycock *et al.*, 1995).

CHAPTER 4*

Cryopreservation of embryonic axes of *Camellia sinensis* (tea): drying, cooling rates, and the thermal properties of tissue water

* Also published as Wesley-Smith J, Vertucci CW, Berjak P, Pammenter NW, Crane J. (1992) Cryopreservation of desiccation-sensitive axes of *Camellia sinensis* in relation to dehydration, freezing rate and the thermal properties of tissue water. *J. Plant Physiol.* **140**: 596-604

Introduction

The limited success of cryopreservation of recalcitrant species may be attributable to desiccation damage, freezing injury or a combination of both. Differential scanning calorimetry (DSC) was used to determine the types of water associated with these two types of injury (Vertucci *et al.,* 1989a,b; Pammenter *et al.,* 1991; Vertucci *et al.,* 1991; Berjak *et al.,* 1992). Removal of non-freezable water was linked to desiccation damage (Pammenter *et al.,* 1991; Berjak *et al.,* 1992). The presence of freezable water in embryonic axes of *Landolphia kirkii* was not necessarily linked to cooling injury if the water content of the axes was less than 0.58 g g^{-1} (Vertucci 1989a,b; Vertucci *et al.,* 1991). Above this water content, necrosis and decreased survival of axes in culture were associated with the presence of a sharp peak at about 0°C in melting thermograms of axes cooled to -70°C (Vertucci *et al.,* 1991). The correlation between the presence of the sharp peak and loss of viability led those authors to speculate that such a peak was indicative of the existence of a particular 'type' of water which was physiologically relevant to freezing damage.

Berjak *et al.* (1993) showed that the melting endotherms of embryonic axes of *Camellia sinensis* (L.) O. Kuntze (tea), flash dried to a range of water contents and cooled at 10°C min^{-1} to -70°C, lacked a sharp peak only at water contents below 0.44 g g^{-1}. Axes flash-dried to water contents less than about 0.40 g g^{-1} showed decreased survival in culture, even in the absence of cooling. Thus the optimal water contents for cryopreservation of tea axes cooled under these conditions, constitute an extremely narrow range which is flanked by desiccation damage on one side, and freezing injury (as indicated by a sharp peak) on

the other. Consequently efforts to cryopreserve tea axes using conventional methods might be hampered by the very narrow window of water contents facilitating survival of freezing, which will be referred to here as the 'permissible' water content range.

Traditional views on the cooling process have favoured slow cooling rates because these encourage the formation of a few, large extracellular ice crystals, over higher rates which result in a larger number of potentially-lethal freezing events both intra- and extracellularly (Meryman, 1956, 1966; Leibo and Mazur, 1971; Fahy *et al.,* 1984; Franks, 1985). In spite of this, rapid cooling has been used to cryopreserve single cells (Moor and Mühlethaler, 1963; Anderson *et al.,* 1966; Mazur and Schmidt, 1968; MacKenzie, 1970; Rebhun and Sander, 1971; Nei, 1977;) and 20-30 μm sections of plant tissues (Sakai, 1966, 1968, 1970). These studies applied the methodology used during cryo-microscopical specimen preparation, where sufficiently rapid cooling can reduce or eliminate visible ice damage within cells. An assumption underlying survival studies using that approach is that by preserving cellular structure, function should also be preserved (Sherman and Kim, 1967; Fujikawa, 1988). While the general consensus (e.g. Farrant *et al.,* 1977b; Franks, 1980; Finkle *et al.*, 1985) is that slow cooling (<0.1°C s^{-1}) promotes the retention of viability and rapid cooling (>>100 °C s^{-1}) the preservation of ultrastructure, both disciplines have the avoidance of cell damage as their common goal. Given that the relatively slow cooling rates used in conventional protocols (*c.* 3 °C s^{-1}; Vertucci, 1989a) restrict survival of recalcitrant embryonic axes to only a narrow range of characteristically-low water contents (see Table 2.1), it was decided to test whether rapid cooling could increase the range of permissible water contents by delaying the onset of freezing damage to higher levels.

One of the prerequisites for cooling sufficiently rapidly to restrict freezing is a small specimen not exceeding 1.0 mm^3 (Stephenson, 1956; Robards, 1974; Robards and Sleytr, 1985; Ryan and Purse, 1985) but preferably close to 0.1 mm^3 (Bailey and Zasadzinski, 1991). Sample size must be kept to such dimensions to ensure an adequate cooling rate throughout the specimen. However, working with such minute specimens is impractical in the context of cryopreservation of recalcitrant embryonic axes. Partially drying the tissue reduces the heat capacity of the tissue and encourages the formation of

glasses in seed tissues (Vertucci 1989b, 1990; Williams and Leopold, 1989; Meryman and Williams, 1980; Leprince and Walters-Vertucci, 1995; Buitink *et al.,* 1996; Williams *et al.,* 1993). Thus, it is suggested that the conditions for optimal cooling may be achieved in larger specimens by partially drying the sample.

The present study was the first of a series of cryopreservation studies exploring the interaction among water content, cooling rate and survival of axes from different species. This study tested whether the rate of cooling to liquid nitrogen temperatures affects the properties of water in embryonic axes of tea and whether or not this is relevant to their survival. Embryonic axes were flash dried to various water contents and subsequently cooled at three different rates, viz. slow (10 C min^{-1}), intermediate (200 C min^{-1}), and rapidly cooling by plunging the specimens into sub-cooled nitrogen. Calorimetric properties of the water present in the axes were recorded by differential scanning calorimetry; ultrastructural preservation was evaluated by freeze-fracture electron microscopy; and survival after cooling of axes was monitored by *in vitro* culture.

Materials and Methods

Plant Material and Drying Treatment

Fruits of *Camellia sinensis* (L.) O. Kuntze were harvested in the Mpumalanga Province of South Africa and transported by air under temperature/pressure-controlled conditions to Fort Collins, CO. USA. Time from harvest to receipt of the materials in Fort Collins did not exceed 7 days. Seeds were immediately removed from their fruits, stored at 6°C and used within 2 weeks of arrival.

Embryonic axes were excised and placed on moist filter paper prior to transfer to the flash drying chamber (Berjak *et al.,* 1990), in which they were dried for 0 to 100 minutes in a stream of compressed air with a flow rate of 10 l min^{-1}. This treatment gave water contents ranging from *c.* 3.1 to 0.10 g g^{-1} dry mass basis. Due to the very high variability of initial water content of recalcitrant seeds, the water content quoted following a particular flash drying treatment is best described by a range rather than a single value.

Differential scanning calorimetry (DSC)

The differential scanning calorimeter compares a sample sealed within an Al pan with a thermally-inert reference pan (i.e. without a sample), and measures the difference in the amount of energy required to heat the two at the same rate (Hirsh *et al.*, 1985; Williams *et al.*, 1993), typically 10°C min^{-1} (e.g. Vertucci 1989a,b; Vertucci *et al.*, 1991). The difference in heat flow between sample and reference pan is displayed as a graph of power (mW) *vs.* temperature (°C). The release of latent heat of fusion during freezing is represented in DSC thermograms by a decrease in power required to maintain the specified cooling rate. Conversely, increased heat input is required to maintain a constant rate of warming as a sample melts, and this is represented as a peak above the baseline. The enthalpy associated with freezing or melting transitions can be evaluated by the area under the curve below or above the baseline, respectively.

To determine if the thermal characteristics of water were altered by cooling rate, DSC warming thermograms from -150 to 20°C of whole axes of tea were recorded with a Perkin Elmer DSC-7 (Perkin Elmer, Norwalk, CT, US) at a scanning rate of 10°C min^{-1}. The DSC was calibrated for temperature using indium (156.6°C) and methylene chloride (-96.5°C) standards, and for energy using indium (27.6 J g^{-1}). Scans of empty Al pans were used to correct for baseline curvature.

Individual axes (sample size of about 1 to 2 mg) of varying water contents were cooled to -160°C at 10°C min^{-1}, at about 200°C min^{-1}, or rapidly cooled. Specimens cooled at 10 or 200°C min^{-1} were hermetically sealed in aluminium pans. The 10°C min^{-1} cooling rate was achieved through programmed cooling in the DSC. The 200°C min^{-1} treatment was achieved by pre-cooling the sample holder of the DSC to -160°C and then loading the sample: this came to temperature (-160°C) in slightly less than 1 min. Very rapid cooling was achieved by securing the axes to the lid of an open DSC pan by means of double-sided adhesive, and rapidly immersing into liquid nitrogen (-196°C) with fine forceps and immediately releasing the axis-lid assembly. (The latter was done so that the specimen did not act as a sink for heat originating from the forceps, which would have reduced the cooling rate of the axes (see Ryan and Purse, 1985b). The complete DSC pan was then

assembled under liquid nitrogen, the sides of the bottom half of the pan being bent over the lid to secure good thermal contact with the specimen. The DSC pan was maintained immersed in the cryogen until it was transferred to the previously cooled stage of the instrument.

Immediately after a warming scan was recorded, the sample plus pan was weighed. The pan was then punctured and heated at 95°C for 36 h and re-weighed. Water content is expressed on a dry weight basis (g g^{-1}).

Warming thermograms were analysed for onset temperature and energy of the endothermic transitions. Onset temperatures were determined as the point of intersection between the baseline and the steepest portion of the peak. The energy of each transition was determined from the area above the baseline. For each cooling rate, the enthalpy per dry weight was regressed against the water content. X-intercepts and slopes of the resulting lines were used to determine the amount of water that did not freeze, and the energy of the melting transition per g of water that froze (Vertucci, 1990).

In some cases, a sharp peak in the melting endotherm was apparent at about 0°C. The presence of this peak has been reported previously and its analysis was described in those papers (Pammenter *et al.,* 1991; Vertucci *et al.,* 1991; Berjak *et al.,* 1992, 1993). Briefly, the area of this transition was calculated separately from the area of the main melting transition and expressed as a function of the water content of the sample. The amount of water associated with the sharp peak was then calculated for a given water content by assuming that the heat of fusion to be 333 J g^{-1} H_2O. In this way, the partitioning of water in the main melting transition and in the sharp peak could be determined as a function of the water content of the tissue.

Electron Microscopy

Freeze-fracture electron microscopy of tea axes was used to assess the degree of ultrastructural preservation attained by the different cooling rates. Embryonic axes, flash dried to various water contents, were mounted on gold planchettes, secured onto ultramicrotomy specimen supports from a Reichert cryo-ultramicrotome (Leica, Vienna,

Austria), and these propelled into sub-cooled liquid nitrogen by means of compressed air generated by a simple spring-loaded piston device. Lowering the temperature of the liquid nitrogen from -196 to -210°C was achieved by placing this cryogen under vacuum (as described by Echlin, 1992). The nitrogen slush thus obtained delays the onset of nucleation boiling around the sample (Leidenfrost phenomenon) that impairs the efficiency of the cooling step. The axes were covered with a thin film of glycerol seconds before cooling since this has been reported to enhance cooling rates in cryogens that exhibit nucleation boiling (Cowley *et al.,* 1961; Luyet, 1961; Robards and Sleytr, 1985)[2]. The term rapid cooling is used here in preference to 'ultra-rapid cooling' since the latter pertains to other methods where higher cooling rates are attained (Gilkey and Staehelin, 1986). An alternative cooling method consisted of immersing specimens mounted on gold planchettes held with forceps into a 15 mm well of melting Freon 22. Although cooling rates were not measured in this study, from subsequent work (see Chapter 5), it is estimated that axes plunged into sub-cooled nitrogen cooled at hundreds of °C s^{-1} and at approximately 50-100°C s^{-1} when plunged into Freon 22.

The specimens were fractured and replicated at -105°C with a Balzers BAF 301 freeze-etching system. Uni-directional shadowing with platinum and rotary carbon coating was carried out within 5 min after fracturing. Specimens were then warmed, and the replicas cleaned by placing in an aqueous chromic acid-sulphuric acid solution (50% v/v) overnight, followed by the full strength mixture for no less than 2 h. Replicas from two axes were collected on 600 mesh copper grids and viewed with JEOL 100 C (JEOL Ltd., Tokyo, Japan) transmission electron microscope at 100 kV.

Survival studies

To determine if rate of cooling to liquid nitrogen temperatures affected survival, tea axes flash-dried to different water contents and cooled at different rates were placed in culture

[2] Even brief exposure to glycerol can induce rapid cellular dehydration in excised biological tissues (Staehelin, pers. comm.), therefore it is possible that the water content of axes at the time of cooling may have been lower than presently reported. However, the likelihood of large discrepancies from the ranges reported was presumably minimised by the presence of an intact the waxy cuticle covering the axis, unlike the situation in excised tissues where diffusion of glycerol is relatively unimpeded by a similar barrier.

and assayed for survival. As detailed above, axes were cooled at 10°C min^{-1} or 200°C min^{-1} in the DSC, while rapidly cooled axes were cooled in sub-cooled nitrogen. All axes were thawed in MS liquid culture medium (Murashige and Skoog, 1962) at 20°C. Axes were allowed to equilibrate in distilled water for 30 min, after which they were surface-sterilized in 1:3 (v/v) dilution of commercial bleach (NaOCl) and 0.2% (v/w) Hibitane (Hibiclens; Stuart Pharmaceuticals, Willmington, DE) for 10 min, rinsed twice in sterile distilled water and placed on a supplemented, solid MS medium. Survival, as indicated by greening and organ development, was assessed at weekly intervals.

Results

The thermal characteristics of water in embryonic axes of tea flash-dried to various water contents and then cooled at slow (10°C min^{-1}), intermediate (200°C min^{-1}) and rapid rates were determined by DSC. Melting endotherms of representative specimens dried to different levels and then cooled at different rates are given in Figures 4.1 – 4.3. Thermograms can be divided into three categories: those that lack an endothermic peak (water contents less than 0.23 g g^{-1}), those with a broad endothermic peak with an onset temperature between -7 and -50°C, and those with an additional sharp peak with onset temperature of about -2°C. The onset temperature of the broad endothermic peak was similar for axes with water contents greater than 0.6 g g^{-1} (Fig 4.4). At water contents less than 0.6 g g^{-1}, onset temperature decreased sharply with water content. There appeared to be no differences in the temperature of the transition for axes of similar water contents that were cooled at different rates. The onset temperature of the sharp melting transition was -2°C and did not vary with water content (Fig. 4.4); This peak was more prevalent in axes cooled at 10°C min^{-1} than it was for axes cooled at faster rates.

Figs 4.1 - 3. Melting thermograms of tea embryonic axes flash-dried to different water contents and cooled to -160°C at 10°C min^{-1} (Fig. 4.1) or 200°C min^{-1} (Fig.4.2), or to *c* -210°C by the rapid cooling method (Fig. 4.3). Thermograms are recorded during warming at 10°C min^{-1}. The figures above each curve indicate axis water content. Note the presence of a sharp peak at low cooling rates and/or high water contents.

Fig. 4.4. Onset temperature of the melting of water in tea axes dried to different levels and cooled at different rates. Onset temperatures of the transitions given by the sharp peaks (illustrated in Figs 1 and 2) are represented by the circled symbols.

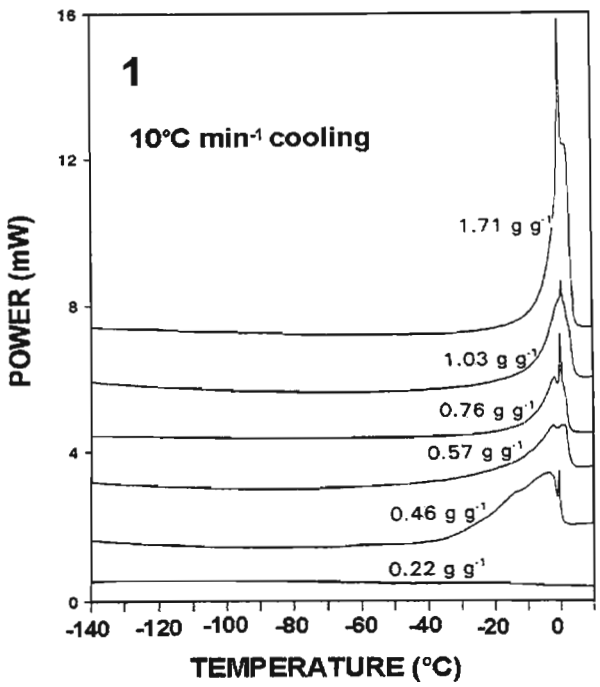
1
10°C min-1 cooling
1.71 g g-1
1.03 g g-1
0.76 g g-1
0.57 g g-1
0.46 g g-1
0.22 g g-1
POWER (mW)
TEMPERATURE (°C)

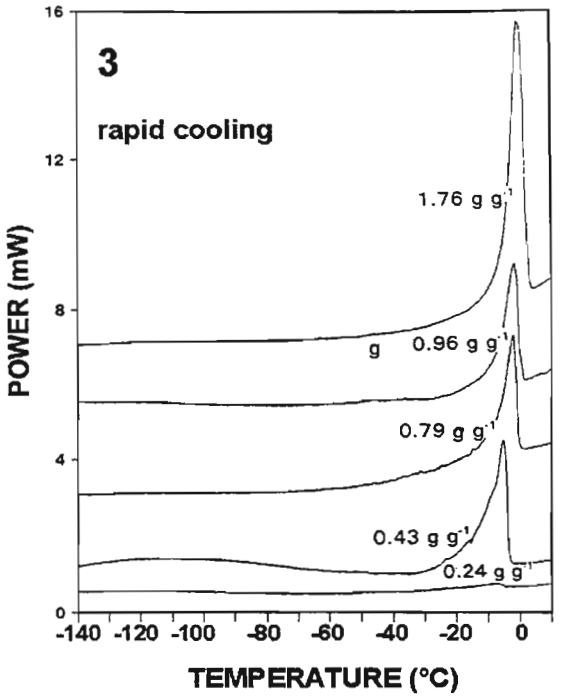
3
rapid cooling
1.76 g g-1
0.96 g g-1
0.79 g g-1
0.43 g g-1
0.24 g g-1
POWER (mW)
TEMPERATURE (°C)

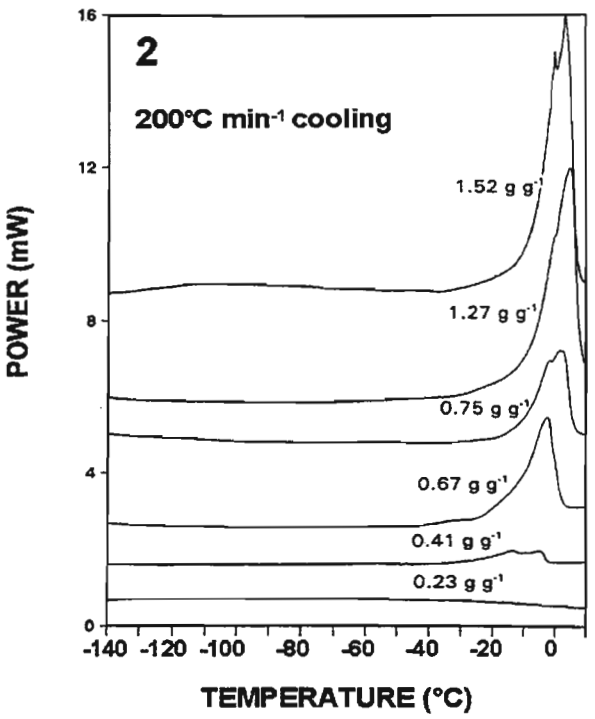
2
200°C min-1 cooling
1.52 g g-1
1.27 g g-1
0.75 g g-1
0.67 g g-1
0.41 g g-1
0.23 g g-1
POWER (mW)
TEMPERATURE (°C)

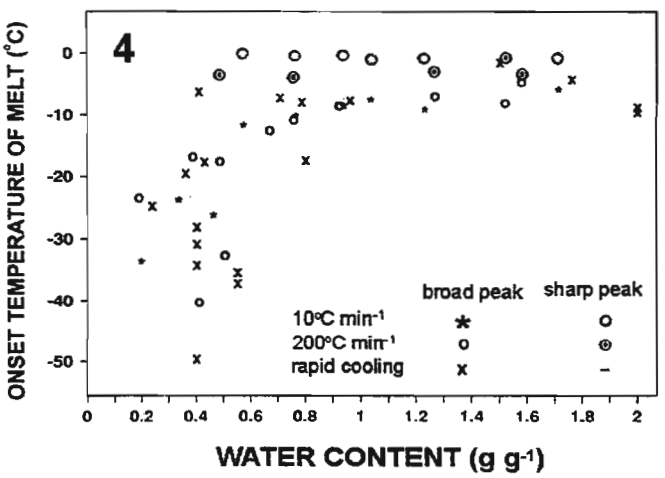
4
broad peak
sharp peak
10°C min-1
200°C min-1
rapid cooling
ONSET TEMPERATURE OF MELT (°C)
WATER CONTENT (g g-1)

To determine the amount of water that did not freeze and the heat of fusion of the water that did freeze, the enthalpy of the melt was regressed against the water content (Fig. 4.5). As reported previously for other species (Vertucci, 1989a; Pammenter *et al.,* 1991; Vertucci *et al.,* 1991; Berjak *et al.,* 1992), the relationships were linear (R^2 = 0.997, 0.994, and 0.972 for 10°C min^{-1}, 200°C min^{-1} and rapid cooling, respectively), and the lines were indistinguishable for the different cooling rates (slope = 303, 304, and 338 J g^{-1} H_2O, respectively). The water content at which no melting transition occurred was also similar among the cooling treatments (x intercept = 0.22, 0.23, and 0.21 g g^{-1}, respectively). Small endothermic transitions with energies ranging from 0.2 to 1.0 J g^{-1} dry mass were often observed at about -120, -80 and -60°C (data not shown). However, there was no apparent change in the energy or temperature of these transitions with either water content or cooling rate.

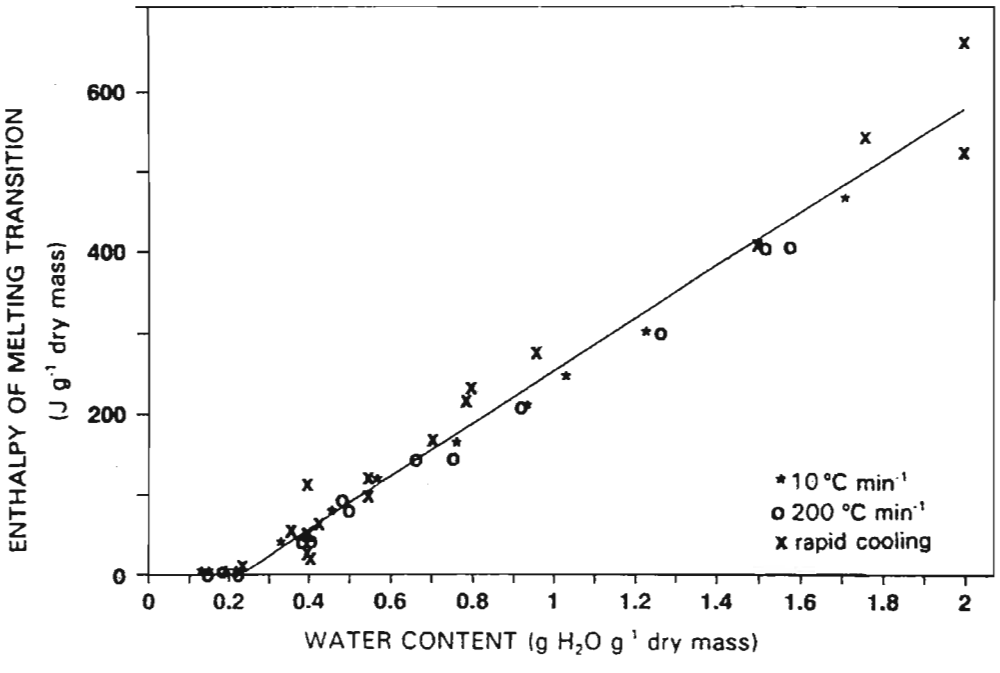

Fig. 4.5. The relationship between water content and the enthalpy of the melting transition of tea axes dried to the different levels and cooled at three rates. Lines are drawn from the least squares fit of the data collected from each cooling rate.

In view of the similarity among the temperature and energies of the melting transitions, and the water contents below which these transitions were not present, it might be assumed that there were no differences in the calorimetric properties of the water in specimens cooled at different rates. However, there was a sharp peak at about -2°C that was most prominent in fully hydrated axes cooled at 10°C min^{-1} and which was not present in rapidly cooled axes (compare Figs 4.1 and 4.3). The sharp peak was less pronounced as axes were dried to lower water contents or cooled at faster rates (Figs 4.1 – 4.3). These trends are expressed as the change in the ratio of water associated with the sharp and broad peaks (Fig. 4.6). In axes cooled at 10°C min^{-1}, the ratio declined from 0.075 at high water content to zero at a water content of 0.44 g g^{-1}. In specimens cooled at 200°C min^{-1}, the maximum value was 0.01, and no sharp peak was present at water contents below 0.8 g g^{-1}. There was no sharp peak in the melting endotherm of axes that were rapidly cooled, irrespective of the water content. Thus, the ratio of water in the sharp peak relative to the broad peak remained constant at 0.

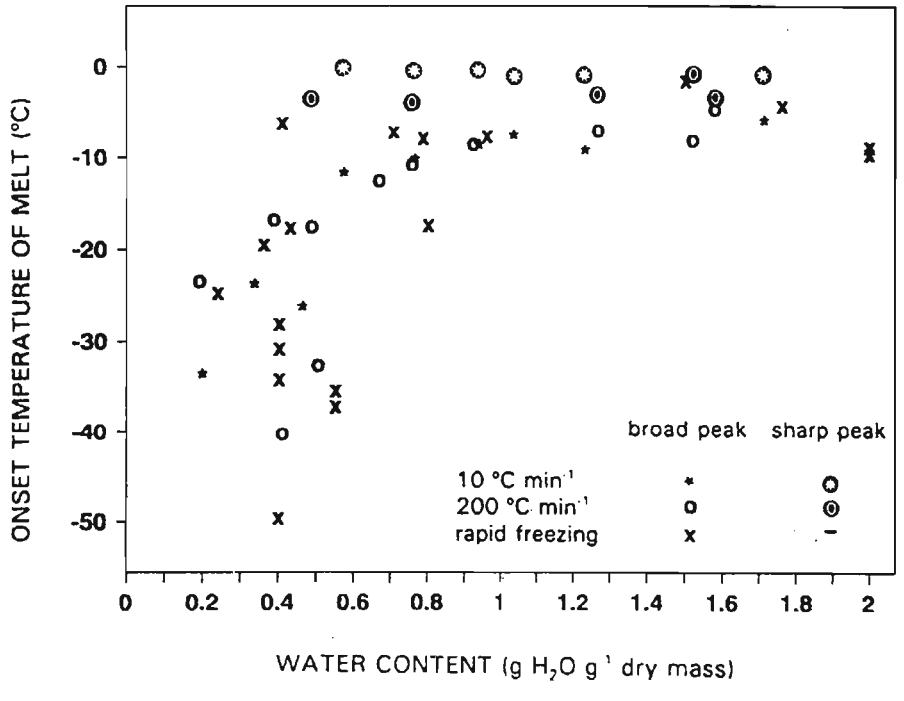

Fig. 4.6. The ratio of the amount of water represented in the sharp peak of the melting endotherm relative to the broad peak for axes dried to different levels and cooled at different rates.

Electron microscopy of freeze-fracture replicas demonstrated the significance of cooling rates on the ultrastructural preservation, as well as the pivotal role played by the water content of the axes. In order to prevent freezing damage, the time spent by hydrated specimens between 0°C and temperatures that preclude ice crystal growth should be minimised. Axes cooled rapidly by plunging into sub-cooled nitrogen showed evidence of ice damage at water contents >1.6 g g^{-1} (Figs 4.7, 4.8). The presence of ubiquitous ice crystals of *c.* 125 nm throughout intracellular compartments obscured fine detail. Nuclei were easily recognised, but identifying other organelles was difficult because of the extensive damage to membranes observed. Ultrastructural damage observed in fully hydrated axes was closely matched by nil survival of such axes *in vitro* (Table 4.1).

Cells flash dried for 20 min to between 1.6 – 1.1 g g^{-1} and cooled rapidly showed no evidence of freezing damage, attested by the high degree of cellular order observed (Figs 4.9 -12). Nuclei, vacuoles and organelles had smooth contours, and no ice inclusions were seen where the plane of fracture exposed the interior of these compartments (Fig. 4.9). Replicas obtained from these axes revealed close association between ER cisternae and vacuoles (Fig. 4.10) than observed in control material (not shown; see Berjak *et al.*, 1989). This phenomenon is also reported to occur in partially dried jackfruit axes (Chapter 3), and suggests *de novo* vacuolation and autophagy. ER profiles were also observed close to well-developed and preserved Golgi cisternae (Fig. 4.11). No evidence of freezing artefacts were observed within the interior of organelles from most of cells examined, even at very high magnifications (Fig. 4.11,12). While membranes in some cells did not share the same smooth profiles those shown here, the absence of damage to these axes is supported by the 100% survival of axes *in vitro* (Table 4.1)

Axes dried for 60 min to 0.7 – 0.4 g g^{-1} and cooled rapidly also showed no signs of freezing damage, although the cytoplasm of these cells was visibly compacted (Figs 4.13,14). *De novo* vacuolation was apparent in these cells, and different stages of autophagy could be seen (Fig. 4.13). In spite of the reduced water status of cells from embryonic axes of tea

Fig. 4.7. Fully hydrated tea axis, rapidly cooled. Meristem-derivative cell showing ubiquitous cavities formed by ice crystals. It is difficult to identify cellular detail other than cell walls and the nucleus (N). Scale bar= 2 μm.

Fig. 4.8. Fully hydrated tea axis, rapidly cooled. Ice crystals averaging 125 μm gave the ground cytoplasm and membrane bounding cellular compartments a rough appearance. Scale bar= 1 μm.

Fig. 4.9. Axes dried for 20 min to 1.6 – 1.1 g g^{-1}, rapidly cooled. The plasmalemma and cellular compartments had smooth profiles, indicating the absence of visible ice crystal damage in these cells. N, nucleus; pl, plasmalemma; V, vacuole; CW, cell wall. Scale bar= 2μm.

Fig. 4.10. Axis dried for 20 min to 1.6 – 1.1 g g^{-1}, rapidly cooled. High degree of structural integrity was preserved. ER cisternae were often closely associated with vacuoles in these partially hydrated cells. N, nucleus; er, endoplasmic reticulum; mf, microfilaments; V, vacuoles. Scale bar= 0.5 μm.

Fig. 4.11. Axis dried for 20 min to 1.6 – 1.1 g g^{-1}, rapidly cooled. Well-developed Golgi stacks (G) and ER cisternae (er) were often seen in close proximity. Scale bar= 0.25 μm.

Fig. 4.12. Axis dried for 20 min to 1.6 – 1.1 g g^{-1}, rapidly cooled. No freezing artefacts or membrane discontinuities were seen in organelles, such as the oil body depicted, even a high magnifications. Scale bar= 0.1 μm.


N
7

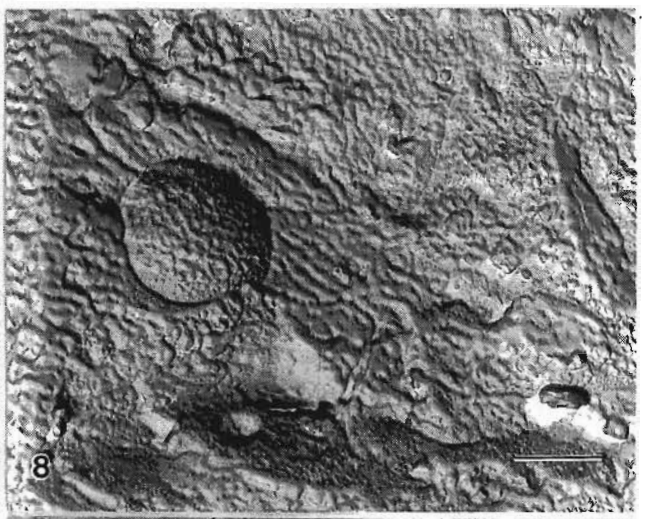
8

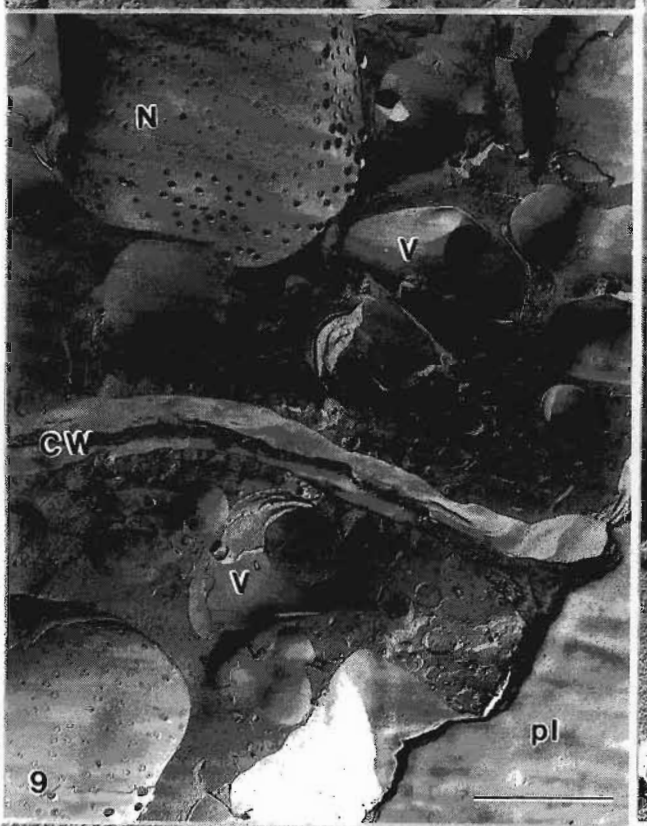
N
V
CW
V
pl
9

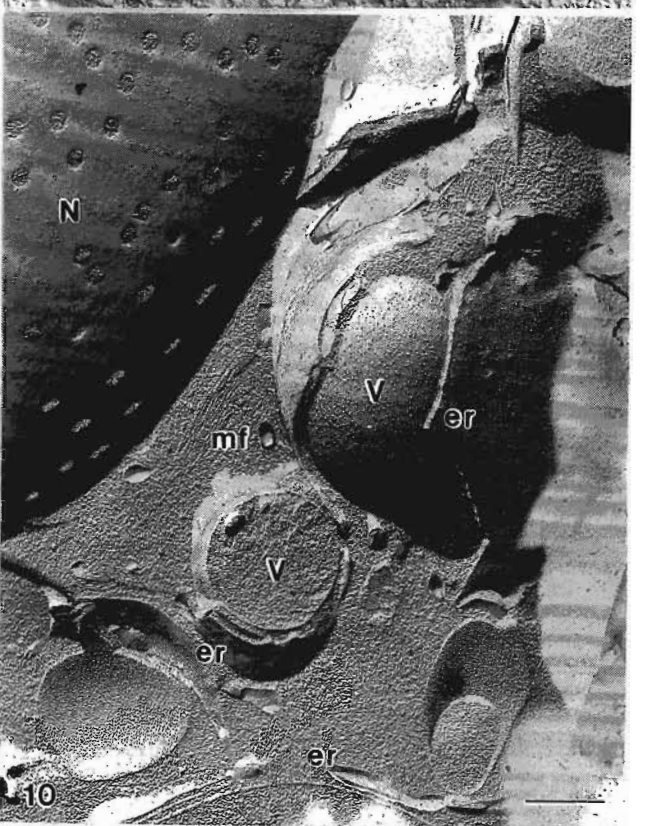
N
V
er
mi
V
er
er
10

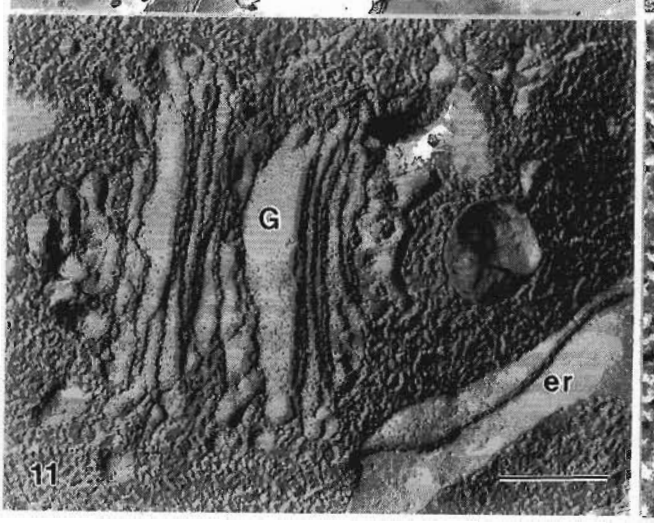
G
er
11

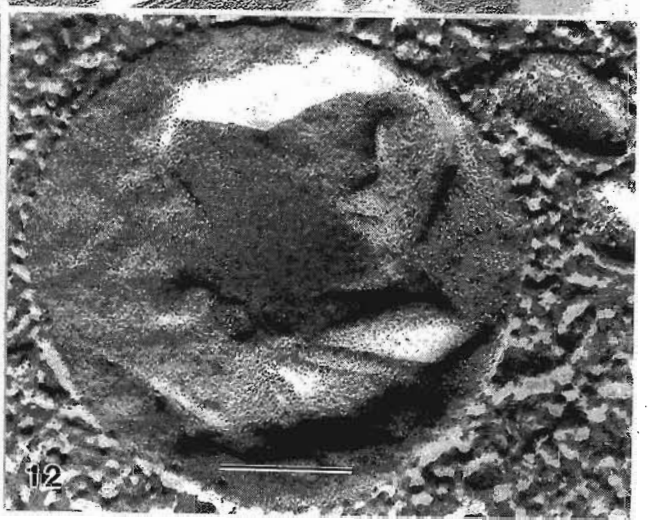
12

seeds, the plasmalemma remained appressed to the cell wall, as also reported for dehydrated axes of other species (Chapters 2, 3).

Axes dried to 1.1 - 0.7 g g^{-1} and cooled in a 15 mm well of molten Freon 22 revealed extensive freezing damage (Fig. 4.7). Freeze-fracture replicas of similarly cooled axes showed extensive segregation of ice and cytoplasmic solution (Figs 4.15,16). It was difficult to identify cellular detail other than cell walls. While the size of ice crystals varied even among adjacent cells (e.g. Fig. 4.15) survival of these axes was low (Table 4.1). Further drying below 0.7 g g^{-1} resulted in reduced freezing damage and a corresponding increase in survival *in vitro* (Table 4.1), although the preservation attained in freeze-fracture replicas did not approximate that attained at equivalent water contents using rapid cooling.

Results of the survival studies are shown in Table 4.1. As described for *Landolphia kirkii* (Vertucci *et al.,* 1991), the responses of embryonic axes in culture could be divided into three broad categories: a. those axes which became necrotic and died within 48 to 72 h after culturing; b. those which showed no signs of necrosis but did not green within a period in excess of 2 months; and c. axes which became green and developed roots and shoots with leaves within 4 weeks in culture.

The viability of *Camellia sinensis* axes flash-dried to different water contents and not cooled (control) declined as water contents approached 0.40 g g^{-1}. Irrespective of the water content, axes cooled at 10°C min^{-1} became necrotic unless dried to the minimum water content tolerated, where only 5% survival was recorded. Survival of axes cooled at 200°C min^{-1} increased as the water content was lowered from 1.1 to 0.40 g g^{-1}. The range of water contents of axes that survived compressed-air plunging into sub-cooled nitrogen broadened to 0.40 - 1.6 g g^{-1}. Axes flash-dried for 20 min to water contents of between 1.6 and 1.1 g g^{-1} showed 100% survival when cooled by this method, with the first instance of expansion and greening occurring after 3 weeks in culture. Rapid cooling of axes dried to lower water contents resulted in relatively slower recovery in culture and also decreased survival. Some of the axes, particularly those at intermediate water contents cooled at intermediate rates, survived but did not show visible germination presumably due to

Fig. 4.13. Axes dried for 60 min to 0.7 – 0.4 g g^{-1}, rapidly cooled. Ultrastructural integrity was preserved, although the cytoplasm was visibly compacted. Note the high density of vesicles in the ground cytoplasm, presumably from disrupted ER and Golgi stacks. Evidence of autophagy (arrowheads) and *de novo* vacuolation was seen. V, vacuole; N, nucleus; AV, autophagic vacuole. Scale bar= 0.5 μm.

Fig. 4.14. Axes dried for 60 min to 0.7 – 0.4 g g^{-1}, rapidly cooled. Partial drying brought cytoplasmic organelles into close contact. N, nucleus; P, plastids; V, vacuole; AV, autophagic vacuole. Scale bar= 0.5 μm.

Figs 4.15 and 16. Axes dried for 40 min to 1.1 – 0.7 g g^{-1} and cooled (while held with forceps) in Freon 22. Cooling at intermediate rates caused severe ice damage, and obscured cellular detail. Neighbouring cells show the presence of ice crystals of different sizes. CW: cell wall. Scale bars in 4.15 and 4.16= 1 μm

Figs 4.17 and 18. Axes dried for 60 min to 0.7 – 0.4 g g^{-1} and cooled (while held with forceps) in Freon 22. This extent of drying reduced freezing damage, but seemingly did not eliminate it completely. pl, plasmalemma. Scale bars, 4.17= 2 μm, 4.18= 0.5 μm.

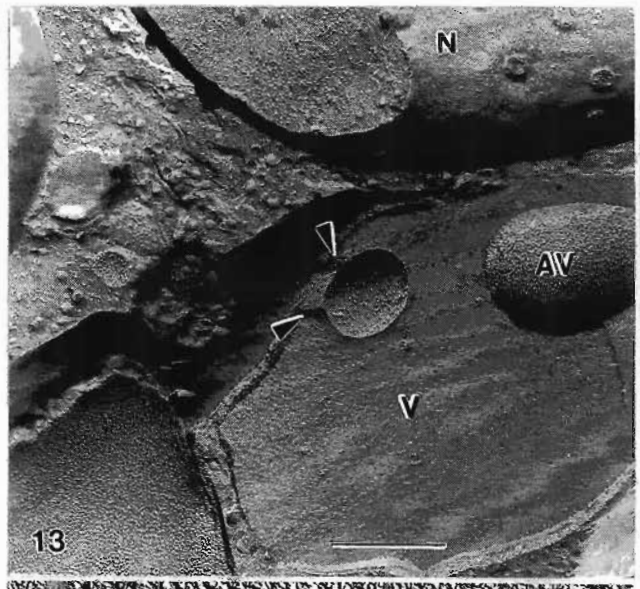
N
AV
V
13


N
AV
V
P
P
14

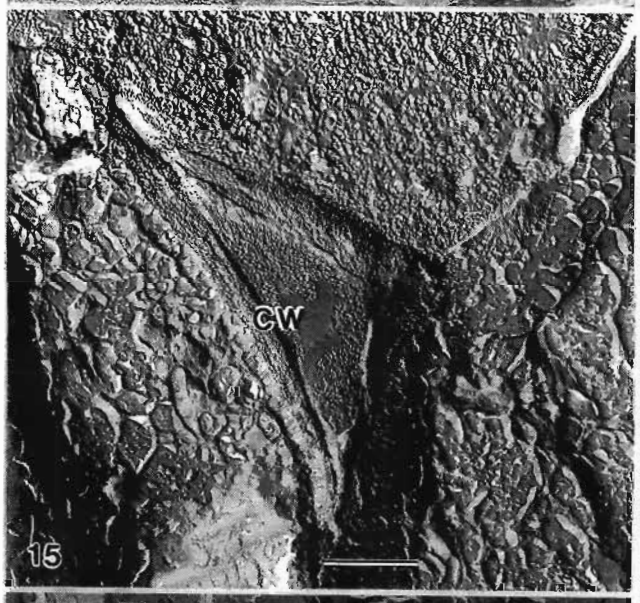
CW
15

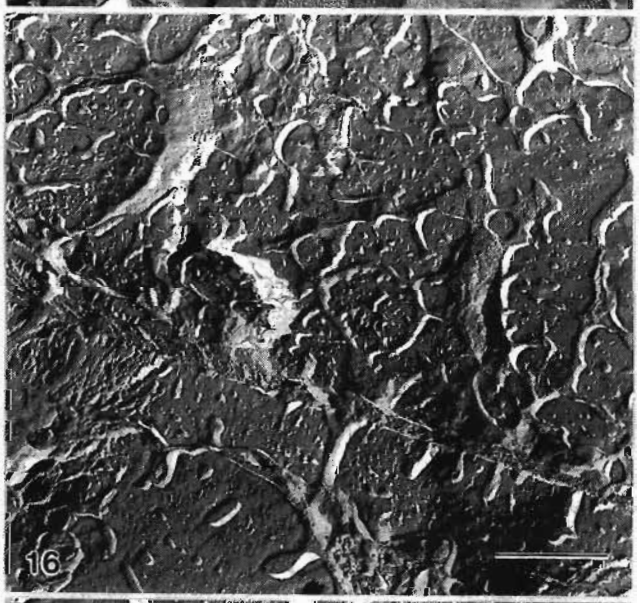
16


17

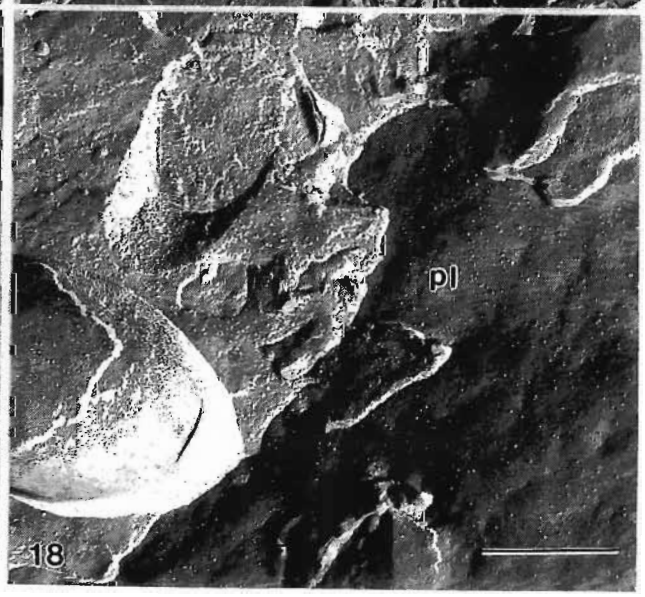
PI
18

freezing injury. Epicotyl necrosis and decreased survival were observed in rapidly cooled axes dried for periods exceeding 20 min. In view of the fact that axes flash-dried to similar water contents in the absence of cooling did not show this damage suggests that a combination of desiccation damage and cooling stress occurred.

Table 4.1. Survival of embryonic axes *in vitro* as a function of water content and rate of cooling to -196°C. Number of axes surviving per treatment are indicated in parenthesis. ns= not studied

DRYING TIME (min)	WATER CONTENT ($g\ g^{-1}$)	CONTROL	10°C min^{-1}	200°C min^{-1}	rapid cooling
0	≥1.6	100% (9/9)	ns	0% (0/10)	0% (0/10)
20	1.6 – 1.1	ns	0% (0/10)	0% (0/10)	100% (8/8)
40	1.1 – 0.7	100% (10/10)	0% (0/14)	20% (2/10)	50% (5/10)
60	0.7 – 0.4	80% (20/25)	5% (1/19)	60% (6/10)	59% (10/17)
>60	0.4 – 0.3	67% (10/15)	14% (4/28)	ns	ns

Discussion

In this study calorimetry, electron microscopy and *in vitro* studies have been combined in order to understand the interacting effects of water content and cooling rate on cooling tolerance of embryonic axes of *Camellia sinensis*. The rapid cooling method utilized here aimed to avoid - or at least minimise - the size of ice crystals formed within cells. Maximum survival was achieved when axes dried below 1.6 g g^{-1} were rapidly injected into sub-cooled nitrogen (Table 4.1). Manipulating parameters such as the thermal load of the axes following partial drying, as well as that of cooling rates attained by different cooling procedures increases present understanding of biophysical aspects involved in the cryopreservation of germplasm.

DSC studies indicate that comparable amounts of water froze in tissues at similar water contents irrespective of the cooling procedure used (Fig. 4.5). However, the presence of a sharp peak in melting thermograms appeared to be particular to the 10°C min^{-1} treatment

at water levels above 0.44 g g^{-1}, and to axes above 0.80 g g^{-1} if cooled at 200°C min^{-1}. *In vitro* survival of axes treated similarly was low, and freeze-fracture replicas revealed ultrastructural damage in axes at > 0.7 g g^{-1} cooled at intermediate rates (Fig. 4.15,16). These findings are in agreement with trends observed for *L. kirkii* (Vertucci *et al.,* 1991), supporting the hypothesis that the presence of a sharp peak in the melting endotherms is invariably associated with lethal cooling injury. Ultrastructural studies revealed that cooling conditions that gave rise to sharp peaks in melting endotherms of cooled axes also resulted in extensive freezing damage. Therefore, it is suggested that the presence of sharp peaks at 0°C may arise from the melting of pure water sequestered within ice crystals during cooling. Since cooling rate and the frequency of nucleation are inversely related (Meryman, 1956, 1966), it is probable that crystals formed during slow cooling may have been large enough to disrupt cellular integrity, and also sufficiently large to be detected by the DSC (sharp peak) during melting. Conversely, the absence of a sharp peak in rapidly cooled axes below 1.6 g g^{-1} does not necessarily mean that ice crystals did not form. It is possible that freezing occurred, but that rapid cooling limited their growth within harmless dimensions and also below detectable levels, in agreement with the suggestion that the presence of intracellular ice is not necessarily lethal (Albrecht *et al.*, 1973; Sherman and Kim, 1967; Mazur and Schmidt, 1968; Mohr and Stein, 1969; Sakai, 1968, 1970; Mazur *et al.,* 1969; Asahina *et al.,* 1970; Bank and Mazur, 1973; Bank, 1974; Vertucci, 1989a; Vertucci *et al.,* 1991, 1995). The extent to which cells tolerate intracellular freezing, and can repair damage induced during this process, is likely to determine survival of axes following cryogenic exposure. The presence of a sharp peak may indicate freezing to an extent that is beyond repair.

If this is true, then the analysis of water partitioning in the sharp and broad peaks of the melting endotherms may be a predictive tool for determining the range of water contents that maximize the cryopreservation of recalcitrant germplasm (Vertucci *et al.,* 1991). The water content at which the onset of desiccation damage occurs will thus determine the lower limit tolerated, although this boundary may need to be higher during exposure to low-temperature stress (Vertucci and Roos, 1993; Vertucci *et al.,* 1994, 1995). At the opposite extreme, the ability of cells to repair freezing damage and give rise to organised growth will

probably determine the upper limit of permissible water content of embryonic axes. Therefore, if tea axes suffer desiccation-induced damage at water contents below 0.40 g g^{-1} (Berjak *et al.*, 1993) and a sharp peak is observed above 0.44 g g^{-1} when they are cooled at 10°C min^{-1} (Fig. 4.1), then the predicted permissible water contents extend between 0.40 and 0.44 g g^{-1}, representing an exceedingly narrow window. Faster cooling resulted in the sharp peak occurring at relatively higher water contents. While the minimum water content tolerated remained unchanged at 0.4 g g^{-1} in axes cooled at 200°C s^{-1} or by rapid injection, the upper limit varied between these treatments. Axes cooled at 200°C min^{-1} survived exposure to -160°C at water contents that ranged between 0.4 and 0.7 g g^{-1}. Survival of axes at the drier end of this range was 60%, decreasing to 0% at water contents above 1.1 g g^{-1}. Rapid cooling extended the window of optimal water content even further, resulting in maximum survival of axes flash dried for 20 min to *c.* 1.6 g g^{-1} (Table 4.1).

Rapid cooling of fully hydrated axes resulted in complete mortality, and freeze-fracture replicas revealed ice crystals averaging 125 nm diameter throughout compartments and in the ground cytoplasm of all cells examined (Fig. 4.7,8). Freezing damage observed was presumably caused by their inability to dissipate the relatively large heat load sufficiently rapidly before extensive freezing occurred. In contrast, the complete survival of rapidly cooled axes at 1.6 – 1.1 g g^{-1} was mirrored by a high degree of ultrastructural preservation in freeze-fracture replicas (Figs 4.9,10). Most cellular structures showed smooth profiles, suggesting a complete absence of ice crystal damage. Long ER cisternae were often closely associated with vacuoles (Fig. 4.10), presumably in response to drying as was also noted for jackfruit axes (Chapter 3). The absence of freezing damage is attested by the visibly intact 3-dimemsional arrangement of Golgi stacks (Fig. 4.11). Freeze-fracture replicas of tea axes dried to 0.7 – 0.4 g g^{-1} revealed vacuoles, organelles and vesicles (presumably of endomembrane origin) which, although intact, were visibly compacted in the cytoplasm of these cells (Fig. 4.13,14). Different stages of autophagy could be seen: an early stage indicated by arrowheads in Figure 4.13, and a more advanced stage (AV) in both Figures 4.13 and 4.14.

Slower cooling rates were deleterious to axes, especially at higher water contents. Cooling axes by plunging into molten Freon was clearly slower than that attained by the compressed-air method, as suggested by the segregated appearance of the cytoplasm observed in replicas from axes even at 1.1 – 0.7 g g^{-1} (Fig. 4.15, 16). Drying to 0.7 – 0.4 g g^{-1} ameliorated the extent of freezing damage observed (Fig. 4.17), and this was supported indirectly by the 60% survival *in vitro* of axes cooled at 200°C min^{-1} (Table 4.1). In spite of this, the ultrastructure of these cells lacked the orderly appearance observed in rapidly cooled axes at equivalent water contents (*cf.* Figs 4.18 and 4.4.14, respectively).

It has been suggested that even brief (<5 s) exposure of axes to undiluted glycerol may have permeated axes sufficiently to reduce the water status and suppress crystallisation in and around cells of embryonic axes, thus explaining the high survival and ultrastructural appearance observed (Staehelin, pers. comm.[3]) However, it is contended that the presence of an intact cuticle around axes is likely to have hindered both dehydration and permeation of tissues (see footnote on page 74). Moreover, efforts were made to observe replicas from cells well within the core of axes, and not just those along the periphery which would have also been exposed to relatively faster cooling. The seemingly paradoxical greater preservation of axes cooled in sub-cooled nitrogen than those cooled in Freon 22 is presently attributed to the longer convective cooling phase attained with the compressed-air injection method than to the suppression of freezing by glycerol. Notwithstanding this, the possible cryoprotective role of glycerol cannot be discounted in the absence of measurements of cooling rates, or water content after glycerol was applied.

Evidence suggests the benefits conferred by partial drying are many-fold. Firstly, partial drying reduces the thermal load of the axes, allowing these to traverse rapidly the critical range of temperatures supporting ice crystal growth. Secondly, the range of the critical temperatures supporting crystallisation is reduced, as the freezing point is lowered (Rasmussen *et al.,* 1975; Meryman and Williams, 1980; Becwar *et al.,* 1983; Vertucci,

[3] **Prof. L.A. Staehelin, Department of Molecular, Cellular and Developmental Biology, 347 University of Colorado, Boulder, CO 80309-0347**

1990; Wesley-Smith *et al.,* 1992; Farrant and Walters, 1998; Pritchard *et al.,* 1995) and the glass transition temperature is raised (Buitink *et al.,* 1996; Leprince and Walters-Vertucci, 1995, Meryman and Williams, 1980; Williams and Leopold, 1989; Williams *et al.,* 1993). Thirdly, drying increases cytoplasmic viscosity, and therefore hinders the process of ice crystal growth by reducing the intracellular mobility of water (Luyet *et al.,* 1962; Williams *et al.,* 1993; Buitink *et al.,* 1998b, 2000; Leprince and Hoekstra, 1998; Leprince *et al.,* 1999).

Although partial drying facilitates survival of axes by minimising freezing damage, survival of axes cooled rapidly decreased at lower water contents (Table 4.1). This suggests the existence of stresses other than those induced by ice damage alone. *In vitro* studies showed epicotyl necrosis was common in cryopreserved axes after drying for periods longer that 20 min, although regeneration of damaged tissues took place once growth was resumed. No browning occurred in axes cryopreserved for 20 min flash-drying, nor in axes flash-dried for longer in the absence of cooling, which suggested epicotyl tissues were increasingly sensitive to sub-zero temperatures at water contents below 1.1 g g^{-1}. It is possible that cells of these tissues may have been prone to phase transitions of molecules other than water during cooling and warming. Transition temperatures of polar lipids in membranes increase with decreasing water content (reviewed by Bryant *et al.*, 2001), and seed lipids *in vivo* have transition temperatures as low as -90°C (Vertucci, 1989a,b). It has been suggested that lipid phase transitions may be an important factor in the viability of desiccation-sensitive tissues (reviewed by Bryant *et al.*, 2001). Embryonic axes of *Landolphia kirkii* dried to water contents where freezing transitions were not observed showed 40% survival when cooled to -70°C (Vertucci *et al.,* 1991) but did not survive exposure to -150°C at any water content when cooled slowly (data not published). Similarly, an additional decline in survival following cooling was observed in embryonic axes of the temperate recalcitrant species *Aesculus hippocastanum* when dried to water contents of about 0.2 g g^{-1} (Pence, 1992). Those observations are consistent with the suggestion that phase transitions of cellular macromolecules may be responsible for damage when axes dried to levels approaching their limit of desiccation tolerance are exposed to very low temperatures.

CHAPTER 5

Measurement of rapid (non-equilibrium) cooling and warming in biological tissues: effects of equipment and handling procedures

Introduction

Achieving (ultra) rapid cooling of hydrated biological specimens is critical to restrict the growth of ice crystals to within a microcrystalline domain (<5 – 10 nm; Moor, 1973; Robards and Sleytr, 1985) and thus preserve the native ultrastructure free from freezing artefacts (Robards, 1974; Robards and Sleytr, 1985; Gilkey and Staehelin, 1986; Echlin, 1992). Stringent conditions are required to meet this goal, such as specimens not exceeding 0.1 mm linear dimension (Bailey and Zasadzinsky, 1991) and conditions ensuring the highest attainable rates of heat transfer during cooling to cryogenic temperatures (Bald, 1987). Many workers (cited below) applied similar principles to survival studies based on the postulate that avoiding freezing damage during cooling and warming would result in both, function as well as structure being preserved upon warming. The enthusiasm initially sparked by the rapid cooling (vitrification) approach pioneered by Luyet and co-workers (Luyet 1960, 1965, 1966; Luyet *et al.*, 1962) was gradually replaced by scepticism, as the difficulty to achieve sufficiently-rapid cooling to prevent lethal damage in cryobiological specimens became apparent (e.g. Meryman, 1957, 1960, 1966; Farrant *et al.*, 1977b). Results from studies where sufficiently rapid cooling was attained were encouraging, although success was limited to only single cells (Moor and Mühlethaler, 1963; Moor, 1964; Anderson *et al.*, 1966; MacKenzie, 1970; Rebhun and Sander, 1971; Plattner *et al.*, 1972; Albrecht *et al.*,1973; Nei, 1977; Fujikawa, 1988) and 20 – 30 μm thick sections of plant tissues (e.g. Sakai, 1966, 1970; Sakai and Otsuka, 1967), and excluded many cell types (e.g. Luyet and Keane, 1955; Shimada and Asahina, 1972a).

Variability

Since the advent of low temperature methods in biological microscopy (see Robards [1974] for an early review), followers of this approach have sought to develop

procedures that facilitate the high cooling rates required to prevent freezing damage (Elder *et al.*, 1982; Costello and Corless, 1978; Moor, 1971; reviewed by Bald, 1987; Ryan,1992). However, the findings of many of those studies could not be compared directly because different specimens and cooling conditions result in very different cooling rates attained. Measurements of cooling rate varied even under similar cooling conditions (see review by Ryan, 1992), probably because cooling data were acquired using temperature probes with different sensitivities (Robards and Sleytr, 1985). Variability is aggravated if specimens exceed *c.* 0.1 mm linear dimension because temperature gradients develop within specimens during non-equilibrium cooling, which means that cooling profiles measured vary depending on the position of the thermocouple within the specimen (Bald, 1975, 1987,1993; Bald and Crowley, 1979). Likewise, the size of the resulting crystals also varies throughout the specimen, being smaller near the periphery and in the centre of a specimen, and largest in between these regions (Van Venrooij *et al.*, 1975). Therefore, it is not surprising that attempts to narrowly define the size of intracellular ice crystal 'critical' to survival of cells cooled ultra-rapidly were frustrated by the extensive variability in cooling rates and consequently in the ice crystal sizes that resulted (e.g. Nei 1976a, 1977).

The extent of variability can be reduced, and comparisons become possible, if mechanical devices are used in preference to manual plunging procedures. Mechanical devices have been shown to increase reproducibility during rapid cooling of biological specimens (Echlin and Moreton, 1976; Costello and Corless, 1978; Robards and Sleytr, 1985). Additionally, information regarding the physical properties of the sample and thermocouple, entry velocity into the cryogen, depth of plunge and temperature of the bulk cryogen should accompany the cooling data, thus providing other workers with a basis for comparison of results (Bald and Robards, 1978; Robards and Sleytr, 1985). This information increases reproducibility of results across laboratories, providing benchmarks that may lead to refinements in the cooling conditions that facilitated the cooling rates required to avoid freezing injury.

Heat transfer

High cooling rates can be achieved if a steep temperature gradient is maintained at the boundary between the tissue and the cryogen (Stephenson, 1956; Gilkey and Staehelin, 1986; Bachmann and Mayer, 1987; Bald, 1987) and the tissue is small. During plunging, heat is removed rapidly by forced convection as the temperature at the interface is maintained close to that of the bulk coolant by the continuous exposure to 'cold' cryogen (Robards and Sleytr, 1985; Bald 1984, 1987). Varying the flow of cryogen over the surface of specimens (travel velocity) and the time during which this takes place (depth of plunge) influences the cooling rate attained (Bald, 1984; Le Murray *et al.*, 1989). Under favourable conditions, the whole specimen approaches the temperature of the bulk cryogen before the end of the plunge. Failure to achieve this results in a shift in heat transfer at the boundary from forced convection (which dissipates heat rapidly) to conduction, which is slower (Bald, 1984, 1987). Heat is likely to build-up as the freezing boundary advances into the specimen, and the latent heat of fusion released has to traverse increasing distances to be dissipated at the boundary with the cryogen (Meryman, 1956, 1960). Extensive ice crystal growth is a likely outcome under these sub-optimal cooling conditions.

Modelling heat transfer in biological tissues is extremely challenging (Meryman, 1966; Bald, 1987). Because of the anomalous behaviour of supercooled water (MacKenzie, 1977; Franks, 1980) and the release of latent heat of fusion upon freezing (Meryman, 1956, 1957, 1966; Bald, 1975, 1987; Bald and Crowley, 1979) it is almost impossible to predict accurately the amount of heat to be dissipated from a specimen during cooling (Bachmann and Mayer, 1987). Many theoretical approaches have attempted to reduce this complexity by modelling heat transfer based on measurements gathered using metallic spheres or blocks of gelatine (e.g. Ryan and Purse, 1985b; Han *et al.*, 1995). However, the value of such studies to cryobiology is limited by the fact that metals and biological tissues have very different thermal diffusivities (Bald, 1984, 1987). Moreover, gelatine blocks cannot truly represent the complex freezing behaviour of membrane-bound compartments within living cells (Meryman, 1966; Banks, 1974; Mazur, 1977, 1984; Franks, 1980) or cells from different tissues.

Therefore, it seems that the complex response of biological tissues to cryogenic cooling can only be approximated at best, and preferably if measurements are gathered from living cells instead of inert materials.

Since water is the largest reservoir of heat in tissues (Bachmann and Mayer, 1987), reducing the water content also reduces the amount of heat to be dissipated, and thus facilitates faster cooling. While partial drying of specimens is discouraged in studies investigating native cell ultrastructure (Gilkey and Staehelin, 1986), in survival studies drying is exploited to reduce the likelihood lethal freezing damage. The study on tea axes (Chapter 4) illustrates the role played by partial drying, and furthermore showed that the extent of drying required varied according to the rate of cooling to cryogenic temperatures. Since cooling rates of axes plunged into sub-cooled nitrogen were not measured, that study could not identify minimum cooling rates associated with increased survival *in vitro*, nor to what extent the dry mass of the specimen would influence such critical rates. The ability to acquire temperature data reliably is essential before the relationship between cooling rate and survival can be explored.

The aim of the present work is to describe a procedure designed to cool embryonic axes of recalcitrant species to cryogenic temperatures under controlled experimental conditions. A spring-loaded device that propels axes and an associated temperature-sensing probe into a cryogen container facilitates rapid cooling of axes for survival, and reliable assessment of the temperature during cooling, under identical plunging conditions. These measurements provide a yardstick to manipulate variables reported to affect the cooling rates within specimens, such as plunging velocity, cryogen type and depth of plunge (Elder *et al.*, 1982; Robards and Sleytr, 1985; Bald, 1987; Ryan, 1992). In particular, the present study investigated

1. The influence of thermocouple size on the cooling and warming rates recorded either within biological tissues of known physical properties or using bare thermocouples

2. The effects of various parameters such as depth of plunge, entry velocity and type of cryogen on the cooling rate recorded using bare thermocouples, or within biological tissues of similar sizes to that of embryonic axes
3. The influence of tissue water content on cooling rates
4. The warming rate within biological tissues, and the likelihood of undesirable warming occurring during handling prior to recovery from cryostorage

Materials and methods

Rapid cooling device and data recording

The plunging apparatus described is based on the cryofixation device of Ryan and Purse (1985a). A diagram of the complete cooling device and data acquisition hardware is shown in Figure 5.1. This spring-loaded device facilitates plunging of axes into a container filled with a cryogen cooled within a bath of liquid nitrogen (Fig. 5.1 a). Cryogen containers were made from copper tubes of 55, 100, 160 or 240 mm in length and 14, 20, 20 and 25 mm inner diameter, respectively, sealed at their lower end, and supported by a metal bracket. Cryogens that froze at -196°C were maintained at a temperature close to their melting point by heat supplied externally. This was achieved using thermal coax wire, coiled in an insulated compartment around the inner container, and which acted as a resistor for current supplied by a custom-built variable power source attached (0-30 V, 0-3 A; [Fig. 5.1 b]).

Axes were mounted singly on cryo-ultramicrotomy specimen supports (Leica, Austria) using a small quantity of low temperature adhesive. Supports with axes were placed inside a plastic sleeve at the lower end of a spring-loaded steel rod (2 mm diameter; [Fig. 5.1 c]). Undesirable pre-cooling of the sample was avoided by two means. Firstly, specimens were loaded at the end of the plunging rod only after this assembly was swung radially away from the cold nitrogen-gas layer above the Dewar container. Secondly, the sample was plunged when a simple catch-release mechanism was operated within seconds after the cryogen container was raised to the top liquid nitrogen

bath and the plunging assembly was returned into position approximately 20 mm above the cryogen. An adjustable threaded fastener along the upper portion of the plunger controlled the depth of travel, in accordance to the depth of the cryogen container.

The rate of cooling in the core of axes was measured using an insulated thermocouple embedded within the hollow interior of a sample holder (Fig. 5.1 c). The position of the thermocouple was adjusted so that only the length required to place the junction in the centre of the tissue protruded outside the holder, thus reducing the likelihood of spurious measurement of temperature during cooling (Bald, 1975; Costello and Corless, 1978; Robards and Sleytr, 1985). Since tissues of even size were used in the present study, this step also ensured that the junction was inserted consistently to the same depth in all specimens. The insulated thermocouple leads ran parallel with the length of the plunging rod and connected to a high-speed amplifier (HSTC 240; Reid and Associates, South Africa; [Fig. 5.1 d]) that amplified the mV range generated at the junction to a corresponding 0 to 10 V scale. Cold-junction compensation provided a reference for temperature measurements, and the amplifier was accurate to 0.4°C over the full measurement range (+35 to -210°C) with piecewise linear approximation (4 breakpoints and 5 segments). The output from the amplifier fed one of the inputs of an HS 508 dual channel oscilloscope (Tie Pie, The Netherlands; [Fig. 5.1 e]). The second channel was used to estimate the velocity of the plunge, as described next.

Velocity during plunging was measured using an infrared sensor and a photodiode assembly secured to the top of the plunger. These elements were mounted facing each other on either side of a rigid film which acted as a guide and consisted of 10 mm opaque squares separated by 1 mm transparent segments (Fig. 5.1 f). Movement of the sensor assembly past transparent regions in the film during the plunge generated voltage pulses that were fed into the second channel of the oscilloscope and displayed synchronously with temperature data. Thus, the start and end of the

plunge could be determined, and velocity calculated by the time separating consecutive pulses, each pair representing a plunging distance of 10 mm.

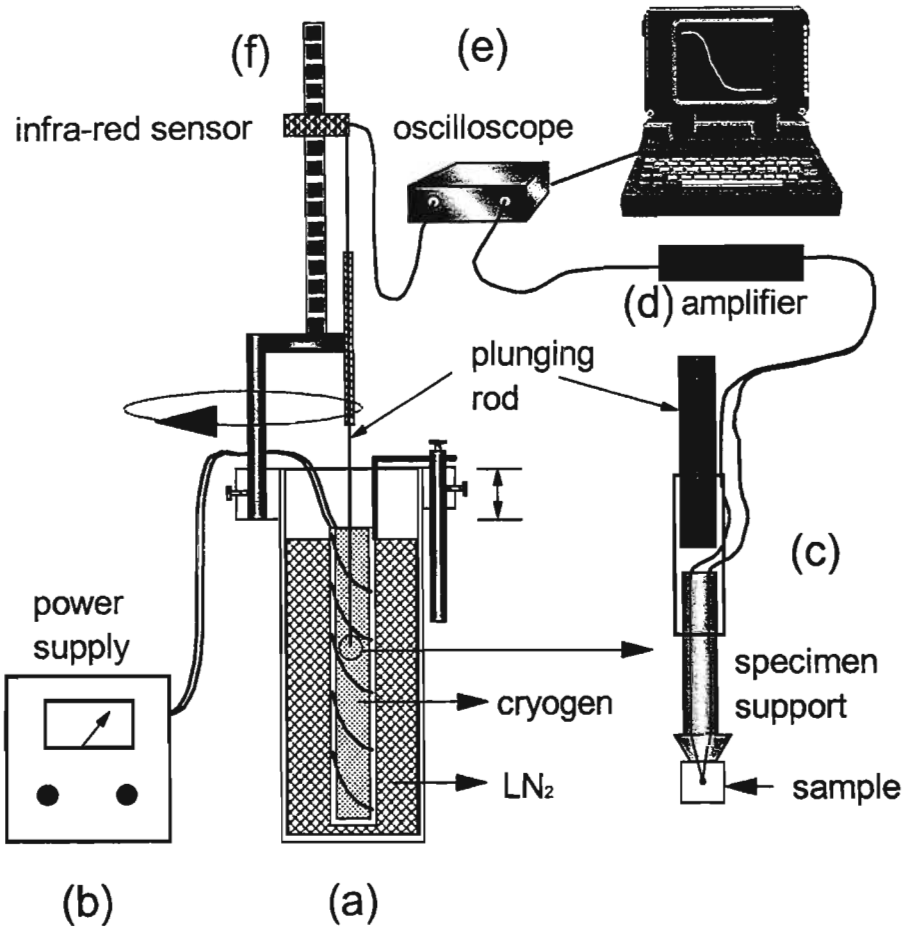

Fig. 5.1. Diagram of the spring loaded device used to achieve rapid cooling of biological tissues, and related equipment to measure plunging velocity and cooling rate. (See text for full description)

The oscilloscope interfaced with a portable computer, which stored and displayed temperature and velocity data. Data collection was standardised at a total of 1000 samples per channel and a frequency ranging between 250 and 12.5 $x10^3$ samples per channel per second. These settings allowed cooling events lasting between 4 and 0.08 s (respectively) to be recorded. The oscilloscope software could also be set to collect 20% of the total number of samples before, and 80% after, reaching the trigger temperature (usually 0°C during cooling). In this way, any evidence of pre-cooling prior to the plunge would become evident. In the present study cooling is expressed

as a rate if the response between two temperatures was linear. Alternatively, the time required to cool (or warm) between two temperatures is given.

Preparation of biological tissues

The response of biological tissues to various cooling and warming treatments was investigated using cotyledonary tissue from horse-chestnut (*Aesculus hippocastanum* L.) seeds collected from trees in Ft Collins, CO, USA. Specimens were prepared by dicing cotyledons manually into cubes with volumes of *c* 33, 7 and 1 mm^3, a dry weight of 14.5, 4.4 and 0.5 mg respectively, and an initial water content of 1.4 ±0.2 g g^{-1} dry mass (g g^{-1}).

Working with tissues of known and even dimensions allowed the effects of cooling parameters to be appreciated without the confounding variability inherent to embryonic axes. Variability was presumably reduced further by the presence of only parenchyma cells within these specimens, instead of an array of different cell types as found in embryonic axes.

The influence of tissue water content on the response of thermocouples to cooling and warming was investigated. Cotyledon cubes were dried from 1.4 ±0.2 to 0.9 ±0.04 or 0.5 ±0.06 g g^{-1} by exposure to an atmosphere of 98% relative humidity for either 24 or 72 h, respectively. Inserting the thermocouple into dry tissue blocks was difficult as these became hard and brittle. This step was assisted by impaling blocks with 3 mm segments of pointed thermocouple wire prior to drying, and replacing this with the temperature probe shortly before cooling.

The combined effect of tissue size and water content on cooling rates was assessed using the same thermocouple (125 μm wire thickness, 300 mm bead size) and plunging at an average 1.2 m s^{-1} into a 240 mm container filled with sub-cooled nitrogen renewed shortly before each plunge. The sizes chosen were similar to those of axes from different species used for this thesis

Thermocouple sensitivity

The thickness of the thermocouple wires, and the diameter of the bead relative to the size of specimens can affect the cooling rate recorded (Robards and Sleytr, 1985). The cooling response of bare Type J (iron / constantan) thermocouples of varying gauges (Table 5.1; Omega Engineering Inc., Stamford, CT, USA) was measured between 0 and -100°C during plunging into sub-cooled nitrogen at an entry velocity of 1.2 m s^{-1} and to a depth of 160 mm. Also, it was desirable to establish whether thermocouples of different bead diameters would affect the cooling rates measured within tissues. Cooling rates were measured using thermocouples of 300, 400 and 590 μm bead diameter inserted into the core of cotyledon tissues at 1.4 and 0.5 g g^{-1}.

Table 5.1. Dimensions of Type J thermocouple (TC) wire and bead size used for temperature measurement. All comparative cooling and warming experiments were performed using the same thermocouple.

TC WIRE DIAMETER (μm)	TC BEAD DIAMETER (μm)
25	70
125	300
125	400
250	590

Travel velocity and depth of plunge

In the present study, the travel velocities attained by springs of three different strengths were measured. The combined effect of travel velocity and depth of plunge on cooling profiles of a bare thermocouple was also investigated. A thermocouple of 125 μm wire thickness and 300 μm bead diameter (Omega Engineering Inc., USA.) was plunged into containers of 55, 100, 160 and 240 mm depth filled with sub-cooled nitrogen at *c.* -210°C (see below), and the cooling rates attained at different travel velocities were recorded.

Cryogens

The cooling rates attainable with the present device using isopentane, propane and sub-cooled nitrogen at -140, -180 and -210°C (respectively), and nitrogen at its boiling point (-196°C) were measured by plunging into the cryogen a thermocouple either bare or within the core of cotyledon tissue. These measurements were conducted using a thermocouple of 125 μm thickness and 300 μm bead diameter (Omega Engineering Inc., USA) plunged at an average velocity of 1.2 m s^{-1}, and to a depth of 160 mm.

Isopentane (Saarchem Pty Ltd., South Africa) and commercial grade propane (Afrox, South Africa) were initially cooled to near freezing temperatures by liquid nitrogen within a well ventilated fume hood. Nitrogen was sub-cooled under vaccum, as described in Chapter 4 (see also Echlin, 1992). Immediately after restoring ambient pressure, the 'slushy' mixture was decanted into the cryogen container previously cooled to ≤ -196°C. Plunging was done within 5 s after filling the receptacle, and contents were replaced by newly sub-cooled nitrogen immediately before the next plunge. These steps ensured that all specimens were treated uniformly, and that the variability in temperature characteristic of sub-cooled cryogens (Bald and Robards, 1978) was minimised. Temperature gradients are known to reduce cooling efficiency (Elder *et al.,* 1982), and were avoided in cryogen baths of propane or isopentane by stirring shortly before a plunge.

The effect of tissue size and water content upon cooling

The limitations imposed by tissues of different size and water content upon the rate of cooling to -60°C using the device described was investigated. Cotyledon cubes with a dry weight of 14.5, 4.4 and 0.5 mg respectively were plunged at water contents ranging from 1.4 to 0.18 g g^{-1}.

Warming rates

Evidence from survival studies suggests that tissues cooled rapidly must also be warmed correspondingly quickly to avoid excessive crystallisation and freezing

damage during warming (Mazur and Schmidt, 1968; Mazur *et al.,* 1969; Leibo *et al.,* 1970). The responses of cotyledon tissues at 1.4 and 0.5 g g^{-1} to warming to 23 or 40°C were investigated. Rapid warming was achieved manually by plunging specimen supports into water to an approximate depth of 100 mm using forceps. Only the rate of warming between -60°C and +5°C is reported presently, because it is at high sub-zero temperatures that warming becomes critical as the melting temperature is approached (Meryman, 1956, 1960; Sakai and Otsuka, 1967). From a cryopreservation perspective, it was also important to determine whether inadvertent warming of tissues ever occurred during transfer between cryogen containers, or prior to plunging in water. By setting the trigger of the oscilloscope to initiate recording at temperatures above -180°C, the temperature of pre-cooled fully and partially hydrated specimens could be monitored for evidence of premature warming during a typical cryopreservation protocol.

Results

Thermocouple size

Thermocouples of different wire thickness and bead diameter plunged into sub-cooled nitrogen cooled linearly from 0 to -100°C at rates that ranged between 243 and *c.* 15 000 °C s^{-1} (Fig. 5.2). One-way analysis of variance (ANOVA) showed that cooling rate increased significantly (P <0.001) with decreasing wire diameter (Fig. 5.2), while multiple range tests (LSD) revealed that for thermocouples of 125 μm wire diameter, 300 μm junctions cooled significantly faster than those of 400 μm (593 ±88 and 1684 ±241°C s^{-1}, respectively; [Fig. 5.2]).

Using the same thermocouple increased the reliability of comparative measurements, but also subjected thermocouples to appreciable wear and tear. Therefore, the sensitivity of the 25 μm wire diameter thermocouple was traded for the greater robustness of a probe 125 μm thick - 300 μm bead diameter. The latter appeared to be an adequate compromise between sensitivity and robustness, and was used in most cooling rate measurements within living tissues.

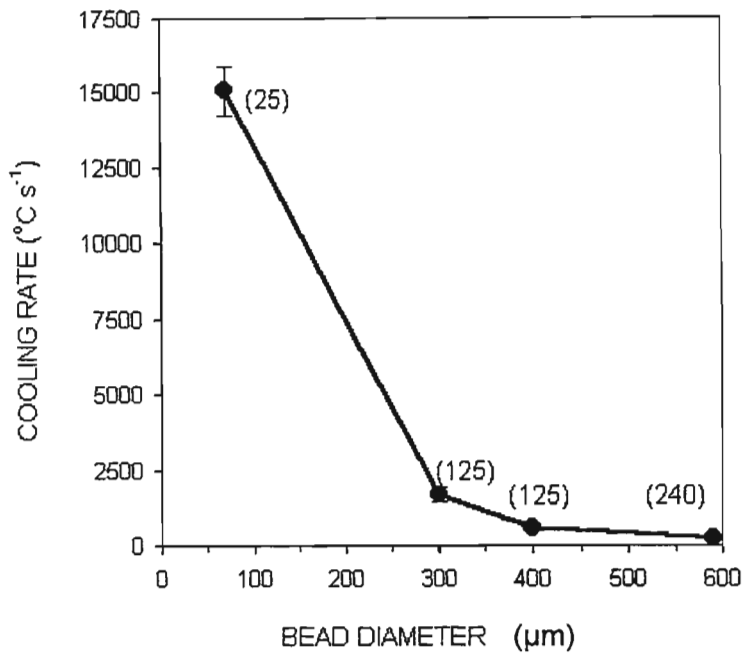

Fig. 5.2. Cooling rate between 0 and -100 C of bare thermocouples of various bead diameters and wire gauges (in parenthesis) plunged at 1.2 m s^{-1} into a 160 mm container filled with nitrogen at -210 C. Bars indicate standard deviation of the mean of 4-10 measurements per thermocouple.

The influence of bead diameter on cooling of tissues of known size at two water contents was assessed. Unlike bare thermocouples, cooling biological tissues was clearly slower as well as non-linear between 0 and -100°C. Accordingly, comparisons between treatments were based upon the time required to cool between 0 and -60°C were compared, as most of cellular water freezes within this temperature range (e.g. Sakai and Otsuka, 1967; Sakai, 1970; Moor, 1973). Multifactor ANOVA performed on the raw data summarised in Table 5.2 showed that bead diameter did not have an effect on cooling, although water content did (P <0.001). One-way ANOVA and multiple range tests (LSD) performed at each water content revealed that for tissues at 1.4 g g^{-1} cooling times were significantly shorter (P <0.05) using the 590 µm instead of the 300 µm bead diameter thermocouple. This suggests that in fully hydrated specimens the thicker thermocouple wire extracted relatively more heat than thinner counterparts during the long cooling times recorded. In contrast, bead diameter had no apparent effect upon cooling time of tissues dried to 0.5 g g^{-1} (Table 5.2).

Travel velocity and depth of plunge

Depending on the strength of the spring used, average travel velocity ranged from 1.2 to 4.4 m s^{-1}, and gave a four-fold increase in the duration of the plunge ranging between 133 and 33 ms for a cryogen container 160 mm deep (Table 5.3). In the present and subsequent chapters, the values indicating the plunging speed describe the average travel velocity of the specimens or axes in the different containers.

Table 5.2. Time required to cool from 0 to -60°C measured by thermocouples of various bead diameters placed in the centre of cotyledon tissues at different water contents plunged at 1.2 m s^{-1} into a 160 mm container filled with sub-cooled nitrogen. Multiple analysis of variance and multiple range tests (LSD) showed water content had a significant effect (P <0.001) on the time required to cool to -60°C, and that bead diameter influenced cooling but only at the higher water content. (Values with the same letters belong to the same group.)

WATER CONTENT ($g\ g^{-1}$)	BEAD DIAMETER (μm)	AVG TIME ±SD (ms)	HOMOGENEOUS GROUPS
1.4	590	694 ±131	a
	400	804 ±65	ab
	300	881 ±131	b
0.5	590	352 ±29	c
	400	314 ±85	c
	300	266 ±51	c

Table 5.3. Velocity of travel at the point of entry into the cryogen, averaged duration of plunge and velocity over a plunging distance of 160 mm

SPRING DESCRIPTION	ENTRY VELOCITY (m s^{-1})	TOTAL PLUNGE TIME (ms)	AVERAGE VELOCITY (m s^{-1})
Slow	0.8	133	1.2
Medium	1.3	65	2.5
Fast	2.7	33	4.4

The combined effect of travel velocity and depth of plunge upon the cooling rate between 0 and -100°C was investigated. A bare 125 μm thermocouple wire (300 μm

junction diameter) was plunged into sub-cooled nitrogen at an average 1.2 or 2.5 m s^{-1} to depths ranging from 55 to 240 mm (Fig. 5.3). The cooling rate during plunging at 2.5 m s^{-1} into the 55 mm container could not be measured accurately as it resulted in excessive splashing. Cooling to -100°C was linear in all treatments. Multifactor ANOVA showed cooling rates were highly dependent upon travel velocity and depths of plunge (P <0.0001). The cooling rate of thermocouples plunged at 1.2 m s^{-1} initially increased with increasing depth of plunge, but appeared to level in containers deeper than 100 mm. A similar trend was observed at 2.5 m s^{-1}, but beyond 160 mm. A comparison between both data sets suggests that that depth of plunge had a greater effect on cooling rate for the faster plunging speed. (Fig. 5.3). However, it is uncertain whether the plateau in cooling rates apparent for deeper containers represents a maximum rate of cooling was reached or, alternatively, variability in the cooling data.

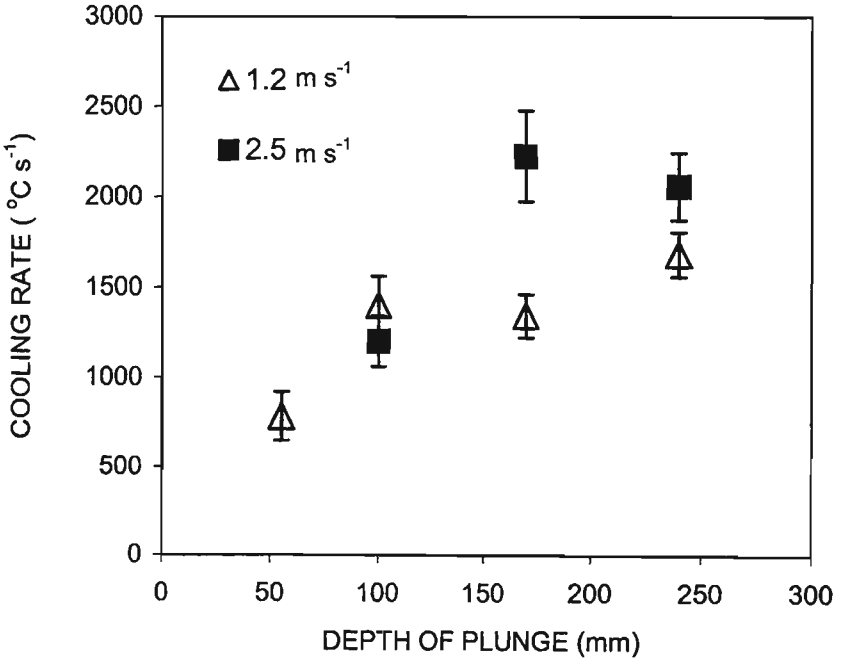

Fig. 5.3. Interaction between depths of plunge and travel velocity. A bare thermocouple (125 μm wire diameter and 300 μm bead diameter) was plunged at an average 1.2 or 2.5 m s^{-1} into containers 55, 100, 160 or 240 mm deep filled with nitrogen at -210°C. The cooling rate was measured between 0 and -100°C. Error bars represent the standard deviation of the mean of 4 – 10 measurements per permutation.

The effect of travel velocity upon cooling rates attained within tissues at water contents of 1.4, 0.9 and 0.5 g g^{-1} plunged into 160 mm of propane is shown in Table 5.4. Travel velocities had no effect upon the time to cool cotyledon tissues at each water content to -60°C, although partial drying to 0.5 g g^{-1} resulted in a significant increase (multifactor ANOVA; P <0.05).

Table 5.4. Time required by cotyledon specimens (7 mm^3 volume, 4.4 mg dry mass) at three water contents to cool between 0 and -60°C during plunging at three speeds into a 160 mm container filled with propane at -180°C. Values with the same letter are not significantly different at 95% confidence interval (Multiple range ANOVA and multiple range test [LSD])

AVERAGE TRAVEL VELOCITY (m s^{-1})	TIME (s) TO REACH -60 C		
	1.4 g g^{-1}	0.9 g g^{-1}	0.5 g g^{-1}
4.4	0.65 ±0.08 **a**	0.71 ±0.07 **a**	0.42 ±0.15 **b**
2.5	0.64 ±0.12 **a**	0.59 ±0.13 **a**	0.42 ±0.14 **b**
1.2	0.76 ±.16 **a**	0.65 ±0.08 **a**	0.45 ±0.10 **b**

Effects of cryogens on bare thermocouples

Representative cooling profiles of a bare thermocouple (125 μm wire, 300 μm bead diameter) plunged into isopentane, propane and nitrogen (either at -196 or sub-cooled to *c.* -210°C) at 2.5 m s^{-1} and to a depth of 160 mm are shown in Figure 5.4 a. This figure also shows the pulses generated by the infrared sensor during motion, indicating the beginning (0 ms) and end (*c.* 65 ms) of the plunge at 2.5 m s^{-1}. Propane provided the fastest cooling, followed by isopentane, sub-cooled nitrogen and lastly saturated nitrogen (Fig. 5.4 a). The peak cooling rates of propane and isopentane during the initial stages of the plunge were 2 x 10^4 and 1.4 x 10^4°C s^{-1} respectively, and contrasted sharply with the timing and lower rates attained by nitrogen, either sub-cooled nitrogen or at its boiling point (Fig. 5.4 b).

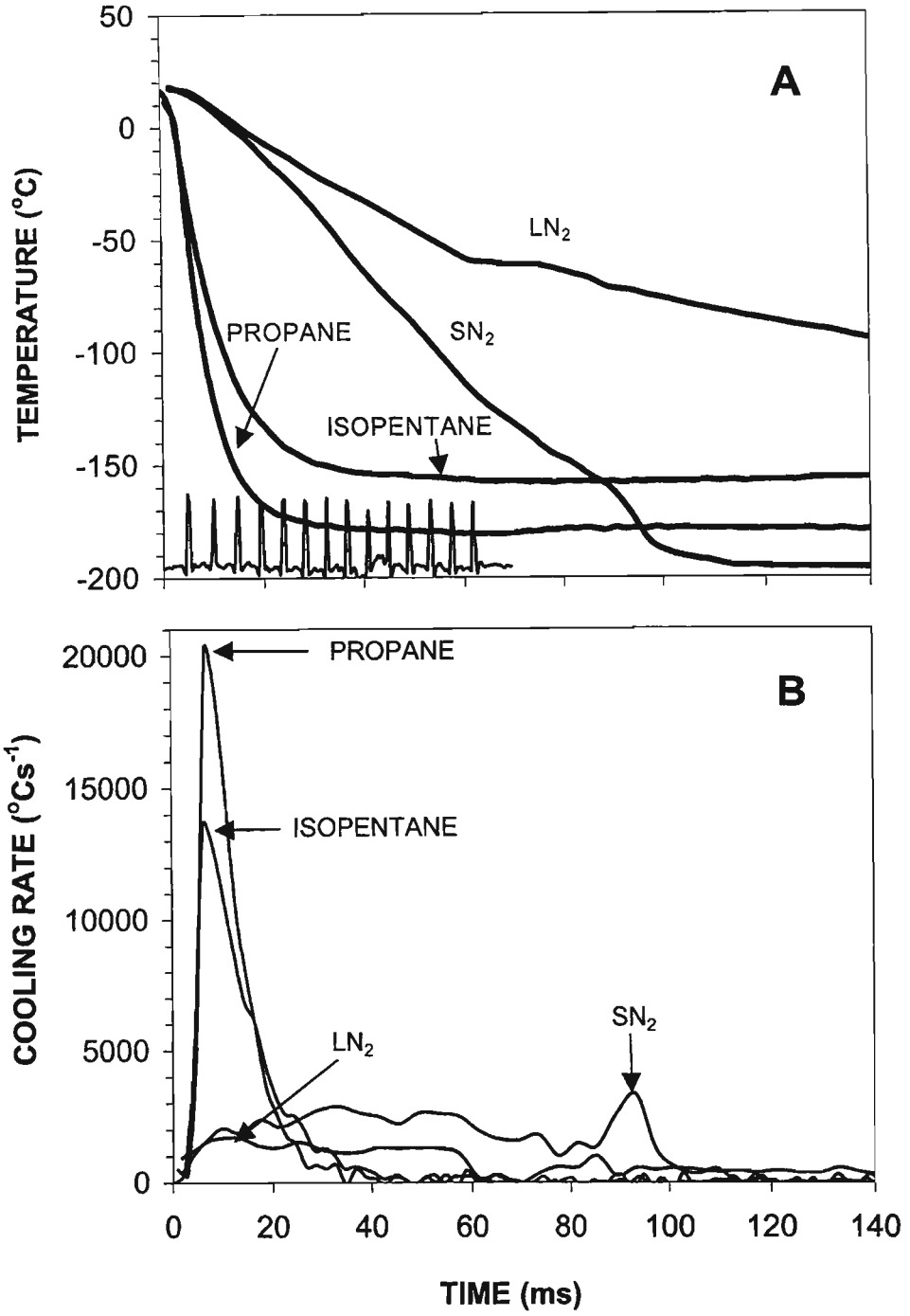

Fig. 5.4. A. Representative cooling profiles of a bare thermocouple (125 μm wire diameter, 300 μm bead diameter) plunged at 1.2 m s^{-1} into a 160 mm container filled with propane (c. -180°C), isopentane (c. -140°C), sub-cooled nitrogen (c. -210°C) and boiling nitrogen _-196°C). The peaks at the base of the chart represent the voltage pulses generated by the infra-red sensor as it moved over transparent regions of the calibrated film, and the troughs separating each peak indicate 10 mm of travel. **B.** Cooling rates calculated using the data displayed in **A.**

The effects of plunging conditions upon cooling in cotyledon tissues

Plunging speed had no effect upon the cooling rates of tissues at water contents of 1.4 – 0.5 g g^{-1} (Table 5.4). Accordingly, 1.2 m s^{-1} became the travel velocity of choice for all subsequent cooling studies because this velocity maximised the convective phase of the plunge (133 ms for a 160 mm container; [Table 5.3]) where cooling is fastest.

The effect of cryogens on cooling of fully hydrated or partially dried tissues was investigated next Fully hydrated cotyledon tissues plunged into propane, isopentane or sub-cooled nitrogen and to a depth of 160 mm, cooled several orders of magnitude slower than bare thermocouples (Fig. 5.5 a; *cf.* Fig. 5.4 a). Regardless of cryogen type, specimens were not cooled below -10 ±5°C after *c.* 133, when they reached the bottom of the cryogen container. After coming to a halt, the rounded cooling profiles suggested large freezing transitions lasting >1 s had occurred. During the stationary stage cooling of fully hydrated tissues was fastest using propane, followed by sub-cooled nitrogen and isopentane, in that order. Drying tissues to 0.5 g g^{-1} resulted in a marked increase in cooling velocity attained in each of the cryogens tested (Fig. 5.5 b), in agreement with the results shown in Table 5.4. Tissues cooled in propane and isopentane cooled linearly to between 0 and -70°C during the plunge (*c.* 133 ms) and relatively slowly thereafter as they approached the respective bulk temperatures. Specimens plunged into sub-cooled nitrogen cooled at a slower rate initially, reaching -70°C after 300 ms, but continued cooling linearly to below -150°C aided by the lower bulk temperature of this cryogen (Fig. 5.5 b).

The thermal properties of tissues appeared to exert the strongest influence on the cooling rates achieved. Reducing the size of the tissue and lowering the water content, either singly or in combination, had marked effects on the time required to cool tissues to target temperatures (e.g. -60°C; Fig. 5.6). Because limiting the length of exposure to high subzero temperatures reduces the likelihood of ice crystal damage, it is clear from Figure 5.6 that larger tissues require a greater extent of drying than smaller ones in order to reduce freezing damage. Conversely, tissues at

higher water contents may be cooled rapidly to 'safe' temperatures precluding crystallisation e.g. -100°C (Moor, 1971; Le Murray *et al.*, 1989) only if they are sufficiently small and cooling conditions are favourable.

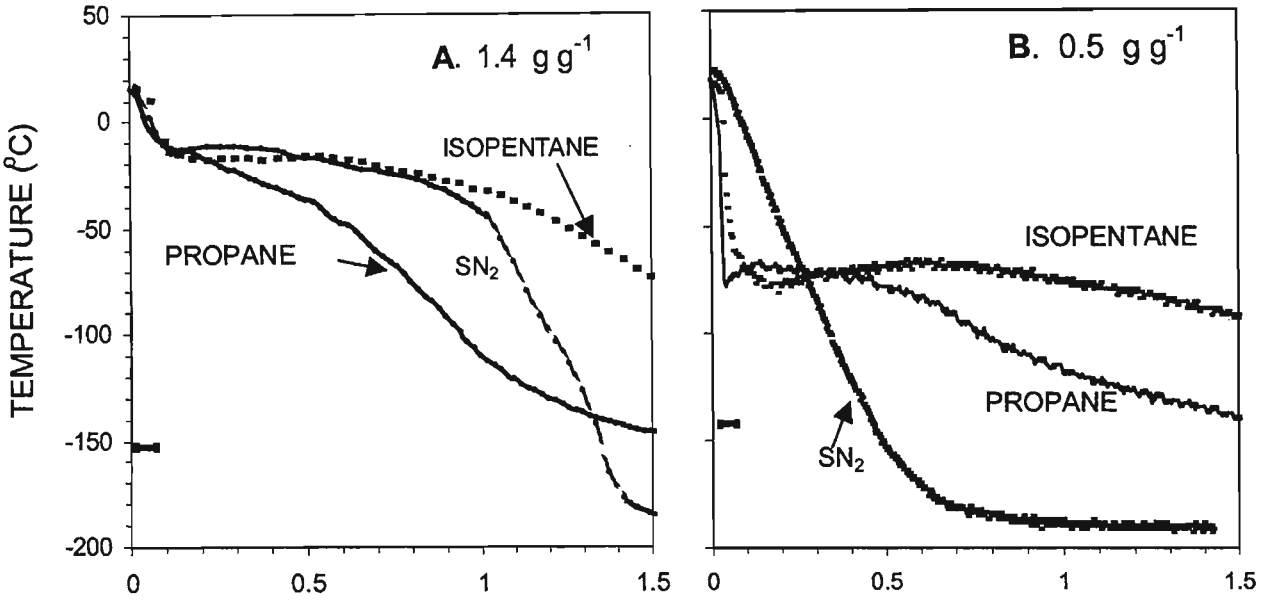

Fig. 5.5. Representative cooling profiles recorded within the core of 4.4 mg (dry weight) diced cotyledon specimens at (a) 1.4 or (b) 0.5 g g^{-1} plunged at 1.2 m s^{-1} into a 160 mm container filled with either propane (c. -180°C), isopentane c. -140°C or sub-cooled nitrogen (SN_2; c. -210°C). The horizontal scale bar represents the duration of the plunge into the cryogen.

Warming of cotyledon tissues

The temperature response of fully hydrated and partially dried (1.4 and 0.5 g g^{-1}, respectively) tissues (4.4 mg dry mass) to warming in water at 23 or 40°C was investigated. Predictably, drier tissues immersed in water at 40°C warmed faster, and fully hydrated tissues at 23°C warmed relatively slowly (Table 5.5). Increasing the water bath temperature from 23 to 40°C reduced significantly the time required by all tissues to reach 5°C. No evidence of warming was observed when tissues at either 1.4 or 0.5 g g^{-1} were transferred between cryogenic containers prior to warming.

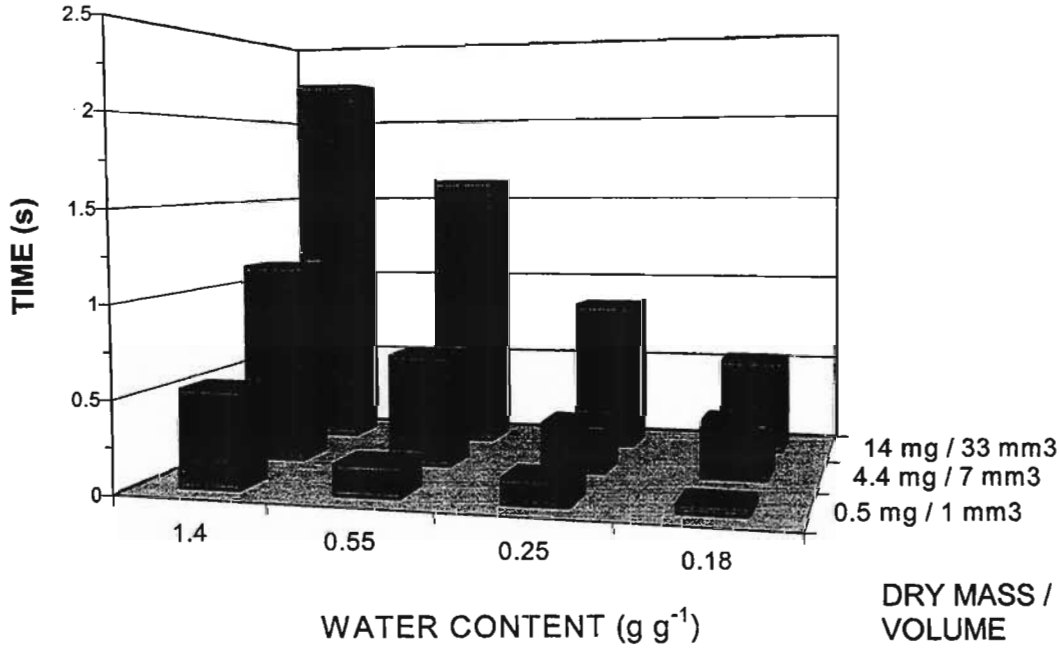

Fig. 5.6. The effects of water content and specimen size on the time required by cotyledon tissues to cool to -60°C during plunging into a 240 mm container of sub-cooled nitrogen. The volumes and dry weights given represent the average of 20 – 30 measurements, and the cooling data shown were taken from representative treatments.

Table 5.5. Time delay during warming fully hydrated and partially dried cotyledon tissues from -60 to +5°C following plunging into water at either 40 or 23°C. Values with the same letters are not significantly different (P >0.05) as indicated by one-way ANOVA and multiple range tests (LSD).

WATER CONTENT ($g\ g^{-1}$)	WARMING TEMPERATURE (°C)	TIME (ms)	HOMOGENEOUS GROUPS
1.4	40	508	ab
	23	877	c
0.5	40	439	a
	23	549	b

Discussion

Numerous works published have dealt with cryofixation of biological tissues for electron microscopy, and the conditions required to avoid freezing damage (see reviews by Robards and Sleytr, 1985; Gilkey and Staehelin, 1986; Menco, 1986; Bald, 1987; Ryan, 1992; Echlin, 1992). Findings from those and similar studies were applied presently to maximise the cooling rate of plant tissues much larger than the size recommended for cryofixation (0.1 mm; Bailey and Zasadzinsky, 1991) and which compared favourably with embryonic axes used in survival studies. The present study was undertaken to identify the conditions permitting the fastest attainable cooling in large specimens. Such conditions could subsequently be applied to restrict freezing damage and enhance survival of embryonic axes of recalcitrant seeds cryopreserved using this rapid cooling approach.

The ability to measure cooling rates reproducibly was a pre-requisite in this study. The rationale behind this was not to define the thermal history of cells at precise locations within the tissue (Bald, 1975; Bald and Crowley, 1979): Instead, emphasis is placed upon recording representative cooling rates that distinguish this method from slower cryopreservation procedures, such as that achieved within cryovials immersed in liquid nitrogen (e.g. Normah *et al.,* 1986; Pritchard and Prendergast, 1986; Vertucci, 1989b) or controlled rates of cooling (e.g. Diaper, 1986; Vertucci *et al.,* 1991; Wesley-Smith *et al.,* 1992). Cooling rate and survival data from axes cooled under defined conditions can then be analysed for trends suggesting favourable combinations of water content and cooling rate for cryopreservation, such trends being based on properties such as axis size and tolerance to partial drying.

The influence of thermocouple size of cooling rates

Studies investigating cooling rates often show different results, because of differences in the cooling conditions or on the size of the thermocouple used (Costello and Corless, 1978; Robards and Sleytr, 1985; Han *et al.,* 1995). Results from the present study show that cooling velocity of bare thermocouples increased with decreasing wire and bead diameter (Fig. 5.2), in agreement with previous studies (Costello and

Corless, 1978; Elder *et al.,* 1982; Han *et al.,* 1995). This effect is due to the lower thermal load (Robards and Sleytr, 1985) and larger surface area to volume ratio of the smaller thermocouples (Bailey and Zasadzinsky, 1991). The influence of thermocouple size on cooling rate observed (Fig. 5.2) questions the reliability of measurements acquired from living tissues using thermocouples of different gauge and / or bead diameters. Results obtained indicate that when the cool-down period of tissues to -60°C is about 0.8 s (Table 5.2), thermocouples of increasing size increase cooling by extracting heat from the sample. This effect was not apparent when tissues were dehydrated to 0.5 g g^{-1} and cooled to -60°C within *c.* 0.3 s. In contrast, thermocouple size has been found to influence cooling of specimens ≤1 mm for cryo-electron microscopy (Robards and Sleytr, 1985). It is possible that the influence of thermocouple size on the cooling rate of partially hydrated tissues was masked by variability inherent in tissues of the sizes presently used. Nevertheless, in the present study comparative measurements of cooling velocity were made using the same thermocouple of 125 μm thickness and *c.* 300 μm bead diameter, which was a suitable compromise between sensitivity and robustness.

Factors affecting the cooling rate of bare thermocouples

Bare thermocouples were cooled faster by variables reported to increase convective cooling, namely increased velocity and plunging distance, and cryogens of high thermal conductivity (Elder *et al.,* 1982; Bald, 1984, 1987; Ryan *et al.,* 1987). Increasing the average travel velocity from 1.2 to 2.5 m s^{-1} increased the flow of 'cold' cryogen over the surface of the thermocouple and aided the rapid removal of heat during forced convection (Fig. 5.3). Previous studies have shown that cooling rates of bare thermocouples increase with entry velocity up to 2 m s^{-1} (Costello and Corless, 1978; Elder *et al.,* 1982] above which a plateau can occur (Ryan *et al.,* 1987). Cooling rates appeared to level out at depths of 100 or 160 mm when thermocouples were plunged at either 1.2 or 2.5 m s^{-1}, respectively. The cooling rate of bare thermocouples was presumably limited by an insulating film of vapour that forms characteristically around objects with high thermal conductivity (e.g. metallic objects) during cooling in cryogens prone to nucleation boiling, such as nitrogen (Bald, 1984).

The thickness of this gaseous layer and the rate of heat loss are reportedly influenced by the travel velocity (Ryan *et al.,* 1987), which explains the difference in maximum cooling rate of thermocouples plunged at either 1.2 or 2.5 m s^{-1} (Fig. 5.3). The increase in cooling rate observed during plunging into a 240 mm container at 1.2 m s^{-1} is presumably due to enhanced cooling by nucleation boiling under those conditions. Results from bare thermocouple experiments indicate that propane and isopentane were the most efficient cryogens, followed by sub-cooled and boiling nitrogen, in that order. These results agree with previous observations (Stephenson, 1956; Elder *et al.,* 1982; Ryan *et al.,* 1987) and provide a benchmark that describes the cooling capabilities of the plunging system described without the confounding variability introduced by biological tissues. However, findings using bare thermocouples should not be used to predict favourable cooling conditions of biological specimens, as both materials have very different physical properties (Bald, 1984, 1987).

Heat transfer in large biological tissues

Biological tissues have characteristically low thermal conductivity, which means that while their boundary quickly approaches the temperature of the cryogen at subzero temperatures, further cooling is limited by the rate of conduction of heat through the tissue (Bald, 1984, 1987). If hydrated tissues are small (*c.* 0.1 mm) heat transfer under favourable cooling conditions appears to be limited predominantly by convection at the boundary (Bailey and Zasadzinsky, 1991). In larger specimens the maximum rate of cooling becomes increasingly limited by conduction of heat through several layers of cells. Therefore, in order to maximise cooling, the sample should be kept under forced convection until the specimen temperature falls below a 'safe' value (e.g. -100°C [Moor, 1971; Le Murray *et al.,* 1989]). In the present study, hydrated tissues failed to cool below -10°C even when plunged into a 240 mm cryogen container filled with sub-cooled nitrogen (not shown). Similarly, increasing the entry velocity conferred no advantage, as this meant that tissues arrived sooner at the bottom of the container still at high subzero temperatures (Table 5.4). The greater cooling ability displayed by propane and isopentane during convective cooling of bare

5.5 a). Collectively, these results suggest that the heat capacity of fully hydrated tissues exceeded by far the amount of heat that could be dissipated by convection under the present plunging conditions. The rate-limiting step appears to be the conduction of heat from the tissue interior to the surface. Most of heat was lost during the stationary stage by conduction over periods ≥1 s, conditions that usually result in reduced survival of axes *in vitro* (Wesley-Smith *et al.,* 2001b; Chapters 6 and 8). Convective cooling can be sustained for longer if the depth of plunge is increased, and plunging distances ≥600 mm appear to be critical to extend the time under forced convection required to achieve favourable cooling of large, hydrated tissues (e.g. Bald and Robards, 1978; Ryan *et al.,* 1987).

Partial drying increases cooling

Cellular water holds the largest reservoir of thermal energy that needs to be dissipated efficiently during rapid cooling (Bachmann and Mayer, 1987), therefore partial drying reduces the thermal load of tissues and favours faster cooling (Table 5.2; Wesley-Smith *et al.,* 1992, 2001b; Chapters 4, 6 and 8) and warming (Table 5.4). Tissues dried to 0.5 g g^{-1} cooled rapidly to *c.* -70°C during forced convection in propane and isopentane (Fig. 5.5 b). The apparently greater efficiency of propane and isopentane is comparable to that observed with bare thermocouples (*cf.* Figs 5.4 and 5.5 b), and suggests that convective cooling effects had become appreciable in partially dried specimens. Although sub-cooled nitrogen was relatively less efficient during forced convection, it facilitated linear cooling to lower temperatures than propane and isopentane, and deserves to be considered as a potential cryogen for cryopreservation of partially hydrated specimens. Evidence suggests that if tissues can tolerate partial drying, the plunging device described is adequate to cool specimens at relatively high rates.

Warming

The beneficial effects of reduced water content were not as marked during warming as they were during cooling. Tissues immersed in water at 23°C warmed faster when partially dried than when fully hydrated (Table 5.4). Like the situation during the

stationary phase after plunging, heat transfer during warming was determined mainly by conduction and thus controlled by the gradient in temperature between the tissue and its surroundings (Meryman, 1956). Accordingly, the warming time of all tissues was reduced significantly (P <0.05) by water at 40 instead of 23°C. Rapid warming reduces intracellular freezing damage by limiting the time available for lethal crystallisation (Mazur and Schmidt, 1968; Bank, 1973; reviewed by Mazur, 1990). The need for rapid warming mirrors the importance of cooling cells sufficiently quickly to temperatures precluding ice growth, a process that is facilitated by partial drying when tissues are large (Fig. 5.6).

The device presently described was chosen to explore the merits of rapid cooling for cryopreservation because it facilitated reproducible temperature measurement with minimum interference to the cooling process. The average cooling rates recorded can serve as a benchmark that can be approximated using simpler, perhaps more practical approaches, also based on the principles of enhancing the rate cooling and warming of (usually) partially hydrated specimens. It is expected that the relationship between water content, cooling rates and properties of embryonic axes will become clearer as more species are investigated using this approach. Determining the minimum cooling rate required to prevent lethal freezing damage in axes from various recalcitrant species is the focus of subsequent chapters.

CHAPTER 6

Is rapid cooling suitable to cryopreserve large embryonic axes? The study of *Aesculus hippocastanum* L. *

* Also published as Wesley-Smith J, Walters C, Pammenter NW, Berjak P (2001) Interactions of water content, rapid (non-equilibrium) cooling to -196°C and survival of embryonic axes of *Aesculus hippocastanum* L. seeds. *Cryobiology* **42**: 196-206

Introduction

Cooling rate is a function of the thermal mass of the material and heat transfer properties of the cooling system (Stephenson, 1956; Meryman, 1956; Bald, 1987). Results presented in the previous chapter (Fig. 5.6) suggest that cooling rates in excess of 100°C s^{-1} are readily attainable in tissues with a dry mass of *c.* 1-2 mg, and when combined with partial drying this approach can facilitate high survival after warming (Chapter 4). However, rapid cooling becomes increasingly difficult for larger axes since, at the same water content, more heat must be dissipated and this heat must be conducted through many layers of cells, which are poor conductors (Meryman, 1960; Bald, 1987). The thermal mass is raised further by the increasing heat capacity of water with increasing supercooling (MacKenzie, 1977; Franks, 1980). Consequently, in order to compensate for an increase in axis size, either an increase in the rate of heat transfer or a reduction in water content - or both - would be required to achieve favourable cryopreservation procedures. Thus, a complex interaction is expected to exist between the physical attributes of embryonic axes (e.g. mass, water content and geometry), the cooling conditions, and survival.

In order to investigate this interaction and assess the broad applicability of rapid cooling for the cryopreservation of embryonic axes of other species, systematic manipulation of variables is required. This was achieved using the plunging device described in Chapter 5, which facilitated cooling under controlled and quantifiable conditions. The present aspect of the study investigated the potential for using rapid cooling to increase the survival of axes of *Aesculus hippocastanum* exposed to

cryogenic temperatures. Previously, a maximum of 100% survival of only shoot poles was achieved for embryonic axes of *A. hippocastanum* by drying them to *c.* 0.28 g g^{-1} and cooling them slowly in cryovials immersed in liquid nitrogen (Pence, 1990, 1992). The objectives of the present study were:

1. To test the hypothesis that rapid cooling increases the upper limit of water contents tolerated by embryonic axes of *A. hippocastanum* exposed to cryogenic temperature;
2. To assess the morphological development of axes *in vitro* following cryopreservation by rapid cooling at various water contents;
3. To evaluate the cooling efficiency of sub-cooled nitrogen and isopentane under controlled plunging conditions and relate this to survival of *A. hippocastanum* axes *in vitro*.

Materials and Methods

Mature *A. hippocastanum* fruits were collected from trees growing in Fort Collins, CO., USA, and seeds were subsequently stored in plastic bags at 15°C. All manipulations were conducted within 30 d of harvest.

Dehydration and water content determination

Axes were excised and kept on moistened filter paper prior to desiccation using the flash-drying chamber described in Chapter 3 (Wesley-Smith *et al.* 2001a). This type of rapid drying allows low water contents to be attained before viability is lost (Pammenter *et al.,* 1991; Wesley-Smith *et al.,* 2001a; Chapter 3). Water contents were determined gravimetrically after axes were dried to a constant weight in an oven at 105°C. The destructive nature of this procedure does not allow the exact water content of cryopreserved axes to be determined. Therefore, axes used in survival studies were dried for specific times and the average water content characterising these drying intervals were determined separately using a sub-sample of 5-10 axes. Water contents from individual axes dried for periods of up to 140 min are shown in

Figure 6.1 and are expressed as g H_2O g dry mass (g g^{-1}), with approximate water potentials (from Farrant and Walters, 1998) in parenthesis in the text.

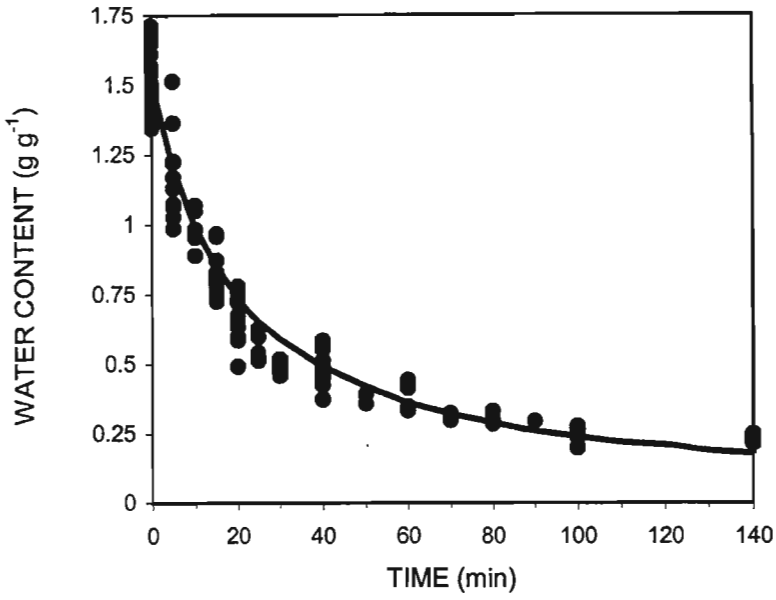

Fig. 6.1. Drying time-course of embryonic axes of *A. hippocastanum*. Data points represent average water contents of 10 axes. The curve shown was fitted using a decay hyperbola and the equation y= ab/(b + x). Axis water content was reduced by approximately 70% during the first 30 min of flash drying and by only 17% after an additional 110 min.

Cooling

Cooling rates were measured using the data-acquisition instrumentation previously described (Wesley-Smith *et al.,* 1999; Chapter 5). In this study a type J thermocouple (200 μm wire, 450 μm bead diameter; Omega Engineering, Stamford, CT, USA) was used to record temperatures in the core of axes at different water contents. Rapid cooling of axes to cryogenic temperatures and measurement of cooling rates were performed using a plunging device previously described (Wesley-Smith *et al.,* 2001b; Chapter 5). Axes were plunged at an average 1.2 m s^{-1} to a depth of 160 mm into a receptacle filled with either isopentane at *c.* -140°C or nitrogen which had been previously sub-cooled to -210°C by placing under vacuum (Echlin, 1992). Following cooling, the supports (each with an individual axis attached) were transferred without warming to liquid nitrogen, and maintained at -196°C until required. Cooling rates were not constant over the entire cooling time course, but were calculated for temperatures between 0 to -40°C assuming linearity. Cooling within this temperature

range induces most of the crystallisation in partially hydrated plant cells (e.g. Sakai and Otsuka, 1967; Moor, 1973).

Survival studies

Following drying, or drying and exposure to cryogenic temperatures, axes were rapidly immersed in distilled water at 40°C for 1 min and subsequently placed on moistened filter paper in the dark for 30 min. Shortly before transfer to *in vitro* culture axes were surface sterilised using the procedure described in Chapter 4 and grown on Woody Plant Medium (Lloyd and McGown, 1980) solidified with 0.7% agar. Because reduced light intensities have been shown to minimise free-radical damage following cryopreservation (Touchell and Walters, 2000), axes in Petri plates were maintained in the dark for 48 h and only then exposed to a 16h:8h light:dark photoperiod at 25°C. Axes were scored as 'normal' when radicles doubled in length and shoots turned green. Axes appearing stunted, bearing callus growth or showing incomplete development of shoot or root were scored as 'abnormal'. Survival was assessed after four weeks *in vitro*. Between 5 and 10 axes were used to assess viability of cooled and control axes at each water content tested.

Electrolyte leakage

Membrane integrity of cells comprising the axes was assessed from the conductivity developed in the bathing water following drying and exposure of axes to cryogenic temperatures (Vertucci, 1989a; Pammenter *et al.,* 1991; Berjak *et al.,* 1992). Electrolyte leakage from individual axes was measured using an ASAC 1000 (Applied Intelligence Systems, Inc.; Neogen, Lansing, MI, USA) conductivity meter. Between 5 and 10 axes were placed individually in wells of the conductivity meter immediately following drying alone or after cryopreservation. Readings were taken at 10 min intervals for a period of 1 h, the results being expressed as leakage rate.

Results

Axes of *A. hippocastanum* had a dry mass of 6 ±1.7 mg, and an initial water content of 1.5 ±0.12 g g^{-1} (Ψ= -2.2 MPa). Flash drying reduced the water content of axes by nearly 70% during the first 30 min, and by only 17% further over the subsequent 110 min (Fig. 6.1). Over 90% survival of control (i.e. not cooled) axes was observed at all water contents between full hydration and 0.25 g g^{-1} (Ψ= -15 MPa), the lowest water content tested (data not shown). However, it was noted that axes dehydrated to 0.25 g g^{-1} (with or without cooling) failed to develop shoots unless protected from direct light during the first 48 h after treatment.

Cooling time-courses were measured in the core of variously hydrated axes plunged into either isopentane or sub-cooled nitrogen (Figs 6.2 a and b, respectively). The vertical dotted lines in Fig. 6.2 represent the approximate end of the plunge into the cryogen, when the axes reached the bottom of the cryogen container after about 0.15 s. Cooling during the plunge into isopentane was rapid, but slowed after plunging was completed especially for axes with high water contents. Changes in cooling rates during and post- plunge into sub-cooled nitrogen were less marked.

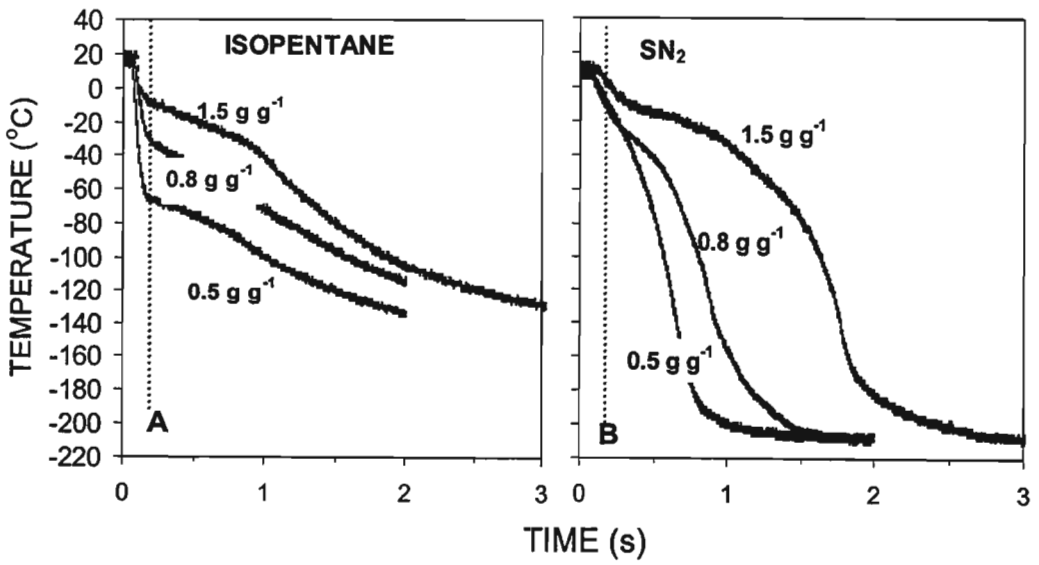

Fig. 6.2. Representative cooling profiles recorded within the core of axes plunged into a) isopentane or b) sub-cooled nitrogen (SN_2) at the water contents indicated. Dotted lines represent the approximate end of the plunge.

During the plunge, isopentane consistently gave more rapid cooling than sub-cooled nitrogen. Axes at water contents of 1.5, 0.8 and 0.5 g g^{-1} cooled to -9 ±4, -30 ±18 and -50 ±10°C, respectively, during the plunge into isopentane, but were not cooled below -15°C during the plunge into sub-cooled nitrogen regardless of water content (Figs 6.2 a and b). Following the plunge, axes in sub-cooled nitrogen cooled faster than those in isopentane, presumably because of the lower temperature of sub-cooled nitrogen (*c.* -210°C) compared with isopentane (*c.* -140°C). Two-way analysis of variance showed that average cooling rates between 0 and -40°C (Table 6.1) differed significantly with axis water content ($P < 0.001$) and cryogen ($P < 0.001$), and that an interaction existed between these factors ($P < 0.001$). Based on the overlap of the confidence intervals (C.I.) of the means, a significant increase in cooling rate in isopentane was observed when axes were dehydrated below 0.75 g g^{-1} (95% C.I. [Table 6.1]). In contrast, the cooling rate of axes plunged into sub-cooled nitrogen increased significantly only when axes had been dehydrated below 0.5 g g^{-1} (Table 6.1), suggesting that isopentane was a faster coolant.

Table 6.1. The rate of cooling (°C s^{-1}) between 0 and -40°C of axes of *Aesculus hippocastanum* of varying water contents when plunged into either isopentane (*c.* -140°C) or sub-cooled nitrogen (*c.* -210°C). Two-way analysis of variance showed a significant effect of water content ($P < 0.001$) and cryogen ($P < 0.001$) on cooling rate, and there was a significant ($P < 0.001$) interaction between these parameters. Values with the same letter constitute homogeneous groups based on overlap of the 95% confidence intervals (C.I.) of the means.

WATER CONTENT (g g^{-1})	**COOLING RATES** (°C s^{-1})			
	ISOPENTANE		SUB-COOLED N_2	
2.0 – 1.0	57 ±28	a	42 ±9	a
1.0 – 0.75	66 ±25	ab	74 ±38	ab
0.75 – 0.5	199 ±50	bc	113 ±23	abc
≤0.5	580 ±156	d	155 ±40	c

Electrolyte leakage was used to evaluate the extent of drying or freezing damage to plasma membranes. Leakage from axes not exposed to cryogens increased only slightly across the water content range above 0.5 g g^{-1}, after which only a small increase in leakage was observed (Fig. 6.3 a). In comparison, a ten-fold increase in electrolyte leakage was observed from fully hydrated axes exposed to either isopentane (Fig. 6.3 b) or sub-cooled nitrogen (Fig. 6.3 c). Electrolyte leakage from cryopreserved axes decreased if these were initially dried prior to cooling (regression analysis showed this effect to be significant [P <0.05]), reaching levels similar to their non-cooled counterparts at water contents of about 0.5 g g^{-1} (Ψ= -10 MPa). Statistical comparison of the regression slopes showed no significant effect of cryogen on leakage rate (P >0.05). This suggests that in spite of the greater apparent cooling efficiency of isopentane, axes cooled in either cryogen sustained equivalent damage during cooling and warming.

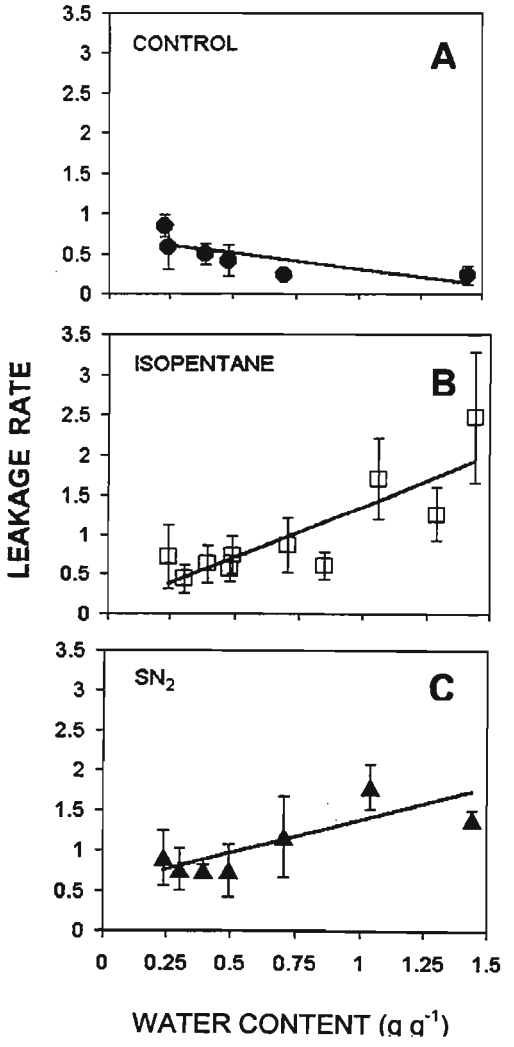

Fig. 6.3. Electrolyte leakage from axes at different water contents which were a) not cooled (control; solid circles), or plunged into b) isopentane (open squares) or c) sub-cooled nitrogen (SN_2; solid triangles).

Data represent averaged leakage rates from 5-10 individual axes at each water content from each treatment.

Regression analysis on data from cooled axes showed a significant decrease (P <0.01) in leakage with increasing drying.

A comparison of the slopes from cooled axes showed no significant difference between treatments.

Axis water content influenced both cooling rates (Fig. 6.4) as well as survival post-warming (Fig. 6.5). The relationships among water content, average cooling rate from 0 to -40°C, and *in vitro* survival suggested four distinct water content ranges.

- Axes above 1.0 g g^{-1} (Ψ= -3.8 MPa) could not be cooled faster than *c.* 100°C s^{-1} irrespectively of the cryogen used (Fig. 4; Table 6.1), and did not survive cryogenic treatment (Figs 6.5 a, b and 6.6 d) irrespective of the cryogen used. Similar cooling rates were attained when axes of 1.0 - 0.75 g g^{-1} (Ψ= -3.8 to -5 MPa) were cooled in either isopentane or sub-cooled nitrogen (Table 6.1; Fig. 6.4).
- Although all axes below 1.0 g g^{-1} survived exposure to isopentane or sub-cooled nitrogen (Figs 6.5 a and b) they developed abnormally, showing shoot necrosis, callus proliferation in radicle tissue or overall stunted growth (e.g. Fig. 6.6 e).
- For axes of 0.75 to 0.5 g g^{-1} (Ψ= -5 to -10 MPa) plunged into isopentane, an increase in cooling rates to an average 200°C s^{-1} was accompanied by a corresponding increase in the proportion of axes developing normally (Figs 6.5 a and 6.6 f). Axes at 0.75 to 0.5 g g^{-1} cooled in sub-cooled nitrogen showed a small increase in average cooling rate from 74 to 113°C s^{-1} (Table 6.1) but, unfortunately, no survival data are available for axes cooled in sub-cooled nitrogen within the 1.0 – 0.5 g g^{-1} water content range because of microbial contamination of cultures.
- At water contents of 0.5 g g^{-1}, differences in the efficiency of the two cryogens were highlighted by the normal development of all axes cooled in isopentane (Fig. 6.5 a), in contrast to the total shoot damage in axes plunged into sub-cooled nitrogen (Fig. 5 b). The cooling rates of axes at ≤0.5 g g^{-1} attained with either cryogen were also markedly different, ranging between 300 and 850°C s^{-1} in isopentane and between 70 and 250°C s^{-1} in sub-cooled nitrogen (Fig. 6.4). With only one exception (Fig. 6.5 a) all cryopreservation trials of axes below 0.5 g g^{-1} (isopentane) and 0.4 g g^{-1} (sub-cooled nitrogen) resulted in complete normal development (e.g. Fig. 6.6 g).

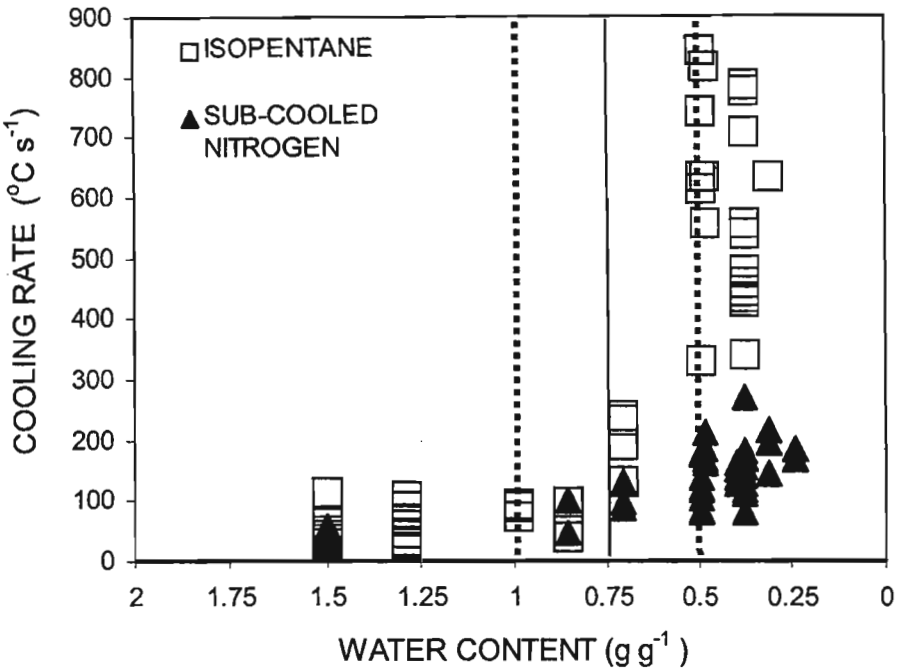

Fig. 6.4. Average cooling rates between 0 and -40°C recorded in the core of axes at various water contents during plunging into either isopentane (open squares) or sub-cooled nitrogen (SN_2; solid triangles). Vertical dotted lines indicate water content ranges that appeared to influence cooling rates of cryopreserved axes.

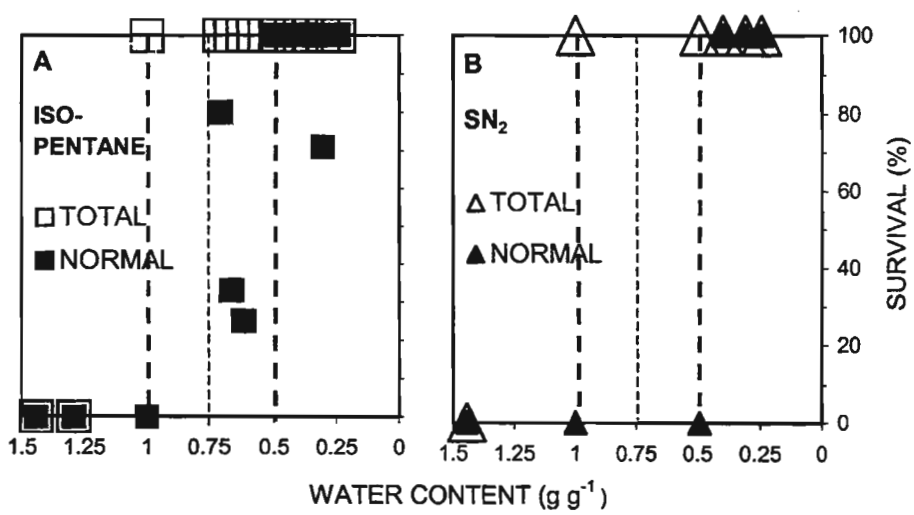

Fig. 6.5. a) Survival of axes at various water contents following cooling in a) isopentane or b) sub-cooled nitrogen (SN_2). Data points represent the percentage survival of 5 - 10 axes expressed as a percentage of the total in each experiment. Solid markers indicate the percentage of axes that developed normally *in vitro*, and open markers represent the proportion that showed callus proliferation, stunted growth or that failed to produce shoots. Vertical dotted lines indicate water content ranges that appeared to influence cooling rates of cryopreserved axes.

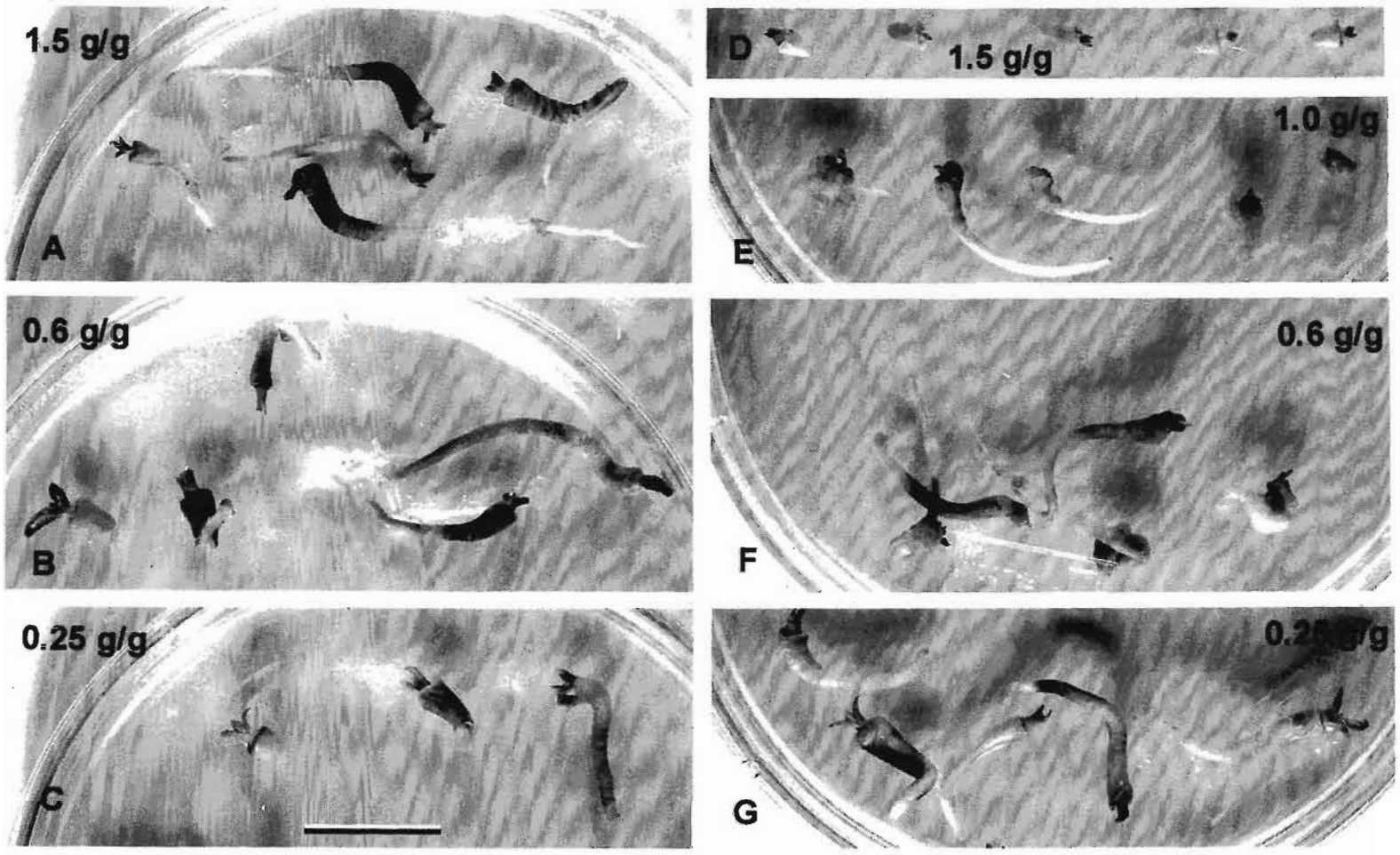

Fig. 6. In vitro survival of embryonic axes of A. hippocastanum at the water contents indicated without cryogenic exposure (A-C) or after cryopreservation with isopentane (D-G). (A-C) Over 90% of control axes developed normally between 1.5 and 2.5 g g^{-1}. (D) Axes at 1.5 g g^{-1} did not survive cryopreservation. (E) At 1.0 g g^{-1} axes survived, but showed evidence of localised freezing damage leading to callus formation. (F) Further drying to 0.6 g g^{-1} increased the incidence of axes developing normally. (G) Complete normal development of axes at 0.25 g g^{-1}. Bar 22.5 mm.

Discussion

This study examined the interaction between moisture content, cooling rate and survival of embryonic axes of *Aesculus hippocastanum* exposed to cryogenic temperatures. In most cases reported, recalcitrant axes are dried to very low water contents and cooled at *c.* 3°C s^{-1} to -196°C in cryovials (e.g. Pritchard and Prendergast, 1986; Vertucci, 1989b; Pence, 1990, 1992, 1995; Chaudhury *et al.*, 1991; de Boucaud *et al.*, 1991; Abdelnour-Esquivel *et al.*, 1992; Chandel *et al.*, 1995). Previously, a highest overall survival of 100% shoot greening and 25% root development for axes of *A. hippocastanum* was obtained at a water content of 0.28 g g^{-1} (Ψ= -12 MPa) following cooling in cryovials (Pence, 1992). In the present study, axes were plunged into isopentane or sub-cooled nitrogen (Fig. 6.2), giving cooling rates between 40 and 850°C s^{-1} (Table 6.1; Fig. 6.4 a). Using this method of cooling, survival increased to 100% for axes with water contents as high as 1.0 g g^{-1} (Ψ= -3.8 MPa; Fig. 4 b) and all axes with water contents less than 0.5 g g^{-1} (Ψ= -10 MPa) developed normally (i.e. both shoots and roots). Rapid cooling thus resulted in both an increase in survival and an increase in water contents at which cryogenic exposure was tolerated.

Rapid cooling was achieved by rapidly plunging individual axes into cryogens. Cooling time courses showed two distinct stages of heat transfer (described in Bald, 1984, 1987), and this was particularly evident in isopentane (Fig. 6.2 a). Forced convection of the coolant over the axis surface leads to a rapid reduction in temperature during the plunge. After the axis comes to rest (vertical line, Fig. 6.2) heat transfer occurs mostly through transient conduction, and temperature changes more slowly. The relatively slower cooling of hydrated specimens was most likely a reflection of the high heat capacity of water (4.2 J g^{-1} $°C^{-1}$ or higher, depending on supercooling; [MacKenzie, 1977; Franks, 1980]) and additional heat production from freezing transitions (*c.* 300 J g^{-1} water; [Farrant and Walters, 1998]). Axes dehydrated to water contents less than 0.75 g g^{-1} cooled more rapidly (Fig. 6.2, Table 6.1), presumably because the removal of water lowered the thermal load of the sample.

Axes dried below 0.75 g g^{-1} cooled faster to -40°C when plunged into isopentane than when plunged into sub-cooled nitrogen (Figs 6.2 and 6.4; Table 6.1) probably because of the relatively higher cooling efficiency of isopentane (Sitte *et al.,* 1987). Liquid nitrogen is generally regarded as an inferior coolant due to the characteristic formation of an insulating layer of gas around warmer objects (Leidenfrost phenomenon; [Luyet, 1961]). Although sub-cooling to -210°C increases the cooling efficiency of nitrogen by delaying the onset of boiling around the sample (Bald, 1987; Steponkus *et al.,* 1990; Wesley-Smith *et al.,* 1992; Han *et al.,* 1995) this cryogen failed to cool axes below -15°C during the plunge (Fig. 6.2). Nevertheless, using the plunging system, embryonic axes were cooled at rates in excess of *c.* 50°C s^{-1}, representing a 10 to 100-fold increase over those attained by the cryovial method.

In fully hydrated axes, water behaves as a dilute solution, with freezing temperatures greater than -5°C and glass transition temperatures below -90°C (Vertucci, 1990; Leprince and Walters-Vertucci, 1995). Assuming the viscosity to be similar to that of pure water (Franks, 1985; Bald, 1987), and the minimum cooling rate equivalent to that required to avoid freezing damage (10^4 °C s^{-1};[e.g. Moor, 1971]), successful cooling of fully hydrated axes requires traversing the -5 to -100°C temperature range within 0.01 s. However, it is difficult (if not impossible; [Franks, 1980; Rasmussen, 1982]) to cool more than 1 mm^3 of hydrated tissue fast enough to prevent crystallisation (Stephenson, 1956; Robards, 1974; Ryan and Purse, 1985; Bald, 1987). Fully hydrated axes of *A. hippocastanum* have estimated volumes of *c.* 15 mm^3, and traversed the critical temperature range of -5 to -90°C within *c.* 1.4 s (Fig. 6.2). Even though the plunging technique cooled hydrated tissues ten times faster than attained with conventional methods, the rates achieved were still approximately 140 times slower than predicted to be necessary to avoid crystallisation. These specimens did not survive cryogenic temperatures (Figs 6.5 a, b and 6.6 d).

Partial drying reduces the requirement for extremely rapid cooling because it abridges the critical temperate range a specimen must traverse rapidly before freezing damage occurs (Moor, 1973; Robards and Sleytr, 1985). Drying lowers the freezing

temperature (Rasmussen *et al.,* 1975; Meryman and Williams, 1980; Becwar *et al.,* 1983; Vertucci, 1990; Wesley-Smith *et al.,* 1992; Farrant and Walters, 1998; Pritchard *et al.,* 1995), elevates the glass transition temperature (Buitink *et al.,* 1996; Leprince and Walters-Vertucci, 1995, Meryman and Williams, 1980; Williams and Leopold, 1989; Williams *et al.,* 1993) and hinders crystallisation by increasing the intracellular viscosity (Buitink *et al.,* 1998b; Leprince and Hoekstra, 1998; Leprince *et al.,* 1999). When specimens are dried to water contents where the glass transition and freezing temperatures are comparable (usually about 0.25 g g^{-1} for tissues containing less than 10% lipid, or specimens at about Ψ= -12 MPa; [Leprince and Walters-Vertucci, 1995; Vertucci, 1990;]), survival becomes almost independent of cooling rate (Vertucci, 1989a,b). Thus, recalcitrant embryos that survive desiccation to about 0.25 g g^{-1} do not undergo lethal freezing damage when cooled slowly to cryogenic temperatures in cryovials (Pritchard and Prendergast, 1986; Chaudhury *et al.,* 1991; de Boucaud *et al.,* 1991; Abdelnour-Esquivel *et al.,* 1992; Pence, 1992, 1995; Chandel *et al.,* 1995).

As cooling and warming become progressively slower, flexibility in the permissible water contents is progressively reduced. The relatively slower cooling method for cryopreserving recalcitrant axes in cryovials requires drying axes to water contents where they are susceptible to desiccation damage (Becwar *et al.,* 1983; Normah *et al.,* 1986; Pammenter *et al.,* 1991; Pritchard, 1991; Vertucci *et al.,* 1991; Berjak *et al.,* 1992; Pammenter *et al.,* 1992, Pritchard *et al.,* 1995). The small window of permissible water contents may be narrowed further by an increasing requirement for water to prevent desiccation damage at lower temperatures (Vertucci and Roos, 1983; Vertucci, 1994, 1995; Vertucci and Farrant, 1995; Buitink *et al.,* 1996). Additionally, axes must be dried rapidly to avoid damage at intermediate water contents (Walters *et al.*, 2001; reviewed in Pammenter and Berjak, 1999; Walters *et al.*, 2002; Chapter 3) and this results in uneven distribution of water among tissues (e.g. Pritchard *et al.,* 1995; Pritchard and Manger, 1998; Chapter 3). The variable water content of different tissues makes axes susceptible to either freezing or desiccation damage when the range of permissible water contents is small.

Increasing the upper limit of permissible water contents for cryopreservation ameliorates this situation, and reduces the exposure of tissues to drying and freezing stress.

The present study demonstrates that the upper limit of permissible water contents for cryopreservation of *A. hippocastanum* axes can be increased by rapid cooling techniques from 0.28 g g^{-1} ([Pence, 1992]; Ψ= -12 MPa) to between 0.50 and 1.0 g g^{-1} (Ψ= -10 to -3.8 MPa, respectively; Fig. 6.4). The results do not separate fully the effects of cooling rate from those of water content on survival, but provide approximations of appropriate water content/cooling rate combinations for successful cryopreservation of *A. hippocastanum* axes. Cooling rates of about 60°C s^{-1} led to complete mortality of axes above 1.0 g g^{-1}, but resulted in 100% survival (albeit abnormal) of axes between 1.0 and 0.75 g g^{-1} (Ψ= -3.8 and -5 MPa, respectively) after cooling in isopentane (Fig. 6.5). The high incidence of disorganized callus proliferation and stunted growth (Fig. 6.6 e) suggests localised freezing damage and a requirement for cooling faster than 60°C s^{-1} at that water content range. Drying to 0.75 -0.5 g g^{-1} (Ψ= -5 to –10 MPa) and cooling rates averaging 200°C s^{-1} raised the proportion of axes developing normally (Fig. 6.5) presumably by further reducing freezing-related injury. (Fig. 4). Normal development was observed in all axes at ≤0.5 g g^{-1} (Ψ= -10 MPa; Fig. 6 g), where cooling rates above *c.* 70°C s^{-1} were sufficient to attain complete cryopreservation (Figs 6.5). Electrolyte leakage below 0.5 g g^{-1} was similar to that of corresponding axes that had not been cooled, further supporting that this combination of water content and cooling rate minimized cellular damage during cryopreservation.

The slopes of the regression lines relating electrolyte leakage from cooled axes to water content did not differ for isopentane and sub-cooled nitrogen treatments, suggesting that the faster initial cooling afforded by isopentane was not an important factor in ameliorating damage. However, it is also possible that this initial faster cooling was beneficial even at axis water contents above 0.75 g g^{-1}, and that the similar levels of electrolyte leakage observed (Fig. 6.3) reflects freezing damage that

occurred on warming and not during cooling. The physical constraints which limit rapid warming (Meryman, 1956), and the high sensitivity of hydrated cells to slow warming following non-equilibrium cooling have been highlighted previously (Mazur 1966, 1990; Meryman, 1966; Sakai *et al.,* 1968; Mazur and Schmidt, 1968; Sakai, 1970; Bank, 1973; Bank and Mazur, 1973).

The superiority of isopentane as a cryogen for cryopreservation studies was suggested by the completely normal development of axes at 0.5 g g^{-1} following cooling at rates ranging between 300 and 850°C s^{-1}. In contrast, corresponding axes plunged into sub-cooled nitrogen were cooled at rates that ranged only from 70 to 200°C s^{-1}. These axes failed to produce shoots, suggesting that cooling rates below 200°C s^{-1} were insufficient to prevent freezing damage and that additional drying to 0.4 g g^{-1} was required before normal development could be attained (Figs 6.5 b and 6.6). Further work is required to assess more comprehensively the relative suitability of these coolants in cryopreservation studies using rapid (non-equilibrium) cooling.

In conclusion, fast cooling to cryogenic temperatures relaxes the stringent conditions required to optimise water contents when cryopreserving recalcitrant embryonic axes. Rapidly traversing the range of temperatures supporting ice crystallisation reduces the likelihood of lethal freezing damage and obviates the need for excessive drying of axes that are sensitive to desiccation. If survival following non-equilibrium cooling is determined primarily by ice crystal size, then the upper limit of allowable water contents is likely to be defined by the highest cooling rate attainable given the size and water content of the axis and the conditions of cooling.

CHAPTER 7

The effects of cytoplasmic concentration (viscosity), cooling and warming rates upon survival of embryonic axes of *Poncirus trifoliata* (L.) RAF.

Introduction

Water content influences cytoplasmic viscosity and, therefore, the mobility of water within cells (Vertucci and Roos, 1990; Williams *et al.,* 1993; Buitink *et al.,* 1998b; Leprince and Hoekstra, 1998; Leprince *et al.,* 1999). When axes are exposed to rapid (non-equilibrium) cooling, the mobility of water and the cooling rate required to prevent the formation of lethal ice crystals are closely related (Luyet *et al.,* 1962; Rall and Fahy, 1985; Rall, 1987). The intracellular viscosity attained by drying to *c.* 0.25 g g^{-1} (Ψ= -12 MPa) is sufficient to limit ice formation during relatively slow cooling, making survival of axes independent of cooling rate (Vertucci, 1989a,b; Wesley-Smith *et al.,* 2001b; Chapter 6). With increasing hydration, the greater mobility of water requires that axes be cooled at correspondingly higher velocities if mechanical freezing injury is to be avoided (Wesley-Smith *et al.,* 1992; 2001b; Chapters 4 and 6). Eventually a threshold is reached, which is set by the difficulty in dissipating the greater heat load of hydrated specimens (Chapters 5 and 6) before freezing damage occurs. Therefore, successful cryopreservation protocols for embryonic axes should strike a balance between the intracellular viscosity (manipulated in the present approach by rapid drying to various water contents) and the conditions determining heat transfer during non-equilibrium cooling. Furthermore, extensive evidence suggests that rapid warming may reduce or avert freezing damage associated with migratory re-crystallisation (Meryman, 1956, 1966; Mazur, 1966, 1977,1990; Mazur and Schmidt, 1968; Sakai *et al.,* 1968; Leibo *et al.,* 1970; Bank, 1973; Bank and

Mazur, 1973). Warming rates that either limit (at best) or exacerbate the growth of ice crystals formed within cells during non-equilibrium cooling are likely to influence survival of embryonic axes at water contents above 0.25 g g^{-1} and, consequently, should also be considered.

It is difficult to separate the effects of cooling rate and water content on survival following rapid cooling, as these variables are co-dependent. Because of their large size and high water content, axes of *Aesculus hippocastanum* above 1.0 g g^{-1} (Ψ= -3.8 MPa) cooled at about 60°C s^{-1}, and did not survive cryogenic exposure (Wesley-Smith *et al.,* 2001b; Chapter 6). Reducing the water content to between 1.0 and 0.75 g g^{-1} did not increase cooling rates appreciably, but resulted in full survival, albeit abnormal growth (Wesley-Smith *et al.,* 2001b; Chapter 6). Further reducing the water content to between 0.75 and 0.5 g g^{-1} facilitated cooling rates averaging 200°C s^{-1} as well as an increase in the proportion of axes that developed normally. While drying below 0.5 g g^{-1} facilitated cooling rates of up to 850°C s^{-1}, cooling at 70°C s^{-1} appeared sufficient to achieve complete survival and normal development of axes in *vitro*. Although that phase of the study demonstrated that rapid cooling increased the permissible water contents for cryopreservation, it could not establish with certainty whether survival of partially-dried axes increased due to the higher cooling rates achieved, or because of the greater viscosity of the cytoplasm. That uncertainty was addressed in the present facet of the investigation using embryonic axes of recalcitrant *Poncirus trifoliata* (L.) seeds. The smaller size of axes of *P. trifoliata* relative to those of *A. hippocastanum* gave greater flexibility in controlling cooling rates, thereby allowing a comprehensive study of the interaction among cooling rate, water content and survival following exposure to cryogenic temperatures. The present study also addresses how the growth of ice crystals that presumably formed during cooling is either inhibited or promoted during warming by using two different warming velocities.

Materials and Methods

Seed material

Mature seeds of *Poncirus trifoliata* (L.) (Rutaceae) were obtained from Willits & Newcomb, Inc (Arvin, CA., USA) and maintained in a sealed container at 5°C. Axes were excised from seeds and accumulated on moistened filter paper about 30 min before drying and /or cryopreservation.

Drying and water content determination

Axes were dehydrated using the flash-drying chamber described by Wesley-Smith *et al.* (2001a; Chapter 3). Water contents were determined gravimetrically using sub-samples of 5 - 10 axes as described previously (Chapters 4, 5 and 6). A drying time course is shown in Figure 1. Axes for survival studies were either cryopreserved or rehydrated immediately after drying.

Cooling

Batches of 5 - 10 axes at various water contents were cooled to cryogenic temperatures using methods that yielded different cooling rates, namely:

Programmed cooling (see also Chapter 4). Constant cooling rates were achieved using a differential scanning calorimeter (DSC 7, Perkin Elmer, Norwalk, CT, USA). Axes were loaded onto DSC pans (without sealing), transferred to the DSC stage, cooled from 20°C to -160°C at 0.17°C s^{-1} (10°C min^{-1}) or 3.3°C s^{-1} (200°C min^{-1}). Axes were then transferred to an adjacent 50 ml container of liquid nitrogen using pre-cooled forceps to avoid re-warming

Immersion in liquid nitrogen. Faster cooling was achieved by immersing axes in liquid nitrogen. Enclosing axes within two different types of container varied the cooling rate attained. In one method, axes were enclosed within envelopes made from a double

layer of commercial light-weight Al foil, folded symmetrically into rectangles measuring 15 mm x 10 mm. Axes were secured within these envelopes by folding back the outermost 2 mm of all open sides. Subsequently, envelopes were held by one corner using fine forceps and immersed in liquid nitrogen (-196°C). Alternatively, axes were enclosed within screw-cap polypropylene containers (catalogue number 5005, Nalgene, Rochester, NY, USA) specially modified for this experiment as follows. Fine nylon mesh was heat-fused to the sawn-off base of the container and to a 15 mm opening in the lid of the container. This alteration secured axes while allowing their relatively quick and direct exposure to liquid nitrogen during cooling.

Plunge cooling. The fastest cooling was attained by plunging axes forcibly into sub-cooled nitrogen. For this purpose, axes were first mounted individually on cryo-ultramicrotomy specimen supports (Leica, Vienna, Austria) using a small amount of low-temperature adhesive. Each holder was subsequently propelled into the cryogen using one of the following methods. Either compressed air was used to propel axes on specimen supports individually into a polystyrene container filled to a depth of *c.* 70 mm with 150 ml sub-cooled nitrogen (Wesley-Smith *et al.,* 1992; Chapter 4); Alternatively, specimen supports were placed at the lower end of the spring-loaded device described in Chapter 5 and plunged at 1.2 m s^{-1} into a 160 mm container also filled with sub-cooled nitrogen at *c.* -210°C s^{-1} (Wesley-Smith *et al.,* 1999, 2001b; Chapters 5 and 6). Nitrogen was sub-cooled as described by Echlin (1992), and in both methods axes attached to supports using a low temperature adhesive (Tissue-Tek, Miles Scientific, USA) were plunged into the cryogen within 5 s after the slush was placed in the containers.

Following cooling, axes were maintained at -196°C for at least 15 min before warming as described below.

Warming

Two warming methods were used to retrieve axes from cryogenic storage:

Rapid. Axes were retrieved from liquid nitrogen storage and warmed by direct immersion in distilled water at 40°C. Specimen carriers with axes attached were plunged individually to a depth of 100 mm using forceps. Axes from other treatments were first transferred to a polystyrene foam cup containing approximately 5 ml of liquid nitrogen, and subsequently decanted into an empty 1000 ml beaker simultaneously with 500 ml of water at 40°C. This procedure ensured rapid warming of axes due to turbulent mixing. Axes were retrieved from the warming bath within one min, and rehydrated as described below.

Slow. Axes warmed slowly were transferred to un-stoppered polypropylene cryovials while under liquid nitrogen, placed on a laboratory bench and allowed to equilibrate to room temperature (20°C) following evaporation of the cryogen. Axes were subsequently immersed in water for 1 min at 40°C before further rehydration as described below.

Measurement of cooling and warming rates

Cooling and warming data were acquired using the system described previously (Wesley-Smith *et al.,* 1999; Chapter 5). Axes of *P. trifoliata* were relatively smaller (0.4 mg dry mass) and were likely to cool faster than larger specimens, such as axes of *Aesculus hippocastanum* (Chapter 6). Faster cooling can reduce freezing damage and facilitate survival of axes at higher water contents (Wesley-Smith *et al.*, 1992; Chapter 4). Since water in dilute solutions is mobile even at temperatures as low as -90 C (Wikefeldt, 1971) it was considered prudent to regard -100 C as the threshold temperature beyond which ice crystal growth would no longer not occur. Accordingly, cooling rates were measured between 0 and -100 C assuming linearity, which was true for all partially dried axes in the 0 to -80 C range. Temperature was measured

within the core of whole axes using a type J thermocouple of 75 μm wire diameter and c. 180 μm bead size (Omega Engineering Inc., Stamford, CT, USA). Segments of thermocouple wire exposed outside the specimen and insulated leads were covered with a fine layer of epoxy resin to prevent spurious measurement of temperature during cooling (Ryan and Purse, 1985b).

The fragile thermocouple could not be inserted into partially dried axes because these became hard and brittle. This problem was circumvented by impaling axes with pointed 3 mm segments of 75 μm wire prior to drying. After drying was completed, the wire segments were replaced with the temperature probe and the axes were cooled immediately.

Cooling rates of axes exposed to nitrogen were measured in 3 - 5 replicates at each water content tested. Cooling rates attained on the stage of the DSC were not measured, axes being assumed to cool at the software-controlled setting of either 3.3 or 0.17°C s^{-1}.

The rate of slow and rapid warming was measured in representative samples at different water contents.

Rehydration of axes and survival assays

Following drying, or immediately after warming from cryogenic storage, axes were placed upon moistened filter paper within closed Petri dishes, at room temperature and darkness for 30 min. Rehydrated axes were surface sterilised using the procedure described in Chapter 3 and cultured aseptically on Petri plates containing half-strength MS medium (Murashige and Skoog, 1962) solidified with 0.7% (w/v) agar. Cultures were kept under dark conditions for 48 h, and subsequently exposed to a 16h:8h light: dark photoperiod (Touchell and Walters, 2000). Survival after

cryopreservation was assessed using 5 - 10 axes per treatment, and experiments were repeated at least twice. Survival data were recorded after four weeks *in vitro*. Axes were scored as 'normal' when radicles doubled in length and shoots showed greening and development. Axes appearing stunted, showing incomplete root or shoot development or the formation of disorganised callus growth were classified as 'abnormal'.

Results

Fully hydrated axes of *P. trifoliata* had an average water content of 1.7 ±0.3 g g^{-1}, and a dry mass of 0.4 ±0.12 mg. The largest decrease in water content (50%) occurred within the first 10 min of flash drying, and declined less than 10% further between 40 and 80 min of drying (Fig. 7.1). Control axes (not cooled) dehydrated to various levels between 1.7 and 0.2 g g^{-1} showed more than 80% survival *in vitro* (data not shown; J. Crane, unpublished observations) .

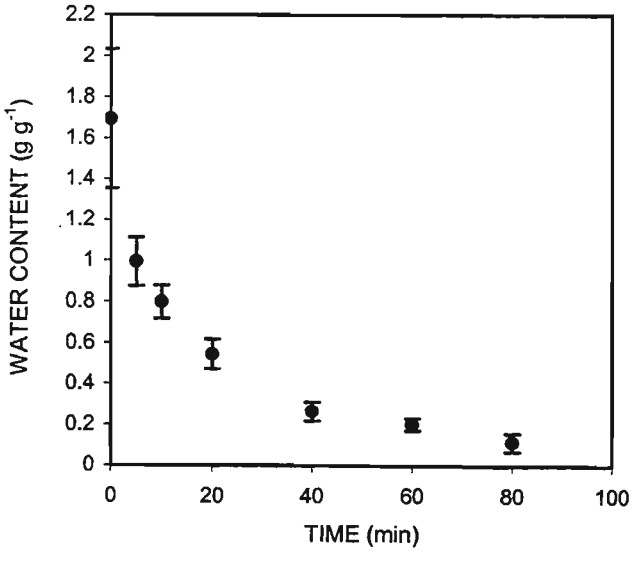

Fig. 7.1. Drying course for axes of *P. trifoliata* . Markers represent the mean of 5-10 axes per drying treatment ± standard deviation.

Cooling rates ranged between 0.17 and *c.* 1300°C s^{-1}, depending on cooling method and axis water content (Table 7.1). Representative cooling profiles of fully hydrated axes are illustrated in Figure 7.2, which highlights the orders of magnitude of

differences in cooling rates achieved. Multiple factor analysis of variance showed that both cooling method and water content each had a highly significant effect on cooling rates ($P < 0.001$), and that their interaction had no effect.

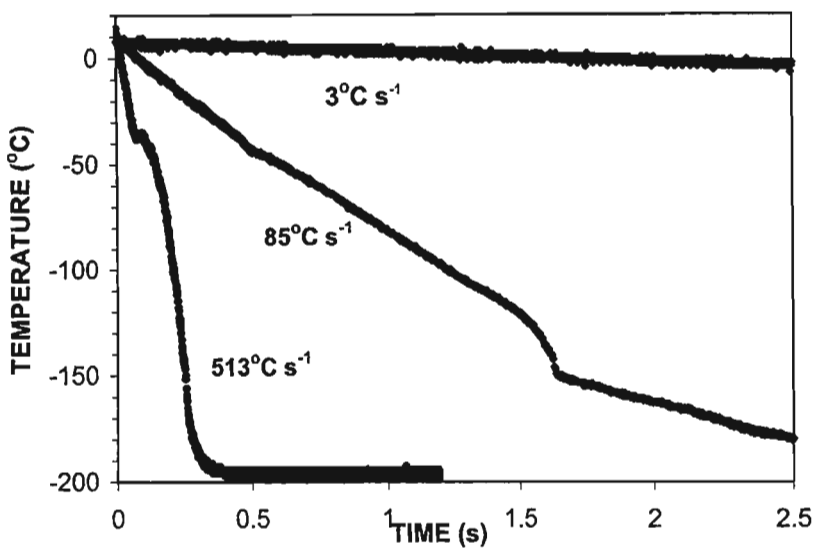

Fig. 7.2. Representative profiles of axes cooled at 3, 85 and 513°C s^{-1} using controlled cooling, the Al foil method and rapid plunging into sub-cooled nitrogen, espectively, clearly illustrates the orders of magnitude that separated these treatments.

Representative cooling profiles of axes plunged into sub-cooled nitrogen at various water contents using the spring-loaded device are shown in Figure 7.3. A representative cooling profile of the bare thermocouple is included in Figure 7.3 for comparison. Axes cooled by forced convection during the plunging phase which lasting approximately 120 ms. Cooling profiles varied among fully hydrated axes (*cf.* 1.7 a and b in Fig. 7.3) probably because of variability in water content (1.7 ±0.3 g g^{-1}) and / or dry mass (0.4 ±0.12 mg). In fully hydrated axes, large freezing transitions delayed cooling below -100°C by 200 - 300 ms (Fig. 7.3). The lowest temperatures attained by fully hydrated axes at the end of the plunge ranged between -40 and

-80°C (Fig. 7.3). Cooling profiles from axes between 0.8 and 0.3 g g^{-1} g g^{-1} showed no visible freezing transitions, and cooling to -100°C was almost linear (Fig. 7.3).

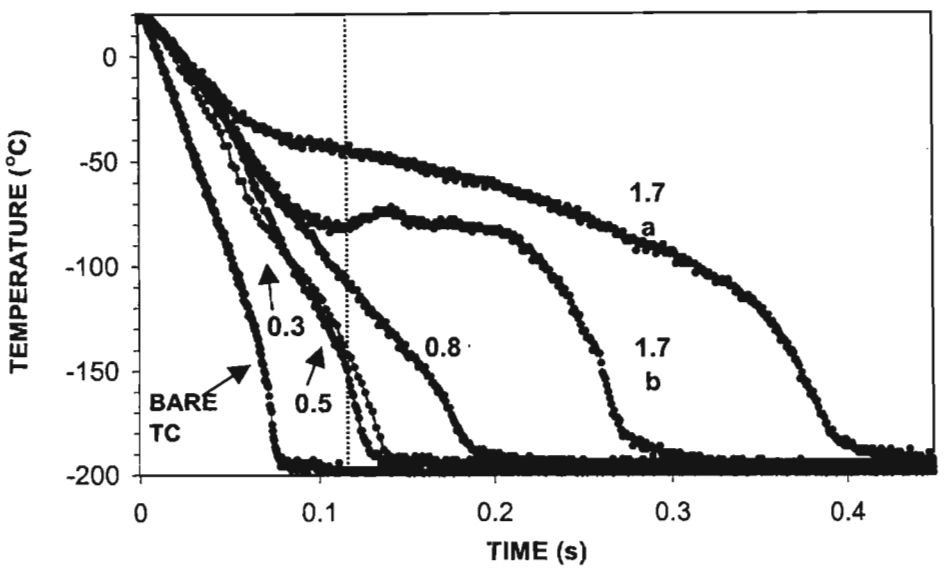

Fig. 7.3. Representative cooling profiles of axes plunged into sub-cooled nitrogen at the water contents indicated. The cooling profile of a bare thermocouple is included for reference. The variable response of fully hydrated axes (1.7 a, b) to identical cooling conditions was ascribed to differences in water content and/or dry mass.

Table 7.1. Cooling rates attained in variously hydrated axes following cooling by various methods. Cooling rates of axes at 0.2 g g^{-1} could not be measured because axes became brittle and were damaged while impaling onto the thermocouple.

COOLING METHOD	AVG COOLING RATE (°C s^{-1}) ± SD			
	Axis water content (g g^{-1})			
	1.7	0.8	0.55	0.26
Spring-loaded plunge	513 ±147	988 ±269	1073 ±414	1282 ±440
Compressed-air injection	414 ±100	686 ±200	863 ±163	959 ±286
Nylon mesh container	200[a]	515 ±112	513 ±9	515[a]
Al foil envelopes	84 ±9	84 ±9	84 ±9	84 ±9
DSC stage	3.3	3.3	3.3	3.3
	0.17	0.17	0.17	0.17

[a] Measured only once.

While dehydrated axes cooled faster than their fully hydrated counterparts, cooling was none the less slower than that of the bare thermocouple plunged under identical conditions. This observation shows that even at 0.3 g g^{-1} the thermal load of axes was sufficiently large to influence the cooling rate, and that the thermocouple did not limit the cooling rates measured inside partially dry axes.

The warming process influenced the length of the exposure of axes cooling by the various methods tested to temperatures favouring crystallisation. Axes between 1.7 to 0.26 g g^{-1} required approximately 150 ±47 ms (data not shown) to warm rapidly from -100 to 0°C. Accordingly, axes spring-driven into sub-cooled nitrogen and warmed rapidly were exposed to harmful temperatures for approximately 360 ms when fully hydrated, and for less than 250 ms below 0.8 g g^{-1} (i.e. 210 and 100 ms during cooling, respectively, and 150 ms during warming). On the other hand, axes cooled at 0.17°C s^{-1} and warmed slowly remained within this critical temperature range for approximately 12 min.

Morphological appearance of cryopreserved axes

Different embryonic tissues from cryopreserved axes responded differently to freezing stress. Cells from the epicotyl showed greatest sensitivity, and cells from the radicle greatest tolerance to cooling. Failure of axes to develop shoots represented the earliest sign of freezing injury, while callus proliferation (usually near the radicle) suggested that extensive damage had occurred, and constituted survival in its most rudimentary form.

Survival

Figure 7.4 illustrates the relationship between cooling rate (x axis; see also Table 7.1) and survival (y axis) of axes at different water contents (horizontal rows) and after warming either rapidly (solid markers) or slowly (open markers). The graphs in the left

column (Figs 7.4 a, c, e, g and i) represent the percentage of axes that survived cryogenic exposure at the conditions stated. Graphs on the right hand column (Figs 7.4 b, d, f, h, j) represent the percentage of the total number of axes cooled that germinated normally.

Categorical data analysis using a log-linear approach (Appendix A; Knoke and Burke, 1980) showed that water content, as well as the rates of cooling and warming, had significant (P <0.01) effect upon survival of axes. Survival was also influenced significantly (P <0.05) by interactions between cooling rate and water content, and also cooling rate and warming rate (Appendix A). Overall, partial drying and rapid warming reduced freezing damage, increasing both total survival (Figs 7.4 a, c, e, g and i) and the proportion of axes that developed normally (Figs 7.4 b, d, f, h, j). For greater clarity, survival data for each water content are presented separately below.

Fully hydrated axes. Axes cryopreserved at 1.7 g g^{-1} suffered extensive freezing damage especially after slow warming (Figs 7.4 a, b). Axes warmed rapidly showed between 60 and 90% survival, and normal development reached an unexpected almost 40% after cooling at 0.17°C s^{-1}, decreasing to <20% at higher cooling rates.

0.8 g g^{-1}. Drying to 0.8 g g^{-1} increased survival of axes after both warming treatments, although rapid warming seemed to be more favourable especially for axes cooled at higher rates (Fig. 7.4 c). Normal development of axes warmed rapidly increased from 0% at 0.17°C s^{-1} to 50% at 3.3°C s^{-1} and 100% at 414°C s^{-1} (Fig. 7.4 d). These results suggest that at 0.8 g g^{-1} a narrow range of optimum cooling rates existed, above and below which damage increased. In contrast, normal development of axes warmed slowly did not exceed 25%, and only after cooling at ≤3.3°C s^{-1} (Fig. 7.4 d).

0.55 g g^{-1}. Survival of axes dried to 0.55 g g^{-1} was ≥80% at all cooling rates and warming rates tested (Fig. 7.4 e). Normal development among axes warmed rapidly followed a similar trend to that observed at 0.8 g g^{-1}, although the apparent optimum cooling range broadened to include slower treatments (Fig. 7.4 f). Normal development of axes warmed rapidly was highest (100%) in axes cooled between 86 and 513°C s^{-1}, decreasing somewhat to approximately 80% at 3.3 and *c.* 1000°C s^{-1}. Among axes warmed slowly, normal development remained below 25%, but the range of favourable cooling rates increased to 0.17 - 84°C s^{-1} (Fig. 7.4 f).

0.26 g g^{-1}. Survival of axes dehydrated to this water content was also ≥80% at all cooling rates and warming rates tested (Fig. 7.4 g). The proportion of axes developing normally after rapid warming, and the range of cooling rates facilitating this, became even greater than at higher water contents (Fig. 7.4 h). In axes warmed rapidly, all cooling rates below about 1000°C s^{-1} resulted in 80 - 100% normal development, which decreased to 65% after cooling at *c.* 1300°C s^{-1}. Axes at 0.26 g g^{-1} showed greater tolerance to slow warming especially after slow cooling, as indicated by >20% normal development at most cooling rates tested.

0.2 g g^{-1}. Drying to this water content led to the highest survival of all axes (Fig. 7.4 i), but also resulted in contrasting germination responses of axes warmed either rapidly or slowly (Fig. 8.4 j). The trends observed suggest that normal development in axes warmed rapidly was higher following rapid cooling whereas the reverse was true for axes warmed slowly (Fig. 7.4 j).

Fig. 7.4. Percentage of axes surviving cryopreservation (a, c, e, g, i) and showing normal development (b, d, f, h, j) after cooling at various rates and warming either rapidly (solid markers; solid lines) or slowly (open markers; dashed lines) at the water contents indicated. (Curves fitted by eye.)

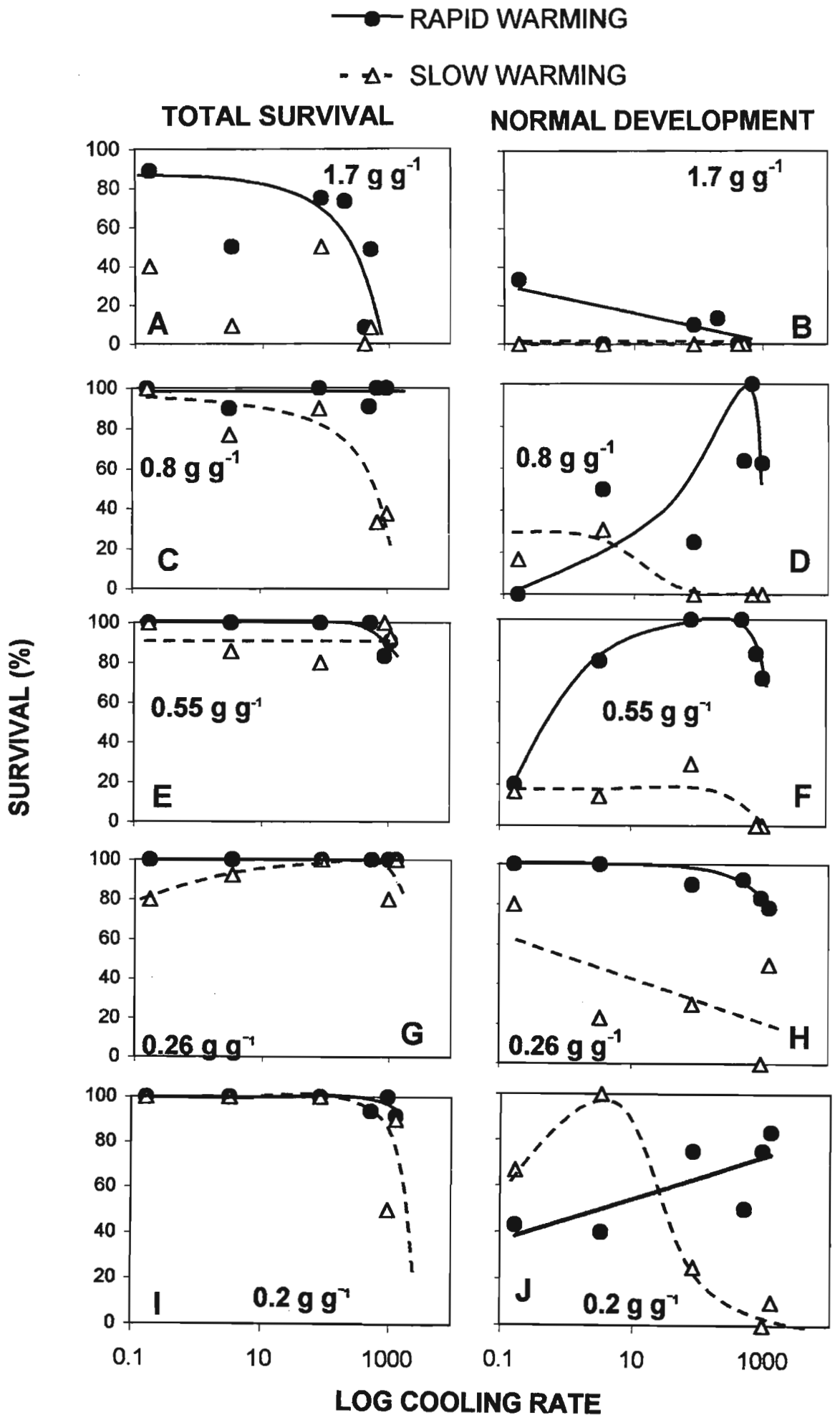
RAPID WARMING
SLOW WARMING
TOTAL SURVIVAL
NORMAL DEVELOPMENT
SURVIVAL (%)
LOG COOLING RATE
1.7 g g-1
0.8 g g-1
0.55 g g-1
0.26 g g-1
0.2 g g-1
A
B
C
D
E
F
G
H
I
J
0
20
40
60
80
100
0.1
10
1000

Discussion

Successful cryopreservation procedures strive to avoid damage associated with freezing or extreme drying either during pre-treatment or during exposure to cryogenic temperatures. The present study investigated the extent to which cooling and warming rates influenced the survival *in vitro* of axes of *Poncirus trifoliata* at various water contents. Results from the present and previous investigations (Wesley-Smith *et al.,* 1992, 2001b; Chapters 4 and 6) support the contention that damage can be avoided if a balance is attained between the time spent at temperatures that promote crystallisation and the relative mobility of water within that range (Luyet *et al.,* 1962; Rall and Fahy, 1985; Rall, 1987). In the present context, the 'time' variable was explored using cooling rates ranging between 0.17 and 1300°C s^{-1} and by warming regimes that either limited or prolonged the exposure to sub-zero temperatures. Additionally, the mobility of water was manipulated by dehydrating axes to various sub-lethal water contents. The results obtained contribute towards increasing present understanding of the response of histologically-complex structures such as embryonic axes to non-equilibrium cooling and warming.

Exposing hydrated tissues to cryogenic temperatures under non-equilibrium cooling conditions often leads to intracellular freezing that, unless restrained, can cause sufficient damage to be lethal (reviewed by Mazur, 1990). If rapid cooling could hinder the arrangement of water molecules into ice (Luyet, 1960, 1965) plunging axes rapidly into nitrogen at *c.* -210°C was the approach most likely to achieve this goal among the methods presently investigated. However, despite the fact that fully hydrated axes plunge-cooled within 120 ms to temperatures where the mobility of water and latent heat of fusion are reportedly reduced (e.g. -40°C; [MacKenzie, 1977; Franks, 1980]), large freezing transitions were observed at the end of the plunge (Fig. 7.3), and survival evidence suggested that the ice crystals formed were damaging

(Fig. 7.4 a). Cooling at 414 or 513°C s^{-1} also appeared insufficient to prevent extensive freezing damage in fully hydrated axes of *P. trifoliata*.

Water constitutes the largest reservoir of thermal energy within cells (Bachmann and Mayer, 1987), and so dehydrating axes reduces their thermal load and facilitates faster cooling (Chapters 5). Lowering the water content from 1.7 to 0.8 g g^{-1} almost doubled the cooling rate of naked axes of *P. trifoliata* propelled mechanically into sub-cooled nitrogen (*c.* -210°C) or immersed in nitrogen at -196°C within meshed containers (Table 7.1). Cooling within fully hydrated axes was presumably limited by the conductivity characteristic of hydrated tissues (Bald, 1987). In contrast, the apparent absence of freezing transitions from temperature profiles of plunge-cooled axes between 0.8 and 0.3 g g^{-1} (Fig. 7.3) suggests that their reduced heat load was dissipated efficiently by convective cooling during the plunge. Cooling rates attained within open mesh containers were lower and also varied less with water content than those attained by mechanical plunging devices, presumably reflecting reduced convective cooling. This trend was accentuated further in axes enclosed within Al envelopes, which cooled at about 84°C s^{-1} irrespectively of their water content. The rate of heat conduction through air pockets and the double layer of Al foil that surrounded the axes may have limited cooling by this method. Therefore, partial drying reduces the thermal load of axes, facilitating faster cooling at rates that can seemingly suppress large freezing events. But while reduced thermal loads appear to be more relevant to methods relying primarily on convective cooling than to those where axes are enclosed within containers, the increase in cytoplasmic concentration that necessarily accompanies partial drying was associated with greater success.

Partial drying increases cytoplasmic viscosity (Buitink *et al.,* 1998b; Leprince and Hoekstra, 1998; Leprince *et al.,* 1999), and in the present study this was associated with increased overall survival of axes cryopreserved at water contents between 1.7

and 0.2 g g^{-1}. Higher viscosity hinders ice crystal growth (Luyet 1960, 1965; Luyet *et al.,* 1962; Franks, 1980; Rall and Fahy, 1985; Rall, 1987) because it reduces the mobility of water (Hirsh *et al.,* 1985; Burke, 1986; Williams and Leopold, 1989; Williams *et al.,* 1993). Additionally, increased cytoplasmic viscosity lowers the freezing temperature (Rasmussen and MacKenzie, 1972; Rasmussen *et al.,* 1975; Meryman and Williams, 1980; Becwar *et al.,* 1983; Vertucci, 1990; Wesley-Smith *et al.,* 1992 [Chapter 4]; Pritchard *et al.,* 1995; Farrant and Walters, 1998) and raises the glass transition temperature (Meryman and Williams, 1980; Williams and Leopold, 1989; Williams *et al.,* 1993; Leprince and Walters-Vertucci, 1995; Buitink *et al.,* 1996). This means that the range of temperatures promoting freezing during cooling and warming is correspondingly reduced, as is the rate required to traverse this region without injury (Robards and Sleytr, 1985). These effects reflected upon the range of cooling rates that favoured normal development *in vitro*. In axes dried to 0.26 g g^{-1}, more than 80% normal development was attained after cooling between 0.1 and 1000°C s^{-1} and warming rapidly (Fig. 7.4 h). At 0.55 g g^{-1} the equivalent favourable range narrowed to 3.3 - 860°C s^{-1} (Fig. 7.4 f). At 0.8 g g^{-1} an even narrower range was observed, where full survival after cooling at 686°C s^{-1} decreased to about 60% at cooling rates of both 988 and 515°C s^{-1} (Fig. 7.4 d). The range of favourable cooling rates also increased with increasing drying among axes warmed slowly, although overall survival remained consistently lower than that attained by rapid warming. Therefore, higher cytoplasmic viscosity induced by drying from 1.7 to 0.26 g g^{-1} appeared to hinder the freezing process increasingly, facilitating survival and normal development of axes after cooling at a wide range of velocities, especially after rapid warming. These results emphasise the greater dependence of axes at higher water contents upon cooling rates sufficiently fast to restrict freezing damage as water becomes increasingly mobile. This finding is highly relevant to the cryogenic storage of recalcitrant axes at water contents above those that are associated with damage, and which promote freezing during cooling to -196°C (e.g. Vertucci *et al.,* 1994).

If rapid cooling is beneficial because it restricts mechanical freezing damage, then the decrease in normal development observed at the highest cooling velocities contradicts this. Increased damage at the highest cooling rates suggests the existence of optimal ranges. While damage at the lower end of such range can be explained readily by reference to excessive crystallisation occurring at slower cooling velocities, accounting for damage caused by cooling at rates above those already facilitating complete survival is challenging. Mechanical damage can be ruled out, since axes cooled at slower rates germinated normally in spite of the greater likelihood of their sustaining intracellular damage. Earlier studies have ascribed damage caused by "rapid" cooling to thermal shock (Lovelock, 1955; Meryman, 1956, 1966; Morris *et al.,* 1983), lipid phase transitions (Williams, 1990) or biochemical injury resulting from the concentration of intracellular solutes that inevitably accompanies freezing (Meryman, 1956, 1960; Franks, 1977, 1980). If intracellular glasses had formed, it is possible that these became unstable at temperatures far below the glass transition temperature (T_g; Williams *et al.,* 1993). It is also possible that in the present study mechanical vibration induced by the sudden stop at the end of the plunge may have been damaging. The latter suggestion could account for the sharp difference in normal development between axes at 0.8 g g^{-1} cooled either by the spring-driven method or by the relatively gentler compressed-air method before rapid warming. Further research is required to explore the occurrence and limits of supra-optimal cooling among embryonic axes of other species.

Cooling at ≥0.17°C s^{-1} (10°C min^{-1}) has been reported to induce intracellular freezing in plant cells (e.g. Sakai and Otsuka, 1967; Sakai and Yoshida, 1967; Sakai *et al.*, 1968; Mohr and Stein, 1969; Morris, 1976; Steponkus, 1984) and yeast (e.g. Mazur and Schmidt, 1969). Therefore, it was unexpected to find that fully hydrated axes developed normally after cooling under conditions presumed to promote - rather than

avoid - equilibrium by intracellular freezing (see review by Mazur, 1990). In the present study, fully hydrated axes cooled at 0.17°C s^{-1} showed 90% survival and 35% normal development after rapid warming. The possibility of survival being due to extracellular freezing is extremely unlikely in view of the 60% mortality and 100% abnormal development of similar axes after slow warming (Figs 7.4 a, b). Alternatively, if intracellular freezing occurred, and it was not lethal, would imply that ice nuclei formed predominantly within non-critical cellular domains and were excluded from others sensitive to freezing damage. This possibility was suggested previously (Sherman and Kim, 1967; Mazur, 1977, 1984) and is supported by extensive evidence suggesting that intracellular freezing is not necessarily lethal (Albrecht *et al.*, 1973; Sherman and Kim, 1967; Mazur and Schmidt, 1968; Mohr and Stein, 1969; Sakai, 1968, 1970; Mazur *et al.,* 1969; Asahina *et al.,* 1970; Bank and Mazur, 1973; Bank, 1974; Vertucci, 1989a; Vertucci *et al.,* 1991, 1995) providing warming is sufficiently rapid (reviewed by Mazur, 1990). The exclusion of ice crystals from some domains could be explained by differences in the solute concentration, membrane permeability and the extent of supercooling endured by various cellular compartments (Meryman, 1966; Sherman and Kim, 1967; Bank, 1974; Mazur, 1977, 1984; Franks, 1980). Since the amount of supercooling influences the number of nuclei formed upon freezing (MacKenzie, 1977; Franks, 1977, 1980; Bald, 1987), cooling fully hydrated axes at either 513 or 0.17°C s^{-1} is likely to result in different distributions of ice within cells. Several studies (Sherman, 1964; Rebhun and Sander, 1971; Bank and Mazur, 1973; Nei, 1976) have provided evidence of the uneven distribution of ice with rapidly cooled cells. Ultrastructural evidence supporting intracellular freezing compatible with survival and normal development was gathered in a subsequent study using axes of *Acer saccharinum* seeds cooled between 3.3 and 77°C s^{-1}, and this is reported in Chapter 9. Presumably in axes of *Poncirus trifoliata* cooling rates above 0.17°C s^{-1} resulted in widespread damage throughout

cellular compartments. It is likely that the pervasive nature of these crystals could underlie the greater sensitivity of axes to slow warming (Mazur, 1984, 1990).

Axes dehydrated to 0.2 g g^{-1} showed contrasting survival depending on whether warming was rapid or slow (Fig. 7.4). Since DSC studies showed no evidence of water freezing in similar axes (J. Crane, unpublished observations) the damage observed cannot be ascribed to ice crystal growth, and possibly reflects stress associated with reduced water content and low temperatures (Vertucci and Roos, 1993; Vertucci *et al.,* 1994, 1995). Axes cooled and warmed rapidly probably benefited from the relatively shorter exposure (*c.* 300 ms) to such harmful conditions. Conversely, it is plausible that slow warming of similar axes allowed sufficient time for deleterious de-mixing of membrane components (e.g. Bryant *et al.*, 2001). At the opposite end of the cooling scale, slow cooling could have predisposed axes to damage caused during imbibition (e.g. Chapter 3). Although speculative, it may be suggested that the reduced damage observed in axes cooled and warmed slowly may reflect beneficial redistribution of cellular water during the brief interval (min) between axes equilibrating to room temperature and being immersed in water, in contrast to rapidly warmed axes which were immediately immersed.

Results obtained in this study support the view of Luyet and colleagues (Luyet 1960, 1965; Luyet *et al.,* 1962) that rapid cooling alone appears to be insufficient to prevent freezing damage, especially in large structures. This would apply to embryonic axes of desiccation-sensitive seeds in general. The potential of rapid (non-equilibrium) cooling as a reliable cryopreservation tool is realised when used in combination with steps that increase cytoplasmic viscosity such as two-step cooling (Sakai and Yoshida, 1967; Farrant *et al.,* 1977a), vitrification solutions (Rall and Fahy, 1985; Rall, 1987; Langis and Steponkus, 1990; Steponkus *et al.,* 1990; Mazur *et al.,* 1993) or partial drying (Rebhun and Sander, 1971; Wesley-Smith *et al.,* 1992, 2001b; Chapters

4, 6 and this chapter). Results here highlight the advantages of exploiting rapid cooling and warming to minimise the extent of drying required to increase survival. This point is illustrated further by reference to an earlier cryopreservation study using embryonic axes of *P. trifoliata* (Radhamani and Chandel, 1992). In that study, axes were enclosed within cryovials which were subsequently wrapped in Al foil, cooled at 3°C s^{-1} and warmed at a rate intermediate to those presently used. Survival was highest (68%) in axes at water contents of 0.16 g g^{-1}, and no survival was attained above 0.25 g g^{-1}. Barring developmental differences between axes used in the two studies, evidence from the present study suggests that even at the same cooling rate (3°C s^{-1}) faster warming alone could have facilitated >80% survival and ≥80% normal development at water contents as high as 0.55 g g^{-1}.

Appendix A. Hierarchical log-linear analysis of the effects of cooling (C), warming (W) and water content (H) on survival (S) of axes of *Poncirus trifoliata*.

Main Effects on Survival	Model	df	L^2 [a]	P	Q^2 (%) [b]
Baseline [c]	[S CHW]	118	416.8	<0.0001	-
Water content	[S CHW][HS]	110	264.2	<0.0001	36.6
Warming	[S CHW][WS]	116	366.7	<0.0001	12.0
Cooling	[S CHW][CS]	108	391.8	0.005	6.0

Interaction Effects	Model	df	L^2 [a]	P	Q^2 (%) [b]
Baseline [c]	[CHW][WS][CS][HS]	98	134.7	0.008	-
Cooling x water content	[CHW][CHS][WS]	58	76.9	0.03	42.9
Cooling x warming	[CHW][WCS][HS]	88	109.8	0.005	18.4
Warming x water content	[CHW][WHS][CS]	90	121.6	0.10	9.7

[a] L^2= Log-likelihood ratio (Knoke and Burke, 1980)

[b] Q^2= (L^2 baseline model - L^2 alternative model) / (L^2 baseline model). An R^2 analogue that reflects the amount of variance not explained by the baseline model, and that is explained by each interaction term.

[c] First Level interaction, incorporating all single order independent terms

CHAPTER 8

A cryopreservation study of embryonic axes of *Acer saccharinum*. Ultrastructural assessment of freezing damage and subsequent recovery *in vitro*

Introduction

It is generally accepted that the presence of intracellular ice is not necessarily lethal (Albrecht *et al.*, 1973; Sherman and Kim, 1967; Mazur and Schmidt, 1968; Sakai, 1968, 1970; Mazur *et al.*, 1969; Asahina *et al.*, 1970; Bank and Mazur, 1973; Bank, 1974; Vertucci, 1989a; Wesley-Smith *et al.*, 1992; Vertucci *et al.*, 1995). However, most cryopreservation procedures endeavour to prevent crystals from forming in the protoplasm, thereby minimising the risk of mechanical injury. In plants this goal can be achieved if the mobility of intracellular water is restricted sufficiently prior to cryogenic exposure, either by drying tissues to low water contents (*c.* $\leq$ 0.4 - 0.2 g H_2O g dry mass; e.g. Vertucci, 1989a,b, Vertucci *et al.*, 1991) or by raising the cytoplasmic viscosity with cryoprotectants (e.g. Morris, 1976; Finkle *et al.*, 1985; Mycock *et al.*, 1995; Thammasiri, 1999; Stewart *et al.*, 2001). An additional protective strategy involves limiting the time of exposure to temperatures promoting ice crystal growth by maximising the cooling and warming rates (Luyet, 1960, 1965; MacKenzie, 1970). Rapid cooling and partial drying have been combined in an approach that facilitates reliable cryostorage of zygotic embryonic axes of recalcitrant (Wesley-Smith *et al.*, 1992, 2001b; Chapters 4, 6 and 7) and germinating orthodox seeds (Wesley-Smith *et al.*, 1995) as well as somatic embryos from both seed types (Mycock *et al.*, 1995).

By restricting the size of ice crystals formed to within harmless limits, rapid cooling makes it possible to cryopreserve axes at relatively higher water contents before lethal limits are reached (Wesley-Smith *et al.*, 1992, 2001b; Chapters 4, 6 and 7). Consequently, this approach is ideally suited to the cryopreservation of desiccation-sensitive material that is damaged by drying to low water contents. The work

embodied in this thesis has explored the complex relationship between properties of the axes (e.g. size, water content), conditions during cooling and warming, and survival of axes *in vitro*. The use of cryoprotectants has been deliberately omitted from those studies in order to appreciate fully the effects of non-equilibrium cooling upon cellular structure and function. Results indicate that survival becomes possible when axes are cooled above a critical rate that is influenced strongly by intracellular viscosity (Wesley-Smith *et al.,* 2001b; Chapters 6 and 7). With increasing hydration, lethal freezing during non-equilibrium cooling can be prevented only if the cooling rate is increased in accordance with the greater mobility of water (Luyet *et al.,* 1962). Accordingly, ≥80% of axes of desiccation sensitive *Poncirus trifoliata* seeds *at* 0.26 g g^{-1} germinated normally *in vitro* after cooling between 0.1 and *c.* 1000°C s^{-1} (Chapter 7). Between 0.26 and 0.8 g g^{-1}, the range of cooling rates required to attain similar survival became narrower and displaced towards the higher end of the scale. Fully hydrated axes at 1.7 g g^{-1} could not be cooled faster than *c.* 500°C s^{-1}, even under the most favourable conditions (Chapter 5). High mortality and abnormal development among surviving axes of *P. trifoliata* suggested that cooling at *c.* 500°C s^{-1} could not prevent extensive freezing damage (Chapter 7). Unexpectedly, that same study showed ≥80% of fully hydrated axes cooled at 3.3 or 0.17°C s^{-1} survived cryogenic exposure, and that up to 35% of those axes developed normally *in vitro*. The present aspect of the study was partly motivated by the paradoxical survival of those axes, cooled at rates that encouraged - rather than restrained – intracellular ice formation (Sakai and Otsuka, 1967; Sakai and Yoshida, 1967; Mohr and Stein, 1969; Morris, 1976; Steponkus, 1984).

Many ultrastructural studies have attempted to establish an association between the size of ice crystals formed within single cells and micro-organisms during rapid (non-equilibrium) cooling and the preservation of functional integrity after warming (e.g. Nei, 1976, 1977; Asahina *et al.,* 1970, Sakai *et al.,* Shimada and Asahina, 1972, 1975; Plattner *et al.,* 1972; Bank, 1973, 1974; Farrant *et al.,* 1977b; Fujikawa, 1980, 1988). Defining the size of ice crystals 'critical' to prevent lethal injury becomes even more difficult in tissues with linear dimensions >0.1 mm. Large temperature gradients

that develop in such tissues during cooling expose cells at different locations to different cooling rates (Bald, 1984, 1987), leading to the formation of a wide range of ice crystals (e.g. Meryman, 1960; Van Venrooij *et al.,* 1975). Establishing 'critical' ice crystal sizes is complicated further by differences in the response to cooling of cells from different tissues (and even within the same tissue) . To gain further insight into the conditions that underlie success or failure during cryopreservation of embryonic axes from desiccation-sensitive seeds, the present study aimed at

1. Evaluating the interaction between cooling rate, warming rate, water content and survival *in vitro* of embryonic axes of *Acer saccharinum* (silver maple) seeds
2. Confirming previous findings that partial drying and increased cooling rate reduces freezing damage, and increases survival of axes warmed rapidly (Wesley-Smith *et al.,* 1992; Chapter 4)
3. Investigating the ultrastructural distribution of ice within cells of fully hydrated axes cooled at different rates, and relating the freezing patterns observed to survival after warming at different rates
4. Exploring the paradoxical possibility that cooling to cryogenic temperatures under conditions that promote the formation of relatively large intracellular ice crystals may confer some protection upon fully hydrated axes against lethal damage
5. Monitoring at light and electron microscopy levels the recovery of fully hydrated axes after cooling by either plunging or at 3.3°C s^{-1} (200°C min^{-1}) followed by rapid warming, and relating the appearance of cells in the solidified state to their ultrastructural development *in vitro.*

Zygotic axes of *A. saccharinum* (silver maple) seeds were selected because earlier attempts to cryopreserve seeds of this species had failed (Becwar *et al.,* 1983). Furthermore, these axes exemplify material commonly encountered in attempts to conserve genetic resources of temperate species producing desiccation-sensitive seeds. The ultrastructure of cells in the solidified state was assessed using freeze-

fracture and freeze-substitution techniques. The freezing patterns observed within the cells were related to cooling rates measured in the core of the axes. Fully hydrated axes were selected for this aspect of the present study because of their greater propensity to freezing damage. The effect of partial drying on the ultrastructure of plunge-cooled axes was also investigated using freeze-fracture. Ultrastructural assessment of the ability of cells to repair was carried out for axes cooled by plunging or at 200°C min^{-1} and only after rapid warming, an approach which reduces freezing injury (reviewed by Mazur, 1990; Chapter 7).

Materials and Methods

Seed Material

Seeds of *A. saccharinum* L. were harvested from a single tree in Ft Collins, CO. (USA). Mature seeds were sorted and stored within plastic bags at 4°C until required. Experiments were conducted within a week after harvesting, as these seeds germinate readily in storage. Embryonic axes were excised and accummulated on moistened filter paper prior to being either dehydrated or cryopreserved.

Dehydration

Embryonic axes were dehydrated rapidly using the flash-drying chamber described by Wesley-Smith *et al.*, 2001a; Chapter 3) and sampled after 0, 20 or 165 min of drying. Five axes from each drying interval were weighed immediately, and water contents were determined gravimetrically after drying to constant weight in an oven at 105°C. Water contents are expressed as g g^{-1} dry mass.

Cooling

Axes were exposed to cryogenic temperatures using three methods, *viz.* plunge cooling, aluminium foil envelopes and controlled-rate cooling.

Plunge cooling

Axes were cooled using the spring-loaded plunging device described in Chapter 5, and the related methodology used in Chapters 6 and 7. Axes were plunged into sub-

cooled nitrogen to a depth of 160 mm and at an average velocity of 1.2 m s^{-1}. Cooled axes were transferred without warming to a liquid nitrogen reservoir, where they were stored in excess of 30 min.

Aluminium foil envelopes

Five axes per treatment were enclosed within Al foil envelopes of similar dimensions to those used for the cryopreservation study of *Poncirus trifoliata* (Chapter 7). The procedure used here differed from the one in Chapter 7 only in that a single layer of foil (instead of two) was presently used. Preliminary temperature measurements indicated that using a double layer of Al foil yielded rates that were slower than those attained in Chapter 7 because of the relatively larger size of axes of *A. saccharinum*. It was expected that using a single layer compensate for the larger size and achieve cooling rates of *c.* 90°C s^{-1}.

Controlled cooling

Axes were also cooled at 3.3°C s^{-1} (200°C min^{-1}) on the stage of a Perkin Elmer DSC 7 differential scanning calorimeter (Norwalk, CT, USA) as described previously (Wesley-Smith *et al.,* 1992; Chapters 4 and 7). Following cooling, the open pans containing the axes were transferred to a container with liquid nitrogen using pre-cooled forceps to prevent warming and were stored for at least 30 min.

Warming

The effects of warming rate on the survival of axes cooled by the three methods were assessed following warming at three velocities. The fastest warming was achieved by direct exposure of axes to water at 40°C. Axes attached to specimen supports were plunged individually and forcefully into water to a depth of 100 mm. Axes cooled by the Al foil method, or on the stage of the DSC, were immersed in <5 ml of liquid nitrogen, and then decanted into an empty beaker synchronously with 500 ml distilled water at 40°C. This step achieved turbulent mixing and maximised the warming process. The identical procedure, but at 4°C, achieved relatively slower warming. The slowest warming rate was achieved by placing axes cooled at various velocities on

the pre-cooled stage of the DSC at –160°C and warming to 20°C at 0.08°C s^{-1} (5°C min^{-1}). Axes cooled rapidly were detached from their specimen supports under liquid nitrogen before placing on Al on the pre-cooled stage of the DSC. After warming was completed, axes from intermediate and slow warming treatments were exposed to water at 40°C for one min to ensure uniformity of experimental conditions. All axes were subsequently allowed to equilibrate on moistened filter for 30 min in the dark, as reduced light intensity minimises the likelihood of deleterious free-radical activity in stressed plant cells (Touchell and Walters, 2000).

Measurement of cooling and warming rates

Cooling rates in the core of axes plunged into the cryogen either bare, or within Al envelopes, were measured using a Type 'J' thermocouple of 125 μm wire diameter and 300 μm bead diameter as described previously (Chapter 5). Cooling and warming rates were measured individually for six axes per treatment. Water within biological tissues freezes mostly between 0 and -40°C (e.g. Sakai and Otsuka, 1967; Moor, 1973), so rates were calculated within this range assuming linearity. Axes placed on the stage of the DSC were assumed to cool at 3.3°C s^{-1} and warm at 0.08°C s^{-1} at the rate controlled by the software.

Survival Studies

The effect of cooling and warming treatments on survival of axes at various water contents was assessed by germination *in vitro*. Axes were surface sterilised using the procedure described in Chapter 3 and grown aseptically on Woody Plant Medium (Lloyd and McGown, 1980) solidified with 0.7% (w/v) agar. Axes in Petri plates were maintained in the dark and at 25°C for 2 d, and gradually introduced to a 16:8 h light: dark photoperiod over 2 d. Survival was assessed using five axes per treatment[1] after four weeks *in vitro*. Axes were scored as 'normal' when the embryonic radicles doubled in length and shoots expanded and turned green. The number of axes

[1] The number of samples used in survival studies was necessarily restricted by the limited time available before mature seeds either germinated in storage (after approximately one week) or were lost after shedding.

showing normal development, failure to develop shoots, stunted development, callus growths or death is expressed as the percentage of the total number of axes per treatment.

Microscopy

The ultrastructure of fully hydrated axes cooled by the three methods described was assessed in the solidified state using freeze-fracture (FF) and freeze–substitution (FS) techniques (described below). The ultrastructure of axes after partial drying for 20 min and plunge cooling was also examined using FF. Hydrated axes sampled at various intervals during recovery *in vitro* (described below) were processed for microscopy using conventional fixation (CF) and resin-embedding procedures.

Freeze fracture

Whole embryonic axes were mounted horizontally on gold planchettes (Bal-Tec, Liechtenstein) using a small amount of commercial silicone sealant, and either plunged rapidly into sub-cooled nitrogen using the spring-loaded device, cooled within Al foil, or placed on the stage of a DSC and cooled at 3°C s^{-1} as described above. Specimens were stored in liquid nitrogen until loading on the pre-cooled stage of a Bal-Tec BAF-060 freeze-fracture instrument (Bal-Tec, Liechtenstein). Axes were planed to a longitudinal median section, shadowed and replicated following standard procedures without etching. Replicas were cleaned by stepwise exposure of specimens to increasing concentrations of Chromerge (Fischer Scientific, USA) over 2 d, and washed by reversing this process. After several rinses in distilled water, replicas were collected on 600 mesh Cu grids (Electron Microscopy Sciences, Fort Washington, PA, USA).

Freeze Substitution

Freeze-substitution is ideally suited to observe cavities within cells formed by ice crystals during cooling (e.g. Sherman and Kim, 1967; Sakai *et al.,* 1968; Fujikawa 1988). The rate of substitution was enhanced by halving axes, previously cooled whole by the methods described, into root and shoot segments under liquid nitrogen

using a scalpel blade. Specimens were subsequently loaded into handling devices and processed using the same FS procedure used in Chapter 2.

Conventional fixation

The recovery of axes after cryopreservation was studied only in axes after cooling by the plunging method or at 3.3°C s^{-1} followed by rapid warming in water at 40°C. Three axes were randomly sampled at each of 0, 0.5, 1, 2.5, 6, 12, 24, 48 and 72 h after warming. Axes were halved transversely into root and shoot segments, and processed conventionally for light and transmission electron microscopy as described in Chapter 2.

Replicas and ultra-thin sections were viewed with a JEOL JEM 1010 (JEOL Ltd., Tokyo, Japan) transmission electron microscope (TEM) at 100 kV, and images were recorded both photographically and digitally. The results from ultrastructural studies were based on observations made on each of three replicates from roots and shoots for each cooling treatment.

Image analysis

The size and frequency of occurrence of ice crystals within solidified cells from different treatments were compared using image analysis. TEM images acquired digitally were analysed using KS 100 image analysis software (Carl Zeiss Vision GmbH, Germany) after calibrating to the appropriate image magnification. Measurements were performed on 5 - 10 cells from radicle and shoot tissues originating from each of three axes prepared for TEM using freeze-substitution. Ice crystal diameters are reported as average values, while the frequency of occurrence is given as the number of crystals per μm^2 area of each cell measured.

Results

Axes of *A. saccharinum* had an initial water content of 2.1 g g^{-1} and an average dry mass of 1.3 ±0.3 mg. Flash drying axes for 20 or 165 min reduced the water contents to 1.0 and 0.25 g g^{-1}, respectively. Axes that were partially dried but not cooled

showed more than 80% survival *in vitro* (J. Crane, unpublished observations), indicating that this extent of drying was not lethal.

Cooling and warming rates

Axes at 2.1, 1.0 or 0.25 g g^{-1} plunged into sub-cooled nitrogen cooled between 0 and -40°C at 94, 150 and 311°C s^{-1}, respectively (Table 8.1). The average cooling rates of axes achieved within Al foil envelopes was 77°C s^{-1} in fully hydrated axes, and was not studied in partially hydrated axes (Table 8.1). Cooling rates of axes on the DSC stage were not measured, as they were assumed to proceed at the software-controlled rate of 3.3°C s^{-1}. One-way analysis of variance (ANOVA) of cooling data showed that fully hydrated axes cooled at similar velocities (P >0.05) when plunged into sub-cooled nitrogen or within Al foil envelopes, and that only drying to 0.25 g g^{-1} increased cooling significantly (P <0.05; Table 8.1).

Fully hydrated axes warmed at an average 177 ±7°C s^{-1} when plunged into water at 40°C, and 67±18°C s^{-1} in water at 4°C. Axes on the stage of the DSC were assumed to warm at the specified rate of 0.08°C s^{-1}.

Table 8.1. Cooling and warming rates of axes. Treatments with the same letter belong to the same homogeneous group (one-way ANOVA, P <0.05). ns, not studied.

WATER CONTENT (g g^{-1})	COOLING (°C s^{-1})		WARMING (°C s^{-1})	
	PLUNGE	Al FOIL	40°C	4°C
2.1	97 ±41 a	77 ±2 a	177 ±7	67 ±18
1.0	150 ±44 a	ns	ns	ns
0.25	311 ±124 b	ns	ns	ns

Survival studies

The effect of water content (x-axis) on survival (y-axis) of axes cooled (horizontal rows) and warmed (columns) by the methods tested are shown in Figure 8.1. Failure to develop shoots appeared to be the earliest sign of freezing damage, in agreement with the findings from previous studies (Chapters 4, 6 and 7). Other abnormalities

included stunted development, callus proliferation or death where damage was most severe. The percentage of axes showing normal development, various abnormalities or death are indicated in Figure 8.1.

Log linear analysis showed that water content and the rate of warming had a highly significant (P <0.001) effect upon survival of cooled axes (Appendix A; Fig. 8.1). While cooling method alone had a marginal effect on survival (P= 0.062), the interaction between cooling rate and water content affected survival significantly (P <0.05; Appendix A). Almost all axes dehydrated to 0.25 g g^{-1} showed 100% normal development at all cooling and warming rates investigated (Figs 8.1 a - i). Unless stated otherwise, the results shown below refer to axes at 2.1 and 1.0 g g^{-1}.

Rapid warming at 177°C s^{-1} was the most favourable procedure of retrieving axes from cryostorage. The total number of axes surviving cryogenic exposure, and the proportion of axes showing reduced freezing damage, were highest after warming at 177°C s^{-1} for all cooling rates tested. However, differences among cooling treatments were noted (Fig. 8.1). Plunge cooling resulted in 100% survival of fully hydrated axes, although shoots failed to develop and 60% of surviving axes showed stunted growth (Fig. 8.1 a). Drying to 1.0 g g^{-1} eliminated stunted development, and while some mortality was observed this was possibly over-emphasised by the necessarily low sample numbers used in the present study. Cooling within Al foil and at 3.3°C s^{-1} also facilitated 100% survival but, in contrast to the plunging treatment, between 20 - 50% of those axes showed development of shoots as well as roots (Figs 8.1 b and c). No marked differences were observed in the survival characteristics of axes at 2.1 and 1.0 g g^{-1} cooled within Al foil or at 3.3°C s^{-1} (Fig. 8.1 b and c).

Survival of axes cooled by the different methods declined progressively with slower warming at 67 and 0.08°C s^{-1} (Fig. 8.1). Axes plunged at 2.1 and 1.0 g g^{-1} showed similar survival percentages to those observed in corresponding axes after rapid warming (compare Figs 8.1 d and a, respectively). However, the greater severity of the damage caused was evident by the increasing proportion of axes showing only

callus growth. Complete mortality occurred when plunge-cooled axes were warmed at 0.08°C s^{-1} (Fig. 8.1 g). On the other hand, axes cooled within Al foil or at 3.3°C s^{-1} appeared to be more tolerant to slow warming than plunge-cooled axes, with the prevalent damage being to shoots after warming at 67°C s^{-1} (Fig. 8.1 e and f, respectively). Partial drying to 1.0 g g^{-1} did not seem to affect survival of these axes (Fig. 8.1 e and f). Warming at 0.08°C s^{-1} resulted in increased damage of axes cooled by these two methods, which appeared to be worse in axes cooled within Al foil envelopes than at 3.3°C s^{-1}. But in spite of the abnormal development observed, some tissue survival was none the less attained, in contrast to the total mortality of corresponding axes cooled by plunging (compare Figs 8.1 h and i with g).

Microscopy

At the light microscope level, median longitudinal sections through the radicle of control axes showed well-defined regions of meristem initials (MI), which gave rise to the root cap (RC) distally and to the ground meristem (GM), elements of the vascular system (VS) and procambium (PC) proximally (Fig. 8.2 a; anatomical terminology after Raven *et al.*, 1992). In the mid-region of axes, the ground meristem gave way to cortical parenchyma cells subtended externally by the epidermis and by immature elements of the vascular system centripetally. The procambium in the radicle differentiated into the pith (P), which like cortical cells, showed abundant starch deposits (Fig. 8.2 d). Longitudinal sections through the epicotyl of axes showed the typical shoot pole structure illustrated in Figures 8.2 b and c. The points where embryonic tissues connect to the cotyledons are indicated (arrows. Fig 8.2 d). Leaf bases enclosed the apical dome, which consisted of an outermost layer of tunica (TU) cells that were small and tightly packed (Fig. 8.2 c). Immediately below is the corpus, which divides in various planes and thus adds bulk to the growing shoot. The corpus is formed by vacuolated central mother cells (CM), which are relatively large, vacuolated and show the presence of starch grains along their periphery. Situated radially around the central mother cells and the tunica were mitotically-active initials of the pith (PTM) and peripheral meristems (PM; Fig. 8.2 c), which gave rise to the procambium and ground meristem of shoots (Fig. 8.2 b).

Fig. 8.1. Survival of embryonic axes at 2.1, 1.0 and 0.25 g g^{-1} after cooling and warming at different rates. Survival figures represent the percentage of axes that developed normally or failed to develop shoots, showed stunted development or died after four weeks *in vitro*. Log-linear statistical analysis of these data is presented in Appendix A..

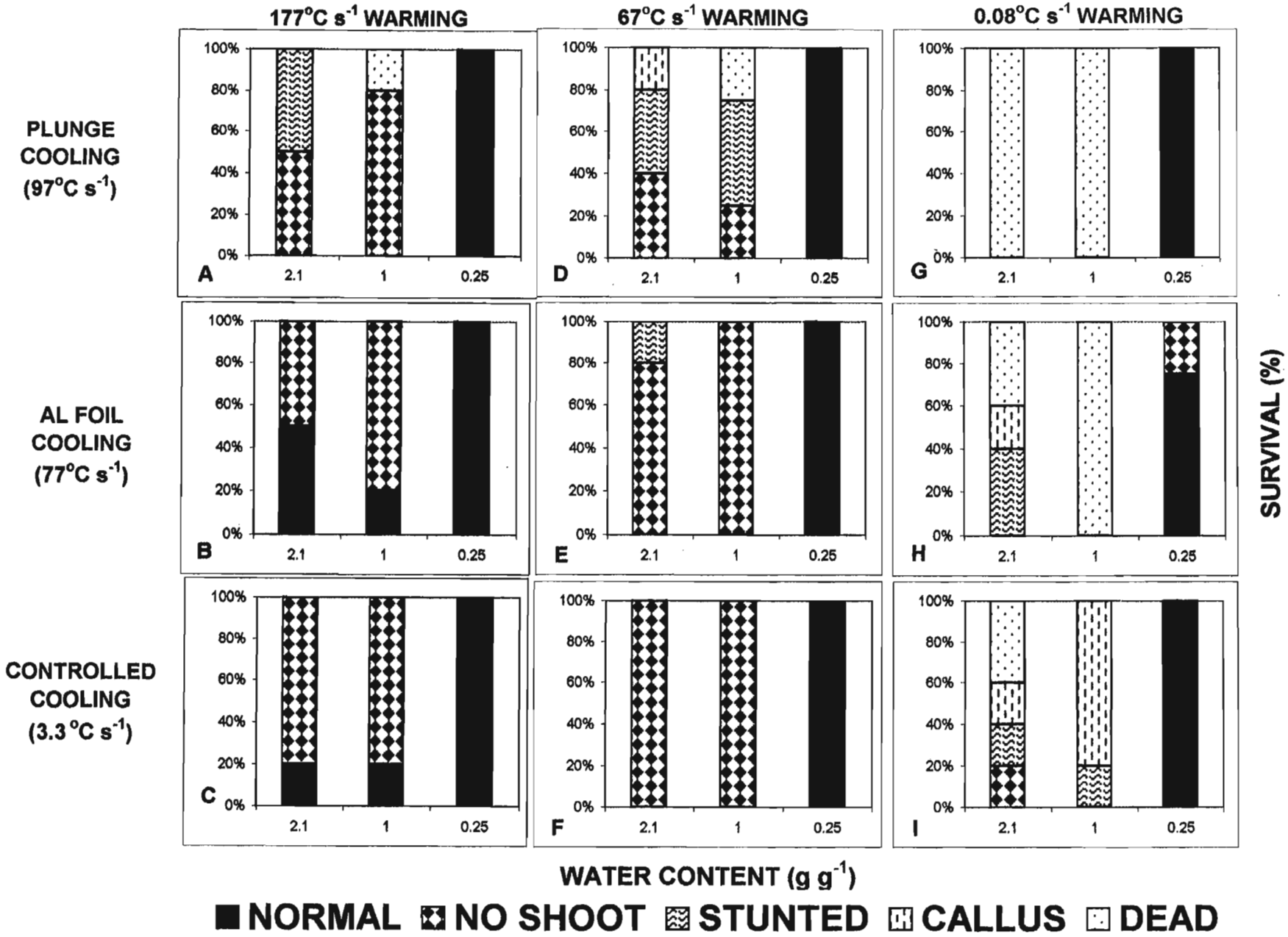
177°C s-1 WARMING
67°C s-1 WARMING
0.08°C s-1 WARMING
PLUNGE COOLING (97°C s-1)
AL FOIL COOLING (77°C s-1)
CONTROLLED COOLING (3.3 °C s-1)
SURVIVAL (%)
100%
80%
60%
40%
20%
0%
A
B
C
D
E
F
G
H
I
2.1
1
0.25
WATER CONTENT (g g-1)
NORMAL
NO SHOOT
STUNTED
CALLUS
DEAD

Fig. 8.2. Fully hydrated control (not cooled) axes. LM; CF. **a)** Radicle, showing meristem initials (*MI*) that give rise distally to the root cap (RC), laterally to the ground meristem (GM) and proximally to the procambium (PC). Bar = 100 μm.; **b)** Shoot pole and epicotyl tissues. Arrows indicate the sites severed during excision to isolate embryonic axes from the cotyledons. Bar = 200 μm. The areas within the frames labelled 'c' and 'd' are enlarged below; **c)** Shoot pole, showing cells of the tunica (TU) and the corpus, collectively made up by the central mother cells (CM), the peripheral meristem (PM) and the pith meristem cells (PTM). Bar = 50 μm; **d)** Longitudinal mid-section of axes magnified from 'b' above, showing the epithelium (EP), cells of the cortex (CO), vascular system (VS) and cells of the pith (P). Bar = 100 μm.

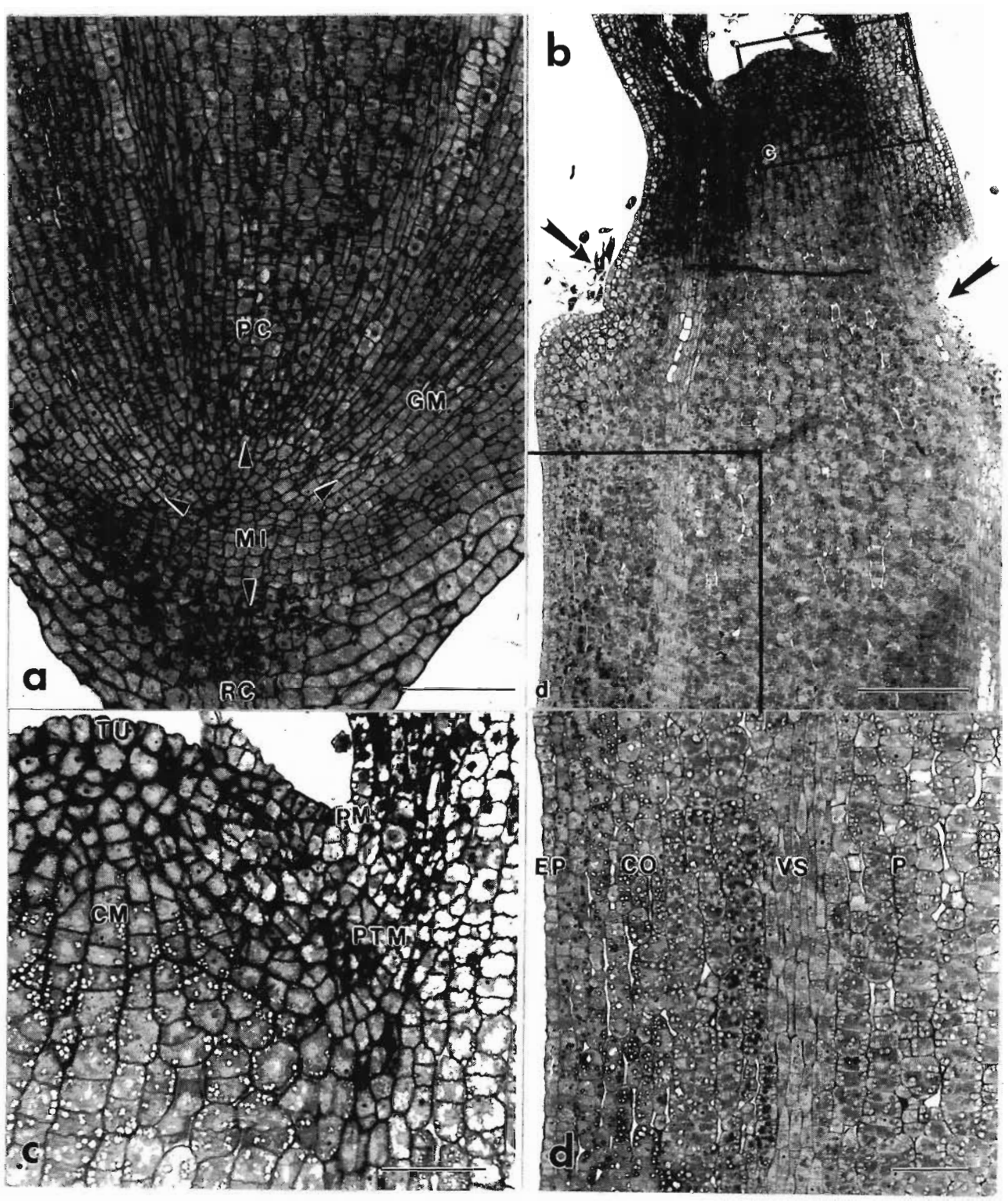
a
PC
CM
MI
RC
b
G
d
TU
PM
CM
PTM
c
EP
CO
VS
P
d

Fig. 8.3. Fully hydrated control (not cooled). **a)** TEM. CF. Whole cell from radicle showing plastids (P) with prominent starch grains. Bar = 2 μm; **b)** Plastid showing plastoglobuli (PG). Bar = 0.5 μm; **c)** Plastids, polysomes and rER (ER). Bar = 0.5 μm; **d)** cisternal (cER) and rough ER profiles. Bar = 0.5 μm; **e)** Central mother cells from shoot apex. Vacuoles (V) mitochondria (M), plastids (P) and lipid bodies are visible. Bar = 0.5 μm.

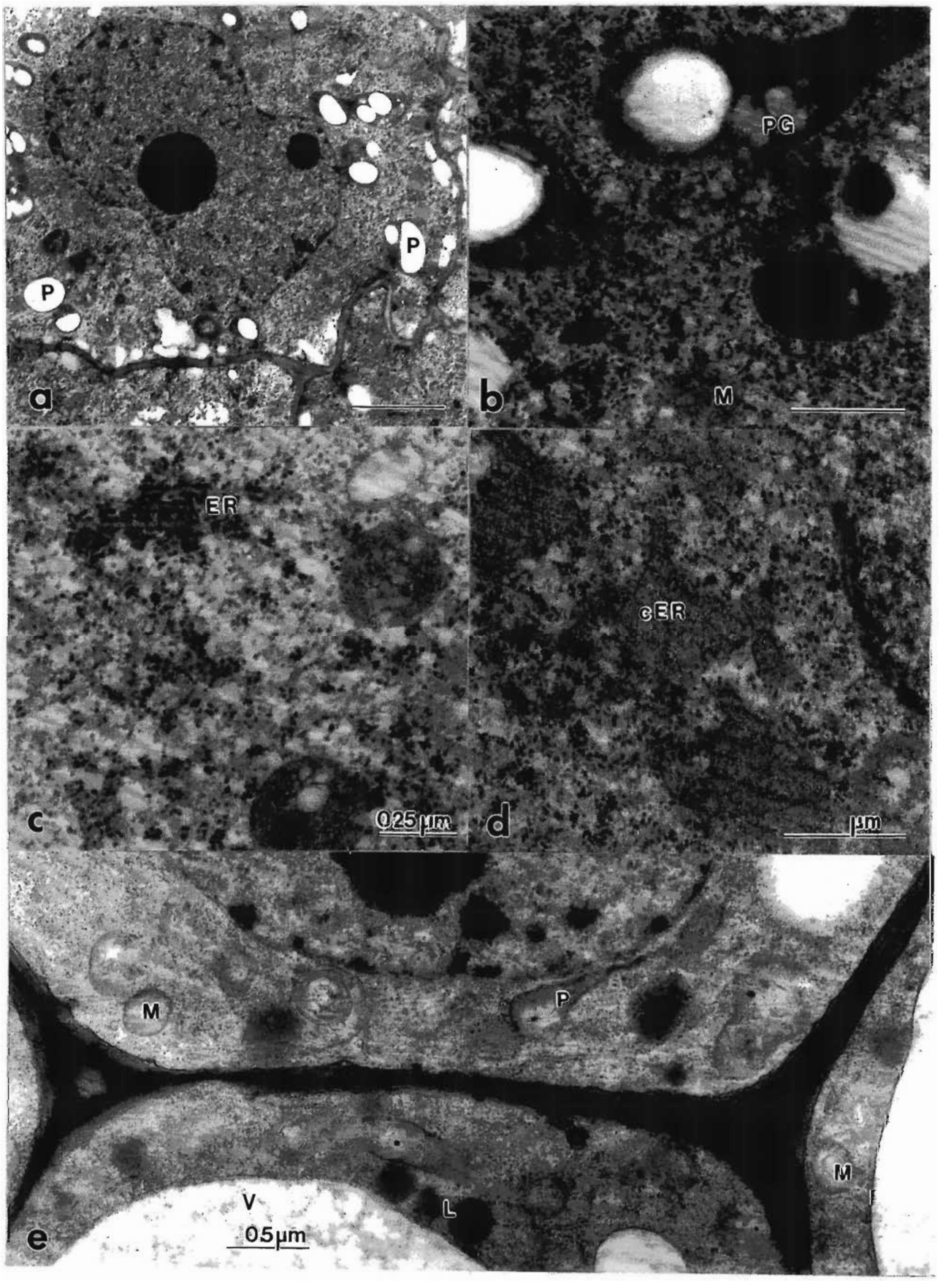
a
P
P
b
PG
M
c
ER
0.25µm
d
cER
µm
e
M
P
M
V
L
05µm

Meristematic cells from the radicle of control material showed characteristically thin, convoluted walls, few and small vacuoles, and centrally positioned nuclei with typically-distributed organelles (Fig. 8.3 a). Nuclei showed undulating profiles and the many plastids (P) contained prominent starch grains (Fig. 8.3 a). Internal differentiation was not clearly visible within the matrix of these electron-dense plastids, but plastoglobuli (PG) were sometimes observed within these organelles (Fig. 8.3 b). Although mitochondria (M) could be recognised (Fig. 8.3 a,b) internal details were difficult to resolve. Polysomes abounded in the cytoplasm of meristematic cells (Figs 8.3 b - d), and also occurred bound to short profiles of endoplasmic reticulum (ER; Fig 8.3 c), and associated with flattened, irregular cisternae presumed to be endoplasmic reticulum (cER; Fig. 8.3 d). In spite of the undulating profile of the cell wall, the plasmalemma remained closely appressed in all cells examined (not shown). Cells from the shoot meristem were turgid and also seemed to be more highly vacuolated than their distal counterparts (Fig. 8.3 e; *cf.* Fig. 8.3 a). Elongated plastids, relatively undifferentiated mitochondria (M), lipid bodies (L) and polysomes both in the cytoplasm and bound to profiles of ER, were observed in these cells (Fig. 8.3 e).

All axes cooled and prepared for microscopy using FF or FS revealed the presence of intracellular ice crystals. The diameter and frequency of ice crystals formed within cells of fully hydrated shoots and roots of all cooling treatments was quantified in sections of FS material using image analysis software. The size of ice crystal sizes formed was extremely variable, even among neighbouring cells, which made it difficult to determine accurately the size and frequency of occurrence of ice crystals within cells cooled by the various methods used. Average values ± standard deviation are provided in Table 8.2. Differences in the distribution of ice crystals among cells from the root and shoot suggested these tissues responded differently to cooling (Table 8.2), in agreement with trends from survival data. Accordingly, differences in the size of ice crystals within cells of the root and shoot among treatments were assessed separately using one-way ANOVA. A log-log plot of mean ice crystal size *vs.* frequency for each individual cell measured, showed that these parameters were

closely related (R^2= 0.97; Fig. 8.4). Ultrastructural results for each treatment are presented below.

Table 8.2. Size and frequency of ice crystals formed within cells from the shoot or root of axes cooled by plunging, within Al envelopes or at 3.3°C s^{-1}. Measurements were performed on 5 - 10 cells from each pole of two axes. Because of the extensive variability in sizes and density, minimum and maximum ranges per radicle or shoot of each treatment are given in preference to mean average values. Treatments with the same letter are not significantly different (0.05).

		ICE CRYSTAL SIZE (μm)		FREQUENCY OF ICE CRYSTALS PER μm^2	
		AVERAGE SIZE	HOMOGENEOUS GROUPS	MIN	MAX
ROOT	Plunge	0.2 ±0.08	a	8	38
	Al foil	0.28 ±0.16	b	5	9
	3.3°C s^{-1}	0.4 ±0.12	c	3	7
SHOOT	Plunge	0.17 ±0.1	a	5	83
	Al foil	0.16 ±0.05	a	8	29
	3.3°C s^{-1}	1.8 ±1.8	b	0.1	4

While fully hydrated axes plunge-cooled at 97°C s^{-1} appeared normal in FF replicas at low magnification (Fig. 8.5 a), closer inspection revealed ice crystals had formed throughout the cytoplasm and most cellular compartments (Fig. 8.5 b). Sections of corresponding FS axes confirmed that widespread nucleation had occurred throughout the cytoplasm, nuclei, vacuoles, and most other organelles (Fig. 8.5 c). The size and frequency of intracellular ice crystals varied between tissues, and occasionally differences between adjacent cells were striking (Fig. 8.5 d). Ice crystals within the radicle of plunge cooled axes formed at a frequency ranging between 8 and 38 nuclei per μm^2 and averaged 0.2 ±0.08 μm diameter (Table 8.2). The relative size of organelles was similar to those observed in corresponding cells from axes that had not been cooled (Fig. 8.3 a-d), indicating that shrinking induced osmotically by ice crystals forming in the ground cytoplasm (e.g. Fujikawa, 1988) during plunge-cooling was minimal. Like cells of the radicle, no compartments within meristematic cells from

the shoot apex appeared exempt from ice crystals (Fig. 8.5 e), which were formed at frequencies of up to 83 crystals μm^{-2} and averaged 0.17 ±0.1 μm diameter (Table 8.2). In these cells only the contour of organelles could be recognised, as ice crystals measuring ≤0.1 μm obliterated internal detail (Fig. 8.5 f). Vacuolar contents (V) often had an even appearance, and it is likely that this represented a solid mass of ice (Fig. 8.5 f).

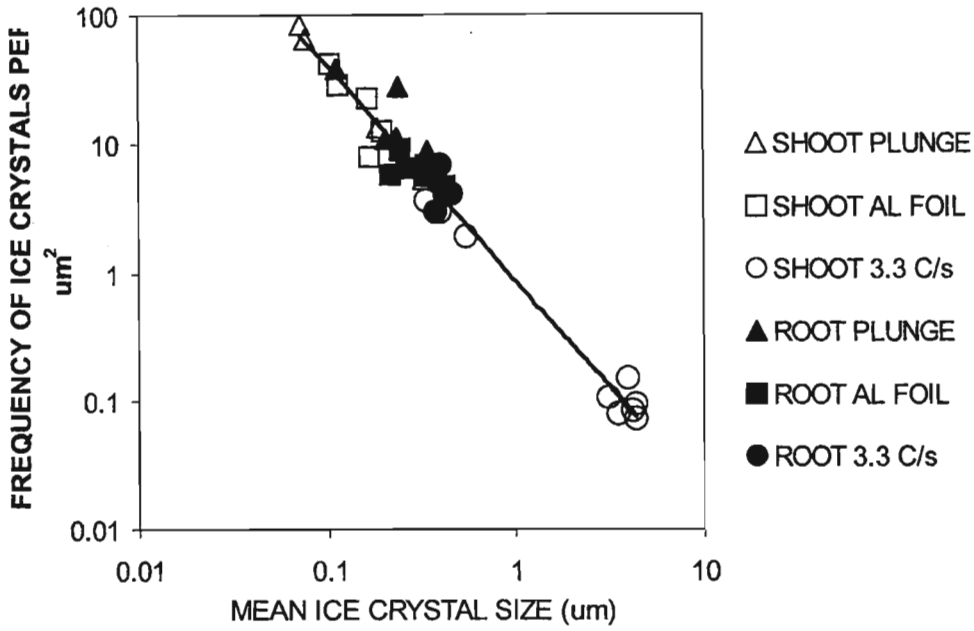

Fig. 8.4. Plot of the frequency of ice crystals formed within cells from the root and shoot in axes cooled at the rates indicated *vs.* mean crystal diameter attained in each case. The trendline fitted using the formula $y= 0.867\ x^{-1.66}$ ($y= cx^b$) returned a $R^2= 0.97$, indicating that these parameters were highly related.

Embryonic axes dehydrated to 1.0 g g^{-1} prior to plunge-cooling at 150°C s^{-1} showed that organelles remained evenly distributed in cells, as observed in axes that were neither dried nor cooled (Fig. 8.6 a). Higher magnifications of rapidly cooled axes at 1.0 g g^{-1} revealed freezing damage to be almost absent in these cells. Nuclei in some cells were somewhat distorted, which was possibly due to drying (Fig. 8.6 b). Some fractures planes showed large areas that resembled either plasmalemma or, alternatively, ER cisternae spanning the region between the periphery and the cell

interior (arrowheads), as also observed in control axes (compare Fig. 8.3 d with Figs 8.6 b and c). However, this interpretation is equivocal, as no intra-membrane particles (IMPs) or ribosomes (seen to abound in fully hydrated cells of non-cooled axes) were visible in association with these structures. Although improbable, the possibility of these structures representing large sheets of ice formed in localised areas within cells cannot be ruled out. Deep etching would have assisted in their identification but, regrettably, this was not done. These structures appeared to interdigitate with vesicles and what is presumed to be the plasmalemma closely appressed to the cell wall (Fig. 8.6 c). Stacks of membrane fragments were occasionally observed attached to the outer leaflet of the nuclear envelope (arrows; Fig. 8.6 d), suggesting that ice crystals or organelles pressing against the nucleus may have interfered with the regular plane of fracture. This suggests that while freezing damage comparable to that observed in fully hydrated axes was never seen after partial drying to 1.0 g g^{-1}, the possibility of some intracellular freezing giving rise to membrane abnormalities and distorted cellular architecture cannot be discounted. Reduced freezing damage is further suggested by the smooth, rounded outlines of mitochondria, vacuoles and plastids (Fig. 8.6 e). Also, profiles of smooth ER could be seen along the periphery of these cells (Figs 8.6 e and f).

Fully hydrated axes cooled within Al foil (76°C s^{-1}) showed widespread freezing similar to that observed in corresponding axes after plunge cooling (Fig. 8.7). Between 5 and 9 crystals μm^{-2} were formed in cells from the radicle, and had diameters that averaged 0.28 ±0.16 μm (Table 8.2). Although nuclei and structures presumed to be ER were visible, most organelles were difficult to identify (Fig. 8.7 a). Sections though corresponding areas in FS preparations confirmed the ubiquitous presence of ice crystals within the cytoplasm and nucleus of these cells (Fig. 8.7 b). Higher magnifications revealed the plasmalemma of cells was seemingly intact, and often closely appressed to the

Fig. 8.5. Fully hydrated axes cooled by plunging into sub-cooled nitrogen (SN_2). **a)** Radicle, FF. N, nucleus. Bar = 3 μm; **b)** Radicle, FF. Plastids (P) and cell wall could be recognised, but widespread ice crystals obscured fine detail in these cells. Bar= 1 μm; **c)** Radicle, FS. Sections of freeze-substituted material revealed the presence of ice crystals throughout all cellular compartments. P, plastid. Bar = 1 μm; **d)** Radicle, FF. Very different freezing patterns were observed, even in adjacent cells. Bar = 1 μm; e) Shoot, FS. Freezing damage was also observed in compartments of cells from the shoot. Bar = 4 μm; **f)** Shoot, FS. The invasive presence of ice crystals within cellular compartments is evident. Bar = 1 μm.

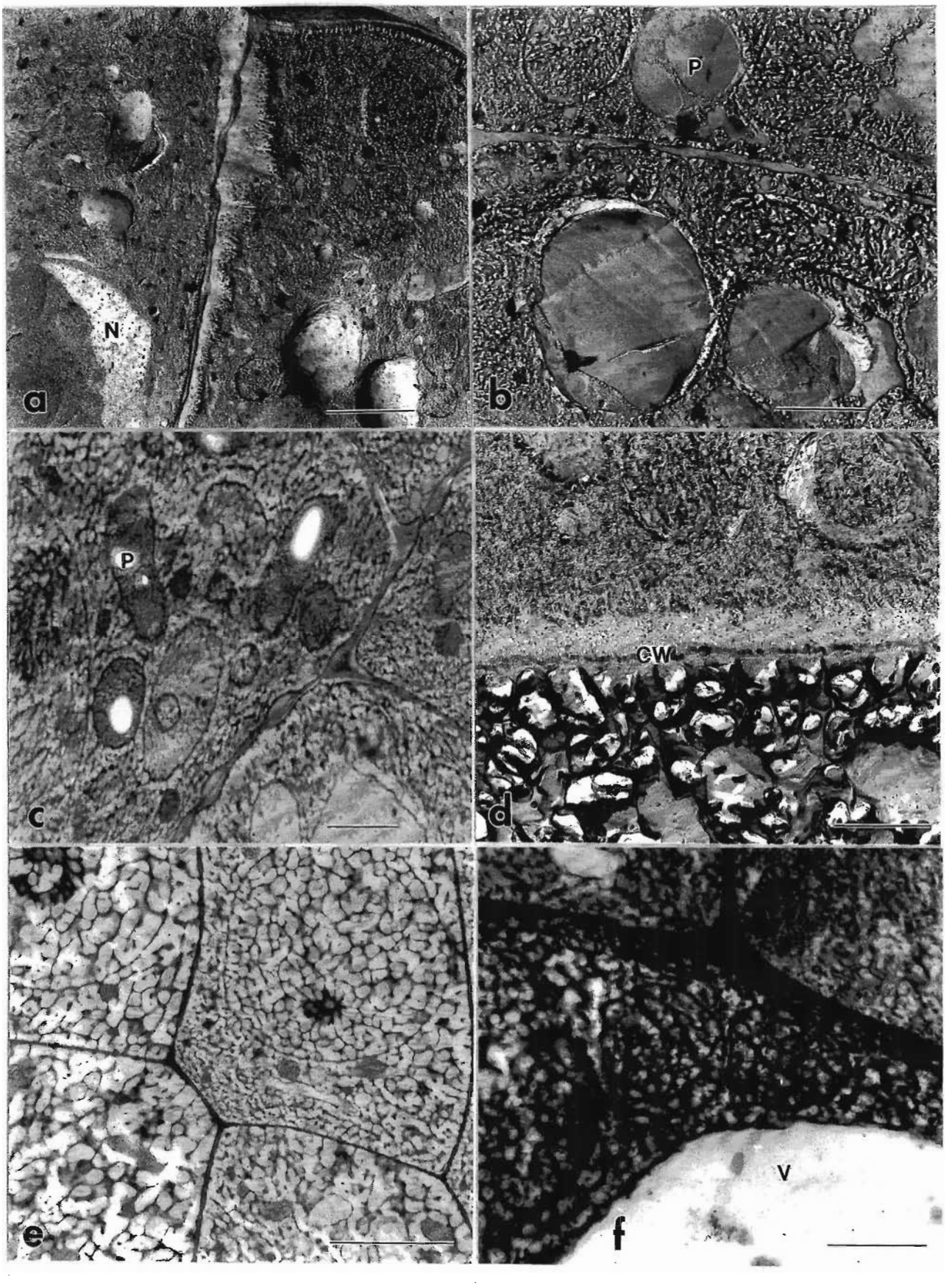
N
a
P
b
P
c
CW
d
e
V
f

Fig. 8.6. Axes partially dried to 1.0 g g^{-1} and cooled by plunging. **a)** Adjacent cells. Bar = 3 μm; **b)** Nuclei often had undulating profiles, probably due to partial drying. Bar = 1 μm; **c)** Large sheets of what is presumed to be either plasmalemma or parallel fractures along ER cisternae (arrowheads). Bar = 0.5 μm; **d)** View of the PF of the inner nuclear envelope membrane showing closely appressed fragments of other membranes. Bar = 0.5 μm; **e-f)** The cytoplasm of these cells appeared devoid of ice artefacts. **e)** Replicas revealed seemingly well-preserved vacuoles (V), ER cisternae and vesicles and rounded organelles, possibly mitochondria (M). Bar = 0.25 μm; **f)** the ordered distribution of ER profiles and vesicles along the cell periphery was apparent. CW, cell wall. Bar = 0.5 μm.

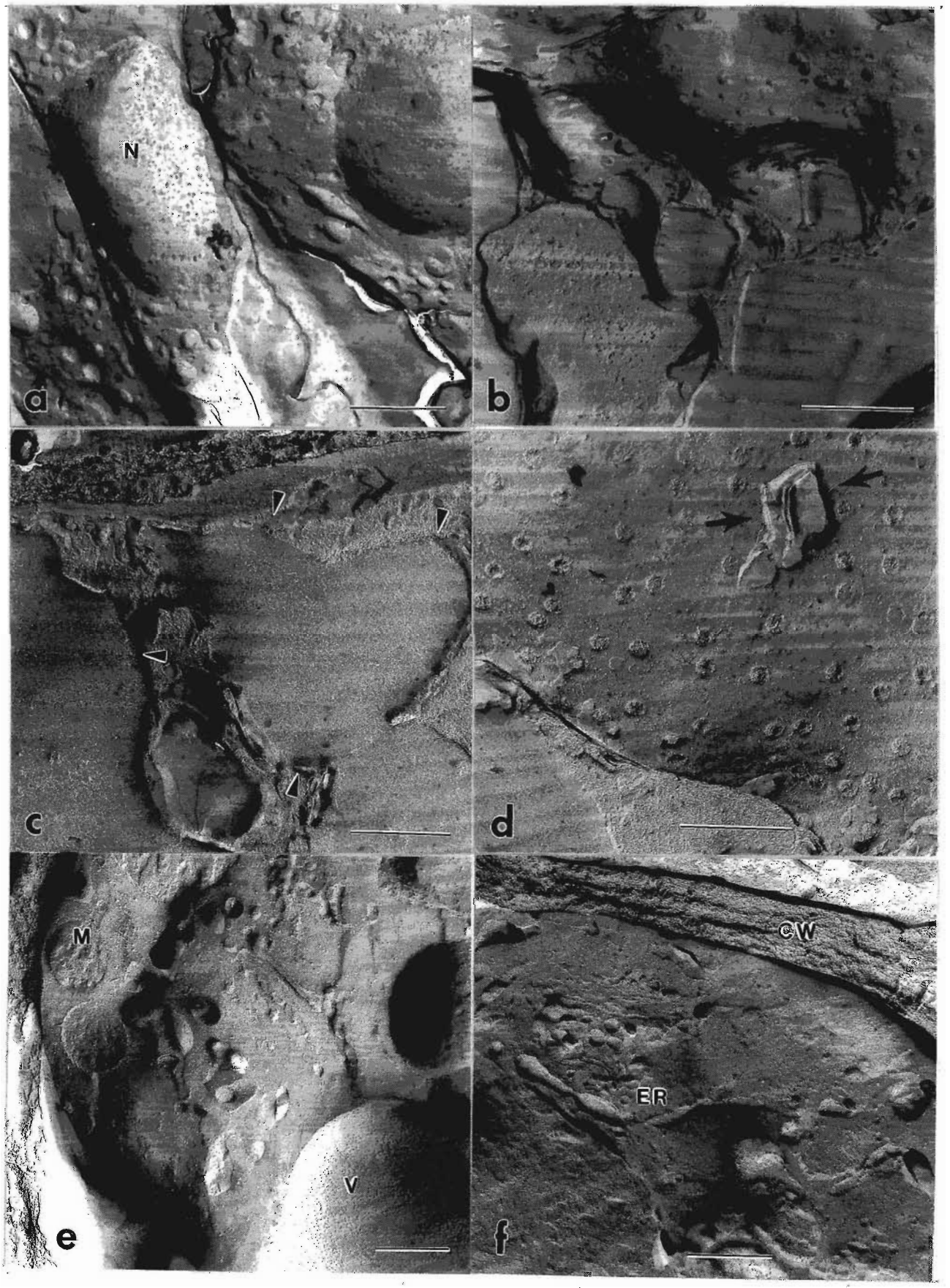
N
a
b
c
d
M
V
e
CW
ER
f

wall by ice crystals in close proximity with the cytoplasmic face (arrowheads; Fig. 8.7 c). Ribosomal subunits and microfilament bundles trapped between ice crystals were also observed (Fig. 8.7 c). Ice crystals also formed on either side of the nuclear envelope, which could be resolved clearly in these cells (Fig. 8.7 d and e). Ice sometimes seemed to traverse the nuclear envelope, presumably through nuclear pores (arrows; Fig. 8.7 d), while in other instances growth occurred within inner and outer leaflets of the nuclear boundary (arrows; Fig. 8.7 e). Significantly, matrices of organelles such as plastids (Fig. 8.7 d) and mitochondria (Figs 8.7 f and g) appeared to be free of ice in approximately 80% of cells investigated. Similar trends were observed in cells from shoot apices, where 60% of cells showed organelles that appeared to be free from ice inclusions (Fig. 8.7 h). Ice crystals within cells of the shoot averaged 0.16 ±0.05 μm and were formed at much lower frequencies than in shoots of plunge-cooled axes (8-29 crystals μm^{-2} instead of 5-83 μm^{-2}, respectively; [Table 8.2]).

Cooling at 3.3°C s^{-1} resulted in the formation of fewer ice crystals that were also significantly larger (P <0.05) and more uniform in size inside cells from the radicle of fully hydrated axes (Table 8.2; Figs 8 a - d). This seemed to result in larger expanses of cytoplasm being free of ice crystals relative to the more finely segregated appearance of the protoplasm in plunge-cooled cells (Fig. 8.8 a). Tubular and cisternal ER profiles were occasionally observed interspersed among these large crystals, apparently intact although visibly compacted (Figs 8.8 b and c). Polysomes had dissociated into ribosomal subunits in these cells (Figs 8.8 c and e). Irregular fracture planes suggest that the ice crystals formed had distorted cellular architecture (e.g. Fujikawa, 1988), such as that of the nucleus shown in Figure 8.8 d. Infrequently, the nucleus (as shown in Figure 8.8 c) seemed to have escaped freezing, although the cross-sectional areas visible in the centre and top left corner of that micrograph (asterisks) suggests that this structure was highly lobed. Like cells cooled by the foil method, ice crystals formed on either side of the nuclear envelope seemingly without disrupting this boundary, although presumably exerting pressure upon it (arrowheads; Fig. 8.8 e).

Fig. 8.7. Fully hydrated axes cooled within Al foil. **a)** Radicle cell, FF, showing extensive ice segregation within the cytoplasm and vacuoles (V). Profiles presumed to be endoplasmic reticulum (ER) were also observed. **b)** FS. Section through a cell from the radicle, showing ice nuclei were present within the nucleus and cytoplasm. Bar = 1 μm.; **c)** Radicle cell, FS, revealing the concentrated appearance of the ground cytoplasm in between ice crystals. Dissociated ribosomes and structures presumed to be of cytoskeletal origin are also visible in this micrograph. The plasmalemma was appressed to the cell wall, and was contacted by numerous ice crystals that seemingly did not cause visible damage. Bar = 2 μm; **d)** Radicle, FS. Closer inspection of the nucleus revealed ice crystals lined the nuclear envelope, occasionally traversing this boundary (arrows). Organelles within this treatment often showed a complete absence of ice inclusions, as attested by the appearance of the amyloplast in this micrographs. Bar = 0.33 μm; **e)** Radicle, FS. Ice crystals were also observed forming within the nuclear envelope, as well as on either side of it. Bar = 0.37 μm; **f, g)** No evidence of freezing artefacts were observed in organelles such as oil bodies (f) or mitochondria (g). Bars for both micrographs = 0.25 μm; **h)** Sections from FS cells from the shoot also showed widespread freezing in nuclear, cytoplasmic and vacuolar compartments, but appeared to be excluded from membrane-bound organelles. Bar = 0.5 μm.

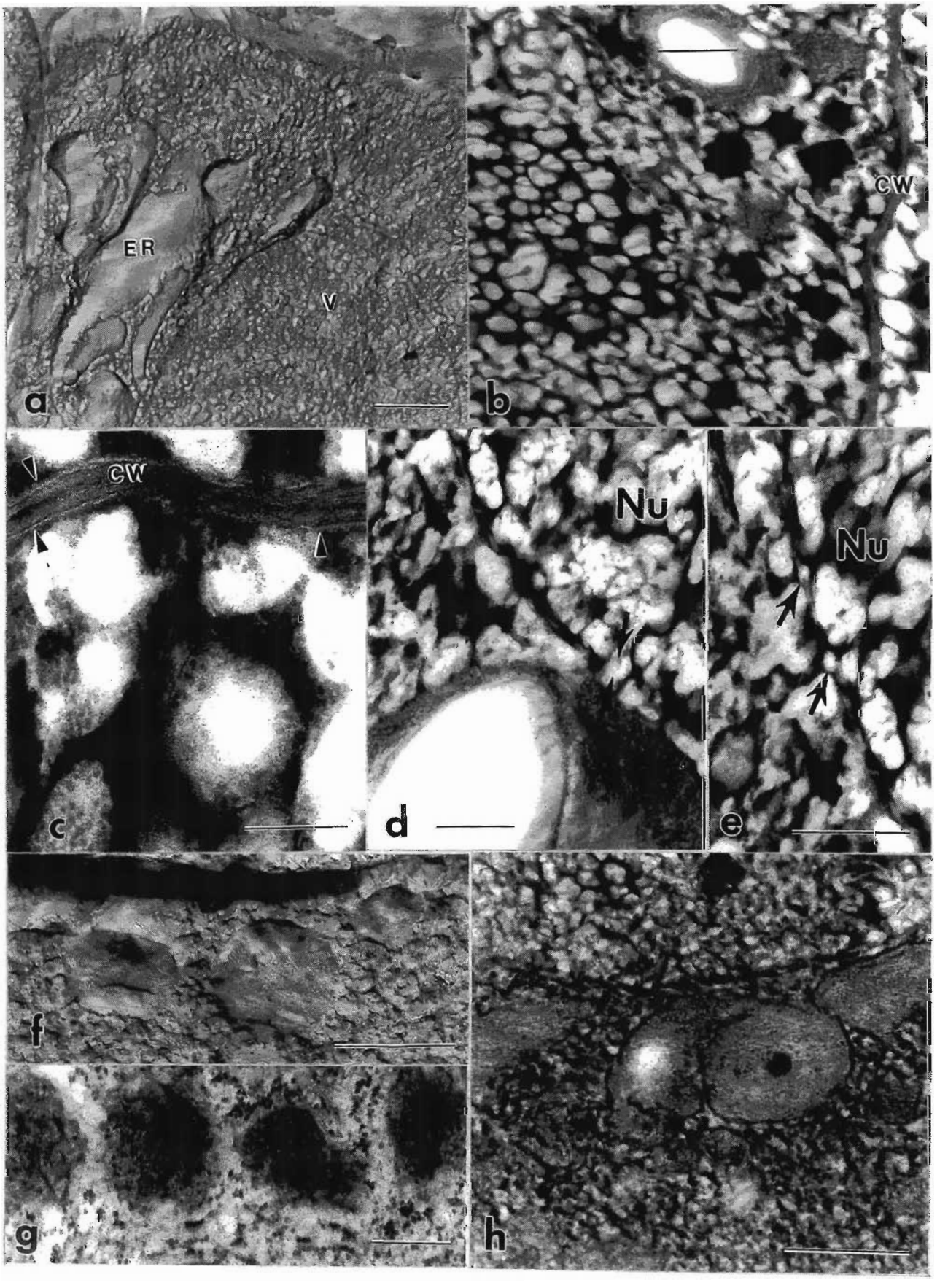
ER
V
a
CW
b
CW
c
Nu
d
Nu
e
f
g
h

In cells from the shoot, the frequency of ice nuclei was relatively lower than in radicle cells (0.1 - 4 crystals μm^{-2}) although crystals grew to 4 μm in some instances. Large areas of unfrozen cytoplasm were also observed, containing ribosomal subunits and compacted - yet seemingly intact - organelles (Fig. 8.8 f).

Freezing damage to the plasmalemma

It is accepted that damage to the plasmalemma usually results in lethal injury. Freeze-fracture electron microscopy can reveal irregularities such as the displacement of intra-membrane particles (IMPs) caused by contact between adjacent membranes or with ice crystals (Fujikawa, 1981, 1988). In the present study the distribution of IMPs of membranes in was assessed by examining freeze-fracture replicas of cells cooled by plunging, within Al foil envelopes or at 3.3°C s^{-1}. Uneven fracture planes were more prominent than aparticulate domains in cell membranes from fully hydrated plunge-cooled axes (Fig. 8.9 a). (The wavy texture of the membranes from radicle cells of plunge-cooled axes shown in Figure 8.9 a is probably an artefact of replication.) Irregular fracture planes and aparticulate domains were also observed occasionally in axes plunge-cooled after drying to 1.0 g g^{-1} (Fig. 8.9 b). The plasmalemma of cells cooled by the Al foil method showed apparently normal distribution of IMPs. Fragments of membranes attached to the plasmalemma were occasionally observed, suggesting that ice crystals could have brought membrane-bound compartments sufficiently close to the cell boundary to presumably alter the plane of fracture (Fig. 8.9 c). Membranes from axes cooled at 3.3°C s^{-1} showed even distribution of IMPs and only infrequently irregular fracture planes (Fig. 8.9 d).

Recovery of axes <u>*in vitro*</u>

The ultrastructure of plunge-cooled cells from the radicle immediately after warming was similar to that of corresponding cells before cryogenic exposure (compare Figs 8.10 a, b with Figs 8.3 a-d). The interiors of these cells showed

Fig. 8.8. Fully hydrated axes cooled at 3.3°C s^{-1} (200°C min^{-1}). **a)** Radicle cell, FF, showing the presence of large intracellular ice crystals separated by regions of apparently unfrozen cytoplasm. Bar = 1 μm; **b)** Closer inspection of radicle cells revealed seemingly intact cellular structures, probably ER cisternae and vesicles, in between large deposits of ice. Bar = 0.25 μm; **c)** Sections of FS radicle cell confirmed the presence of large ice crystals, and relatively large areas of the cytoplasm that, although compacted, showed no visible segregation. The nucleus (Nu) shown, appeared to be free from visible ice but also highly lobed, as suggested by the areas marked with an asterisk (*). Bar = 0.5 μm; **d)** FF replicas showed compacted, yet intact, cellular structures in radicle cells. Bar = 0.25 μm; **e)** While large ice crystals were often noted on either side of the nuclear envelope in FS cells from the radicle, the integrity of this boundary was apparently maintained (arrowheads). Bar = 0.25 μm; **f)** FS cells from shoot tissues had a similar appearance, with organelles within highly compacted areas of cytoplasm trapped between large expanses of ice. Bar = 0.25 μm.

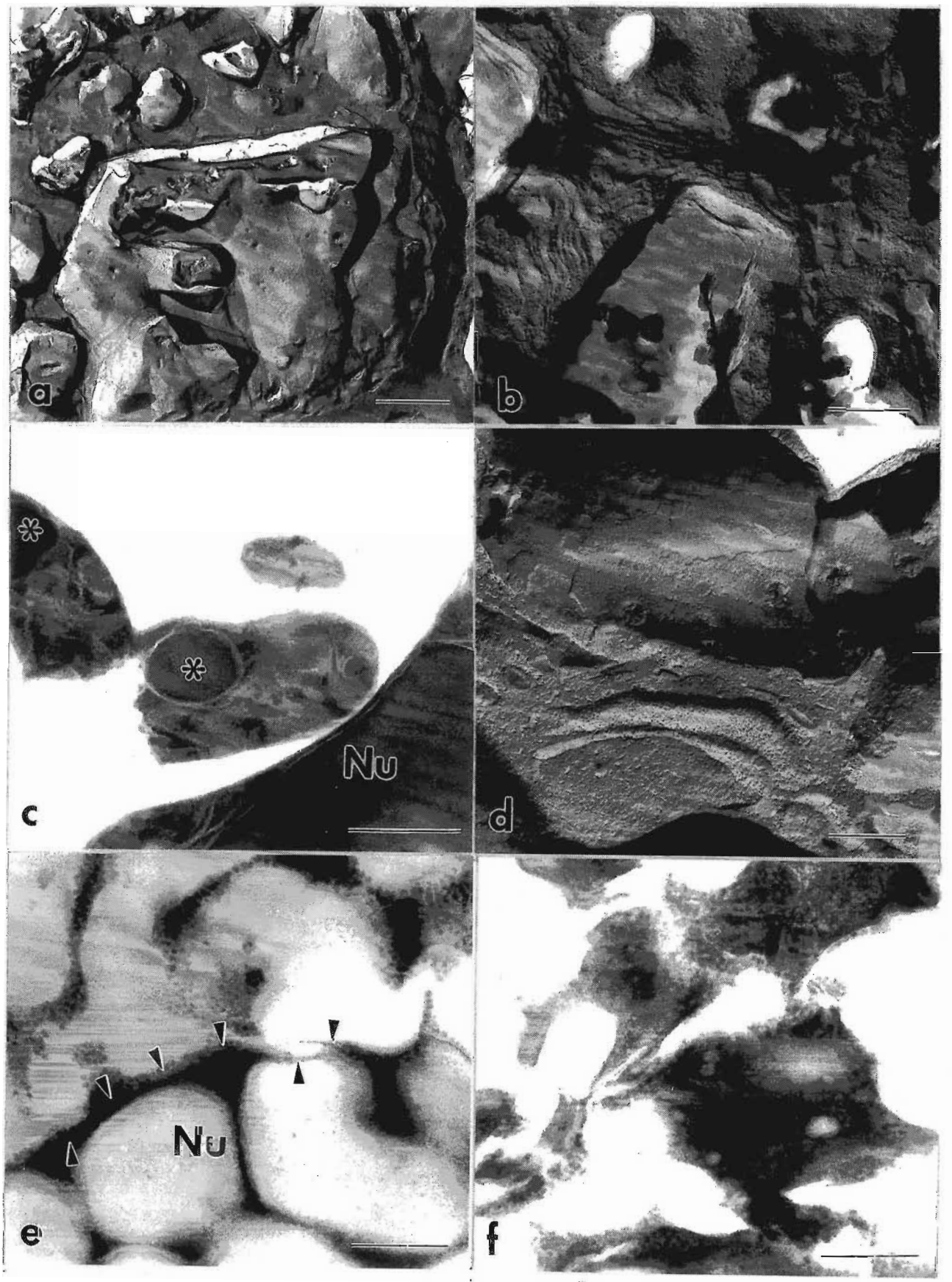
a
b
c
Nu
d
e
Nu
f

little evidence of the distortion observed while in the solidified state. However, some signs of freezing damage were occasionally noted, such as plasmalemma vesiculation, diffuse appearance of tonoplasts and nuclear envelopes, and dilated cisternae of ER (not shown). The plasmalemma and tonoplasts of most cells from the hypocotyl of axes showed no visible disruption 2.5 h after warming (Fig 8.10 c). Organelles appeared intact and randomly distributed (Fig. 8.10 c). Autophagy by - and fusion of - vacuoles were also noted in these cells, and continued to be manifested 6 h after warming (Fig. 8.10 d). Profiles of ER seemingly increased in number and length in these cells (Fig. 8.10 d). However, there were signs of degradation in these cells also. In particular, plastid membranes dissolution was advanced (arrowheads), and previously discrete lipid bodies showed evidence of confluence (arrow; Fig. 8.10 d). Long ER profiles and increased vacuolation by fusion of pre-existing compartments was also noted (Fig. 8.10 d). In contrast, cells from the shoot meristem showed evidence of freezing damage almost immediately after warming. After the elapse of 30 min from warming, the nuclear envelope of most of these cells showed localised swelling (arrowheads), plasmalemma and tonoplast seemed diffuse, and electron dense vesicles were frequently observed in their vicinity (Fig. 8.10 e). After 2.5 h recovery, damage to the nuclear envelope had become intensified, and osmiophilic deposits were prominent both within the nuclear envelope and generally in these cells (Fig. 8.10 f). In instances where damage was most severe, complete cell breakdown had accompanied loss of vacuolar integrity (Fig. 8.10 g).

Transmission electron microscopy (TEM) showed that distal meristem and meristem-derivative cells of plunge-cooled axes appeared to be engaged in cell repair after 24 h recovery (not shown). However, median longitudinal sections through these axes showed at light microscopy (LM) level that root growth originated from cells of the ground meristem and procambium of axes (Fig. 8.11 a). After 48 h recovery, axes showed root elongation and geotropism (Figs 8.11 b and c) and, remarkably, the root cap and probably some meristem initials as well

Fig. 8.9. Freeze fracture replicas showing the distribution of intra-membrane particles (IMPs) on the plasmalemma of cells cooled by plunging either **(a)** fully hydrated, or **(b)** after partial drying to 1.0 g g^{-1}. Irregular fracture planes and areas free from IMPs were sometimes observed in membranes of axes cooled rapidly; **c)** Cooling fully hydrated axes by the foil method resulted in evenly distributed IMPs, although fractures also revealed the remains of membranes from other cellular structures; **d)** In spite of the large size of ice crystals formed, IMPs were evenly distributed along the plasmalemma of axes cooled at 3.3°C s^{-1}. Bar for Figs a – d = 0.2 μm

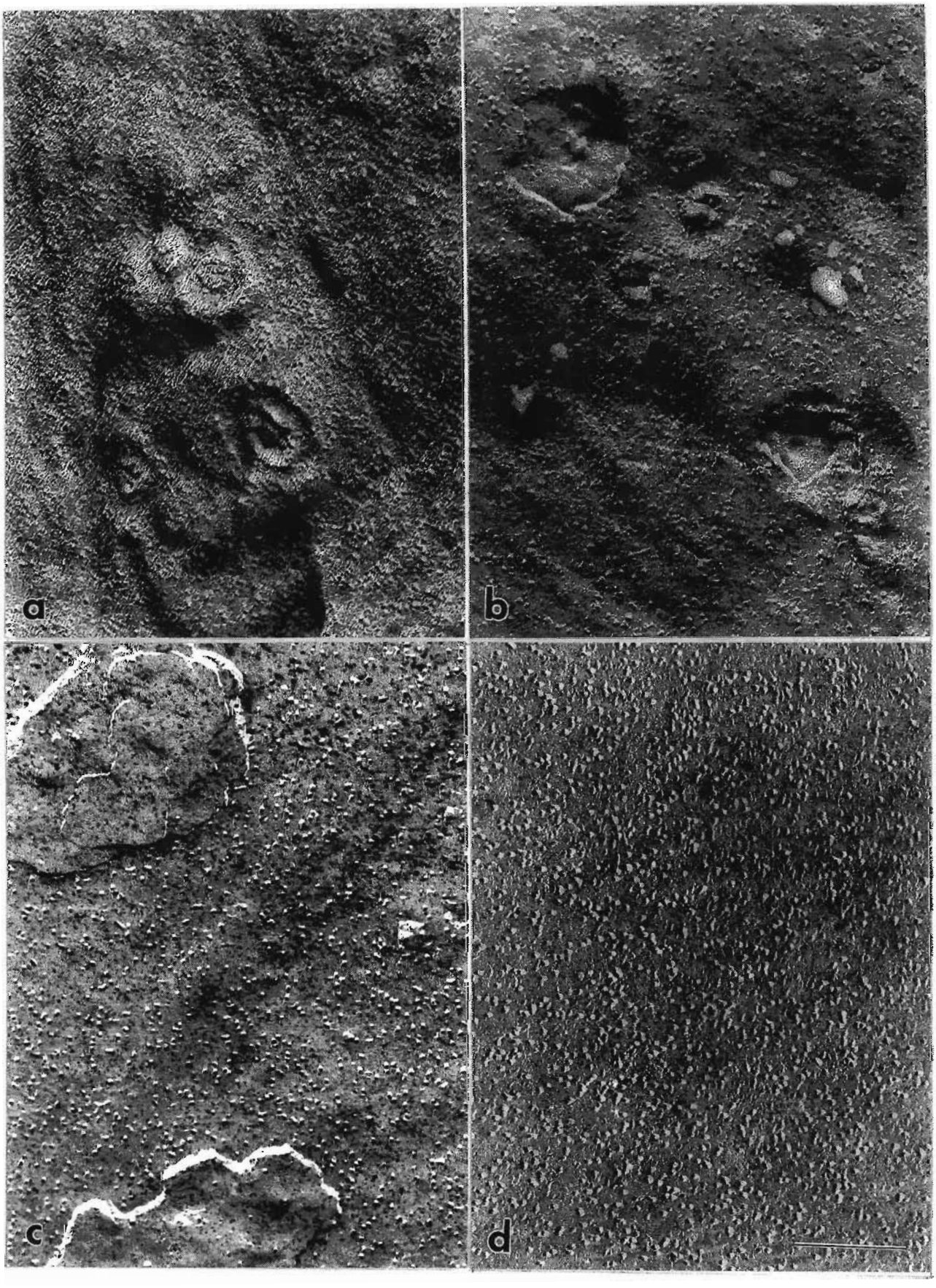
a
b
c
d

were seemingly displaced by this renewed growth (Fig. 8.11 c and d). The mid region of axes examined at this stage showed consistently that cortical cells (CO) were the most tolerant of rapid cooling, and that elements of the vascular tissue (VS) and cells within the pith had been damaged by cryogenic exposure (Fig. 8.11 e). Large voids were observed within the pith of these axes (asterisks), presumably areas where severe freezing damage had induced cell lysis (Figs 8.11 b and c) At LM level, cells of shoot tissues appeared severely plasmolysed (not shown), suggesting that irreversible membrane damage had occurred, which explained the absence of development *in vitro*.

Meristematic cells from axes cooled at 3.3°C s^{-1} were also remarkably similar to control cells immediately after warming, with little apparent evidence of the distortion caused by intracellular crystals (Fig. 8.12 a; *cf.* Fig. 8.8). Plasmalemma, tonoplast and nuclear envelope integrity appeared to have been maintained in these cells (Fig. 8.12 a). After 2.5 h recovery the early phases of autophagy involving the sequestering of ground cytoplasm and some organelles by ER cisternae was commonly seen, suggesting cellular repair mechanisms had been activated (Fig. 8.12 b). Short ER profiles and autophagic vacuoles (AV) continued to be observed after 6 h recovery, and organelles appeared irregularly distributed in cells, suggesting that freezing may have affected the cytoskeleton of these cells (Fig 8.12 c). Cells from tissues in the shoot were visibly affected by freezing, with their appearance in axes fixed 2.5 h after warming suggesting that the extent of damage varied among cells (Fig 8.12 d). After 6 h recovery, many cells showed localised swelling of the nuclear envelope (arrowheads), as well as tonoplast irregularities and electron-dense vesicles close to the plasmalemma (Fig. 8.12 e).

The histological appearance typical of axes cooled at 3.3°C s^{-1} after 72 h *in vitro* is illustrated by the median section through a whole axis in Figure 13 a, and by images of selected areas at higher magnifications. The normal appearance of roots in germinating axes (Fig. 8.13 b) reflects the absence of visible freezing

Fig. 8.10. TEM of rapidly cooled axes at various intervals after warming during recovery *in vitro*. CF. **a) 0 min.** Cell from the distal meristem immediately after warming showed no striking evidence of the freezing insult previously experienced. Cellular architecture resembled that of control (not cooled) axes (*cf.* Fig. 3). Bar = 2 μm; **b) 0 min**. Closer inspection of radicle cells immediately after warming showed the integrity of membranes and cellular compartments had not been visibly disrupted during cryogenic exposure. Bar = 0.5 μm; **c) 2.5 h**. Cells appeared intact 2.5 h after warming. Autophagy and fusion of existing vacuoles was also observed. Bar = 2 μm; **d) 6 h**. Profiles of ER seemingly increased in number and length in these cells, and evidence of autophagy was frequently observed. However signs of damage were also noted, such as dissolution of plastid membranes (arrowheads), confluence of lipid bodies (arrow). Bar = 2 μm; e – f) Meristematic cells from the corpus region of shoots showed signs of damage almost immediately after warming. **e) 30 min**. Plasmalemma and tonoplasts seemed diffuse, and electron dense vesicles were frequently observed along the cell boundary. Localised swelling of the nuclear envelope was also noted (arrowheads). Bar = 1 μm; **f) 2.5 h**. Damage to the nuclear envelope was clearly seen, and osmiophilic deposits were prominent both within the nuclear envelope and along membranes in these cells. Bar = 0.5 μm; **g) 2.5 h**. In cells where damage was most severe complete lysis was apparent. Nu, nucleus.

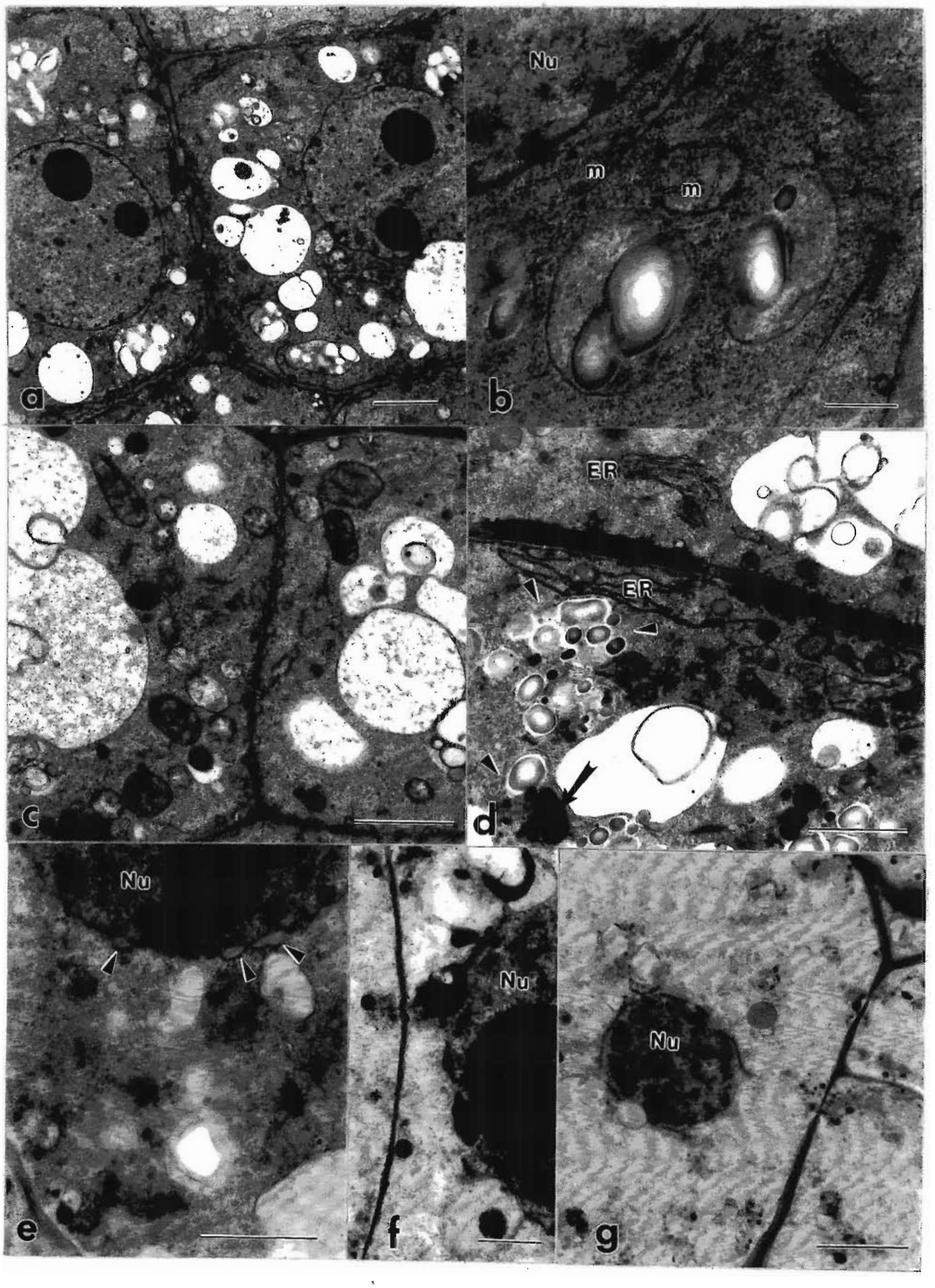
a
b
Nu
m
m
c
d
ER
ER
e
Nu
f
Nu
g
Nu

Fig. 8.11. Light microscopy of axes during germination *in vitro* following plunge cooling in sub-cooled nitrogen at full hydration **a)** After 24 h longitudinal sections showed that root growth originated from cells of the ground meristem and procambium of axes. Bar = 100 μm **b)** After 48 h recovery, the root cap and probably some meristem initials were seemingly displaced by this renewed growth from proximal tissues. Large voids developed in the core of many axes, suggesting cell breakdown due to irreparable freezing damage. (Note that voids occurred in the tissue and not the sections cut, which would have indicated poor fixation/infiltration instead.) Bar = 200 μm **c)** Longitudinal section through a different axis after 48 h *in vitro*, showing voids (asterisks) in the pith and intense staining of distal tissues suggesting the presence of active meristem-like cells. (Framed area is enlarged in Fig. 8.11 d.) Bar = 300 μm. **d)** Higher magnification revealed how growth from proximal tissues appeared to displace the root cap during germination *in vitro*. These cells are presumed to be driving germination, although cell division is not apparent in this section. **e)** Cortical cells (CO) of the hypocotyl were the most tolerant of rapid cooling, while elements of the vascular tissue (VS), cells within the pith and shoot (not shown) were damaged by cryogenic exposure.

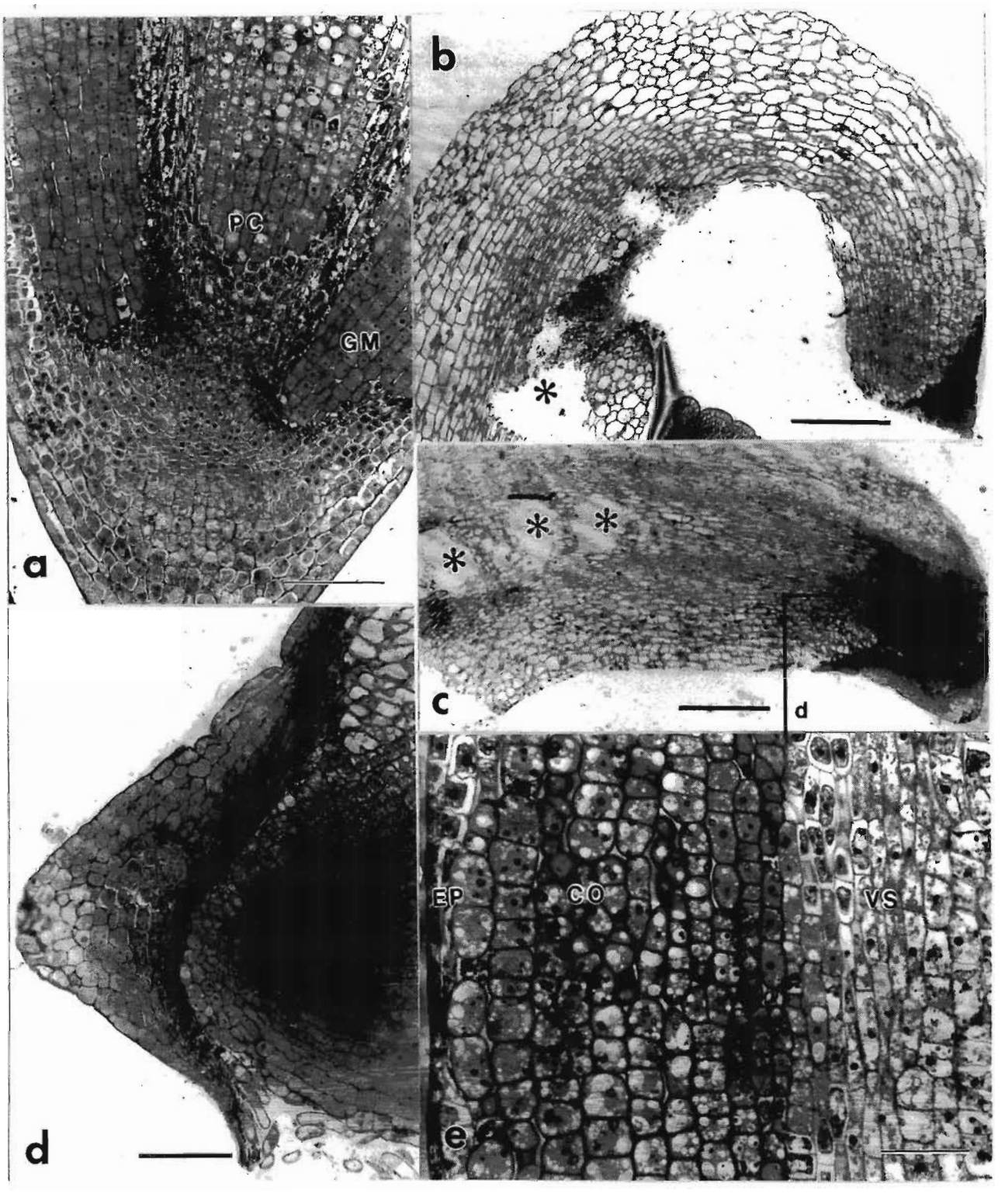
a
PC
GM
b
*
c
*
*
*
d
d
EP
CO
VS
e

damage in distal cells of the radicle at TEM level. Freezing damage resulted in voids within the pith and occasionally localised constrictions that limited normal cell expansion of cells near the epidermis (Fig. 8.13 c). Mid-sections of these axes, unlike that of plunge-cooled axes, showed that cortical cells suffered greater damage than those within the pith (Fig. 8.13 d). While many cells from the shoots showed signs of freezing damage, large pockets of cells had apparently survived in regions of the peripheral meristem and also near the procambium of shoots after 72 h (arrows; Figs 8.13 e and f, respectively)

Discussion

The present study explores the interaction among cooling and warming rates, water content and survival of embryonic axes of *Acer saccharinum* seeds. The results obtained confirm that, at least in many temperate species, axes that tolerate drying to water contents approaching 0.25 g g^{-1} can also withstand cryogenic exposure under a wide range of cooling and warming conditions (compare Pritchard and Prendergast, 1986 and Pence, 1990, 1992 with Wesley-Smith *et al.,* 1992, 2001b; Chapters 4, 6 and 7, and Berjak *et al.,* 1999). At higher water contents the risk of intracellular freezing increases, and cooling and warming conditions appear to have increasingly critical effects upon the survival of cryopreserved axes. Ultrastructural evidence presented here also confirms previous observations suggesting that intracellular freezing and survival are not incompatible (Sherman and Kim, 1967; Mazur and Schmidt, 1968; Sakai, 1968, 1970; Asahina *et al.,* 1970; Bank and Mazur, 1973; Bank, 1974; Vertucci, 1989a; Wesley-Smith *et al.,* 1992; Vertucci *et al.,* 1995; Aker *et al.,* 1999). However, the present facet of this study also revealed unexpected resilience of cells from some tissues, which appeared to tolerate larger intracellular ice crystals to a greater extent than relatively smaller ones. The results presented contribute towards current understanding of the response of non-cryoprotected cells to cooling rate, the sensitivity of different cellular compartments to freezing, the variable

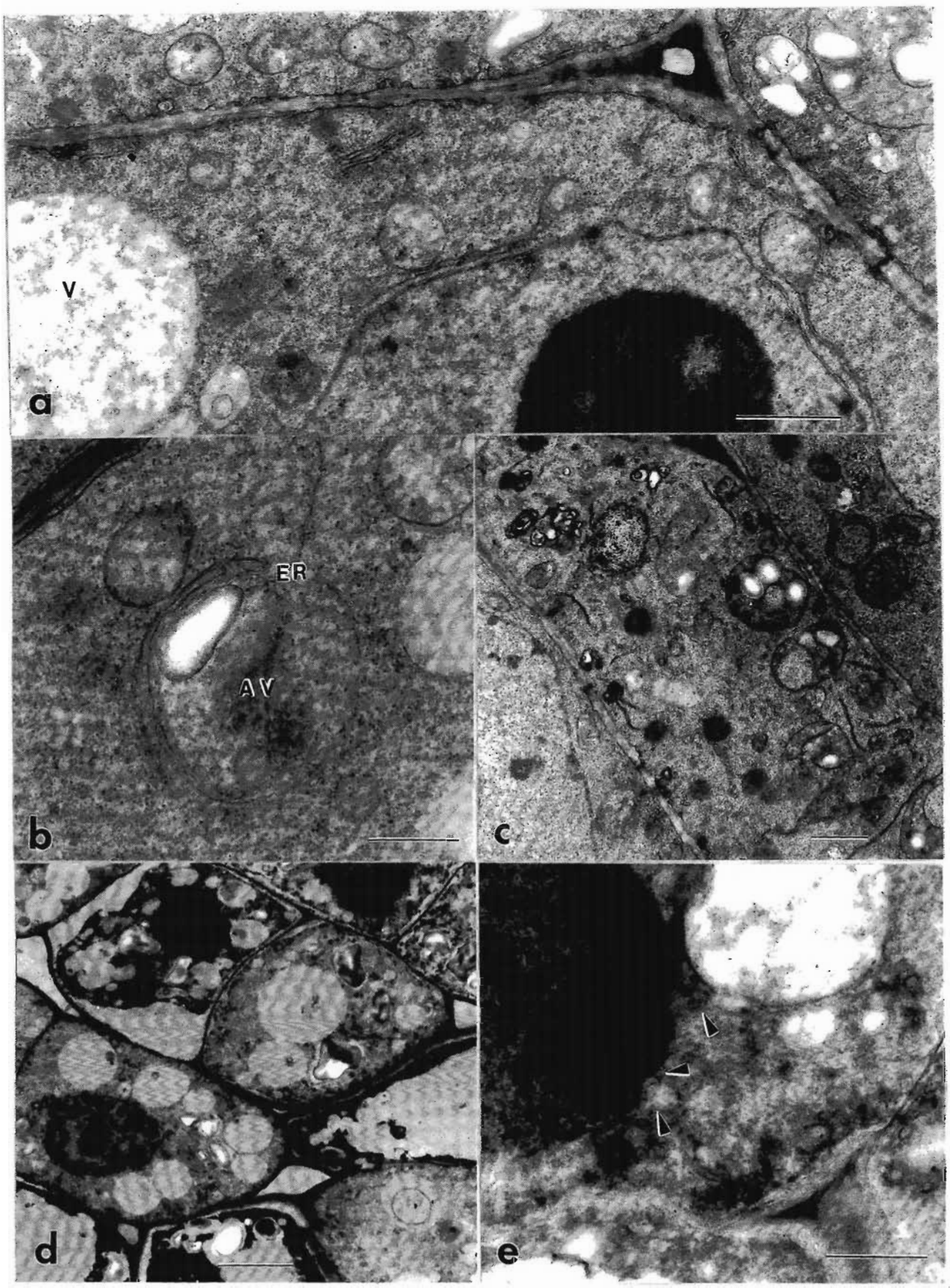
V
a
ER
AV
b
c
d
e

Fig. 8.12. TEM of axes at various intervals after cooling at 3.3°C s^{-1} while fully hydrated, and warmed rapidly **a) 0 min.** Cells resembled closely the appearance of control (not cooled) cells. Bar = 1 μm; **b) 2.5 h** after recovery the early phases of autophagy suggested cellular repair mechanisms had been activated. Bar = 0.5 μm. **c) 6 h.** Organelles appeared irregularly distributed in these cells, which suggested the cytoskeleton had probably been disrupted by cryogenic exposure. Bar = 1 μm; **d, e)** Cells from tissues of the shoot. **d) 2.5 h.** The extent of damage varied among cells. Bar = 3 μm; **e) 6 h.** Localised swelling of the nuclear envelope (arrowheads), tonoplast irregularities and electron-dense vesicles close to the plasmalemma were observed, supporting similar findings made in cells from the corpus of rapidly cooled axes. Bar = 1 μm.

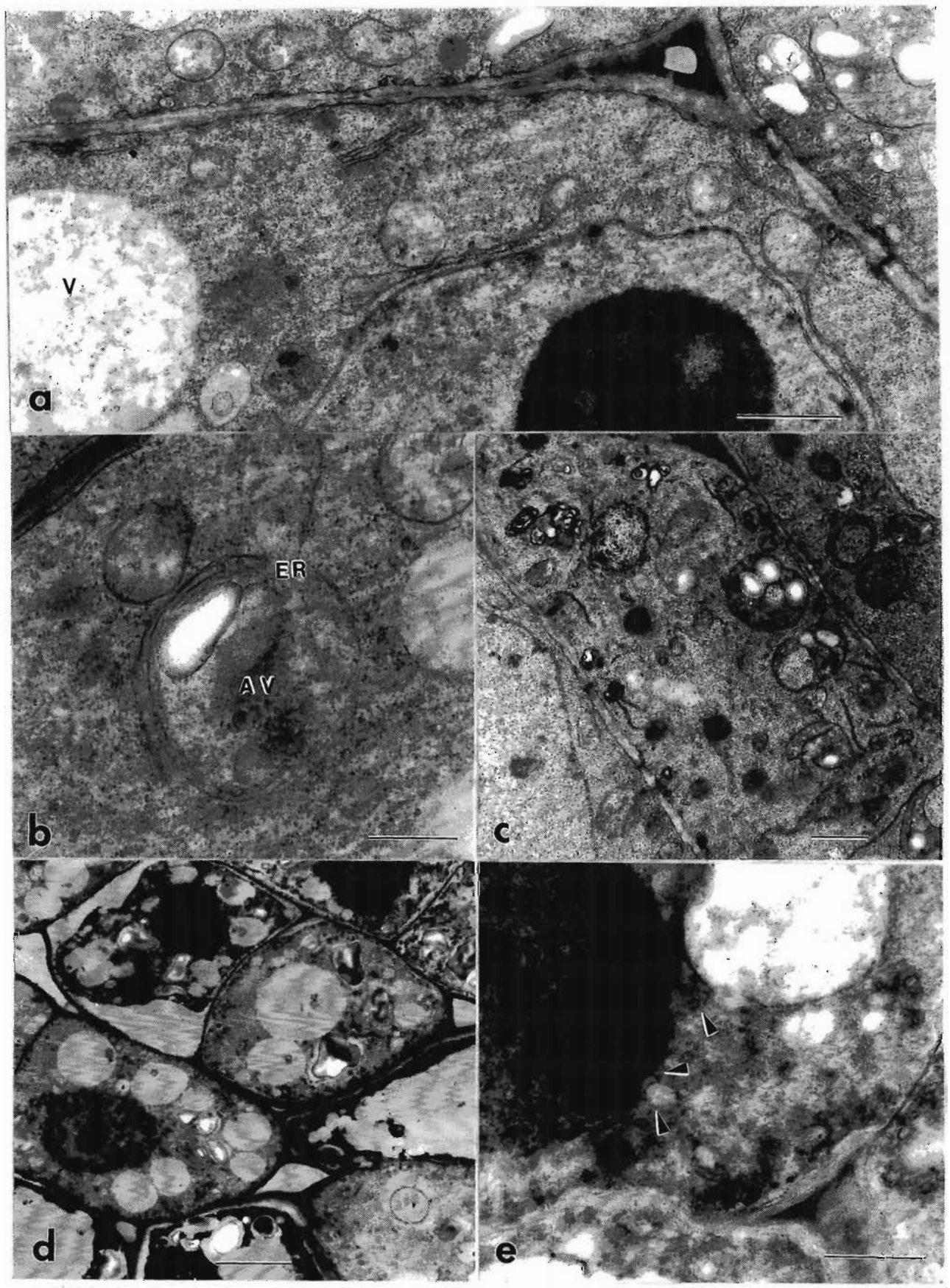
V
a
ER
AV
b
c
d
e

Fig. 8.13. Light microscopy of axes at various intervals during germination *in vitro* following cooling at 3.3°C s^{-1} at full hydration and rapid warming. **a)** Whole axis showing the location of regions investigated at higher magnification in c, d and e below. Bar = 500 μm; **b)** Distal tissues of a germinating axis after 72 h *in vitro*. Bar = 200 μm; **c)** Necrotic areas within the pith of axes were also observed in slowly cooled axes. Note the seemingly normal appearance of surviving cells from the pith surrounding this region. Occasionally surface lesions resulted in constriction during expansion and growth of axes, giving axes a 'warty' appearance. Bar = 200 μm; **d)** Cells from the mid-region of hypocotyls (see Fig. 8.13 a) on either side of the vascular system, but especially within the procambium cylinder, displayed increased tolerance to cryogenic exposure. This contrasted with the situation in plunge-cooled cells, where cortical cells appeared more resilient than tissues deeper into the axis (*cf.* Fig. 8.11 e). Tissues within the procambium cylinder (PC) or lying close to the epidermis (EP) are indicated. Bar = 1 μm; **e, f)** Pockets of cells from the shoot survived cryogenic cooling, and in many instances were able to restore function in partially damaged tissues and resume normal shoot development. **e)** The darkly stained appearance of cells presumed to be of primary and pith meristematic origin (arrows) suggests these cells were alive. In contrast, the highly vacuolated cells of the central mother cells, and those below the leaf bases close to the epidermis showed varying degrees of damage, ranging from severe plasmolysis to complete cell breakdown. Bar = 50 μm; **f)** This micrograph clearly illustrates the localised survival of cells (arrows) from shoots cooled by this treatment. Bar = 200 μm.

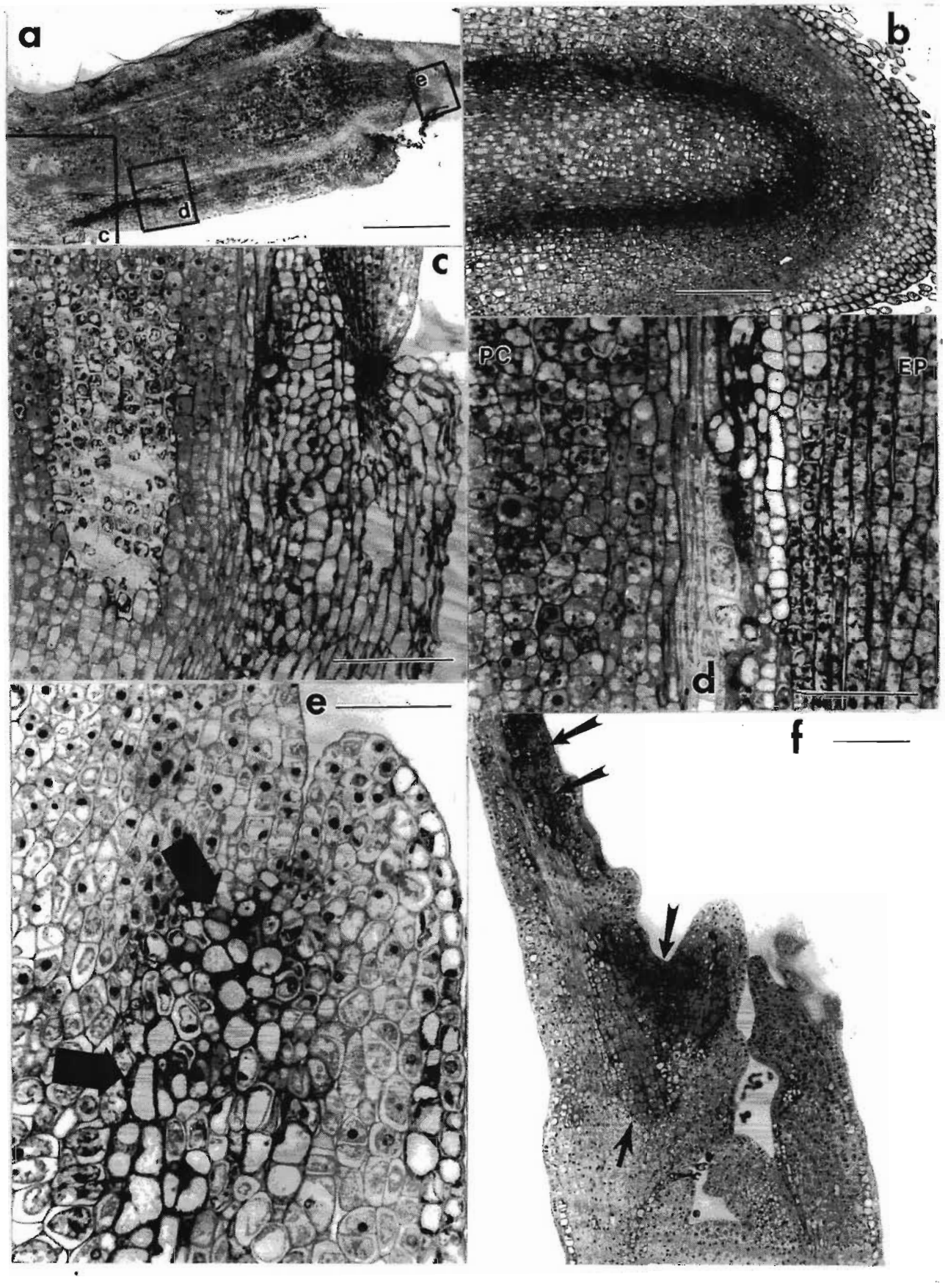
a
b
c
d
e
PC
EP
f

response among axis tissues and the ability of axes as units to restitute damage and re-initiate growth after warming.

Cooling rates

Cooling fully hydrated axes of *A. saccharinum* by plunging and by the Al foil method unexpectedly resulted in similar (P >0.05; Table 8.1) cooling rates between 0 and -40°C. In the study described in Chapter 8, fully hydrated (1.7 g g^{-1}) axes of *Poncirus trifoliata* (0.4 mg dry mass) cooled at 86°C s^{-1} when enclosed within a double layer of Al foil and immersed in liquid nitrogen, and at 500°C s^{-1} during plunging into sub-cooled nitrogen (Chapter 8). In the present case, using a single layer of Al foil also limited the cooling rate attained to about 80°C s^{-1}, but the relatively larger thermal load of fully hydrated *A. saccharinum* axes (1.2 mg dry mass) precluded cooling faster than *c.* 100°C s^{-1} during plunging into sub-cooled nitrogen. Partial drying reduced the thermal load to be dissipated from axes during plunging, resulting in cooling rates of 150°C s^{-1} in axes at 1.0 g g^{-1}, and a significant (P <0.05) increase to 311°C s^{-1} in axes dried to 0.25 g g^{-1} (Table 8.1). The trend presently observed is similar to, and cooling rates intermediate between, those measured under similar cooling conditions within the larger *Aesculus hippocastanum* (6 mg dry mass) and the relatively smaller axes of *P. trifoliata* (Chapters 6 and 7, respectively see also Chapter 5)

Distribution of ice within cells

Previous studies (Sakai and , 1967; Sakai and Yoshida, 1967; Sakai *et al.*, 1968; Mohr and Stein, 1969; Bank and Mazur, 1973; Morris, 1976; Steponkus, 1984) suggest that even the slowest cooling rate tested here (3.3°C s^{-1}) would have been too fast to prevent supercooling of the cell interior and thus limit freezing to only the extracellular medium (Mazur, 1966, 1977). Supercooling increases the likelihood of intracellular freezing, and influences both the number and size of nuclei that are capable of initiating ice crystal growth. A greater extent of supercooling below the equilibrium freezing point reduces the critical size of nuclei capable of initiating freezing, increasing the number of potential nucleation sites (Meryman, 1956, 1966;

Mazur, 1977). Methods such as rapid plunging of naked specimens into sub-cooled cryogens enhance supercooling within very small specimens cryofixed for electron microscopy (Franks, 1980; Bald, 1987). Although rapidly cooled hydrated axes probably do not supercool to the same extent as smaller specimens and freeze at relatively higher subzero temperatures (Meryman, 1966), it was nevertheless expected that cooling at $\geq$77°C s^{-1} or 3.3°C s^{-1} would result in very different distributions of ice within cells. Electron microscopical analysis of FF replicas and sections of FS material confirmed not only that in fully hydrated axes freezing had occurred intracellularly, but that the size and frequency of ice crystals formed in both roots and shoots differed between axes cooled at either $\geq$77°C s^{-1} or 3.3°C s^{-1} (Table 8.2).

The smaller size of ice crystals formed during relatively rapid cooling ($\geq$77°C s^{-1}) agrees with theoretical predictions (Meryman, 1956, 1957, 1966; Van Venrooij *et al.*, 1975; Mazur, 1977; Bald, 1987). However, although it was expected that rapid cooling would reduce the proportion of cellular water converted into ice (*sensu* Luyet, 1965; MacKenzie, 1977), Figure 8.4 suggests that equivalent amounts of water froze in axes cooled rapidly or slowly. Previously, DSC studies also showed no difference in the amount of ice per unit weight of tissue formed within axes cooled using similar procedures comparable to those used presently (Wesley-Smith *et al.,* 1992; Chapter 4). Evidence from both studies suggest that, at least for fully hydrated axes of >1 - 2 mg, not even the fastest cooling rates attainable can reduce the fraction of cellular water that freezes.

Although cooling rates measured in the core of axes during cooling by plunging or within Al foil envelopes were statistically similar (Table 8.1), these two methods resulted in different distributions of ice within cells. Ice inclusions were ubiquitous in cells from plunge-cooled axes (Fig. 8.5), but absent from the matrices of plastids, mitochondria and ER domains in 60-80% of cells of axes cooled within Al foil envelopes (Figs 8.7 b - h). Given the unstable nature of supercooled water (Franks, 1980; Bachmann and Mayer, 1987; Bald, 1987) it is probable that the sudden stop at

the end of the plunge may have contributed to the differences observed between these two treatments. It is proposed that mechanical vibration may have induced widespread (and potentially lethal) nucleation throughout all cellular compartments at a time when axes had cooled only to high subzero temperatures. The possibility of freezing occurring in some but not others has been proposed previously, and explained in terms of differences in chemical composition, viscosity, membrane permeability or in the extent of supercooling endured during non-equilibrium cooling (e.g. Meryman, 1966; Sherman and Kim, 1967; Bank and Mazur, 1973; Nei, 1976a; MacKenzie, 1977; Mazur, 1977; Franks, 1980). While the possible significance of freezing damage within intracellular compartments 'critical' to survival has been recognised for a long time (e.g. Sherman and Kim, 1967; Mazur, 1984) it has seldom been related to functional integrity (e.g. Sherman, 1962, 1964) or survival studies.

In the present study, the ultrastructural damage suggested by the ubiquitous presence of ice in hydrated cells after plunge cooling was paralleled by the inability of corresponding axes to develop shoots *in vitro*, and by the incidence of stunted development in 60% of these axes (Fig. 8.1 a). In axes cooled by the foil method freezing was confined mainly to the ground cytoplasm, nucleus and vacuole, resulting in 100% survival *in vitro* that included up to 50% normal development (Fig. 8.1 b). Survival and normal development of axes cooled slowly at 3.3°C s^{-1} was similar to that attained by the foil method, confirming that damage in both treatments was equally low (compare Figs 8.1 c and b, respectively). The ultrastructure of slowly cooled cells contrasted with that of axes cooled rapidly, revealing relatively fewer and larger intracellular ice crystals (Table 8.2), which gave the cytoplasm a less segregated appearance (Fig. 8.7 c, d, f). Organelles within these apparently ice-crystal free regions seemed compacted and negatively stained and, like axes cooled by the foil method, showed no visible sign of freezing damage. This suggests strongly that the absence of visible ice from cellular compartments could be germane to preserving greater functional integrity of axes cooled within Al foil envelopes or at 3.3°C s^{-1}.

Uneven distribution of intracellular ice within cells cooled at different velocities has been noted previously. Erythrocytes cooled at an optimum 16°C s^{-1} for survival showed ice crystals of approximately 0.1 μm confined to the centre of cells, but none visible along the periphery (Nei, 1976a). Sherman (1962) reported that cells from mouse skin tissues and parakeet tumours survived large intracellular crystals formed during slow cooling at 1.1°C min^{-1}, but were damaged by smaller ice crystals formed during faster cooling at 40°C s^{-1}. Subsequently, Sherman (1964) found that during intracellular freezing, mitochondria of mouse kidney cells suffered greater damage when cooling was rapid (40°C s^{-1}) and ice crystals formed were 5 - 17 times smaller than after slower cooling at 1 - 3°C min^{-1}. Rebhun and Sander (1971) observed that large areas within partially dehydrated eggs of a marine clam remained free from ice crystals after rapid cooling (>100°C s^{-1}) to cryogenic temperatures, presumably due to water migrating from this region towards crystals formed elsewhere in the cell.

It is possible that ice formed during cooling at the expense of water not immediately associated with structure (i.e. 'bulk' water) may dehydrate the cytoplasm and sub-cellular compartments sufficiently to suppress further freezing events. In the present study, cooling between 3.3 and 76°C s^{-1} may have induced such innocuous type of freezing within the cytoplasm and nucleus of most cells of embryonic tissues, especially within roots. Conversely, cooling by the plunging method seemingly failed to exclude ice from forming in compartments such as mitochondria, plastids, ER and possibly the nuclear envelope. Therefore, it appears that during non-equilibrium cooling of hydrated tissues, at least within embryonic axes of certain species, less damage is caused by cooling that encourages the formation of fewer and larger crystals than faster rates which aim to minimise ice crystal growth, but can promote widespread (lethal) nucleation.

The growth of ice crystals within hydrated axes can be hindered by partial drying (Wesley-Smith *et al.,* 1992, 2001b; Chapters 4 and 6) because it increases cytoplasmic viscosity and therefore reduces the mobility of water within cells (Buitink *et al.,* 1998b; Leprince and Hoekstra, 1998; Leprince *et al.,* 1999). In the present

studies, axes dried to a sub-lethal 0.25 g g^{-1} before cooling consistently developed normally irrespective of the warming rate, thus attesting to the limited availability of water for deleterious ice crystal growth in these cells. Above this water content, cells tend to freeze intracellularly, becoming increasingly dependent upon rapid warming to ensure ice crystals melt before growing to lethal sizes as suggested by previous studies (e.g. Sakai, 1966; Mazur and Schmidt, 1968; Mazur *et al.*, 1969; Leibo *et al.*, 1970; Bank, 1973; Bank and Mazur, 1973; Mazur, 1977, 1984, 1990). Presently, drying to 1.0 g g^{-1} presumably increased cytoplasmic viscosity sufficiently to reduce the extent of ultrastructural damage observed in cells from fully hydrated axes following plunge cooling (compare Figs 8.5 and 8.6). However, plunge cooled axes at 1.0 g g^{-1} failed to develop shoots even after rapid (177°C s^{-1}) warming (Fig. 8.1 a), suggesting that the cytoplasm of cells from these tissues was still too dilute to escape lethal freezing damage. Slower warming (67°C s^{-1}) exacerbated the damage observed in axes at both 2.1 and 1.0 g g^{-1}, while warming at 0.08°C s^{-1} was lethal at these water contents (Figs 8.1 d and g, respectively). Rapid warming (177°C s^{-1}) was also more favourable than slower regimes to axes cooled by the foil method or at 3.3°C s^{-1}. However, similar axes cooled by these methods and warmed at 67°C s^{-1} or 0.08°C s^{-1} appeared to endure less damage than corresponding axes cooled by plunging, and differences between axes at 2.1 and 1.0 g g^{-1} were also less marked. These observations agree with the proposal that damage in plunge-cooled axes arises from unrestrained growth of ice nuclei within organelles and endomembrane compartments, especially during prolonged warming. Axes cooled at slower rates appeared to be more tolerant of slower warming, as previously suggested (Mazur and Schmidt, 1968). This is probably due to the greater margin for growth afforded by the absence of immediate membranous boundaries if ice crystals are formed within the cytoplasm or nucleus, rather than within compact, membrane-bound organelles. It seems inevitable that extended ice crystal growth eventually leads to severe damage, but it is uncertain whether this arises from mechanical deformation, extreme freeze-induced drying, or from the deleterious effects of drying and low temperature combined (Vertucci and Roos, 1993; Vertucci *et al.*, 1994, 1995).

Ice crystals reportedly do not become lethal until they exceed a critical size (Sakai and Otsuka, 1967; Sakai *et al.*, 1968), which additionally varies among cell types (e.g. Moor, 1964; Shimada and Asahina, 1972; Nei, 1973). In agreement with the findings of Nei (1976a, 1977), the present study could not determine accurately the size of ice crystals critical for survival: cooling at rates as dissimilar as 3.3 or 76°C s^{-1} yielded similar survival in spite of large differences in the sizes of crystals formed (Table 8.2; Fig. 8.4). Conversely, ice crystals of similar size were formed within the shoots of axes cooled by rapid plunging or within Al foil (Table 8.2), and yet post-warming damage was greater in the former (compare Figs 8.1 b and a, respectively). This supports earlier proposals that survival of axes may have been influenced more by the intracellular *location* of ice than by the *size* of the crystals formed (Sherman and Kim, 1967; Mazur, 1984). It should be emphasised that presumably all cellular compartments are equally important to survival, but that some of these may tolerate freezing to a greater extent than others. While the maximum size attained must ultimately be important, large crystals formed within smaller compartments are more likely to disrupt membranes sooner than corresponding ones formed in the nucleus, vacuoles or in the cytoplasm. It is also possible that not all individuals of a particular organelle type will be similarly affected, and that there is a critical proportional threshold of damage to vital organelles (e.g. mitochondria) which, if executed, could be lethal.

Of the numerous explanations of freezing damage that have been proposed previously, damage to the plasmalemma (e.g. Mazur, 1966; Nei, 1976b; Fujikawa, 1980; Steponkus, 1984; Acker and McGann, 2001) and to sub-cellular compartments (Sherman and Kim, 1967; Mazur, 1977, 1984) seem most relevant to the present study. Freeze-fracture replicas of axes cooled by the methods presently described revealed irregular fracture planes that possibly reflect altered membrane structure (Fig. 8.9). It has been suggested that irregular fracture planes develop where membranes are brought into close contact by large physical forces, such as dehydration and large ice crystals. According to one view (Fujikawa 1980, 1988), localised changes in membrane structure result in fracture planes that reportedly

deviate above or below the area of membranes in close contact instead of cleaving along hydrophobic domains, resulting in localised stripping (Fig. 8.9 b) or stacking (Figs 8.5 d, 8.9 c) of adjacent membrane layers. A contrasting explanation of this phenomenon was initially proposed by Armond and Staehelin (1979). Those authors suggested that fracture planes occurred preferentially within the relatively weaker hydrophobic domains of lipids, which remain appressed to membranes after being excluded by physical stresses. Either way, such membrane structural alterations could account for the high electrolyte leakage associated with reduced survival in hydrated axes of *Aesculus hippocastanum* following rapid cooling (Wesley-Smith *et al.,* 2001b; Chapter 6). It is unclear to what extent membrane damage contributed to the decrease in survival observed *in vitro* in the present study. Many cells from tissues prone to freezing damage, such as those from the shoot, appeared irreversibly plasmolysed during recovery (Fig. 8.13 e) suggesting loss of plasmalemma integrity. Conversely, cells of the root meristem of plunge-cooled axes appeared organised and each had a visibly-intact plasmalemma, but these failed to expand and grow before being displaced by growth originating proximally in the axis (Fig. 8.11 a). This observation, in conjunction with others made presently, emphasises that damage to the plasmalemma is just one of a number of possible causes underlying cellular damage during freezing.

Physical damage to cellular compartments could destroy the ordered partitioning of ions, macromolecules and enzymes across selectively permeable membranes. The similarity between the site and nature of the injuries in axes cooled slowly or rapidly suggests the nuclear envelope is equally prone to freezing damage as the plasmalemma during intracellular freezing, and is likely to prove similarly lethal. In previous studies freezing damage within mitochondria of liver cells resulted in a marked decrease in respiration (Sherman, 1964), while loss of tonoplast integrity (e.g. Fig. 8.9 h) was found to be lethal in non-acclimated Jerusalem artichokes following freezing (Murai and Yoshida, 1998). The increased solute concentration of the cytoplasm that inevitably accompanies freezing reportedly affects polymeric structures (Franks, 1980) such as polysomes (e.g. Figs 8.7c, 8.8 c and e). Similarly,

cytoskeletal elements reportedly depolymerise in response to freezing and increased solute concentration, particularly of Ca^{2+} ions ([Bartolo and Carter, 1991). Damage to intracellular Ca^{2+} stores such as ER cisternae (Hepler *et al.*, 1990) could also cause cytoplasmic levels of Ca^{2+} to rise and thus preclude cytoskeletal reassembly in recovering cells.

Recovery in vitro

The extent of ultrastructural deformation observed in frozen cells makes it almost as challenging to account for the survival obtained as it does to explain the causes underlying damage. The significance of findings from cells in the solidified state can be fully appreciated only if the structural and functional integrity are assessed after warming (Sherman and Kim, 1967; Nei, 1976a). It is noteworthy that while membranes may appear intact immediately after warming this is not unequivocal proof that this is, in fact, the case. Ultrastructural changes were observed after 30 min had elapsed, which presumably allowed sufficient time for cells to equilibrate to ambient conditions and for damage sustained during cryogenic exposure to become apparent. Accordingly, in the present study the structure of cells from axes after cooling and rapid warming was examined at various intervals ranging from minutes to days after warming, and survival was assessed after a four-week period.

Recovery of axes *in vitro* can be assumed to progress at three levels, *viz.* the ability of individual cells to repair damage, the recovery of a critical number of cells to sustain function within each tissue, and the ability of tissues to resume interactions that facilitate growth. Ultrastructural evidence suggesting cell repair processes was first noted after 2.5 h recovery in cells of axes cooled by plunging or at 3.3°C s^{-1}. The similar ultrastructural events (e.g. increased autophagy, ER proliferation, vacuolation) in axes during recovery *in vitro* suggests that a common spectrum of mechanisms was activated for intracellular repair. Nevertheless, repair did not invariably follow where extensive damage occurred, such as in cells of the shoot of plunge-cooled axes. While presumably the response of cells to damage is initiated shortly after warming, the ability of cells to recover probably depends on the extent of the injury.

Likewise, the ability of axes to germinate normally seemed to be influenced by the location of tissues damaged during cryogenic exposure as well as by the proportion of cells capable of sustaining organised growth within these tissues.

Light microscopy provided invaluable information regarding the recovery of tissues from axes plunged into sub-cooled nitrogen or cooled at 3.3°C s^{-1}. Cell expansion (and presumably cell division) were evident in the ground meristem and procambium regions of the embryonic radicle from plunge-cooled axes after 24 h *in vitro* (Fig. 8.10 a). Many of the cells from both these primary meristems remain meristematic and are presumed to initiate germination in these axes. As mentioned above, this proximal renewed growth subsequently displaced cells of the root cap, meristem initials and their derivatives (Fig. 8.11 b - d) probably because the latter had endured damaged that prevented these developing at the same rate or, perhaps, at all. In contrast, tissues of axes cooled at 3.3°C s^{-1} germinated normally (Fig. 8.12 b), suggesting that less damage had occurred within cells from these axes. The recovery of cells from mid-regions of axes cooled by either treatment contrasted sharply. In axes plunged rapidly, cells of the pith suffered greater damage than cortical cells, possibly due to the slower cooling and warming within the core (Fig. 8.10 e). Although the reverse was mostly true in axes cooled at 3.3°C s^{-1}, cells on either side of the vascular tissues appeared to survive cryogenic exposure (Fig 8.13 d). It is probable that survival of a greater proportion of cells capable of assuming a meristematic rôle led to the apparently normal root development observed in axes cooled at 3.3°C s^{-1}. This notwithstanding, large areas of cells within the pith of both cooling treatments often showed voids where cell breakdown presumably had occurred (Figs 8.11 b, c and 8.13 e). It is contended that these lesions could be responsible for the apparently stunted development of some axis and, in extreme cases, for callus growth where only isolated groups of cells survive cryopreservation.

Cells from the shoot of plunge-cooled axes appeared plasmolysed after 24 h, suggesting that irreparable freezing damage had occurred. Conversely, survival of isolated groups of ≥20 cells was observed in leaf primordia from shoots from axes

cooled at 3.3°C s^{-1} (Fig. 8.12 e - f). The capacity of hydrated cells of pea (*Pisum sativum*) to regenerate growth from regions other than the meristem proper following cryogenic exposure has been reported previously for embryonic axes (Berjak *et al.*, 1995) and cryoprotected shoot apical meristems (Haskins and Kartha, 1980). In both studies surviving cells were capable of cell division and organised growth. The 20% of fully hydrated axes which presently showed normal shoot development (Fig. 8.2 c) suggests that at least in some axes surviving cells were able to restore organised growth and allow near-normal development to proceed. While it is uncertain what conferred surviving cells greater freezing tolerance, but close proximity to the peripheral meristem and procambium was frequently noted (Figs 8.13 c and f).

Appendix A. Hierarchical log-linear analysis of the effects of cooling (C), warming (W) and water content (H) on survival (S) of axes of *Acer saccharinum*.

Main Effects on Survival	Model	df	L^2 [a]	P	Q^2 (%) [b]
Baseline [c]	[S CHW]	52	213.85	-	-
Water content	[S CHW][HS]	48	93.26	<0.0001	56.4
Warming	[S CHW][WS]	48	175.91	<0.0001	17.7
Cooling	[S CHW][CS]	48	204.91	0.0625	4.2

Interaction Effects	Model	df	L^2 [a]	P	Q^2 (%) [b]
Baseline [c]	[CHW][WS][CS][HS]	40	20.24	-	-
Cooling x water content	[CHW][CHS][WS]	32	4.58	0.05	77.4
Warming x cooling	[CHW][WCS][HS]	32	12.39	>0.4	39
Warming x water content	[CHW][WHS][CS]	32	15.91	>0.8	21.5

[a] L^2= Log-likelihood ratio (Knoke and Burke, 1980)

[b] Q^2= (L^2 baseline model - L^2 alternative model) / (L^2 baseline model). An R^2 analogue that reflects the amount of variance not explained by the baseline model, and that is explained by each interaction term.

[c] First Level interaction, incorporating all single order independent terms

CHAPTER 9

Rapid drying and cooling as a reliable approach to cryopreserve embryonic axes of recalcitrant seeds: A critical appraisal

The purpose of the present thesis was to develop a procedure that facilitates the long-term storage of embryonic axes of recalcitrant species. An approach that combines harmless rapid drying to low water content, and rapid (non-equilibrium) cooling to temperatures where metabolic activities are in a state of suspended animation, is described. The inadequacies of conventional protocols to cryopreserve recalcitrant axes, and the manner in which the approach presently described overcomes these obstacles, is discussed below.

Drying to low water contents

The long-term preservation of embryonic axes requires that all metabolic activities be halted without injury, followed by storage at water contents and subzero temperatures that preclude degradative reactions (Walters, 1998). Cells of desiccation tolerant (orthodox) seeds become metabolically quiescent and equilibrate to ambient relative humidity during their final phases of development (Bewley, 1979; Kermode *et al.*, 1985). Loss of most or all freezable water facilitates storage at cryogenic temperature without freezing injury (e.g. Stanwood, 1985; Vertucci 1989a,b). In contrast, desiccation sensitive (recalcitrant) propagules are shed fully hydrated (Ψ= > -1.5 MPa) and therefore require drying to increase the likelihood of survival after cryogenic exposure. Embryonic axes from highly recalcitrant species do not tolerate drying to <0.5 g g^{-1} (e.g. *Avicennia marina* [Farrant *et al.,* 1993]) and are killed by cryogenic exposure at those water contents. Axes from many temperate species and some tropical species tolerate drying to 0.35 - 0.25 g g^{-1} under favourable conditions (Chapter 3) and have been reported to survive cryogenic exposure (Pritchard and Prendergast, 1986; Vertucci 1989a,b; Pence, 1990, 1992, 1995; Chaudhury *et al.,* 1991; de Boucaud *et al.,* 1991; Vertucci *et al.,* 1991; Abdelnour-Esquivel *et al.,* 1992; Chandel *et al.,* 1995; Pritchard *et al.,* 1995;

Chapters 4, 6, 8 and 9). However, their survival as entire axes is equivocal, as frequently incomplete development or only callus growth follows retrieval from cryogenic conditions (reviewed by Berjak *et al.*, 1996).

Deleterious combination of low water content and low temperature

Evidence suggests that storage stability is attained at water content optima that are strongly dependent upon temperature and the nature of reserves within cells (Vertucci and Roos, 1990, 1993; Vertucci *et al.,* 1994; Buitink *et al.,* 1998a, 2000; Walters, 1998). Results from those studies suggest that the optimum water content increases with decreasing storage temperature. This means that in spite of tolerating drying to water contents that preclude freezing, axes can nevertheless sustain damage during exposure to subzero temperatures (e.g. Vertucci *et al.,* 1994). The exact nature of damage caused by the combination of low water content and low temperature is not clear, but demixing of membrane components is a strong possibility (reviewed by Bryant *et al.*, 2001). Increasing axis water content ameliorates this type of damage but, paradoxically, also increases the likelihood of freezing damage during cooling to subzero temperatures. This clearly illustrates the dilemma faced by genebank operators attempting to determine favourable conditions facilitating long-term storage stability in desiccation-sensitive germplasm with minimum loss of viability.

Glasses, and their significance to germplasm conservation

Germplasm should be stored under conditions that preclude or minimise degradative reactions in order to attain maximum storage stability (Walters, 1998). Water content and temperature affect the viscosity of the cytoplasm, and thus the rates of reactions that take place within cells. A rapid decrease in temperature, a large increase in viscosity, or both, can lead to the formation of an amorphous solid state within cells, referred to either as syrup, rubber or glass depending on its viscosity (e.g. Roos and Karel, 1991). These states are thermodynamically unstable, and their tendency to restore equilibrium can be restricted by reducing their molecular mobility at temperatures below the glass transition range (T_g; Williams *et al.,* 1993; Leopold *et al.,* 1994). Glasses can be regarded as the natural outcome of seed drying (Walters, 1998), and are

particularly relevant to seed storage stability because they hinder deleterious chemical reactions requiring diffusion (Burke, 1986; Williams *et al.,* 1993; Leopold *et al.,* 1994; Leprince and Walters, 1997). Glasses have been reported to occur at ambient temperature in orthodox seeds dried to ≤ 0.12 g g^{-1} (e.g. Williams and Leopold, 1989; Bruni and Leopold, 1992). They have also been reported to prevent intracellular freezing in tissues of cold-acclimated trees after freeze-dehydration and temperatures ≤ -28°C (Hirsh *et al.,* 1985). While the ability to form intracellular glasses has been linked to increased storage longevity in desiccation tolerant seeds (Burke, 1986; Williams and Leopold, 1989; Leopold *et al.,* 1994), glass transitions do not necessarily confer desiccation tolerance to seeds (Buitink *et al.*, 1996).

Glasses and desiccation-tolerance

Although it appears there is a spectrum of phenomena implicated in the acquisition and loss of desiccation-tolerance, clear-cut differences in the events that confer storage stability on desiccation tolerant, but not sensitive, seed types remain elusive. There appears to be no difference in the calorimetric properties of water from these seed types (Vertucci, 1990; Pammenter *et al.,* 1991; Berjak *et al.,* 1992, 1993; Sun *et al.,* 1994; Buitink *et al.,* 1996; reviewed by Vertucci and Farrant, 1995). It has been suggested that perhaps the manner in which water interacts with macromolecular structures could explain differences in levels of desiccation tolerance (reviewed by Vertucci and Farrant, 1995). It was initially proposed that high ratios of oligosaccharides were beneficial to seed longevity because they elevated T_g and thus increased storage stability at ambient temperatures by restricting molecular mobility (Leopold *et al.,* 1994). Different lines of evidence suggest that while soluble sugars are important in conferring storage stability, they cannot account fully for differences in desiccation sensitivity (Buitink *et al.*, 1996). Buitink *et al.* (2000) found that different oligosaccharide concentrations do not affect T_g or change the molecular mobility within glasses of cells. Secondly, sugars accumulate in appropriate levels and ratios in maturing embryonic axes of some recalcitrant seed species (Berjak *et al.,* 1989; Farrant *et al.,* 1992, 1993; Finch-Savage, 1992), and yet these propagules display sensitivity to extreme drying. Glasses have been reported to form in cells of desiccation sensitive cotyledons (Sun *et al.,* 1994) and by sugar solutions

extracted from axes of desiccation sensitive seeds (Koster, 1991). Glasses were observed in both those studies, but even at water contents corresponding to the limit of desiccation tolerance these formed at temperatures only below -25°C. This evidence emphasises the inescapable fact that desiccation tolerant embryos survive loss of freezable water to levels favouring glass formation at ambient temperature (hydration level 2; [Vertucci and Farrant, 1995]) but recalcitrant axes do not. Therefore, there is a need for protocols that facilitate long-term storage of recalcitrant axes by reducing damage during drying as well as during cooling to sufficiently low temperatures.

Conventional storage procedures are inadequate for recalcitrant seeds

Drought or subzero temperatures seldom occur in the natural habitats of plants showing recalcitrant seed storage behaviour (Chin and Roberts, 1980), and it is likely that these propagules do not possess adequate mechanisms to cope with these stresses. Favourable procedures to cryopreserve embryonic axes should thus strive to reduce stress during drying, cooling and, as an inevitable corollary, warming and recovery. Conventionally, recalcitrant axes are cooled at approximately 3°C s^{-1} (e.g. Pritchard and Prendergast, 1986; Pence, 1990, 1992, 1995; Chaudhury *et al.,* 1991; de Boucaud *et al.,* 1991; Abdelnour-Esquivel *et al.,* 1992; Chandel *et al.,* 1995; Pritchard *et al.,* 1995) and, in order to prevent freezing damage axes, must first be dried to water contents equivalent to those attained by equilibrium freezing procedures prior to rapid cooling to -196°C (reviewed by Mazur, 1990). Drying recalcitrant axes to such low water contents is often deleterious, and can result in abnormal development and death on rehydration even before exposure to cooling stress. The success of this type of procedure relies heavily on the ability of axes to *endure* the rigours of extreme drying and relatively slow cooling, which possibly explains the lack of success with recalcitrant species that are chilling sensitive (e.g. Chin and Roberts, 1980) or that do not tolerate the extent of drying that this approach demands (e.g. *Trichilia dregeana* [Kioko *et al.,*1998]; jackfruit; [Thamassiri, 1999]).

The present strategy: avoiding stress

The work presented in this thesis explores strategies aimed at *avoiding* stress during pre-treatments commonly used such as prolonged drying, or that induced by freezing during cryogenic exposure, *viz.* non-equilibrium drying, cooling and warming. It is hypothesised that survival after cryogenic exposure would be increased if the potentially deleterious effects associated with each of those steps could be avoided or, at least, minimised. In particular, it is contended that restricting the growth of ice to within harmless levels by sufficiently rapid cooling would allow axes at relatively higher water content to be cryopreserved. It was expected that by increasing present understanding of the physiological and biophysical factors resulting in survival or death among axes from different species could lead to the development of a cryopreservation model with broad applicability and predictive value. The use of cryoprotectants was deliberately omitted so as not to obscure the response of cells to drying and cooling treatments. Aspects therefore investigated included the response of axes to differences in drying, cooling and warming rates, and heat transfer processes influencing the distribution of ice among cells of axes cooled under various conditions. The effects of these variables, and their interactions, upon the survival *in vitro* of axes of *Artocarpus heterophyllus* (jackfruit), *Camellia sinensis* (tea), *Aesculus hippocastanum* (horse chestnut), *Poncirus trifoliata* (trifoliate orange) and *Acer saccharinum* (silver maple) seeds are discussed below.

The importance of rapid drying

Ice forms readily in dilute solutions at subzero temperatures (Luyet, 1966; Franks, 1980) and within hydrated cells this process is usually lethal (Mazur, 1966, 1977). Increasing the intracellular solute concentration decreases the molecular mobility of water and therefore hinders ice crystal growth during non-equilibrium cooling (Luyet *et al.*, 1962; Fahy, 1984). In the present study, cytoplasmic concentrations were manipulated by rapid (flash) drying (Berjak *et al.*, 1990) in a chamber at low relative humidity (Wesley-Smith *et al.*, 2001a; Chapter 3). Axes of jackfruit dehydrated for ≤90 min using this approach and rehydrated immediately could attain lower water contents and with minimal injury relative to slower drying procedures over 2-3 d. Freeze-substitution

allowed the structure of partially dried axis cells to be appraised reliably without evidence of rehydration artefacts characteristic of aqueous fixation protocols (Wesley-Smith, 2001; Chapter 2). Partial drying to 0.7 g g^{-1} did not affect axes of jackfruit dried rapidly, but marked the onset of increased electrolyte leakage and decreased survival of axes dried slowly. It was expected that TEM sections would reveal differences between these treatments that explained the incipient damage observed in slowly dried cells. Axes dried rapidly or slowly to 0.7 g g^{-1} showed undifferentiated mitochondria, numerous Golgi stacks and increased ER profiles, which possibly indicated a homoiostatic response to the water deficit experienced. No plasmalemma or tonoplast abnormalities were observed in meristem and meristem-derivative cells of axes from either treatment. However, after rehydration membrane abnormalities were observed in slowly dried axes, suggesting that damage occurred either during rehydration or alternatively during drying, but required additional water to become apparent (Wesley-Smith *et al.,* 2001a; Chapter 3). Damage to axes dried slowly was probably caused by deleterious biochemical reactions occurring at intermediate water contents due to unregulated metabolism (Vertucci, 1993; Salmen Espindola *et al.,* 1994; Leprince and Hoekstra, 1998; Pammenter *et al.*, 1998; Leprince *et al.,* 1999, 2000; Walters *et al.,* 2001; reviewed by Vertucci and Farrant, 1995; Pammenter and Berjak, 1999; Walters 2001) culminating in complete mortality with further drying to 0.4 g g^{-1}. Based on this evidence, rapid drying became the method of choice to increase the cytoplasmic viscosity prior to cryogenic storage.

Rapid drying and differential drying

Studies on embryonic axes of jackfrfuit showed that rapid drying resulted in uneven distribution of water (Wesley-Smith *et al.,* 2001a; Chapter 3). Cells from the cortex dried more than cells within the procambium cylinder, and probably the relatively exposed meristematic tissues from the shoot dried to a greater extent than distal meristematic cells, as has been reported for *Trichilia dregeana* axes (J. Kioko, University of Natal, Durban, South Africa; pers. comm.) Differential drying is presumably caused by a lag in diffusion as water is withdrawn preferentially from outermost cell layers, establishing a steep gradient between the dry conditions at the boundary and the relatively hydrated

interior. Such uneven drying implies that in axes dried rapidly to intermediate water contents (e.g. 0.7 – 0.45 g g^{-1}; hydration level 4 [Vertucci and Farrant, 1995], germinative cells within the core were exposed to relatively shorter, and less intense, drying than cortical cells. Furthermore, evidence suggests that exposure of axes to short, mild drying stress stimulates an ultrastructural response (e.g. Chapter 3) which could be associated with an increase in vigour often observed during germination of partially dried recalcitrant embryos (Farrant *et al.,* 1985; Probert and Brierley, 1989). Although speculative, it is probable that the same response could be beneficial to axes during subsequent cryogenic exposure, but this possibility remains to be confirmed.

Slow drying leads to water being more evenly distributed in axes, exposing meristematic cells to relatively greater and longer drying stress. It is possible that this prolonged water deficit reduces vigour and predisposes axes negatively for cryogenic storage (Berjak *et al.*, 1999; Kioko *et al.*, 1998). Given that meristematic tissues from the shoot appear to be more sensitive to desiccation than corresponding tissues of the hypocotyl (Pritchard and Prendergast, 1986; Pritchard, 1991; Fu *et al.,* 1993; Pritchard and Manger, 1998; Kioko *et al.*, 1998; Chapter 3), it is likely that they are damaged first during drying irrespectively of the drying rate. Although not reported here, preliminary investigations have shown that protecting the shoot pole from excessive drying by covering these structures using a thin coating of wax is advantageous. Minimising stress experienced meristem and meristem-derivative cells of axes prior to cooling is presumably advantageous, as those cells are the primary determinants of normal germination after retrieval from cryostorage (see Chapter 8).

Implications of a narrow window of permissible water contents

The need for rapid drying to avoid injury, and the uneven distribution of water that results from it, imply that in order for whole axes to survive cryogenic exposure the cooling procedure must accommodate a wide range of cellular water contents. However, conventional cryopreservation protocols do not allow such margin of variability, which results in tissues suffering varying extents of damage during this procedure. As with desiccation stress, shoots are the first tissues to be damaged during freezing, and while

root development may not be affected, the development of a normal plantlet in such instances is uncommon. Axes sustaining severe freezing damage typically showed isolated pockets of surviving cells, usually near the embryonic radicle, giving rise to disorganised callus growth (Berjak *et al.*, 1998; Chapter 6). Cooling treatments that result in high mortality of axes, or lethal damage at tissue level within these, may inadvertently bias preservation in favour of axes showing particular cellular traits. Such selection could possibly lead to genetic shifts that could compromise the goal pursued, *viz.* conserving heterogeneity within a population of seeds. If callus growth is the only form of survival attainable, plantlets could possibly be re-generated from explants by somatic embryogenesis (e.g. Pence, 1991). Preferably, abnormal development of axes should be avoided by the use of cryopreservation procedures that minimise damage caused by severe desiccation (e.g. Fu *et al.*, 1993; Pritchard and Manger, 1998), freezing injury (Wesley-Smith *et al.*, 2001b), or a combination of these (Normah *et al.*, 1986; Pritchard and Prendergast, 1986; de Boucaud *et al.*, 1991; Vertucci *et al.*, 1995; Chmielarz, 1997; Kioko *et al.*, 1998; Chapters 4, 6, 8 and 9).

Cooling rates and permissible water content ranges

The water content range that separates freezing and desiccation damage among recalcitrant embryos cryopreserved by conventional procedures (e.g. Pritchard and Prendergast, 1986; Radhamani and Chandel, 1992; Pence, 1992; Chandel *et al.*, 1995) can be extremely narrow. Axes tolerating drying to 0.35 – 0.25 g g^{-1} avoid freezing injury presumably because water does not freeze at these water contents (Vertucci, 1989a,b, 1990; Pammenter *et al.*, 1991; Vertucci *et al.*, 1991; Berjak *et al.*, 1992; Wesley-Smith *et al.*, 1992; Farrant and Walters, 1995; Pritchard *et al.*, 1995; Pritchard and Manger, 1998). Drying below this range results in damage even when axes are dehydrated very rapidly, and in the absence of cooling (reviewed in Vertucci and Farrant, 1995; Pammenter and Berjak, 1999; Walters *et al.*, 2001). Conversely, above that range water becomes increasingly mobile and available for ice crystal growth, resulting in freezing damage within cells cooled at *c.* 3°C s^{-1}. Consequently, axes that fall outside this narrow window of permissible water contents are damaged by excessive drying or by freezing either wholly or in part (Chapter 4). Therefore, strategies to increase the range of

permissible water content are required to reduce freezing damage and increase post-warming survival. Increasing the rate of cooling can achieve this goal (Chapters 4 and 7).

The study on mature axes of tea (*Camellia sinensis*; Chapter 4) showed that the rapid cooling approach could be applied to cryopreserve organised tissues and not just single cell layers or suspensions. Rapid cooling increased the range of permissible water content relative to that attained using slower cooling methods. In that study, survival of axes dried (but not cooled) decreased from 100% above 1.6 g g^{-1} to 67% after flash drying to 0.4 – 0.3 g g^{-1}, a range presumed to mark the onset of desiccation damage in that species (Chapter 4; Berjak *et al.*, 1993). Axes dried rapidly to this low water content and cooled at 0.08°C s^{-1} (10°C min^{-1}) showed maximum survival of only 14%. Following cooling at 3.3°C s^{-1} (200°C min^{-1}) the upper limit of tolerated water content increased to 0.7 g g^{-1}, where 60% survival was noted. Yet even faster cooling at rates, estimated at hundreds of °C s^{-1}, resulted in 100% normal germination of axes of up to 1.6 g g^{-1}. Freeze-fracture replicas obtained from similar axes showed superior preservation of ultrastructure and no evidence of ice crystal damage, which mirrored the complete survival of axes *in vitro*. In contrast, axes at water contents above 1.6 g g^{-1} did not survive rapid cooling, and freeze-fracture replicas of those axes revealed the presence of ice nuclei of *c.* 125 nm throughout every cellular compartment of the cells examined. At all cooling rates, the upper limit of permissible water content appeared to be determined by the occurrence of lethal freezing damage, albeit at different values, while the lower limit was set by the onset of desiccation damage at about 0.4 - 0.3 g g^{-1} irrespective of the cooling rate.

DSC, sharp peaks and survival

DSC studies provided further evidence that freezing damage determined the upper limit of permissible water content. Melting endotherms of axes cooled to $\leq$ -70°C at different velocities revealed the presence of sharp endothermic peaks with onset temperature of -2°C (Pammenter *et al.*, 1991; Berjak *et al.*, 1992, 1993). Studies conducted in parallel showed that these sharp peaks were associated with decreased survival of axes post-

warming (Pammenter *et al.*, 1991; Vertucci *et al.*, 1991; Wesley-Smith *et al.*, 1992; Berjak *et al.*, 1993). Sharp peaks occurred above 0.46 and 0.67 g g^{-1} in tea axes cooled at 10 or 200°C min^{-1}, respectively, and were not observed in axes cooled rapidly (Chapter 4). Several findings led to the conclusion that these sharp peaks represented melting of ice crystals large enough to be detectable, as well as lethal. Firstly, sharp peaks were seen only at water contents above those where survival *in vitro* no longer occurred. Secondly, sharp peaks occurred consistently at about 0°C irrespective of the axis water content, suggesting the melting of pure water. They were more pronounced in axes at higher water contents, reflecting the greater availability of water for freezing. Finally, finding that sharp peaks were not observed when axes were cooled rapidly irrespective of the water content supported the view that rapid cooling restricted the ultimate size attained by ice crystals (e.g. Meryman, 1960). However, while ice crystals formed within fully hydrated axes may have been too small to be detected, they were lethal none the less. Thus, the presence of sharp peaks in melting endotherms can be regarded as indicative of lethal damage, but their absence does not necessarily imply survival.

Cooling rates and the proportion of cellular water that freezes

Previous studies (e.g. Sakai and Otsuka, 1967; Sakai and Yoshida, 1967; Sakai *et al.*, 1968; Mohr and Stein, 1969; Bank and Mazur, 1973; Morris, 1976; Steponkus, 1984) have shown that cooling rates ≥10°C min^{-1} exceed the limit required for equilibrium freezing, resulting in supercooling of the cell interior and subsequent freezing. Increasing the rate of cooling can limit the amount of ice formed (Luyet *et al.*, 1962; Luyet, 1965; MacKenzie, 1977). This implies that while complete avoidance of intracellular freezing during non-equilibrium cooling seems unattainable in large (>0.1 mm) hydrated tissues (Luyet, 1960; Rasmussen, 1981; Franks, 1980), rapid cooling to temperatures below *c.* -130°C may none the less limit the amount of ice formed. The high survival of axes of *Camellia sinensis* at 1.6-1.1 g g^{-1} and the apparent absence of ice crystals in freeze-fracture replicas support that observation (Chapter 4). In contrast, melting endotherms recorded using DSC at a warming rate of 10°C min^{-1} suggested that there were no differences in the amount of ice formed among axes cooled at 10 or

200°C min^{-1}, or very rapidly in sub-cooled nitrogen. Two possible interpretations are suggested for this apparent contradiction:

1. All cellular water was converted into ice, irrespective of cooling velocity and water status (e.g. Meryman, 1957). Differences in survival are explained by the absence of damage when ice crystals formed during rapid cooling were small, yet numerous, in contrast to the increasingly larger (and lethal) sizes of the relatively fewer crystals formed at 200 and 10°C min^{-1} (see Chapter 8). Warming at 10°C min^{-1} did not affect the amount of ice formed in those axes.

2. Different cooling rates resulted in various amounts of ice being formed during cooling, being smallest after rapid cooling and increasingly larger with slower cooling. However, slow warming at rates typical of DSC studies (e.g. 10°C min^{-1} [Vertucci, 1989a,b]) allowed sufficient time for ice crystals re-crystallise into larger structures that, upon melting, negated differences in the initial amounts of ice formed at each cooling rate. Survival of axes cooled rapidly was high because rapid warming prevented deleterious re-crystallisation during retrieval from cryostorage, whereas axes cooled at slower rates were damaged on cooling, irrespectively of the warming rate (Mazur, 1990). No exothermic events were visible in endotherms because heat released during re-crystallisation was probably too diffuse to be detected.

Further studies are required to establish with certainty whether or not rapid cooling attained under the present conditions can limit the amount of ice formed within axes at various water contents. If the second interpretation is correct, then it may be inappropriate to investigate the calorimetric properties of water in dilute solutions cooled very rapidly using warming rates that allow re-crystallisation to occur.

Measurement, reproducibility and heat transfer

The success attained cryopreserving axes of *C. sinensis* promoted further research to test the applicability of these findings to other species. It became immediately apparent that cooling rates needed to be quantified reliably, and cooling procedures achieved

reproducibly, in order to allow meaningful comparisons between treatments and among cryopreservation trials. Although the compressed-air method used in Chapter 4 was highly practical and efficient for survival studies, it did not allow reproducible measurement of cooling rates within specimens. The plunging device adapted from the cryofixation apparatus described by Ryan and Purse (1985) fulfilled both requirements (Chapter 5). Springs of variable strength gave the plunging rod sufficient travel velocity to impel individual axes mounted either on an ultramicrotomy holder (Reichert, Vienna, Austria) or on similar supports bearing a thermocouple that enabled temperature measurement during cooling. Additionally, this device allowed manipulation of variables (e.g. travel velocity, depth of plunge, cryogen type) known to increase the rate of cooling of small specimens for cryo-electron microscopy (reviewed by Gilkey and Staehelin, 1986; Menco, 1986; Ryan, 1992). The influences of bare thermocouples of different gauges and bead diameters upon the cooling rates recorded were also identified. This was important to reduce the likelihood of spurious temperature measurements arising from the influence of the thermocouple, allowing the response of axes to changes in the cooling conditions to be assessed reliably. It must be emphasised that the rationale behind measuring cooling rates was not to describe the thermal history at different locations of the axes, which is known to vary extensively during non-equilibrium cooling in large (>0.1 mm) specimens (Bald, 1984, 1987). Instead, measurements made within the core of axes during cooling were intended to record *average* values for whole axes, using thermocouples that provided a suitable compromise between sensitivity and robustness (Chapter 5). Such measurements helped to explore relationships among water content, cooling rate and survival of axes from different species, which are pivotal to the investigations reported in this thesis. Furthermore, these measurements highlighted the orders of magnitude that separate cooling rates achieved by this device relative to those attained by conventional methods. Although cryopreservation of fully hydrated axes may not be attainable under the conditions presently described, the cooling rates facilitated by this plunging device has never-the-less increased the window of permissible of axes from several species.

Overcoming the limitations to rapid cooling imposed by axis size

Cryofixation of specimens for electron microscopy require stringent conditions in order to avoid freezing artefacts. Water stores the largest reserve of heat within cells (Bachman and Mayer, 1987), and in order to attain the benchmark rate of $\geq 10^4$ °C s^{-1} (e.g. Moor, 1971) under favourable cooling conditions at atmospheric pressure, hydrated specimens should not exceed 0.1 mm linear dimensions (Bailey and Zasadzinsky, 1991). Therefore, it was not surprising that cooling rates within axes of *Aesculus hippocastanum* measuring *c.* 15 mm^3, and at water contents of 1.5 g g^{-1}, did not exceed 50-100°C s^{-1} or survive cryogenic exposure (Chapter 6). The difficulty of dissipating heat efficiently from hydrated specimens >0.1 mm, and the loss of viability that invariably follows, has led to the firmly-entrenched view (e.g. Farrant *et al.*, 1977; Franks, 1978, 1980; Bald and Robards, 1978; Skaer, 1982; Finkle *et al.*, 1985) that cooling rates required to preserve structure *vs.* function are mutually exclusive in specimens larger than single cells and 20-30 μm slices of tissue. In contrast to that view, the present study shows that, at least with embryonic axes, it is possible to lower the heat capacity to levels where the benefits of convective cooling (Bald, 1987) become apparent, and temperatures preventing crystallisation are reached without lethal injury. Admittedly, partial drying could be considered artefactual and inappropriate if the ultrastructure of the fully hydrated condition were sought after (see Gilkey and Staehelin, 1986). However, from a cryobiological perspective, combining rapid cooling and partial drying enabled the structure and function of organised tissues to cryogenic exposure to be investigated at a wider range of water contents (and in the absence of cryoprotectants) than would have been possible using slower conventional methods.

Heat transfer

Achieving sufficiently rapid cooling in hydrated biological specimens is hindered by the relatively inefficient conduction of heat through the tissues, and this process becomes increasingly difficult if specimens exceed 100 μm linear dimension (Bailey and Zasadzinsky, 1991). Furthermore, water shows an anomalous increase in specific heat with increasing supercooling, thus increasing the heat load to be dissipated during rapid cooling (Franks, 1980; Bachmann and Mayer, 1987; Bald, 1987). The rate of heat

transfer can be increased by conditions favouring convective cooling, such as cryogens of high heat transfer coefficient (e.g. propane, isopentane), increased travel velocity and greater depth of plunge (Elder *et al.,* 1982; Robards and Sleytr, 1985; Bald, 1987; Ryan, 1992; Chapter 5). In spite of attempts to increase the cooling rate by manipulating the plunging conditions, the heat capacity of axes remained the strongest determinant of cooling rate attained (see Fig. 5.6; [Bachmann and Mayer, 1987]). This is also illustrated by comparing the cooling profiles of fully hydrated axes of *Poncirus trifoliata* (Chapter 7) and *Aesculus hippocastanum* (Chapter 6). Axes of *P. trifoliata* cooled linearly from 0 to between -40 and -80°C during forced convection, whereas axes of *A. hippocastanum* seldom cooled below -15°C by the end of the plunge. In order to increase the convective cooling phase in fully hydrated axes, plunge distances of *c.* 1 m similar to that of the device of Bald and Robards (1978) would be required. However, this seemed unwarranted in the present study given that partial drying to water contents well above the limit of desiccation tolerance consistently increased cooling and facilitated survival of axes from all species tested. Likewise, while propane and isopentane displayed greater cooling efficiency (Bald, 1984), sub-cooled nitrogen was found more convenient to use in terms of safety and cost, and easier to regulate at its optimum cooling temperature (*c.* -210°C) especially in the deeper container tested (240 mm). Axes of all species presently reported could be successfully cryopreserved using sub-cooled nitrogen, albeit at somewhat lower water content than would have been required with isopentane or propane. Had this not been the case, recourse to more efficient cryogens or longer depth of plunge would have followed.

It is relevant to mention here that coating specimens with various substances has been reported to increase the cooling rate in cryogens prone to nucleation boiling (Cowley *et al.,* 1961; Luyet, 1961). Axes of *C. sinensis* were coated with a thin layer of glycerol seconds before injecting into sub-cooled nitrogen (Chapter 4). This method resulted in the highest permissible water content attained so far for axes cooled rapidly using the methods described in the present thesis. Unfortunately, no data are available to indicate whether or not this coating enhanced cooling rates, or whether those results reflected a presumably highly viscous cytoplasm of the mature seeds used in that study. The

potential benefits conferred by such coverings to the survival of axes during rapid cooling deserve further attention.

Testing the effect of increasing axis size upon the upper limits to rapid cooling

The study on *C. sinensis* indicated that higher cooling rates reduce freezing damage and raise the upper limit of water content permitting survival (Chapter 4), a premise that would subsequently become central to this thesis. It was important to determine whether this hypothesis would also apply to embryonic axes larger than the 1 - 2 mg dry mass typical of *C. sinensis*. Axes of desiccation sensitive *A. hippocastanum* (horse chestnut) seeds weigh approximately 6 mg (dry mass) and were thus suitable to test this hypothesis. The potential of isopentane and sub-cooled nitrogen as cryogens for cryopreservation was also tested in that study. While differences in cooling efficiency between these cryogens were observed, the cooling rates attained were not sufficiently different to be contrasted. The effect of cooling rate upon survival of axes could also not be assessed adequately, because cooling rates increased with decreasing water contents (see Chapter 5). Therefore, it was not possible to distinguish whether the increase in survival observed with increasing drying was due to the higher cooling rates attained, or resulted from the higher viscosity of axes at lower water contents. In spite of these difficulties, the study on axes of *A. hippocastanum* provided estimates of suitable water content/cooling rate combinations facilitating survival. Cooling rates of about 60°C s^{-1} led to complete mortality of axes above 1.0 g g^{-1}, but resulted in 100% survival (albeit abnormal) of axes between 1.0 and 0.75 g g^{-1} (Chapter 6). Evidently, partial drying increased the cytoplasmic concentration sufficiently to reduce lethal damage in these axes. Notwithstanding this, high electrolyte leakage and abnormal development suggested extensive cellular damage had occurred, and that cooling rates above 60°C s^{-1} were required to prevent damage at that water content range. Further drying to 0.75 - 0.5 g g^{-1} raised the proportion of axes developing normally, and also increased cooling rates to *c.* 200°C s^{-1}. At $\leq$ 0.5 g g^{-1}, axes cooled above 70°C s^{-1} showed completely normal development and electrolyte leakage similar to that of control axes. This suggested that in these axes partial drying had increased intracellular viscosity sufficiently to preclude damage even at such comparatively low cooling rates. However,

freezing transitions can occur at water contents above 0.1 – 0.3 g g^{-1} in *A. hippocastanum* axes (Farrant and Walters, 1998), and therefore survival of axes between 0.5 and 0.25 g g^{-1} was probably still dependent upon cooling rate. This is supported indirectly by the low survival and incomplete development of *A. hippocastanum* axes above 0.28 g g^{-1} following slow cooling at *c.* 3°C s^{-1} in an earlier study (Pence, 1992). In the present study, cooling between 70 and 800°C s^{-1} increased the upper limit of permissible water content to 0.5 g g^{-1} for completely normal development, and to 1.0 g g^{-1} for axes that survived fully, but showed abnormal germination (Wesley-Smith *et al.*, 2001b; Chapter 6).

Cooling rate, viscosity and survival

The trends observed in Chapter 6 agree closely with the findings of the X-ray diffraction study of Luyet *et al.* (1962). Those authors found that crystallisation in gelatine specimens of different concentrations was unhindered below 10% (w/v), and completely inhibited above 70% (w/v) at all cooling rates tested. Between concentrations of 50 and 70% (w/v), cooling rates ≥2 000°C s^{-1} inhibited crystallisation, and slower cooling resulted in varying degrees of hindrance. However, gelatine specimens and biological tissues are intrinsically different due to the presence of membrane-bound compartments of varying solute concentrations in the latter, which lead to striking differences in the complexity of the response to cooling (Meryman, 1966; Bank, 1974; Franks, 1980). In the present study, the ability to assess germination of embryonic axes exposed to cryogenic temperatures at various water contents provides indisputable evidence of the amount of damage induced by the different treatments, and of the extent to which cells recover from such insult. From the practical viewpoint, exploring the effects of cytoplasmic viscosity, cooling and warming rates upon survival contributes towards formulating recommendations of favourable conditions required for cryostorage of, at least, temperate recalcitrant embryonic axes.

Drying confers numerous advantages

Partial drying alone, without any additional protection, was sufficient to prepare embryonic axes adequately for cryogenic exposure, although the extent of drying

required varied among species according to their size. The advantages of partial drying are numerous. In addition to lowering the thermal load of embryonic axes, partial drying increases cytoplasmic viscosity (Buitink *et al.,* 1998b; Leprince and Hoekstra, 1998; Leprince *et al.,* 1999), thus influencing their ability to withstand cryogenic temperatures (Chapter 6). Increased viscosity reduces cytoplasmic mobility, hindering ice crystal growth by slowing the diffusion of water molecules to the growing ice crystal (Luyet *et al.,* 1962; Franks, 1980). Secondly, increased cytoplasmic solute concentration lowers the freezing temperature T_m (Meryman and Williams, 1980; Becwar *et al.,* 1983; Vertucci, 1990; Wesley-Smith *et al.,* 1992; Pritchard *et al.,* 1995; Farrant and Walters, 1998; Chapter 4) and consequently the temperature of homogeneous nucleation T_h (Rasmussen and MacKenzie, 1972; Rasmussen *et al.,* 1975). Lowering T_h leads to greater supercooling, favouring high densities of nuclei of necessarily small size, and also reducing the amount of latent heat of fusion released during freezing (MacKenzie, 1977; Franks, 1980). Thirdly, increased viscosity raises the glass transition temperature (Meryman and Williams, 1980; Williams and Leopold, 1989; Williams *et al.,* 1993; Leopold *et al.,* 1994; Leprince and Walters-Vertucci, 1995; Buitink *et al.,* 1996) that, combined with the lowering of T_m, results in reduced ranges of temperatures supporting crystallisation during cooling and warming. The latter is highly significant to the cryopreservation of large axes using this approach, as the cooling rate required to traverse this region without injury is correspondingly reduced (Robards and Sleytr, 1985). Evidence thus suggests that the benefits conferred by increased cytoplasmic viscosity can be exploited to offset the size disadvantage of recalcitrant axes during rapid non-equilibrium cooling.

Separating the effects of water content and cooling rate upon survival

The study on *A. hippocastanum* showed that the rapid cooling device facilitated survival of relatively large axes, although the cooling rate attainable within fully hydrated axes was limited to *c.* 60°C s^{-1} even under the most favourable conditions (Chapter 6). The relatively smaller size of axes of *Poncirus trifoliata* (0.4 mg dry mass) allowed cooling rates between 0.17 *c.* 1 300°C s^{-1} to be attained using various methods (Chapter 7), thus making it possible to investigate separately the effects of cooling and water content

upon survival. This study furthered the findings from the study on tea axes (Chapter 4) because, in addition to investigating a larger number of cooling rates, it also contrasted the effects of two very different warming rates. The experiments using *P. trifoliata* essentially explored the extent to which viscosity inhibited or promoted ice crystal growth to damaging sizes.

Between 0.26 and 0.8 g g^{-1}, normal development of axes of *P. trifoliata* increased with increasing viscosity, at almost all cooling rates and at both warming velocities. Most significantly, that study revealed viscosity-dependent ranges of cooling rates that facilitated normal development. On rapid warming, more than 80% of axes at 0.26 g g^{-1} showed normal development after cooling between 0.1 and 1000°C s^{-1}, while at 0.55 g g^{-1} this range narrowed to 3.3 - 863°C s^{-1} and at 0.8 g g^{-1} equivalent survival was attainable only at 686°C s^{-1}. This indicated that axes at low water contents survived relatively independently of cooling rate, but nevertheless benefited from rapid warming. Conversely, axes at higher water contents required correspondingly higher cooling to compensate for the greater mobility of water (Buitink *et al.,* 1998b; Leprince and Hoekstra, 1998; Leprince *et al.*, 1999) and inhibit lethal crystallisation. This finding is highly relevant to recalcitrant axes requiring storage at water contents above those that lead to desiccation damage, but which can sustain injury during slow cooling (e.g. Vertucci *et al.,* 1994). Normal development among axes warmed slowly was almost invariably lower than that after rapid warming, but increased markedly at lower water contents and especially at slower cooling rates (≤ 3.3°C s^{-1}). In fact, axes at 0.2 g g^{-1} cooled at 3.3°C s^{-1} and warmed slowly showed the highest survival at this water content. Radhamani and Chandel (1992) and Normah and Sitti Dewi Serimala (1997) recorded *c.* 70 - 100% survival of axes of citrus species at 0.19 - 0.12 g g^{-1} cryopreserved within cryovials (at *c.* 3.3°C s^{-1}) and warmed at rates intermediate between those used here. Although remaining to be confirmed, results from the present investigation suggest that the higher survival of axes of *P. trifoliata* at 0.2 g g^{-1} warmed slowly may arise from the requirement for either slow or delayed rehydration in the water-stressed tissues, and are presumably damaged by direct immersion in water during rapid warming (Chapter 7). The reasons why slow warming is damaging to axes cooled at higher velocities are

speculative from these data, and require further investigation. The high survival attained in the studies of Radhamani and Chandel (1992) and Normah and Sitti Dewi Serimala (1997) suggests that applying the rapid cooling approach to cryopreserve axes of citrus species may not be warranted, given the high tolerance to drying, and slow cooling and warming that these axes exhibit. However, only an assessment of the long-term stability of axes in storage can test the merits of each approach, and such studies remain to be done.

Is there a maximum cooling rate tolerated?

The terms 'rapid' or 'slow' cooling can have very different meanings among cryobiologists. A conventional approach defines 'rapid' cooling as that rate associated with the transition from extra-cellular to intracellular freezing which is usually considered lethal (e.g. Mazur, 1966, 1977; Fujikawa, 1988). Intracellular freezing almost certainly occurred at the non-equilibrium cooling rates used in the present thesis (e.g. Sakai and Otsuka, 1967; Sakai and Yoshida, 1967; Mohr and Stein, 1969; Bank and Mazur, 1973; Morris, 1976; Steponkus, 1984). Accordingly, 'rapid cooling' has been used in the present context to describe rates aimed at restricting the growth of ice crystals to within harmless dimensions. It became imperative to quantify the cooling rates that led to survival or death of axes in order to allow meaningful comparisons among axes from different species. In spite of the difficulties of accurately describing the cooling rates within large biological tissues (Bald, 1975; Bald and Crowley, 1979), the cooling rates recorded provide close approximations that separate the rapid non-equilibrium approach presently used from slower cooling approaches, such as within cryovials or at controlled rates.

The trends observed in chapters 4, 6 and 8 showed that faster cooling facilitated survival of axes at higher water contents, presumably because it limited the growth of intracellular ice. Therefore, it was unexpected to find that the fastest cooling rates were not necessarily the most favourable. For example, survival of axes of *P. trifoliata* between 0.8 and 0.26 g g^{-1} decreased if cooled faster than 500°C s^{-1} (Chapter 8). The reason(s) underlying the decline in survival are not clear. Growth of ice crystals to lethal

sizes can safely be ruled out, since slower cooling rates yielded higher survival. The possibility of devitrification and crystallisation of glasses formed in partially dehydrated axes during rapid cooling cannot be discounted. If glasses did form in axes of *P. trifoliata* it is possible that axes could have been damaged if warming was insufficiently fast. The phase separation that inevitably accompanies freezing (irrespective whether this occurs during cooling or after devitrification) is known to interfere with biochemical and biophysical equilibria within cells (Franks *et al.,* 1990). Since glasses become increasingly brittle at temperatures below T_g (Williams *et al.,* 1993), it is also possible that vibration induced by the mechanical devices used to achieve rapid cooling may be responsible for the damage observed. Even vitrification could not prevent potentially harmful physical or biochemical changes associated with low temperatures, such as lipid phase transitions (Franks, 1977) or the differential expansion of lipid and protein components in the plasmalemma (thermal shock; Lovelock, 1955; Meryman, 1956, 1966; Morris *et al.,* 1983). However, these suggestions are speculative, and further work is required to identify whether similar supra-optimal rates occur during non-equilibrium cooling in axes from other species.

Survival in the presence of intracellular ice crystals

Earlier it was concluded that failure to dissipate the relatively large thermal mass of fully hydrated axes could lead to extensive freezing damage. Fully hydrated axes of *P. trifoliata* sustained severe freezing damage in spite of cooling linearly to ≤ -40°C at rates of *c.* 500°C s^{-1}, and even after rapid warming. In contrast, an unexpected 90% survival and 35% normal development was observed in axes cooled slowly at 0.17°C s^{-1} (10°C min^{-1}). The possibility of extracellular freezing accounting for the survival observed is ruled out by the 60% mortality and abnormal development of those axes that survived slow warming. This paradox could not be explained in the absence of ultrastructural evidence. At the time, seeds of the temperate recalcitrant *Acer saccharinum* had become available, and the cryopreservation study using axes from those seeds was further prompted by the fact that previous attempts (Becwar *et al.*, 1983) had failed.

Survival of *A. saccharinum* axes after rapid cooling was compared with that resulting from two commonly used procedures, *viz.* cooling at 3.3°C s^{-1} and within Al foil envelopes (Chapter 8). As for the *P. trifoliata* study, this work investigated the effectiveness of cytoplasmic viscosity in inhibiting damage by varying the time of exposure to potentially deleterious cryogenic temperatures. In particular, this study assessed ultrastructurally the apparent contradiction that intracellular freezing could play a stabilising role in cryopreserved fully hydrated axes. Freeze-fracture and freeze-substitution enabled the freezing patterns within cells of roots and shoots from axes cooled by the various methods to be observed and quantified. These results were then related to the appearance of corresponding tissues at various intervals during recovery, and to the overall survival after four weeks *in vitro*.

Fully hydrated axes cooled by plunging, or within Al foil envelopes cooled at similar rates (77 - 97°C s^{-1}) and appeared to form equivalent amounts of ice (Chapter 8). Ice crystals of a wide range of sizes were prominent in the nucleus, vacuoles and cytoplasm of cells from root and shoot tissues from both treatments. The most salient difference between these treatments was the occurrence of freezing within all cellular compartments in 60 - 80% of cells from plunge-cooled axes, in contrast with the situation for the axes cooled within Al foil envelopes or at 3.3°C s^{-1} where mitochondria, plastids and endomembranes showed no evidence of ice. Normal development was higher in axes cooled by either of the latter methods than in those cooled by plunging, suggesting that the presence of ice within organellar compartments of rapidly cooled cells was damaging. Since damage was greater in plunge-cooled axes than after cooling within Al foil in spite cooling at a similar rate, it is possible that mechanical vibration could be detrimental to axes during rapid cooling, and result in the relative distributions of ice observed. Furthermore, this observation supports the earlier proposal that increased injury during plunge cooling was due to the method of cooling and not the rate *per se* (Chapter 7). The growth of ice nuclei formed within confined, membranous compartments is likely to cause mechanical damage more readily than equivalent crystals formed in relatively open locations if crystal growth occurs at equivalent rates. Therefore, it is contended that the all-pervasive presence of ice within cells of axes

cooled rapidly underlies their greater sensitivity to slow warming. Axes cooled at slower rates appeared to be more tolerant of slower warming, which is probably due to the greater margin for ice crystal growth afforded by the absence of immediate membranous boundaries when these are formed within the cytoplasm or nucleus. However, in axes cooled rapidly slow warming allows the additional growth of ice within compact, membrane-bound organelles, and it is contended that these may be responsible for the damage observed. It seems inevitable that ice crystal growth that is extended in space and time eventually leads to severe damage, but it is uncertain whether this arises from mechanical deformation, extreme freeze-induced drying, or from the deleterious effects of drying and low temperature combined (Vertucci and Roos, 1993; Vertucci *et al.,* 1994, 1995).

Lethal ice crystal damage: size or location?

Evidence suggests intracellular ice is compatible with survival provided a 'critical size', which varies among cell types, is not exceeded (Moor, 1964; Sakai and Otsuka, 1967; Sherman and Kim, 1967; Mazur and Schmidt, 1968; Sakai *et al.*, 1968, 1970; Mazur *et al.,* 1969; Asahina *et al.,* 1970; Shimada and Asahina, 1972; Bank and Mazur, 1973; Nei, 1973; Bank, 1974; Fujikawa, 1988; Vertucci, 1989a; Wesley-Smith *et al.,* 1992; Vertucci *et al.,* 1995). Attempts to identify the size of "critical" ice crystals within histologically complex structures such as embryonic axes cooled at non-equilibrium velocities seem to be a futile exercise. Accurate measurements are not possible because of the extensive variability in cooling rates between cells at different positions of the sample (Bald, 1975; Van Venrooij *et al.*, 1975; Bald and Crowley, 1979), differences in water content, degree of vacuolation, varying sensitivity to drying and/or freezing of different tissues, etc. In agreement with the findings of Nei (1976a, 1977), the present study could not determine accurately the size of ice crystals critical for survival: cooling at rates as dissimilar as 3.3 or 76°C s^{-1} yielded similar survival in spite of large differences in the sizes of crystals formed (Chapter 8). Evidence supports the proposal that survival of axes may have been influenced more by the intracellular *location* of ice than by the *size* of the crystals formed. It should be emphasised that presumably all

cellular compartments are equally important to survival, but that some of these may tolerate freezing to a greater extent than others (Sherman and Kim, 1967).

The elusive basis of freezing damage

Physical damage to cellular membranes can destroy the ordered partitioning of ions, macromolecules and enzymes. Damage to the plasmalemma is regarded as the prime site of freezing injury (e.g. Steponkus, 1984), and the ability to exclude vital stains or to respond to an externally applied osmotic stress (e.g. Sakai, 1971; Sakai and Yoshida, 1967; Steponkus, 1984; Acker and McGann, 2001) are tests commonly used to assess survival. In Chapter 8, ultrastructural damage to the plasmalemma is described, which became apparent within minutes after warming (Chapter 8). However, cells must sustain injuries of a more subtle (e.g. biochemical) nature during drying (Chapter 3) or cryogenic exposure (Chapters 4 and 8) that do not become immediately apparent in specimens until some time has lapsed after the stress is removed. Consequently, assays of survival or ultrastructural integrity applied immediately after a trial may not necessarily reflect survival in the longer-term. Conducting ultrastructural and survival studies in parallel gave greater confidence when relating structure to function in the *Camellia sinensis* study (Chapter 4). Similarly, it was remarkable that survival of *Acer saccharinum* axes occurred at all, given the extensive deformation observed in freeze-fracture and freeze-substitution images (Chapter 8). It is highly likely that the absence of *in vitro* germination data and ultrastructural assessment at regular intervals during recovery, would have led to conclusions different to those presently reached.

The role of microscopy in relating structure and function

In the same manner as reliable survival data are required to support ultrastructural observations, so are sound methodological procedures required for microscopical investigations relating to function. Examples are presented where the methods used may have led to equivocal conclusions in areas of study closely related to the theme of this thesis.

Many studies of desiccation tolerance in plants have relied upon findings from dehydrated tissues prepared for electron microscopy using aqueous processing protocols (see Chapter 2). Phenomena commonly reported as "plasmolysis" or "plasmalemma pulling away from the cell wall" in air-dried material have been shown to be artefacts of aqueous fixatives (Wesley-Smith, 2001; Chapter 2). Aqueous fixatives allow walls of dry cells to expand unhindered, while restricting the expansion of the plasmalemma and cell contents to greater extent, presumably by crosslinking. The unavoidable tearing of plasmalemma and plasmodesmatal connections that usually results have often been mistaken for evidence of desiccation damage (e.g. Webster and Leopold 1977; Fincher Chabot and Leopold 1982; Sargent *et al.,* 1981; Sack *et al.,* 1988; Berjak *et al.,* 1989; Schneider *et al.,* 1993; Quartacci *et al.,* 1997). Evidence suggests that damage to membranes probably had occurred during drying, but becomes apparent only on rehydration and not necessarily as observed in aqueously fixed specimens (Chapter 2, 3).

Another view commonly held (and largely unchallenged) arises primarily from the study of Farrant *et al. (*1977), and has led to the firmly entrenched dogma among cryobiologists and microscopists alike that the cooling rates required to preserve structure or function are opposed (see also Franks, 1977, 1980; Bald and Robards, 1978; Skaer, 1982; Finkle *et al.*, 1985). Farrant and co-workers compared the appearance of Chinese hamster fibroblasts freeze-substituted after "rapid" cooling at 8°C s^{-1} (473°C min^{-1}) with the appearance of cells after conventional fixation. Based on the finding that the volume and appearance such "rapidly" cooled cells (in spite of "numerous intracellular ice cavities") resembled unfrozen controls, but were dead after warming (at an unspecified rate), those authors concluded that achieving structural preservation by rapid cooling does not imply function is retained as well. Clearly, that and other similar studies (e.g. Bank and Mazur, 1972) failed to achieve the necessary cooling rates used in microscopical investigations of hydrated cells, which is probably why their results contrast sharply with those from studies that did (Moor and Mühlethaler, 1963; Moor, 1964; Anderson *et al.,* 1966; Sakai, 1967; Mazur and Schmidt, 1968; Bachmann and Schmitt, 1971; Plattner *et al.,* 1972). Unfortunately, many other

studies where rapid cooling was attained parallel survival studies were either not undertaken (e.g. Bank and Mazur, 1973; Steere, 1969) or not reported (e.g. Shimada and Asahina, 1975).

Results presented in this thesis attest to the fact that cooling rates that preserve structure can also maintain structural integrity (Chapter 4). Although dissipating heat efficiently is challenging (Chapter 5), results presented in this thesis show that manipulating the water content can overcome this obstacle and facilitate survival of axes from several temperate recalcitrant species successfully. While it would be naïve to advocate rapid cooling as the universal solution to the challenges of cryobiology, present results underline its potential, particularly where conventional approaches have failed. In contrast, the conventional perception of rapid cooling as detrimental for survival is supported by aspects of some of the studies presently undertaken (Chapters 7 and 8). However, these cooling rates are several orders of magnitude higher than those reported to be lethal by Farrant *et al.* (1977b), and it is probable that the underlying cause of damage is different in each case. Further studies are required to establish whether non-equilibrium cooling is deleterious when it fails to hinder the conversion of a critical proportion of water into ice, a process which has both mechanical and biochemical consequences (Meryman, 1956, 1966; Franks, 1977, 1980). Evidence presented also suggests that the distribution of intracellular ice could be decisive as to whether damage is lethal or repairable. It is not unreasonable to assume that innocuous intracellular freezing occurs in many successful cryopreservation procedures, and that it is far more commonplace than expected. Lastly, cellular membranes of many organisms are likely to be sensitive to low temperatures, as previously suggested by proponents of the 'cold shock' phenomenon (Lovelock, 1955; Luyet and Keane, 1955; Morris *et al.*, 1983). In this regard, microscopy has played an important role in increasing present understanding in cryobiology, and is likely to continue doing so as the level of refinement of instruments and techniques open new avenues for research.

Freeze-fracture and freeze-substitution have provided valuable insights into the effects of drying and/or cooling rate upon cells and tissues. Critics of the freeze-substitution

technique (e.g. Bank, 1973; Franks, 1980) maintain that warming tissues to -80°C allows some re-crystallisation to occur. This implies that the size of the cavities observed in freeze-substituted preparations do not necessarily reflect the freezing patterns within axes used in survival studies. That view is not endorsed by present (Chapters 3 and 8) or earlier studies (e.g. Gilkey and Staehelin, 1986; Steinbrecht, 1985; Kiss *et al.,* 1990), which emphasise the reliability of FS as an important tool in studies of desiccation tolerance as well as in low temperature biology. It could be argued that had re-crystallisation occurred during substitution, axes of *Acer saccharinum* from all three cooling treatments would have had a similar appearance, which was clearly not the case (Chapter 8). While FS revealed damage that would have been difficult to reconcile with survival in the absence of corresponding *in vitro* studies, future similar studies may confirm that certain cell types can withstand intracellular freezing to a greater extent than previously thought possible.

REFERENCES

Abdelnour-Esquivel A, Villalobos V, Engelmann F (1992) Cryopreservation of zygotic embryos of *Coffea* spp. *Cryo-Lett.* **13**: 297-302

Acker JP, McGann LE (2001) Membrane damage occurs during the formation of intracellular ice. *Cryo-Lett.* **22**: 241-254

Albrecht RM, Orndorf GR, MacKenzie AP (1973) Survival of certain microorganisms subjected to rapid freezing on membrane filters. *Cryobiology* **10**: 233-239

Altus DP, Hallam ND (1980) Fine structure of hydrated and air-dry leaves of *Sporobulus stapfianus* Gandoger, a drought tolerant grass. *Micron* **11**: 515-516

Anderson NG, Green JG, Mazur P (1966) Centrifugal freezing. I. A system for rapid freezing of aqueous cell suspensions. *Natn. Cancer Inst. Monogr.* **21**: 415-430

Asahina E, Hisada Y, Emura M (1967) Microscopic observations of innocuous intracellular freezing in very rapidly cooled tumor cells. *Contrib. Inst. Low Temp. Sci. Series* B **15**: 36-59

- , Shimada K, Hisada Y (1970) A stable state of frozen protoplasm with invisible intracellular ice crystals obtained by rapid cooling. *Exp. Cell Res.* **59**: 349-358

Assy-Bah B, Engelmann F (1992) Cryopreservation of mature embryos of coconut (*Cocos nucifera* L.) and subsequent regeneration of plantlets. *Cryo-Lett.* **13**: 117-126

Aubert S, Gout E, Bligny R, Marty-Mazars D, Barrieu F, Alabouvette J, Marty F, Douce R (1996) Ultrastructural and biochemical characterization of autophagy in higher plants subject to carbon deprivation: control by the supply of mitochondria with respiratory substrates. *J. Cell Biol.* **133**: 1251-1263

Bachmann L, Schmitt WW (1971) Improved cryofixation applicable to freeze-etching. *Proc. Nat. Acad. Sci. U.S.A.* **68**: 2149-2152

- , Mayer E (1987) Physics of water and ice: implications for cryofixation. *In:* RA Steinbrecht, K Zierold (eds) *Cryotechniques In Biological Electron Microscopy*. Springer-Verlag, Heidelberg, Berlin, pp. 3-34

Bailey SM, Zasadzinsky AN (1991) Validation of convection-limited cooling of samples for freeze-fracture electron microscopy. *J. Microsc.* **163**: 307-320

Bald WB (1975) A proposed method for specifying the temperature history of cells during the rapid cool-down of plant specimens. *J. Exp. Bot.* **26**: 103-119

- (1984) The relative efficiency of cryogenic fluids used in the rapid quench cooling of biological samples. *J. Microsc.* **134**: 261-270

- (1985) The relative merits of various cooling methods. *J. Microsc.* **140**: 17-40

- (1987) *Quantitative Cryofixation* Adam Hilger, Bristol, Philadelphia,

- (1993) Real cooling and warming rates during cryopreservation. *Cryo-Lett.* **14**: 207-216

- , Robards AW (1978) A device for the rapid freezing of biological specimens under precisely controlled and reproducible conditions. *J. Microsc.* **112**: 3-15

- , Crowley AB (1979) On defining the thermal history of cells during the freezing of biological materials. *J. Microsc.* **117**: 395-409

Bank H (1973) Visualization of freezing damage. II. Structural alterations during warming. *Cryobiology* **10**: 157-170

- (1974) Freezing injury in tissue cultured cells as visualized by freeze-etching. *Exp. Cell Res.* **85**: 367-376
- , Mazur P (1972) Relation between ultrastructure and viability of frozen-thawed Chinese hamster tissue-culture cells. *Exp. Cell Res.* **71**: 441-454
- , Mazur P (1973) Visualization of freezing damage. *J. Cell Biol.* **57**: 729-742
Bartolo ME, Carter JV (1991) Microtubules in mesophyll cells of nonaclimated and cold-acclimated spinach. *Plant Physiol.* **97**: 175-181
Becwar MR, Stanwood PC, Leonhardt KW (1983). Dehydration effects on freezing characteristics and survival in liquid nitrogen of desiccation-tolerant and desiccation-sensitive seeds. *J. Am. Soc. Hort. Sci.* **108**: 613-618
Bergfeld R, Schopfer P (1984) Transitory development of rough endoplasmic reticulum aggregates during embryo maturation in seeds of mustard (*Sinapsis alba* L.). *Eur. J. Cell Biol.* **34**: 27-33
Berjak P, Pammenter NW (1994) Recalcitrance is not an all-or-nothing situation. *Seed Sci. Res.* **4**: 263-264
- , Dumet D (1996) Cryopreservation of seeds and isolated axes of neem (*Azadirachta indica*). *Cryo-Lett.* **17**: 99-104
- , Pammenter NW (1997) Progress in the understanding and manipulation of desiccation-sensitive (recalcitrant) seeds. In: RH Ellis, M Black, AJ Murdoch, TD Hong (eds) *Basic And Applied Aspects Of Seed Biology.* Academic Publishers, Dordrecht, Kluwer, pp. 689-703
- , Dini M, Pammenter NW (1984) Possible mechanisms underlying the differing dehydration responses in recalcitrant and orthodox seeds: desiccation associated subcellular changes in propagules of *Avicennia marina*. *Seed Sci. Technol.* **12**: 365-384
- , Farrant JM, Pammenter NW (1989) The basis of recalcitrant seed behaviour. In: RB Taylorson (ed.) *Recent Advances In The Development And Germination Of Seeds.* Plenum Press, New York, pp. 89-108
- , Pammenter NW, Vertucci CW (1992) Homoiohydrous (recalcitrant) seeds: developmental status, desiccation sensitivity and the state of water in axes of *Landolphia kirkii* Dyer. *Planta* **186**: 249-261
- , Vertucci CW, Pammenter NW (1993) Effects of developmental status and dehydration rate on characteristics of water and desiccation-sensitivity in recalcitrant seeds of *Camellia sinensis*. *Seed Sci. Res.* **3**: 155-166
- , Farrant JM, Mycock DJ, Pammenter NW (1990) Recalcitrant (homoiohydrous) seeds: the enigma of their desiccation sensitivity. *Seed Sci. Technol.* **18**: 297-310
- , Walker M, Watt MP, Mycock DJ (1999) Experimental parameters underlying failure or success in plant germplasm cryopreservation: a case study on zygotic axes of *Quercus robur* L. *Cryo-Lett.* **20**: 251-262
- , Mycock DJ, Watt P, Wesley-Smith J, Hope B (1995) Cryostorage of pea (*Pisum sativum*) and implications for the successful cryopreservation of plants with recalcitrant seeds. In: YPS Bajaj (ed.) *Biotechnology in Agriculture and Forestry.* Springer-Verlag, Berlin, pp. 292-307
- , Mycock DJ, Wesley-Smith J, Dumet D, Watt MP (1996) Strategies for the *in vitro* conservation of hydrated germplasm. In: MN Normah, MK Narimah, MM

Clyde (eds) *In Vitro Conservation Of Plant Genetic Resources*. Percetakan Watan Sdn. Bhd., Kuala Lumpur, Malaysia, pp. 19-52

- , Kioko JI, Walker M, Mycock DJ, Wesley-Smith J, Watt MP, Pammenter NW (1998) Cryopreservation – An elusive goal. In: M Marzalina, KC Khoo, N Jayanthi, FY Tsan, B Krishnapillay (eds) *Recalcitrant Seeds*, FRIM, Kuala Lumpur, Malaysia, pp. 96-109

Bewley JD (1979) Physiological aspects of desiccation tolerance. *Annu Rev. Plant Physiol.* **30**: 195-238

Browning AJ, Gunning BES (1977) An ultrastructural and cytochemical study of the wall-membrane apparatus of transfer cells using freeze-substitution. *Protoplasma* **93**: 7-26

Bruni F, Leopold AC (1992) Cytoplasmic glass formation in maize embryos. *Seed Sci. Res.* **2**: 251-253

Bryant G, Koster KL, Wolfe J (2001) Membrane behaviour in seeds and other systems at low water content: the various effects of solutes. *Seed Sci. Res.***11**: 17-25

Buitink J, Walters-Vertucci C, Hoekstra FA, Leprince O (1996) Calorimetric properties of dehydrating pollen: analysis of a desiccation-tolerant and an – intolerant species. *Plant Physiol.* **111**: 235-242

- , Walters C, Hoekstra FA, Crane J (1998a) Storage behaviour of *Typha latifolia* pollen at low water contents: Interpretation on the basis of water activity and glass concepts. *Physiologia Plantarum* **103**: 145-153

- , Claessens MMAE, Hemminga MA, Hoekstra FA (1998b) Influence of water content and temperature on molecular mobility and intracellular glasses in seed and pollen. *Plant Physiol.* **118**: 531-541

- , Leprince O, Hemminga MA, Hoekstra FA (2000) The effects of moisture and temperature on the ageing kinetics of pollen: interpretation in terms of molecular mobility. *Plant Cell Environ* **23:** 967-974

Bullock GR (1984) The current status of fixation for electron microscopy: a review. *J Microsc.* **133**: 1-15

Burke MJ (1986) The glassy state and survival of anhydrous biological systems. In: AC Leopold (ed.) *Membranes, Metabolism And Dry Organisms.* Cornell University Press, Ithaca, pp. 358-363

Buttrose MS (1973) Rapid water uptake and structural changes in imbibing seed tissues. *Protoplasma* **77**: 111-122

Calistru C, McLean M, Pammenter NW, Berjak P (2000) The effects of mycofloral infection on the viability and ultrastructure of wet-stored recalcitrant seeds of *Avicennia marina* (Forsk.) Vierh. (2000) *Seed Sci. Res.* **10**: 341-353

Chandel KPS, Chaudhury R, Radhamani J, Malik SK (1995) Desiccation and freezing sensitivity in recalcitrant seeds of tea, cocoa and jackfruit. *Ann. Bot.* **76**: 443-50

- , Chaudhury, R, Radhamani, J (1996) Cryopreservation of embryos / embryonic axes – a novel method for the long-term conservation of recalcitrant seed species. In: MN Normah, MK Narimah, MM Clyde (eds) *In Vitro Conservation Of Plant Genetic Resources*. Percetakan Watan Sdn. Bhd., Kuala Lumpur, Malaysia, pp. 53-71

Chaudhury R, Chandel KPS (1994) Germination studies and cryopreservation of seeds of black pepper (*Piper nigrum* L.) – a recalcitrant species. *Cryo-Lett.* **15**: 145-150

- , Radhamani J, Chandel KPS (1991) Preliminary observations on the cryopreservation of desiccated embryonic axes of tea (*Camellia sinensis* [L.] O. Kuntze) seeds for genetic conservation. *Cryo-Lett.* **12**: 31-36

Chin HF (1992) Seed banks – conserving the past for the future. Keynote address *23rd ISTA Congress,* Buenos Aires, Argentina

- , Roberts EH (1980) *Recalcitrant Crop Seeds.* Tropical Press Sdn. Bhd., Kuala Lumpur, Malaysia

- , Krishnapillay B, Alang ZC (1988) Media for embryo culture of some tropical recalcitrant species. *Pertanika* **11**: 357-363

- , Krishnapillay B, Stanwood PC (1989) Seed moisture: recalcitrant vs. orthodox seeds. In: *Seed Moisture*, Crop Science of America Special Publication no. 14.

Chmielarz P (1997) Preservation of *Quercus robur* L. embryonic axes in liquid nitrogen. In: RH Ellis, M Black, AJ Murdoch, TD Hong (eds) *Basic And Applied Aspects Of Seed Biology.* Academic Publishers, Dordrecht, Kluwer, pp. 765-769

Costello MJ, Corless JM (1978) The direct measurement of temperature changes within freeze-fracture specimens during rapid quenching in liquid coolants. *J. Microsc.* **112**: 17-37

Cowley CW, Timson WJ, Sawdye JA (1961) Ultra rapid cooling techniques in the freezing of biological materials. *Biodynamica* **170**: 317-329

Craig S, Staehelin LA (1988) High pressure freezing of intact plant tissues. Evaluation and characterisation of novel features of the endoplasmic reticulum and associated membrane systems. *Eur. J. Cell Biol.* **46**: 80-93

Crévecoeur M, Deltour R, Bronchart R (1976) Cytological study on water stress during germination of *Zea mays. Planta* **132**: 31-41

Davidson AL, Newcomb W (2000) Novel ultrastructural observations of pea (*Pisum sativum*) root nodules cells by high pressure freezing and propane-jet freezing techniques. *Protoplasma* **213**: 55-66

de Boucaud M-T, Brison M, Ledoux C, Germain E, Lutz A (1991) Cryopreservation of embryonic axes of recalcitrant seed *Juglans regia* L. *cv* Franquette. *Cryo-Lett.* **12**: 163-166

Diaper MP (1986) Practical techniques for cooling biological samples at 0.3 – 100°C min^{-1}. *Cryo-Lett.* **7**: 279-290

Ding B, Turgeon R, Parthasarathy MV (1991) Routine cryofixation of plant tissues by propane jet freezing for freeze-substitution. *J. Electron Microsc. Techn.* **19**: 107-117

Dong Z, McCully ME, Canny MJ (1994) Retention of vacuole contents of plant cells during fixation. *J. Microsc.* **175**: 222-228

Drennan PM, Berjak P (1982) Degeneration of the salt glands accompanying foliar maturation in *Avicennia marina* (Forsskål) Vierh. *New Phytol.* **90**: 165-176

Dumet D, Engelmann F, Chabrillange N, Dussert S, Duval Y (1994) Effect of various sugars and polyols on the tolerance to desiccation and freezing of oil palm polyembryonic cultures. *Seed Sci. Res.* **4**: 307-313

- , Engelmann F, Chabrillange N, Duval Y, Dereuddre J (1993) Importance of sucrose for the acquisition of tolerance to desiccation and cryopreservation of oil palm somatic embryos. *Cryo-Lett.* **14**: 243-250
Dyke G (1997) How to avoid bad statistics. *Field Crop Res.* **51**: 165-187
Echlin P (1992) *Low-Temperature Microscopy and Analysis*. Plenum Press, New York
Echlin P, Moreton R (1976) Low temperature techniques for scanning electron microscopy. *Scanning Electron Microsc.* **1**: 753-761
Elder HY, Gray CC, Jardine, JN, Chapman JN, Biddlecombe WH (1982) Optimum conditions for cryoquenching of small tissue blocks in liquid coolants. *J. Microsc.* **126**: 45-61
Engelmann F (1997) Importance of desiccation for the cryopreservation of recalcitrant seed and vegetatively propagated species. *Plant Genetic Resources Newsletter*, No. **112**: 9-18
Fahy GM, MacFarlane DR, Angell CA, Meryman HT (1984) Vitrification as an approach to cryopreservation. *Cryobiology* **21**: 407-426
Farrant J, Walter CA, Lee H, McGann LE (1977a) Use of two-step cooling procedures to examine factors influencing cell survival following freezing and thawing. *Cryobiology* **14**: 273-286
- , Walter CA, Lee H, Morris GJ , Clarke KJ (1977b) Structural and functional aspects of biological freezing techniques. *J. Microsc.* **111**: 17-34
Farrant JM, Walters C (1998) Ultrastructural and biophysical changes in developing embryos of *Aesculus hippocastanum* in relation to the acquisition of desiccation tolerance to drying. *Physiologia Plantarum* **104**: 513-524
- , Berjak P, Pammenter NW (1985) The effect of drying rate on viability retention of recalcitrant propagules of *Avicennia marina*. *South Afr. J. Bot.* **51**: 432-438
- , Berjak P, Pammenter NW (1986) The increasing desiccation sensitivity of recalcitrant *Avicennia marina* seeds with storage time. *Physiologia Plantarum* **67**: 291-298
- , Pammenter NW, Berjak P (1988) Recalcitrance: a current assessment. *Seed Sci. Technol.* **16**: 155-166
- , Pammenter NW, Berjak P (1989) Germination-associated events and the desiccation sensitivity of recalcitrant seeds - a study on three unrelated species. *Planta* **178**: 189-198
- , Pammenter NW, Berjak, P (1992) Development of the recalcitrant (homoiohydrous) seeds of *Avicennia marina*: anatomical, ultrastructural and biochemical events associated with the development from histodifferentiation to maturation. *Ann. Bot.* **70**: 75-86
- , Pammenter NW, Berjak P (1993) Seed development in relation to desiccation-tolerance: a comparison between desiccation-sensitive (recalcitrant) seeds of *Avicennia marina* and desiccation-tolerant types. *Seed Sci. Res.* **3**: 1-13
- , Pammenter NW, Berjak P, Walters C (1997) Subcellular organization and metabolic activity during the development of seeds that attain different levels of desiccation tolerance. *Seed Sci. Res.***7**:135-144
Fincher Chabot J, Leopold AC (1982) Ultrastructural changes of membranes with hydration in soybean seeds. *Am. J. Bot.* **69**: 623-633

Finch-Savage WE (1992a) Embryo water status and survival in the recalcitrant species *Quercus robur* L.: evidence for a critical moisture content. *J. Exp. Bot.* **43**: 663-669
- (1992b) Seed development in the recalcitrant species *Quercus robur* L.: germinability and desiccation-tolerance. *Seed Sci. Res.* **2**:17-22
- , Grange RI, Hendry GAF, Atherton NM (1993) Embryo water status and loss of viability during desiccation in the recalcitrant species *Quercus robur* L. In: D Côme, F Corbineau (eds) *Fourth International Workshop On Seeds. Basic And Applied Aspects Of Seed Biology. Vol. 3*, ASFIS, Paris, pp. 723-730
Finkle BJ, Zavala ME, Ulrich JM (1985) Cryoprotective compounds in the viable freezing of plant tissues. In: KK Kartha (ed.) *Cryopreservation Of Plant Cells And Organs.* CRC Press, Boca Raton, Florida, pp. 75-113
Franks F (1977) Biological freezing and cryofixation. *J. Microsc.* **111**: 3-16
- (1980) Physical, biochemical and physiological effects of low temperature and freezing – Their modification by water soluble polymers. *Scanning Electron Microscopy*. II. SEM Inc. AMF O'Hare, Chicago, 349-360
- (1985) Biophysics and biochemistry at low temperatures. Cambridge University Press, Cambridge
- , Mathias SF, Hatley RHM (1990) Water, temperature and life. *Phil. Trans. R. Soc. Lond.* B 326: 517-533
Fu JR, Xia QH, Tang LF (1993) Effects of desiccation on excised embryonic axes of three recalcitrant seeds and studies on cryopreservation. *Seed Sci. Technol.* **21**: 85-95
Fujikawa S (1980) Freeze-fracture and etching studies on membrane damage on human erythrocytes caused by formation of intracellular ice. *Cryobiology* **17**: 351-362
- (1981) The effect of different cooling rates on the membrane of frozen human erythrocytes. In: GJ Morris, A Clarke (eds) *Effects Of Low Temperatures On Biological Membranes.* Academic Press, London, New York, pp. 323-334
- (1988) Artificial biological membrane ultrastructural changes caused by freezing. *Electron Microsc. Rev.* **1**: 113-140
- (1994) Seasonal ultrastructural alterations in the plasma membrane produced by slow freezing in cortical tissues of mulberry (*Morus bombyciz* Koidz. Cv Goroji). *Trees* **8**: 288-296
- , Takabe K (1996). Formation of multiplex lamellae by equilibrium slow freezing of cortical parenchyma cells of mulberry and its possible relationship to freezing tolerance. *Protoplasma* **190**: 189-203
George MF, Becwar MR, Burke MJ (1982) Freezing avoidance by deep undercooling of tissue water in winter-hardy plants. *Cryobiology* **19**: 628-639
Gilkey JC, Staehelin LA (1986) Advances in ultrarapid freezing for the preservation of cellular ultrastructure. *J. Electron Microsc. Techn.* **3**:177-210
Grout BWW (1979) Low temperature storage of imbibed tomato seeds: a model for recalcitrant seed storage. *Cryo-Lett.* **1**: 71-76
- , Shelton K, Pritchard HW (1983) Orthodox behaviour of oil palm seed and cryopreservation of the excised embryo for genetic conservation. *Ann. Bot.* **52**: 381-384

Hallam ND (1976) Anhydrous fixation of dry plant tissue using non-aqueous fixatives. *J. Microsc.* **106**: 337-345
- , Gaff DF (1978) Re-organization of fine structure during rehydration of desiccated leaves of *Xerophyta villosa*. *New Phytol.* **81**: 349-355
- , Luff SE (1980) Fine structural changes in the leaves of the desiccation-tolerant plant *Talbotia elegans* during extreme water stress. *Bot. Gaz.* **141**: 180-187
Han RH, Hua TC, Ren HS (1995) Experimental investigation of cooling rates of small samples during quenching into sub-cooled LN_2. *Cryo-Lett.* **16**: 157-162
Haskins RH, Kartha KK (1980) Freeze preservation of pea meristems: cell survival. *Can. J. Bot.* **58**: 833-840
Hilling B, Amelunxen F (1985) On the development of the vacuole. II. Further evidence for endoplasmic reticulum origin. *Eur. J. Cell Biol.* **38**: 195-200
Hirsh AG, Williams RJ, Meryman HT (1985) A novel method of natural cryoprotection. *Plant Physiol.* **79**: 41-56
Hong TD, Ellis RH (1990) A comparison of maturation drying, germination and desiccation tolerance between developing seeds of *Acer pseudoplatanus* and *Acer platanoides* L. *New Phytol.* **116**: 589-596
- , Ellis RH (1996) *A protocol to determine seed storage behaviour.* IPGRI, Rome.
Hu J, Guo CG, Shi SX (1993) Partial drying and post-thaw preconditioning improve the survival and germination of cryopreserved seeds of tea (*Camellia sinensis*). *Plant Genetic Resources Newsletter* No. 93: 1-4
Huang AHC (1992) Oil bodies and oleosins in seeds. *Annu. Rev. Plant Physiol. Plant Mol. Biol.* **43**: 177-200
Journet EP, Bligny R, Douce R (1986) Biochemical changes during sucrose deprivation in higher plant cells. *J. Biol. Chem.* **261**: 3193-3199
Kandasamy MK, Kristen U (1989) Ultrastructural responses of tobacco pollen tubes to heat shock. *Protoplasma* **153**: 104-110
Kartha KK (1985) Meristem culture and germplasm conservation. In: KK Kartha (ed.) *Cryopreservation Of Plant Cells And Organs.* CRC Press, Boca Raton, Florida, pp. 115-134
Kasai M, Niwa K, Iritani A (1980) Survival of mouse embryos frozen and thawed rapidly. *J. Reprod. Fert.* **59**: 51-56
Kellenberger E (1991) The potential of cryofixation and freeze-substitution: observations and theoretical considerations. *J. Microsc.* **161**: 183-203
Kermode AR, Bewley JD (1985) The role of maturation drying in the transition from seed development to germination. I. Acquisition of desiccation tolerance and germinability during development of *Ricinus communis* L. seeds. *J. Exp. Bot.* **36**: 1906-1915
King MW, Roberts EH (1989a) Maintenance of recalcitrant seeds in storage. In: HF Chin and EH Roberts (eds) *Recalcitrant Crop Seeds.* Tropical Press, Kuala Lumpur, Malaysia, pp. 53-89
- , Roberts EH (1989b) A strategy for future research into the storage of recalcitrant seeds. In: HF Chin, EH Roberts (eds) *Recalcitrant Crop Seeds.* Tropical Press, Kuala Lumpur, Malaysia, pp. 53-89

Kioko J, Berjak P, Pammenter NW, Watt MP, Wesley-Smith J (1998) Desiccation and cryopreservation of embryonic axes of *Trichilia dregeana* SOND. *Cryo-Lett.* **19**: 15-26

Kiss JZ, Giddings ThH, Staehelin LA, Sack FD (1990) Comparison of the ultrastructure of conventionally fixed and high pressure frozen / freeze substituted root tips of *Nicotiana* and *Arabidopsis*. *Protoplasma* **157**: 64-74

Klein S, Pollock BM (1968) Cell fine structure of developing lima bean related to seed desiccation. *Am. J. Bot.* **55**: 658-672

Knoke D, Burke PJ (1980) *Log-linear models*. Sage University paper on Quantitative Applications in the Social Sciences. Sage Publications, Newbury Park

Koster KL (1991) Glass formation and desiccation tolerance in seeds. *Plant Physiol.* **96**: 302-304

Lancelle SA , Hepler PK (1992) Ultrastructure of freeze-substituted pollen tubes of *Lillium longiflorum*. *Protoplasma* **167**: 215-230

- , Callaham DA, Hepler PK (1986) A method for the rapid freeze fixation of plant cells. *Protoplasma* **131**: 153-165

- , Torrey JG, Hepler PK, Callaham DA (1985) Ultrastructure of freeze-substituted *Frankia* strain HFPCcl3, the actinomycete isolated from root nodules of *Casuarina cunninghamia*. *Protoplasma* **127**: 64-72

Langis R, Steponkus PL (1990) Cryopreservation of rye protoplasts by vitrification. *Plant Physiol.* **92**: 666-671

Le Murray PW, Robards AW, Waites PR (1989) Countercurrent plunge cooling: a new approach to increase reproducibility in the quick freezing of biological tissue. *J. Microsc.* **156**: 173-182

Leibo SP, Farrant J, Mazur P, Hanna Jr MG, Smith LH (1970) Effects of freezing on marrow stem cell suspensions: Interactions of cooling and warming rates in the presence of PVP, sucrose, or glycerol. *Cryobiology* **6**: 315-332

Leopold AC, Sun WQ, Bernal-Lugo I (1994). The glassy state in seeds: analysis and function. *Seed Sci. Res.* **4**: 267-274

Leprince O, Walters-Vertucci C (1995) A calorimetric study of the glass transition behaviors in axes of bean seeds with relevance to storage stability. *Plant Physiol.* **109**: 1471-1481

- , Hoekstra FA (1998) The responses of cytochrome redox state and energy metabolism to dehydration support a role for cytoplasmic viscosity in desiccation tolerance. *Plant Physiol.* **118**: 1253-1264

- , Buitink J, Hoekstra F (1999) Axes and cotyledons of recalcitrant seeds of *Castanea sativa* Mill. exhibit contrasting responses of respiration to drying in relation to desiccation sensitivity. *J. Exp. Bot.* **50**: 1515-1524

- , Harren FJM, Buitink J, Alberda M, Hoekstra FA (2000) Metabolic dysfunction and unabated respiration precede the loss of membrane integrity during dehydration of germinating radicles. *Plant Physiol.* **122**: 597-608

Lloyd G, McGown B (1980) Commercially-feasible micropropagation of mountain laurel, *Kalmia latifolia* by use of shoot-tip culture. *Comb. Proc. Int. Plant Prop. Soc.* **30**: 421-427

Lott JNA (1974) Cell walls in *Curcubita maxima* cotyledons in relation to imbibition. *Can. J. Bot.* **52**: 1465-1468

Lovelock JE (1955) Haemolysis by thermal shock. *Brit. J. Haematol.* **1**: 117-129.
Luyet B (1960) On the mechanism of growth of ice crystals in aqueous solutions and on the effect of rapid cooling in hindering crystallization. In: AS Parkes, AU Smith (eds) *Recent Research In Freezing And Drying*. Blackwell, Oxford, pp. 3-22
- (1961) A method for increasing the cooling rate in refrigeration by immersion in liquid nitrogen and other boiling baths. *Biodynamica* **8**: 331-352
- (1965) Phase transition encountered in the rapid freezing of aqueous solutions. *Ann. N.Y. Acad. Sci.* **125**: 502-521
- (1966) Anatomy of the freezing process in physical systems. In: HT Meryman (ed.) *Cryobiology*. New York, Academic Press, pp. 115-138
- (1970) Physical changes occurring in frozen solutions during rewarming and melting. In: GEW Wolstenholme, M O'Conner (eds) *The Frozen* Cell. Churchill Ltd., London, pp. 27-50
- , Gonzales F (1951) Recording ultra rapid changes in temperature. *Proc. Am. Soc. Refrig. Eng.*, pp. 1191-1193, 1236
- , Keane J Jr (1955) A critical temperature range apparently characterized by sensitivity of bull semen to high freezing velocity. *Biodynamica* **7**: 281-292
- , Tanner J, Rapatz G (1962) X-ray diffraction study of the structure of rapidly frozen gelatin solutions. *Biodynamica* **9**: 21-46
MacKenzie AP (1970) Death of frozen yeast in the course of slow warming. In: GEW Wolstenholme, JA O'Conner (eds) *The Frozen Cell*. Churchill Ltd., London, pp. 89-96
- (1977) Non-equilibrium freezing behaviour of aqueous systems. *Phil. Trans. R. Soc. Lond.* B. **278**: 167-189
Marty F (1999) Plant vacuoles. *Plant Cell* **11**: 587-599
Matile P (1975) The lytic compartment of plant cells. In: M Alfert, W Beermann, G Rudkin, W Sandritter, P Sitte (eds) *Cell Biology Monographs Vol. 1*. Berlin: Springer-Verlag, pp. 40-84
Mazur P (1966) Physical and chemical basis of injury in single-celled micro-organisms subjected to freezing and thawing. In: HT Meryman (ed.) *Cryobiology*, Academic Press, New York, pp. 213-315
- (1977) The role of intracellular freezing in the death of cells cooled at supraoptimal rates. *Cryobiology* **14**: 251-272
- (1984) Freezing of living cells: mechanisms and implications. *Am. J. Physiol.* **247**: C125-C142
- (1990) Equilibrium, quasi-equilibrium and non-equilibrium freezing of mammalian embryos. *Cell Biophys.* **17**: 53-92
- , Schmidt J (1968) Interaction of cooling velocity, temperature, and warming velocity on the survival of frozen and thawed yeast. *Cryobiology* **5**: 1-17
- , Farrant J, Leibo SP, Chu EHY (1969) Survival of hamster tissue culture cells after freezing and thawing. *Cryobiology* **6**: 1-9
- , Cole KW, Schreuders PD, Mahowald AP (1993) Contributions of cooling and warming rate and developmental stage to the survival of *Drosophila* embryos cooled to -205°C. *Cryobiology* **30**: 45-73
McCully ME, Canny MJ (1985) The stabilisation of labile configurations of plant cytoplasm by freeze-substitution. *J. Microsc.* **139**: 27-33

Menco BPM (1986) A survey of ultra-rapid cryofixation methods with particular emphasis on applications to freeze-fracturing, freeze-etching, and freeze-substitution. *J. Electron Microsc. Techn.* **4**: 177-240

Mersey B, McCully ME (1978) Monitoring the course of fixation of plant cells. *J. Microsc.* **114**: 49-76

Meryman HT (1956) Mechanics of freezing in living cells and tissues. *Science* **124**: 515-521

- (1957) Physical limitations of the rapid freezing method. *Proc. Roy. Soc. Lon. Ser.* B **147**: 452-459

- (1960) The mechanism of freezing in biological systems. In: AS Parkes, AU Smith (eds) *Recent Research In Freezing And Drying*. Blackwell, Oxford, pp. 23-39

- (1966) Review of biological freezing. In: HT Meryman (ed.) *Cryobiology*. Academic Press, London, New York, pp. 1-114

-, Williams RJ (1980) Mechanisms of freezing injury and natural tolerance and the principles of artificial cryoprotection. In: LA Withers, JT Williams (eds) *Crop Genetic Resources – The Conservation Of Difficult Material*. IUBS Série B42, Reading, pp. 5-37

-, Williams RJ (1985) Mechanisms of cooling injury and natural tolerance and the principles of artificial cryoprotection. In: KK Kartha (ed.) *Cryopreservation Of Plant Cells And Organs*. CRC Press, Boca Raton, pp. 13-47

Mohr WP, Stein M (1969) Effect of different freeze-thaw regimes on ice formation and ultrastructural change in tomato fruit parenchyma tissue. *Cryobiology* **6**: 15-31

Moor H (1964) Die gefrier-fixation lebender zellen und ihre anwendung in der elektronmikroscopie. *Zeitschrift für Zellforshung* **62**: 546-580

Moor H (1971) Recent progress in the freeze-etching technique. *Phil. Trans. Roy. Soc.* B **261**: 121-131

- (1973) Cryotechnology for the structural analysis of biological material. In: EL Benedetti, P Favard (eds) *Freeze Etching: Techniques And Applications*. Société Française de Microscopie Électronique, Paris, pp. 11-19

-, Mühlethaler K (1963) Fine structure in frozen-etched yeast cells. *J. Cell Biol.* **17**: 609-628

Moriyasu Y, Oshumi YO (1996) Autophagy in suspension-cultured cells in response to sucrose starvation. *Plant Physiol.* **111**: 1233-1241

Morris GJ (1976) The cryopreservation of *Chlorella*. 1. Interactions of rate of cooling, protective additive and warming rate. *Arch. Microbiol.* **107**: 57-62

-, Coulson G, Meyer MA, McLellan, Fuller BJ, Grout BWW, Pritchard HW, Knight SC (1983) Cold shock – A widespread cellular reaction. *Cryo-Lett.* **4**: 179-192

Murai M, Yoshida S (1998) Vacuolar membrane lesions induced by a freeze-thaw cycle in protoplasts isolated from deacclimated tubers of Jerusalem artichoke (*Helianthus tuberosus* L.). *Plant Cell Physiol.* **39**: 87-96

Murashige T, Skoog E (1962) A revised medium for rapid growth and bio-assays with tobacco tissue cultures. *Physiologia Plantarum* **15**: 473-497

Mycock DJ, Wesley-Smith J, Berjak P (1995) Cryopreservation of somatic embryos of four species with and without cryoprotectant pre-treatment. *Ann. Bot.* **75**: 331-336

Nei T (1973) Growth of ice crystals in frozen specimens. *J. Microsc.* **99**: 227-233
- (1976a) Freezing injury to erythrocytes. I. Freezing patterns and post-thaw hemolysis. *Cryobiology* **13**: 278-286
- (1976b) Freezing injury to erythrocytes. II. Morphological alterations and cell membranes. *Cryobiology* **13**: 287-294
- (1977) Structure and function of frozen cells: freezing patterns and post-thaw survival. *J. Microsc.* **112**: 197-204

Normah MN, Chin HF, Hor YL (1986) Desiccation and cryopreservation of embryonic axes of *Hevea brasiliensis* Muell.- Arg. *Pertanika* **9**: 299-303
- , Sitti Dewi Serimala MN (1997) Cryopreservation of seeds and embryonic axes of several *Citrus* species. In: RH Ellis, M Black, AJ Murdoch, TD Hong (eds) *Basic And Applied Aspects Of Seed Biology*. Academic Publishers, Dordrecht, Kluwer, pp. 817-823

Öpik H (1980) The ultrastructure of coleoptile cells in dry rice (*Oryza sativa* L.) grains after anhydrous fixation with osmium vapour. *New Phytol.* **85**: 521-529
- (1985) The fine structure of some dry seeds tissues observed after completely anhydrous chemical fixation. *Ann. Bot.* **56**: 453-466

Pammenter NW, Berjak P (1999) A review of recalcitrant seed physiology in relation to desiccation-tolerance mechanisms. *Seed Sci. Res.* **9**: 13-37
- , Vertucci CW, Berjak P (1991) Homeohydrous (recalcitrant) seeds: dehydration, the state of the water and viability characteristics in *Landolphia kirkii*. *Plant Physiol.* **96**: 1093-1098
- , Vertucci CW, Berjak P (1993) Responses to dehydration in relation to non-freezable water in desiccation-sensitive and –tolerant seeds. In: D Côme, F Corbineau (eds) *Fourth International Workshop On Seeds. Basic And Applied Aspects Of Seed Biology*. ASFIS, Paris, pp. 867-872
- , Berjak P, Farrant JM, Smith MT, Ross G (1994) Why do recalcitrant seeds die? *Seed Sci. Res.* **4**: 187-191
- , Farrant JM, Berjak P (1984) Recalcitrant seeds: short-term storage effects in *Avicennia marina* (Forsk.) Vierh. may be germination-associated. *Ann. Bot.* **54**: 843-846
- , Greggains V, Kioko JI, Wesley-Smith J, Berjak P, Finch-Savage WE (1998) Effects of differential drying rates on viability retention of recalcitrant seeds of *Ekebergia capensis*. *Seed Sci. Res.* **8**: 463-471

Parthasarathy MV (1995) Freeze-substitution. In: DW Galbraith, HJ Bohnert, DP Bourque (eds) *Methods In Plant Cell Biology* **49**, Part A. Academic Press, San Diego, pp. 57-69

Pence VC (1990) Cryostorage of embryo axes of several large-seeded temperate tree species. *Cryobiology* **27**: 212-218
- (1991) Cryopreservation of immature embryonic axes of *Theobroma cacao*. *Plant Cell Rep.* **10**: 144-147
- (1992) Desiccation and the survival of *Aesculus*, *Castanea*, and *Quercus* embryo axes through cryopreservation. *Cryobiology* **29**: 391-399
- (1995) Cryopreservation of recalcitrant seeds. In: YPS Bajaj (ed.) *Biotechnology In Agriculture And Forestry, Vol 32 Cryopreservation of Plant Germplasm I.* Berlin, Heidelberg: Springer-Verlag, pp. 29-50

Perner E (1965) Elektronmikroskopische untersuchungen an zellen von embryonen im zustand völliger samenruhe. I. Mitteilung. Die zelluläre strukturordnung in der radicula lufttrockner samen von *Pisum sativum*. *Planta* **65**: 334-357

Platt KA, Oliver MJ, Thomson WW (1994) Membranes and organelles of dehydrated *Selaginella* and *Tortula* retain their normal configuration and structural integrity – Freeze fracture evidence. *Protoplasma* **178**: 57-65

- , Oliver MJ, Thomson WW (1997) Importance of the fixative for reliable ultrastructural preservation of poikilohydric plant tissues. Observations on dry, partially, and fully hydrated tissues of *Selaginella lepidophylla*. *Ann. Bot.* **80**: 599-610

Plattner H, Fischer WM, Schmitt WW, Bachmann L (1972) Freeze etching of cells without cryoprotectants. *J. Cell Biol.* **53**: 116-126

Pritchard HW (1991) Water potential and embryonic axis viability in recalcitrant seeds of *Quercus rubra*. *Ann. Bot.* **67**: 43-49

- (1995) Cryopreservation of seeds. In: JG Day, MR McLellan (eds) *Methods In Molecular Cell Biology, Vol. 38: Cryopreservation and Freeze Drying Protocols*, Humana Press, Totowa, NJ, pp. 133-143

- , Prendergast FG (1986) Effects of desiccation and cryopreservation on the *in vitro* viability of embryos of the recalcitrant seed species *Araucaria hunsteinii* K. Shum. *J. Exp. Bot.* **37**: 1388-1397

- , Manger KR (1998) A calorimetric perspective on desiccation stress during preservation procedures with recalcitrant seeds of *Quercus robur* L. Cryo-Lett. **19** [Suppl1]: 23-30

- , Tompsett PB, Manger K, Smidt WJ (1995) The effect of moisture content on the low temperature response of *Araucaria hunstenii* seed and embryos. *Ann. Bot.* **76**: 79-88

Probert RJ, Brierley ER (1989) Desiccation intolerance in seeds of *Zizania palustris* is not related to developmental age or the duration of post-harvest storage. *Ann. Bot.* **64**: 669-674

Quartacci MF, Forli M, Rascio N, Dalla Vechia F, Bochicchio A, Navari-Izzo F (1997) Desiccation-tolerant *Sporobolus stapfianus*: lipid composition and cellular ultrastructure during dehydration and rehydration. *J. Exp. Bot.* **48**: 1269-1279

Radhamani J, Chandel KPS (1992) Cryopreservation of embryonic axes of trifoliate orange (*Poncirus trifoliata* [L.] RAF.). *Plant Cell Reports* **11**: 372-374

Rall WF (1987) Factors affecting the survival of mouse embryos cryopreserved by vitrification. *Cryobiology* **24**: 387-402

Rall WF, Fahy GM (1985). Ice free cryopreservation of mouse embryos at -196°C by vitrification. *Nature* **313**: 573-575

Rasmussen DH (1982) Ice formation in aqueous systems. *J. Microsc.* **128**: 167-174

- , MacAuley MN, MacKenzie AP (1975) Supercooling and nucleation in single cells. *Cryobiology* **12**: 328-339

- , MacKenzie AP (1972) Effect of solute on ice-solution interfacial free energy; calculation ffrom measured homogeneous nucleation temperatures. In: HHG Jellinek (ed.) *Water Structure At The Water-Polymer Interface*, Plenum, New York, pp. 126-145

Raven PH, Evert RF, Eichorn SE (1992) *Biology Of Plants*. Worth Publishers, New York, pp. 470-519

Rebhun LI, Sander G (1971) Electron microscope studies of frozen-substituted marine eggs I. Conditions for avoidance of intracellular ice crystallization. *Am. J. Anat.* **130**: 1-16

Reed BM (1996) Pre-treatment strategies for the cryopreservation of plant tissues. In: MN Normah, MK Narimah, MM Clyde (eds) *In Vitro Conservation Of Plant Genetic Resources*, Percetakan Watan Sdn. Bhd., Kuala Lumpur, Malaysia, pp. 73-87

Robards AW (1974) Ultrastructural methods for looking at frozen cells. *Sci Prog. Oxf.* **61**: 1-40

- , Sleytr UB (1985) Low temperature methods in biological electron microscopy. In: AM Glauert (ed.) *Practical Methods In Electron Microscopy, Vol 10*. Elsevier, Amsterdam

Roberts EH (1973) Predicting the storage life of seeds. *Seed Sci. Technol.* **1**:499-514

- , King MW (1980) The characteristics of recalcitrant seeds. In: HF Chin, EH Roberts (eds) *Recalcitrant Crop Seeds*. Tropical Press, Kuala Lumpur, Malaysia, pp. 1-5

Roos Y, Karel M (1991) Amorphous state and delayed ice formation in sucrose solutions. *Int. J. Food Sci. Technol.* **26**: 553-566

Ryan KP (1992) Cryofixation of tissues for electron microscopy: a review of plunge cooling methods. *Scanning Microscopy*, Vol 6, III. SEM Inc. AMF O'Hare Chicago, pp. 349-60

- , Purse DH (1985a) A simple plunge-cooling device for preparing biological specimens for cryo-techniques. *Mikroskopie* (Wien) **42**: 247-251

- , Purse DH (1985b) Plunge cooling of tissue blocks: determinants of cooling rates. *J. Microsc.* **140**: 47-54

- , Liddicoat MI (1987) Safety considerations regarding the use of propane and other liquefied gases as coolants for rapid freezing purposes. *J. Microsc.* **147**: 337-340

- , Purse DH, Robinson SG, Wood JW (1987) The relative efficiencies of cryogens used for plunge-cooling biological specimens. *J. Microsc.* **145**: 89-96

Sack FD, Leopold CA, Hoekstra FA (1988) Structural correlates of imbibitional injury in *Typha* pollen. *Am. J. Bot.* **75**: 570-578

Sakai A (1966) Survival of Plant tissues at super-low temperatures. IV. Cell survival with rapid cooling and rewarming. *Plant Physiol.* **41**: 1050-1054

- (1968) Mechanism of survival in plant cells at super-low temperatures by rapid cooling and rewarming. *Cryobiology* **4**: 165-173

- (1970) Some factors contributing to the survival of rapidly cooled plant cells. *Cryobiology* **8**: 225-234

- , Otsuka K (1967) Survival of plant tissue at super-low temperatures V. An electron microscope study of ice in cortical cells cooled rapidly. *Plant Physiol.* **42**: 1680-1694

- , Yoshida S (1967) Survival of plant tissue at super-low temperature VI. Effects of cooling and rewarming rates on survival. *Plant Physiol.* **42**: 1695-1701

- , Otsuka K, Yoshida S (1968) Mechanism of survival in plant cells at superlow temperatures by rapid cooling and rewarming. *Cryobiology* **4**: 165-173
Salmen Espindola L, Noin M, Corbineau F, Côme D (1994) Cellular and metabolic damage induced by desiccation in recalcitrant *Araucaria angustifolia* embryos. *Seed Sci. Res.* **4**: 193-201
Sargent JA, Mandi SS, Osborne DJ (1981) The loss of desiccation tolerance during germination: an ultrastructural and biochemical approach. *Protoplasma* **105**: 225-239
Schneider K, Wells B, Schelzer E, Salamini F, Bartels D (1993) Desiccation leads to the rapid accumulation of both cytosolic and chloroplastic proteins in the resurrection plant *Craterostigma plantigeneum* Hochst. *Planta* **189**: 120-131
Seewaldt V, Priestley DA, Leopold AC, Feigenson GW (1981) Membrane organization in soybean seeds during hydration. *Planta* **152**: 19-23
Senaratna T, McKersie BD (1986) Loss of desiccation tolerance during seed germination: a free radical mechanism of injury. In: AC Leopold (ed.) *Membranes, Metabolism And Dry Organisms*. Cornell University Press, Ithaca, pp. 85-101
Sherman JK (1962) Survival of higher animal cells after the formation and dissolution of intracellular ice. *Anat. Rec.* **144**: 171-191
- (1964) Effect of size of intracellular ice on consumption of oxygen and nuclear alteration of mouse kidney cells. *Anat. Rec.* **149**: 591-604
- , Kim KS (1967) Correlation of cellular ultrastructure before freezing, while frozen, and after thawing in assessing freeze-thaw induced injury. *Cryobiology* **2**: 61-74
Shimada K, Asahina E (1972a) Types of cell freezing and post-thaw survival of individual HeLa cells. *Cryobiology* **9**: 51-56
- , Asahina E (1972b) Innocuous ice crystallisation within ascites tumor cells of rat by rapid freezing. *Low Temperature Sci. Ser. B* **30**: 65-75
- , Asahina E (1975) Visualization of intracellular ice crystals formed in very rapidly frozen cells at -27°C. *Cryobiology* **12**: 209-218
Simon EW, Raja Harun RM (1972) Leakage during seed imbibition. *J. Exp. Bot.* **23**: 1076-1085
Sitte H (1996) Advanced instrumentation and methodology related to cryoultramicrotomy: a review. *Scanning Microscopy International.* AMF O'Hare, Chicago, [Suppl 10], pp. 387-466
- , Edelmann, L, Neumann K (1987) Cryofixation without pretreatment at ambient pressure. In: RA Steinbrecht, K Zierold (eds) *Cryotechniques In Biological Electron Microscopy.* Springer-Verlag, Heidelberg, Berlin, pp. 87-113
Skaer H (1982) Chemical cryoprotection for structural studies. *J. Microsc.* **125**: 137-148
Smith MT (1991) Studies on the anhydrous fixation of dry seeds of lettuce (*Lattuca sativa* L.). *New Phytol.* **119**: 575-584
- , Berjak P (1995) Deteriorative changes associated with the loss of viability of stored desiccation-tolerant and desiccation-sensitive seeds. In: J Kigel, G Gallili (eds) *Seed Development And Germination*. Marcel Dekker Inc. New York, pp. 701-746

Spurr AR (1969) A low viscosity epoxy resin embedding medium for electron microscopy. *J. Ultrastruct. Res.* **26**: 31-43
Staehelin LA, Chapman RL (1987) Secretion and membrane recycling in plant cells. *Planta* **171**:43-57
Stanwood PC (1985) Cryopreservation of seed germplasm for genetic conservation. In: KK Kartha (ed.) *Cryopreservation Of Plant Cells And Organs*. Boca Raton, CRC Press, pp. 199-226
Stanwood PC, Bass LN (1981) Seed germplasm preservation using liquid nitrogen. *Seed Sci. Technol.* **9**: 423-437
Steere RL (1969) Freeze-etching and direct observation of frezing damage. *Cryobiology* **3**: 137-150
Steinbrecht RA (1985) Recrystallization and ice crystal growth in a biological specimen, as shown by a simple freeze-substitution method. *J.Microsc.* **140**: 41-46
Steinbrecht RA, Müller M (1987) Freeze-substitution and freeze-drying. In: RA Steinbrecht, K Zierold (eds) *Cryotechniques In Biological Electron Microscopy*. Springer-Verlag, Berlin, Heidelberg, pp. 149-172
Stephenson JL (1956) Ice crystal growth during the rapid freezing of tissues. *J. Biophys. Biochem. Cytol.* **2** (Suppl.) 45-52
Steponkus PL (1984) Role of the plasma membrane in freezing injury and cold acclimation. *Annu. Rev. Plant Physiol.* **35**: 543-584
- , Myers SP, Lynch DV, Gardner I, Bronshteyn V, Leibo SP, Rall WF, Pitt RE, Lin TT, MacIntyre RJ (1990) Cryopreservation of *Drosophila melanogaster* embryos. *Nature* **345**: 170-172
Stewart P, Taylor M, Mycock D (2001) The sequence of preparative procedures affects the success of cryostorage of cassava somatic embryos. *Cryo-Lett.* **22**: 35-42
Sun WQ, Irving TC, Leopold AC (1994) The role of sugar, vitrification and membrane phase transition in seed desiccation tolerance. *Physiologia Plantarum* **90**: 621-628
Swift JG, Buttrose MS (1972) Freeze-etch studies of protein bodies in wheat scutellum. *J. Ultrastruct. Res.* **40**: 378-390
Thammasiri K (1999) Cryopreservation of embryonic axes of jackfruit. *Cryo-Lett.* **20**: 21-28
Thomson WW (1979) Ultrastructure of dry seed tissue after a non-aqueous primary fixation. *New Phytol.* **82**: 207-212
- , Platt KA (1997) Conservation of cell order in desiccated mesophyll of *Selaginella lepidophylla* ([Hook and Grev.] Spring). *Ann. Bot.* **79**: 439-447.
Tiwari SC, Polito VS, Webster BD (1990) In dry pear (*Pyrus comminis* L.) pollen, membranes assume a tightly packed multilamellate aspect that disappears rapidly upon hydration. *Protoplasma* **153**: 157-168
Tompsett PB, Pritchard HW (1993) Water status changes during development in relation to germination and desiccation tolerance of *Aesculus hippocastanum* L. seeds. *Ann. Bot.* **71**: 107-116
- (1987) Desiccation and storage studies on *Dipterocarpus* seeds. *Ann. Appl. Biol.* **110**: 371-379

Touchell D, Walters C (2000) Recovery of embryos of *Zizania* pallustris following exposure to liquid nitrogen. *Cryo-Lett.* **21**: 261-70

Van Venrooij GEPM, Aretsen AMHJ, Hax WMA, Ververgaert PHJT, Verhoeven JJ, Van der Horst HA (1975) Freeze-etching: freezing velocity and crystal size at different locations in samples. *Cryobiology* **12**: 46-61

Vander Willigen C, Pammenter NW, Mundree SG, Farrant JM (2001) Some physiological comparisons between the resurrection grass *Eragrostis nindensis* and the related desiccation-sensitive species *E. curvula. Plant Growth Reg.* (in press)

Vertucci CW (1989a) Relationship between thermal transitions and cooling injury in pea and soybean seeds. *Plant Physiol.* **90:** 1121-1128

- (1989b) Effects of cooling rate on seeds exposed to liquid nitrogen temperatures. *Plant Physiol.* **90**: 1478-1485
- (1990) Calorimetric studies of the state of water in seed tissues. *Biophys. J.* **58**: 1463-1471
- (1993) Towards a unified hypothesis of seed aging. In: D Côme, F Corbineau (eds) *Fourth International Workshop On Seeds. Basic And Applied Aspects Of Seed Biology.* Paris: ASFIS, pp. 739-746
- , Roos EE (1990) Theoretical basis of protocols for seed storage. *Plant Physiol.* **94**: 1019-1023
- , Roos EE (1993) Theoretical basis of protocols for seed storage II. The influence of temperature on optimal moisture levels. *Seed Sci. Res.* **3**: 201-213
- , Farrant JM (1995) Acquisition and loss of desiccation tolerance. In: J Kigel, Galili G (eds) *Seed Development And Germination.* Marcel Dekker Inc., New York, Basel, Hong Kong, pp. 237-271
- , Berjak P, Pammenter NW, Crane J (1991) Cryopreservation of embryonic axes of a homeohydrous (recalcitrant) seed in relation to calorimetric properties of tissue water. *Cryo-Lett.* **12**: 339-350
- , Crane J, Porter RA, Oelke EA (1994). Physical properties of water in *Zizania* embryos in relation to maturity status, water content and temperature. *Seed Sci. Res.* **4**: 211-224
- , Crane J, Porter RA, Oelke EA (1995). Survival of *Zizania* embryos in relation to water content, temperature and maturity status. *Seed Sci. Res.* **5**: 31-40

Vigil EL, Steere RL, Wergin WP, Christiansen MN (1984) Tissue preparation and fine structure of the radicle apex from cotton seeds. *Am. J. Bot.* **71**: 645-659

- , Steere RL, Wergin WP, Christiansen MN (1985) Structure of plasma membrane in radicles from cotton seeds. *Protoplasma* **129**: 168-177

Walters C (1998) Understanding the mechanism and kinetics of seed aging. *Seed Sci. Res.* **8**: 223-244

- , Pammenter NW, Berjak P, Crane J (2001) Desiccation damage, accelerated ageing and respiration in desiccation tolerant and sensitive seeds. *Seed Sci. Res.***11**: 135-148
- , Farrant JM, Pammenter NW, Berjak P (2002) Desiccation and damage. In: Black M, Pritchard HW (eds) Desiccation And Plant Survival (in press)

Weakley BS (1981) *A beginner's handbook in biological transmission electron microscopy.* Curchill Livingstone, New York, pp.18-48

Webb MA, Arnott HJ (1982) Cell wall conformation in dry seeds in relation to the preservation of structural integrity during desiccation. *Am. J. Bot.* **69**: 1657-1668

Webster BD, Leopold AC (1977) The ultrastructure of dry and imbibed cotyledons of soybean. *Am. J. Bot.* **64**: 1286-1293

Wesley-Smith J (2001) Freeze-substitution of dehydrated plant tissues: artefacts of aqueous fixation revisited. *Protoplasma* **218**: 154-167

Wesley-Smith J, Vertucci CW, Berjak P, Pammenter NW, Crane J. (1992) Cryopreservation of desiccation-sensitive axes of *Camellia sinensis* in relation to dehydration, freezing rate and the thermal properties of tissue water. *J. Plant Physiol.* **140**: 596-604

Wesley-Smith J, Berjak P, Pammenter NW, Vertucci CW (1995) Ultrastructural evidence of freezing in embryonic axes of *Pisum sativum* L. at various water contents. *Ann. Bot.* **76**: 54-64

Wesley-Smith J, Walters C, Pammenter NW, Berjak P (1999) Rapid freezing of embryonic axes of recalcitrant species. In: M Marzalina, KC Khoo, N Jayanthi, FY Tsan, B Krishnapillay (eds) *Recalcitrant Seeds*. FRIM, Kuala Lumpur, pp. 132-139

Wesley-Smith J, Pammenter NW, Walters C, Berjak P (2001a). The effects of two drying rates on the desiccation tolerance of embryonic axes of recalcitrant jackfruit (*Artocarpus heterophyllus* Lamk.) seeds. *Ann. Bot.* **88**: 653-664

Wesley-Smith J, Walters C, Pammenter NW, Berjak P. (2001b) Interactions of water content, rapid (non-equilibrium) cooling to -196°C and survival of embryonic axes of *Aesculus hippocastanum* L. seeds. *Cryobiology* **42**: 196-206

Wikefeldt P (1971) Growth of an ice phase in frozen tissue studied by proton NMR-spectroscopy. *Cryobiology* **8**: 589-593

Williams WP (1990) Cold induced lipid phase transitions. *Phil. Trans. R. Soc. Lond.* B **326**: 555-570

Williams RJ, Leopold AC (1989) The glassy state in corn embryos. *Plant Physiol.* **89**: 977-981

- , Hirsh AG, Takahashi TA, Meryman HT (1993) What is vitrification and how can it extend life? *Japanese J. Freezing Drying* **39**: 1-10

Winston PW, Bates DH, (1960) Saturated salt solutions for the control of humidity in biological research. *Ecology* **41**: 232-237

Withers LA, Street HE (1977) Freeze-preservation of cultured plant cells III. The pre-growth phase. *Physiologia Plantarum.* **39**:171-178

- , Engelmann F (1998) *In vitro* conservation of plant genetic resources. In: A Altman (ed.) *Biotechnology In Agriculture*. Marcel Dekker Inc., New York, pp. 57-88

Wood MJ, Farrant J (1980) Preservation of mouse embryos by two-step freezing. *Cryobiology* **17**:178-180

Yatsu LY (1983) Electron microscopy of dry peanut (*Arachis hypogaea* L.) seeds crushed for oil removal. Fixation and embedding of anhydrously prepared tissues. *Protoplasma* **117**: 1-6